Neural Plasticity

Neuronal Plasticity in the Entorhinal Cortex

Guest Editors: C. Andrew Chapman, Roland S. G. Jones, and Min Jung

Neuronal Plasticity in the Entorhinal Cortex

Neuronal Plasticity in the Entorhinal Cortex

Guest Editors: C. Andrew Chapman, Roland S. G. Jones, and Min Jung

Copyright © 2008 Hindawi Publishing Corporation. All rights reserved.

This is a special issue published in volume 2008 of "Neural Plasticity." All articles are open access articles distributed under the Creative Commons Attribution License, which permits unrestricted use, distribution, and reproduction in any medium, provided the original work is properly cited.

Editor-in-Chief

Gal Richter-Levin, University of Haifa, Israel

Editorial Board

Robert Adamec, Canada
Cristina M. Alberini, USA
Shimon Amir, Canada
Hymie Anisman, Canada
Edi Barkai, Israel
Timothy Bliss, UK
Clive Raymond Bramham, Norway
Anna Katharina Braun, Germany
Sumantra Chattarji, India
Leonardo G. Cohen, USA
David Diamond, USA
Gabriele Flügge, Germany
Eberhard K. Fuchs, Germany
Zygmunt Galdzicki, USA
Yuji Ikegaya, Japan
John T. Isaac, USA
Marian Joels, The Netherlands
Min Jung, Korea
Leszek Kaczmarek, Poland
Jeansok J. Kim, USA
Monica Di Luca, Italy
Sonia J. Lupien, Canada
Stephen A. Maren, USA
M. Silvana Oitzl, The Netherlands
Denis Paré, USA
Bruno Poucet, France
Kerry J. Ressler, USA
Katherine W. Roche, USA
Benno Roozendaal, USA
Michael J. Rowan, Ireland
Pankaj Sah, Australia
Susan J. Sara, France
Menahem Segal, Israel
Michael G. Stewart, UK
Robert Stickgold, USA
Oliver Stork, Germany
David J. Sweatt, USA
Donald A. Wilson, USA
Lin Xu, China

Contents

Hindawi Publishing Corporation
Neural Plasticity
Volume 2008, Article ID 314785, 2 pages
doi:10.1155/2008/314785

Editorial

Neuronal Plasticity in the Entorhinal Cortex

C. Andrew Chapman,[1] Roland S. G. Jones,[2] and Min Jung[3]

[1] *Center for Studies in Behavioral Neurobiology, Department of Psychology, Concordia University, Montreal, QC, Canada H4B 1R6*
[2] *Neuronal Networks Research Group, Department of Pharmacy and Pharmacology, University of Bath, Bath BA2 7AY, UK*
[3] *Neuroscience Laboratory, Institute for Medical Sciences, Ajou University School of Medicine, Suwon 443-721, South Korea*

Correspondence should be addressed to C. Andrew Chapman, andrew.chapman@concordia.ca

Received 15 December 2008; Accepted 15 December 2008

Copyright © 2008 C. Andrew Chapman et al. This is an open access article distributed under the Creative Commons Attribution License, which permits unrestricted use, distribution, and reproduction in any medium, provided the original work is properly cited.

The entorhinal cortex (EC) is a unique and fascinating structure, constituting a highly parallel interface between phylogenetically old cortex (hippocampus) and higher neocortical areas. The literature related to the EC has increased dramatically in the past 30 years. A simple PubMed search for EC lists around 20–40 articles per year in the early 1980s. This more than doubled by the beginning of the 1990s and doubled again by the start of the new century. Throughout the current decade, some 220–250 papers per year relating to structure, function, and pathology of the EC have been published, and the numbers are still rising. It has become increasingly apparent that the EC can no longer be regarded as a simple relay between the hippocampus and neocortex, but is a dynamic processor of both efferent and afferent information. In recent years, there has been burgeoning interest in synaptic plasticity at entorhinal synapses particularly in relationship with learning and memory functions of limbic structures. Neuroplasticity in the EC clearly takes many forms. In addition to the "input" and "output" roles that have long been ascribed to the superficial and deep layers, functions of the entorhinal area have been studied with respect to differences in the medial and lateral divisions, prominent state-dependent theta- and gamma-frequency population activities, membrane conductances that shape cellular and network activities, the neurophysiology of synaptic inputs from other regions and interlaminar connections, and the powerful roles of modulatory transmitter systems and local inhibition. The discovery of grid cells in the EC has led to strong interest in the role of the area in spatial processing. On the other side of the coin, long-term adaptive changes in EC function also appear to play pivotal roles in neuropathological states, particularly epilepsy, schizophrenia, and Alzheimer's disease.

Contributions to this special issue of Neural Plasticity provide an overview of some of the theoretical and methodological approaches that are being applied to understand the functions and mechanisms of neuroplasticity within the EC. The research contained in this special issue deals mainly with findings derived from animal research. It is clear, however, that research using a variety of techniques is providing insight into entorhinal function in human and clinical populations.

The significance of plasticity in the EC is best understood within the context provided by anatomical knowledge of the extrinsic and intrinsic connectivity of this area. Canto et al. have provided an excellent overview of the anatomical organization of the EC. Their analysis of intrinsic and extrinsic connections, in relationship to laminar organization and neuronal subtypes, heavily underscores our increasing perception of the EC as a dynamic interactive processor essential to hippocampal function, rather than a passive route of information entry and exit. The EC is tightly intertwined with circuitries of the hippocampal formation and other cortical areas, and its particular contributions to sensory processing, learning, memory, and motor behavior have been difficult to define. Lipton and Eichenbaum present evidence dealing with the complementary roles of the EC and hippocampus in episodic memory. They have found that medial EC neurons show stronger trajectory-dependent firing whereas hippocampal place cells show greater spatial specificity. Based on these observations, they propose roles of the hippocampus and medial EC in encoding sequences of events and disambiguating overlapping experiences, respectively. A contribution by Bevilaqua et al. also highlights the role of the EC in extinction learning and how this is affected by ageing. They raise the possibility that ageing-associated

impairment of extinction may occur in part because of degenerative changes in the EC.

Several articles in the special issue have investigated mechanisms of long-term, activity-dependent synaptic plasticity. Ma et al. observed differences in the induction of long-term synaptic potentiation (LTP) in the superficial neurones of the EC; LTP in horizontal (potentially extrinsic) inputs required NMDA receptor activation whereas LTP in interlaminar (intrinsic) inputs did not. This underlines the potential complexity of information processing in neurones that provides the bulk of hippocampal afferent inputs. Hernández et al. have found that prenatal malnutrition has lasting effects on the capacity of the EC to express LTP, and it is possible that this reduced plasticity may contribute to deficits in learning and memory in the adult. In addition to LTP, there is a growing body of literature dealing with characteristics of long-term *depression* (LTD) in the EC. Kourrich et al. have investigated the postsynaptic signaling mechanisms that mediate entorhinal LTD, and provide further evidence for the roles of calcium-dependent signaling and protein phosphatases in the expression of LTD in the superficial layers. Much of the interest in long-term changes in synaptic strength has traditionally been driven by interest in mnemonic processes and neurological disorders. Short-term activity-dependent changes in synaptic strength also have powerful influences on ongoing synaptic transmission in the EC. In this issue, Chamberlain et al. have continued their work on the role of presynaptic NMDA autoreceptors in excitatory transmission in layer V of the EC. They demonstrate that presynaptic NR2B subunits are critical in enhancement of both spontaneous glutamate release and frequency-dependent facilitation of action potential-driven release. The kinetics of these receptors provide an optimal facilitation frequency of 3–6 Hz, and the authors speculate on the possible involvement of the autoreceptors in generation of delta/theta oscillations in mnemonic processing and epileptogenesis.

The EC is subject to the powerful influence of several neuromodulatory transmitters including acetylcholine, serotonin, and dopamine. One of the articles in the special issue, from Caruana and Chapman, describes the dose-dependent, bidirectional effect of dopamine on the amplitude of evoked synaptic responses in layer II of the lateral EC. The significance of this bidirectional effect for entorhinal function is as yet unclear, but there are interesting parallels with bidirectional effects of dopamine in prefrontal cortex.

Oscillatory neuronal population activities are known to contribute to the synchronization of neuronal activity in cortical areas throughout the brain, and the mechanisms that generate theta- and gamma-frequency activities in the EC are being examined. Kainic acid induces powerful gamma oscillations in layer III of the EC, and Stanger et al. demonstrate here that the GLU_{K5} subunit is required for kainate-induced gamma activity in the EC. Morgan et al. also examined kainate-induce oscillations in the beta/gamma range in EC with respect to the action of cannabinoid receptors. Their experiments suggest that CB1 receptors are constitutively active in the EC and that antagonists or inverse agonists enhanced beta/gamma oscillations in layer II but suppressed oscillations in layer V, again pointing to differential control of synchrony in neurons providing afferent input to the hippocampus and those receiving output from it. Hasselmo and Brandon have examined how oscillations in membrane potential in entorhinal neurons, combined with the unique persistent firing activity in these cells, may contribute to several phenomena. This provides an excellent example of how quantitative analysis of cellular and network properties of the EC can lead to a greater understanding of mechanisms of cognition and behavior. The role of oscillatory activity in regulating large-scale interactions between the hippocampal formation and the neocortex has come under increased study in the past several years as several labs have begun to examine concurrent changes in oscillatory EEG activity in hippocampus and neocortex associated with sleep and waking states. In the current issue, Axmacher et al. describe results obtained from scalp and intracranial EEG recordings from epilepsy patients that show increased correlations between oscillations in the neocortex and medial temporal lobe including the rhinal cortex during non-REM sleep; the increased correlation may support mechanisms related to memory consolidation.

Our hope is that this special issue of Neural Plasticity will serve to emphasize the diversity of phenomena related to neural plasticity in the EC, and to highlight the importance of these effects, particularly in relationship to the increasing perception of the participation of the EC in mnemonic function of temporal lobe memory circuits and its related roles in integration of spatial information.

C. Andrew Chapman
Roland S. G. Jones
Min Jung

Hindawi Publishing Corporation
Neural Plasticity
Volume 2008, Article ID 381243, 18 pages
doi:10.1155/2008/381243

Review Article

What Does the Anatomical Organization of the Entorhinal Cortex Tell Us?

Cathrin B. Canto,[1] Floris G. Wouterlood,[2] and Menno P. Witter[1,2]

[1] *Department of Neuroscience, Kavli Institute for Systems Neuroscience and Centre for the Biology of Memory, Norwegian University of Science and Technology (NTNU), Building MTFS, 7489 Trondheim, Norway*
[2] *Department of Anatomy and Neurosciences, Institute for Clinical and Experimental Neurosciences, VU University Medical Center, Amsterdam, P.O. Box 7057, 1007MB Amsterdam, The Netherlands*

Correspondence should be addressed to Menno P. Witter, menno.witter@ntnu.no

Received 6 February 2008; Accepted 23 May 2008

Recommended by Roland S. G. Jones

The entorhinal cortex is commonly perceived as a major input and output structure of the hippocampal formation, entertaining the role of the nodal point of cortico-hippocampal circuits. Superficial layers receive convergent cortical information, which is relayed to structures in the hippocampus, and hippocampal output reaches deep layers of entorhinal cortex, that project back to the cortex. The finding of the grid cells in all layers and reports on interactions between deep and superficial layers indicate that this rather simplistic perception may be at fault. Therefore, an integrative approach on the entorhinal cortex, that takes into account recent additions to our knowledge database on entorhinal connectivity, is timely. We argue that layers in entorhinal cortex show different functional characteristics most likely not on the basis of strikingly different inputs or outputs, but much more likely on the basis of differences in intrinsic organization, combined with very specific sets of inputs. Here, we aim to summarize recent anatomical data supporting the notion that the traditional description of the entorhinal cortex as a layered input-output structure for the hippocampal formation does not give the deserved credit to what this structure might be contributing to the overall functions of cortico-hippocampal networks.

Copyright © 2008 Cathrin B. Canto et al. This is an open access article distributed under the Creative Commons Attribution License, which permits unrestricted use, distribution, and reproduction in any medium, provided the original work is properly cited.

1. INTRODUCTION

The entorhinal cortex (Brodman area 28) derives its name from the fact that it is partially enclosed by the rhinal (olfactory) sulcus. This feature is particularly striking in nonprimate mammalian species, but also in primates at least the anterior part of the entorhinal cortex is bordered laterally by a rhinal sulcus. Interest in the entorhinal cortex arose around the turn of the 20th century when Ramon y Cajal, in his seminal studies on the anatomy of the nervous system, described a peculiar part of the posterior temporal cortex which is strongly connected to the hippocampus with fibers that merge in the angular bundle and perforate the subiculum. Cajal was so struck by this massive connection that he suggested that the physiological significance of the hippocampus had to be related to that of the entorhinal cortex. At that time, he assumed that the entorhinal cortex was part of the olfactory cortex and so was, therefore, the hippocampus. He even stated that if this part of the posterior temporal cortex, which he called the sphenoidal cortex/angular ganglion, would be visual, so would be the hippocampus [1]. How right he was, in more than one way. Today we conceive the entorhinal cortex as the nodal point between the hippocampal formation on the one hand and a variety of multimodal association areas of the cortex such as parietal, temporal, and prefrontal cortex on the other hand. So, multimodal sensory and highly processed unimodal inputs converge at the level of the entorhinal cortex. This input in turn is conveyed to the hippocampal formation. We also know that the entorhinal cortex harbors different subdivisions, which specifically mediate the connectivity with functionally different sets of cortical and subcortical areas in the brain. This has led to the now quite widely accepted concept of parallel input/output channels as originally proposed by us and others [2–5]. Recent electrophysiological recordings in lateral and medial

entorhinal cortices of the rat have further elaborated on this point in showing that cells in the medial subdivision are spatially modulated, whereas in the lateral entorhinal cortex such modulation is largely absent [6–9]. Cells in the lateral entorhinal cortex most likely convey olfactory [5, 10, 11] and somatosensory information [12–15].

Our current insights into the functional relevance of the hippocampal formation, and how its anatomy is related to function, are much more detailed than what we know about the entorhinal cortex. It therefore seems attractive to turn the argument of Cajal around by stating that in view of the findings that the hippocampus is crucially involved in conscious, declarative memory processes so should be the entorhinal cortex. This conjecture is apparently supported by available functional studies. Although the specific functional contributions of the entorhinal cortex to memory remain to be established, they are most likely different from, but complementary to, those of the hippocampus [5, 16, 17]. The finding of the grid cells in medial entorhinal cortex, as well as head direction and conjunctive cells, and the notion that converging inputs of a limited number of grid cells onto a single CA1 neuron are sufficient to result in the well-established place cell properties [17–19] kindled a renewed interest in the anatomical organization of the entorhinal cortex [20]. A review of the anatomical organization, as part of a special issue on entorhinal cortex, is therefore appropriate. We aim to provide a comprehensive description of the entorhinal cortex, with particular emphasis on the intrinsic organization, based on data from studies in the rat, extensively referring to, rather than repeating, previously published accounts.

2. DEFINITION OF THE ENTORHINAL CORTEX, SUBDIVISIONS, AND OVERALL ARCHITECTURE

A cortical area can be defined in many different ways, using a variety of different criteria, such as location, connectivity, cyto- and chemoarchitectonics. For the entorhinal cortex, all these approaches have been applied, resulting in a confusing variety of borders, subdivisions, and description of layers. A good lead, since it has withstood over a century of arguments, is the definition of the entorhinal cortex on the basis of its connectivity with the hippocampus as originally suggested by Cajal [1]. In view of increasing insights into the connectivity of the hippocampal formation and its subdivisions, quite a few authors have chosen to take projections to the dentate gyrus as a good defining criterion, in particular in combination with certain cytoarchitectonic features. In this paper, such a combined definition will be used and described below.

The entorhinal cortex is surrounded by a number of cortical areas. Anteriorly, it meets with olfactory and amygdaloid cortices, such as the piriform (olfactory) cortex laterally, and medially it is bordered by the periamygdaloid cortex and the posterior cortical nucleus of the amygdala. On its medial side, the entorhinal cortex merges with structures that belong either to the hippocampal formation or the parahippocampal region, such as the amygdalo-hippocampal transition, and the parasubiculum. The lateral and posterior borders are with the other two major constituents of the parahippocampal region, the perirhinal cortex laterally and the parahippocampal cortex (in nonprimate species generally referred to as postrhinal cortex) posteriorly. The lateral and posterior borders are quite easy to establish on the basis of a variety of cytoarchitectonic and chemoarchitectonic features. The most prominent features are that the fairly large-sized cells of layer II in the entorhinal cortex are replaced by much smaller neurons in the perirhinal and postrhinal cortices, the lamina dissecans disappears, and these changes coincide with similarly striking changes in the density of parvalbumin-positive neuropil, high in entorhinal cortex, virtually absent in perirhinal and parahippocampal areas. The mirror-image pattern appears when staining for heavy metals (Timm stain) or the calcium binding protein calbindin. All additional criteria that have been described seem to coincide with these borders. The anterior and medial borders, in contrast, are somewhat harder to establish. They apparently coincide with a rather striking change in the ease with which layers II and III can be differentiated from each other as well as with a loss of differentiation between the deep layers (medial border) or even complete disappearance of the deep layers (anterior border). Combined with subtle changes in chemoarchitectonic features and connectional differences, an overall consensus has now been reached (for further details see [21–25]).

Attempts to subdivide the entorhinal cortex have, likewise, been numerous (see [26], for a detailed review cf. [27]). Whereas Cajal, similar to Lorente de Nó did not see much merit to subdivide the entorhinal cortex based on cytoarchitectonic criteria [28, 29], it was Brodmann [30] who parcelled the entorhinal cortex field 28 into two fields: a lateral area 28a, and a medial area 28b on the basis of cytoarchitectonic criteria. Lorente de Nó [29] instead argued that the projections to the hippocampal formation support to distinguish between lateral, intermediate, and medial entorhinal subdivisions. The use of these two fundamentally different approaches, connectivity versus architecture, has continued till today, although a merged approach is now becoming accepted. Cytoarchitectonic parcellation schemes are useful tools to describe experimental data about connectivity and data on for example the distribution of receptors [2, 22, 31–33]; they help to navigate through data. Connectionally based subdivision-schemes may better serve our understanding of the possible functional contributions [34]. In view of the strong implications of the human entorhinal cortex in a variety of brain diseases (see, e.g., [35, 36]), the development of animal models for such diseases depends strongly on our capabilities to extrapolate the definition of the entorhinal cortex from rodents to nonhuman and human primates. With this aim in mind, combinations of the different approaches may lead to the most detailed and reliable subdivision.

A good start to subdivide the entorhinal cortex is to use the entorhinal-to-dentate projection, which has been documented in extensive detail in a variety of species. On the basis of the terminal distribution of this projection in the rat and the mouse, it seems plausible to divide the entorhinal cortex into two subareas, generally referred to as

the lateral and medial entorhinal cortices (LEC and MEC, resp.). These areas roughly correspond to the description of Brodmann's areas 28a and b, respectively [25, 30, 37, 38]. In the monkey [39], the terminal distribution of the entorhinal-to-dentate projection does not provide such a clear criterion to functionally subdivide the entorhinal cortex. However, a second connection, which has been proposed to functionally subdivide the entorhinal cortex, is the input of the presubiculum. In all nonprimate mammalian species studied so far, including rat, guinea pig, and cat, the innervation of the entorhinal cortex by presubicular fibers is restricted to a more caudal and dorsal portion, that coincides with a cyto- and chemoarchitectonically well-defined area, now called MEC [40–44]. Also in the monkey, inputs from the presubiculum distribute to only a restricted posterior portion of the entorhinal cortex ([45, 46]; Witter and Amaral, unpublished observations), which may thus represent the homologue of MEC as defined in nonprimates.

A note of caution should be added here: the choice for the terms lateral and medial entorhinal cortex is not simply related to a particular anatomical position of these areas in relation to the hippocampal formation and the rhinal fissure. In general, the lateral area occupies a more rostrolateral position versus a more caudomedial position for the medial area (see Figure 1(a)).

The lamination of the entorhinal cortex generally is considered the prototype of the transition between the three-layered allocortex and the six-layered neocortex [26]. The superficial plexiform or molecular layer (layer I) is relatively free of neurons and, in general, contains a dense band of transversely oriented fibers. The outermost cell layer (layer II) varies considerably in appearance among the rostro-to-caudal and lateral-to-medial extent, but mainly contains so-called "stellate" or "modified pyramidal cells." Overall, cells in layer II are fairly large, making them distinctly different from layer II cells in the adjacent cortical regions with the exception of the parasubiculum. In the latter area, neurons of layer II are as large as or somewhat larger than those of the entorhinal cortex, but entorhinal cells stain darker with a Nissl stain. Layer III is a wide layer of loosely arranged, large to medium sized cells that are predominantly of the pyramidal type. The deep border of layer III is the cell-sparse fiber layer called the lamina dissecans (sometimes referred to as layer IV). The lamina dissecans is better developed in the medial entorhinal cortex although species differences are apparent. The next cell layer (layer V) is clearly stratified and sometimes subdivided into a superficial layer of large to medium-sized, darkly stained pyramidal cells, which is sometimes referred to as layer Va. Note that in some lamination schemes, more particularly so in primates, this layer is referred to as layer IV thus resulting in some confusion when compared to the present scheme where the lamina dissecans is referred to layer IV. Subsequent deeper portions of layer V (layer Vb/Vc) have an overall stratified appearance and mainly consist of rather small pyramidal cells with a moderately dense packing. In the deepest cell layer VI, which is delineated by the white matter, multiple layers can be distinguished, more in particular in primates. However, since the appearance of layer VI is highly variable at different lateromedial and rostrocaudal levels, generally no further differentiation between sublayers is made.

3. EXTRINSIC CONNECTIVITY

3.1. Entorhinal hippocampal connectivity

Entorhinal connections with the hippocampal formation in the rat have been comprehensively described and reviewed in a number of recently published papers and reviews to which the reader is referred for further details [2, 47–52]. To summarize, all regions of the entorhinal cortex project to all parts of the hippocampal formation, the dentate gyrus, fields CA3, CA2, CA1, and the subiculum. Overall, entorhinal fibers synapse most often onto the dendrites of principal cells, that is, on spines, where they form asymmetrical, excitatory synapses. Entorhinal fibers also terminate on inhibitory interneurons, forming both putative excitatory as well as inhibitory synapses with the dendrites of these interneurons [38, 47, 52–54]. In the dentate gyrus, entorhinal axons distribute largely to the outer two-thirds of the molecular layer, although differences between species may exist with respect to the precise terminal distribution in relation to the origin of these projections in either LEC or MEC [38, 55]. The projections to the dentate gyrus arise largely from neurons in layer II. However, projections that arise from the deep layers have been systematically observed, and it is likely that these deep originating fibers show a differential terminal distribution, largely innervating the inner molecular layer of the dentate gyrus ([56]; see also [38]). The same cells in layer II also form the main origin of the projection that distributes to the outer portions of stratum lacunosum-moleculare of CA3 and CA2 [38, 49]. In all species studied, the projections to CA1 and the subiculum originate from cells in layer III of both LEC and MEC. The terminations of the latter projections exhibit a transverse topography. The rostral entorhinal cortex in the monkey and LEC in the rat project to the region around the border between CA1 and subiculum (distal CA1, *furthest away from the dentate gyrus*, and proximal subiculum, *closest to the dentate gyrus*) whereas caudal entorhinal cortex in the monkey and MEC in the rat project to proximal CA1 (*close to the dentate gyrus*) and distal subiculum (*far from the dentate gyrus*) [55, 57, 58].

The CA1-subicular projections are topographically organized along the transverse or proximodistal axis as well, such that parts of CA1 and subiculum that receive comparable inputs that are either from LEC or MEC are connected to each other [59–61]. Finally, the projections from CA1 and subiculum back to deep layers of LEC or MEC grossly reciprocate the forward projections [51, 62, 63] (see Figures 1(a), 1(b)). These data thus indicate that the entorhinal-CA1-subiculum circuitry exhibits a high degree of fidelity, which suggests that this circuitry may permit a highly ordered processing of information. The functional relevance of this strikingly precise organization needs yet to be established. In this respect, it is of interest that the CA1 and entorhinal projections targeting the same population of subicular neurons do not seem to have a high incidence

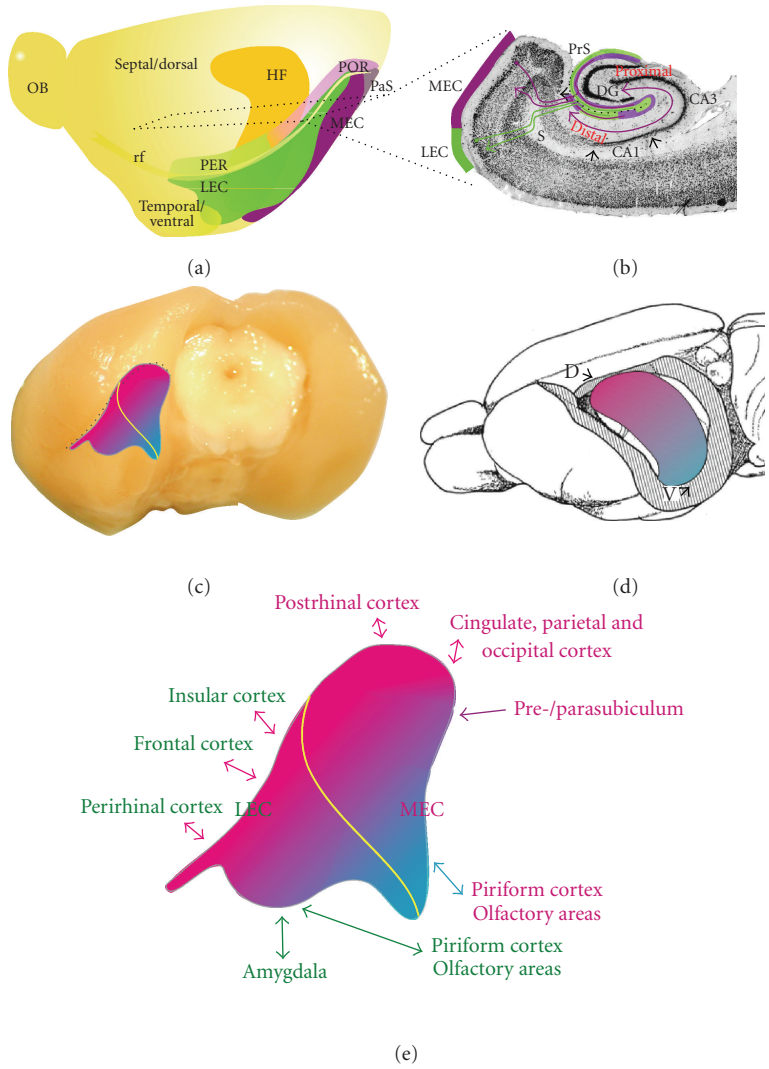

Figure 1: Schematic representation of the overall organization of the entorhinal cortex and its connectivity. (a) Position of the entorhinal cortex and surrounding cortices and hippocampus in the rat left hemisphere. Indicated are the dorsoventral extent of the hippocampus, positions of LEC and MEC, and the approximate position of a representative horizontal section, illustrated in (b). (b) Horizontal section illustrating entorhinal-hippocampal connectivity (see text for more details). (c) and (d) Representation of the topographical arrangement of entorhinal-hippocampal reciprocal connections. A dorsolateral band of entorhinal cortex (magenta) is preferentially connected to the dorsal hippocampus. Increasingly, more ventral and medial bands of entorhinal cortex (purple to blue) are connected to increasingly more ventral levels of the hippocampus. Yellow line in (c) indicates the border between LEC and MEC. (e) Enlarged entorhinal cortex, taken from (c), indicating the main connectivity of different portions of entorhinal cortex. Brain areas preferentially connected to LEC are printed in green, those connected to MEC are in magenta. The color of the arrows indicates preferential connectivity to the dorsolateral-toventromedial bands of entorhinal cortex (magenta or blue, resp.) or that no preferential gradient is present (green).

of convergence [64]. In contrast, in CA1, inputs from CA3 and entorhinal cortex do converge on pyramidal cells as well as onto interneurons with a very high incidence [54]. A final point to make with respect to entorhinal-hippocampal connectivity has to do with the topographical organization along the long axis of the hippocampus. Although the orientation of the hippocampus in various species is quite different [2, 65] in all species the structure has an impressive length, measuring from about 7 mm in mice, through 9–11 mm in rats, up to 4.5–5 cm in humans. It has now been established that in all species studied, entorhinal-hippocampal connectivity is present as described above, the striking difference being that different portions along the long axis of the hippocampal formation are connected to different bands of the entorhinal cortex. These bands are differently distanced from the lateral and posterior borders of the entorhinal cortex with the adjacent perirhinal and postrhinal (rodent) or parahippocampal (primates) cortices (see Figures 1(c), 1(d)). In the rat, this longitudinal topography has been shown to be closely related to the spatial properties of neurons in both structures. Neurons in the dorsal hippocampus and the related dorsal portions

of entorhinal cortex, more in particular of the medial entorhinal cortex, exhibit firing patterns that, although qualitatively as well as quantitatively very different, both represent fairly small areas of the environment. In contrast, cells that are more ventrally positioned in both hippocampus and entorhinal cortex show much larger spatially tuned firing fields [8, 9, 66]. Interestingly, the relationships in this respect between the dorsal to ventral axes both in the entorhinal cortex and the hippocampus are reflected in a comparable relationship with respect to the behavioral effects of selective lesions. Whereas lesions in the dorsal hippocampus and dorsal part of the entorhinal cortex have comparable detrimental effects on spatial learning and recall, ventral lesions do not. The latter have a profound effect in fear related behavior, which is in turn not effected by dorsal lesions [16, 67].

3.2. Entorhinal cortical connectivity

The most comprehensive systematic series of studies on entorhinal connectivity in the rat is from the Burwell lab [13–15, 68–71], with some added studies describing one or a few inputs or outputs in greater detail [22, 72]. All these studies are in line with earlier influential reports in the monkey that the perirhinal and parahippocampal cortices form the major cortical link for the entorhinal cortex [73, 74]. In general, the perirhinal cortex projects to rostrolateral parts of the entorhinal cortex, whereas the parahippocampal (primates) or postrhinal (nonprimates) cortex projects preferentially to caudodorsal portions of the entorhinal cortex [3, 68, 75]. In addition to the perirhinal/parahippocampal connections, the pre- and parasubiculum [23, 44] and olfactory-related structures provide prominent inputs to the entorhinal cortex and, in case of olfactory domains, receive a similarly strong output from the entorhinal cortex. As mentioned above, the spatial distribution of the input from the presubiculum is currently considered to be one of the defining features of MEC in different species. Though typically not as strong, additional cortical afferents and efferents of the entorhinal cortex are widespread. Cortical afferents are dominated by piriform input, but input also arises in frontal, cingular, retrosplenial, insular, parietal, and even visual areas. Similar to what was reported for the monkey, in the rat projections from the cingulate and retrosplenial cortices preferentially project to the more caudal portions of the lateral, intermediate, and medial bands of the entorhinal cortex [23, 72, 76–78]. Cortical efferents are widespread, largely reciprocating the cortical afferents. Note that species differences are apparent indicating that whereas in the rat cortico-entorhinal reciprocal connectivity is rather limited and confined to the areas close to the rhinal sulcus [22, 79], such connections in the monkey are more common and involve a more widespread domain of the entorhinal cortex [75, 80].

Although we will address the layered organization of the entorhinal cortex in more detail below, it is relevant to point out that entorhinal-cortical projections largely arise from deep layers, primarily from layer V pyramidal neurons. Possible exceptions are the entorhinal-infralimbic and entorhinal-olfactory projections, which appear to arise in layers II and III as well [22, 81]. Regarding entorhinal afferents, it is clear that most show a distribution largely confined to the superficial layers I–III with the exception of inputs from infralimbic, and prelimbic areas together with cingular and retrosplenial inputs that show a striking preference for deep layers of the entorhinal cortex [72].

3.3. Entorhinal subcortical connectivity

Studies conducted in multiple species indicate extensive subcortical connectivity for the entorhinal cortex. Although differences exist with respect to the detail of the information, it is safe to conclude that the entorhinal cortex has connections with the basal forebrain, claustrum, amygdala, basal ganglia, thalamus, hypothalamus, and brainstem (for review see [70]). The entorhinal cortex sends projections to the nucleus accumbens [82–85] and receives inputs from the ventral tegmental area [86]. The entire entorhinal cortex has strong reciprocal connections with the claustrum [32, 87–90]. Additional connections exist with basal forebrain structures, in particular the medial septal nucleus, the nucleus of the diagonal band, and the substantia innominata [32, 86, 91–93]. It is most likely that entorhinal projections to basal forebrain structures arise in layers II and V.

Entorhinal-amygdala connectivity has been studied in rather detail in both monkey and rat. For recent reviews, the reader is referred to McDonald [94], Pitkänen et al. [33]; see also Burwell and Witter [70]. Although all parts of the entorhinal cortex are connected with the amygdala, the rostral subfields are more strongly interconnected with the amygdala than the caudal subfields. Whereas in monkey the primary connections are with the lateral and accessory basal nuclei [95, 96], in rat the most prominent inputs arise from the lateral, basal, and accessory basal nuclei [97]. Amygdala input terminates primarily in layer III of the entorhinal cortex, and the return projection originates predominantly from cells in layer V.

The entorhinal cortex is connected with thalamic and hypothalamic structures. Major thalamic input arises in midline nuclei, particularly the reuniens, paratenial, and periventricular nuclei [31, 86, 98–100]. Additional but weaker inputs have been described from the anteromedial thalamic nucleus [101], and the ventromedial nucleus of the hypothalamus [102]. In the rat, it has been shown that the entorhinal cortex reciprocates the reuniens input [103]. In the monkey, additional projections have been reported to end in the magnocellular portion of dorsal medial nucleus, the medial pulvinar, and the dorsolateral nucleus [98, 104]. The entorhinal cortex also receives input from midbrain structures such as the dorsal raphe nucleus, the median raphe, and locus coeruleus [86, 105, 106]. Details about entorhinal innervations from these important modulatory regions of the brain are not available yet.

4. INTRINSIC ORGANIZATION OF THE ENTORHINAL CORTEX

Our understanding of the entorhinal cortex is still rather premature, and to a large extent, influenced by our current

functional concept for MEC. The generally accepted division of the entorhinal cortex into at least two functionally different domains stresses the need for an answer to the questions whether or not they differ with respect to their intrinsic wiring and neuronal makeup, in addition to their gross differences with respect to cortical and subcortical connectivity summarized above. The entorhinal network, *grosso modo*, encompasses three different (groups of) elements, elements receiving inputs, elements that provide output, and elements that contribute to the intrinsic architecture of the area. This subdivision into three functionally different elements and roles to be played by different neurons does not necessarily have an exclusive character; it is actually quite likely that all three elements might be an integral part of one and the same neuron; however, specializations may occur.

Compared to the details known for the hippocampal formation and some parts of the neocortex, such as the visual or barrel cortices in rodents, our understanding of the entorhinal cortex is rather in its infancy. The first detailed description of the morphology of entorhinal neurons, based on Golgi impregnated material, was published in 1933 by Lorente de Nó [29]. Over the years, this initial description has been extended, adding details and new cell types, based on a variety of different techniques. Here, we will summarize the main cell types that are currently known with a focus on their local connectivity and in particular addressing the question whether or not the lateral and medial subdivisions differ with respect to the overall main cell types. We will summarize (see Figure 2) data from previously published reviews [107] supplemented with some recently obtained, yet unpublished own data.

4.1. Cell types in entorhinal cortex

Layer I

In layer I throughout the entorhinal cortex, Lorente de Nó described two cell types; horizontal cells and short axis cylinder cells, nowadays known as multipolar neurons (MPNs). This latter category constitutes the majority of cells in layer I, and generally, they are non- or sparsely spiny. MPNs are quite often positive for calretinin (CR) and GABAergic, and two types have been described. Small CR positive MPNs are more often located just deep to layer Ia [108], whereas CR positive MPNs with a laterally extending dendritic tree are mainly located deep in layer I [108]. From the perikaryon of MPNs three to five short, curved smooth dendrites arise that branch after a short distance and radiate within layer I, sometimes extending into layer II [108, 109]. The diameter of the dendritic tree is around 100 μm in small or 150 μm in the other MPNs, respectively. Own recent data indicate that the axons of layer I neurons travel towards layer II and III [110] where they most likely provide feed-forward inhibition to principal cells [111, 112]. A minority of CR positive layer I neurons can be glutamatergic or contain calbindin D28K (CB) or neuropeptide-Y (NPY) [113].

Horizontal cells are located in the transitional zone between layers I and II [29, 114, 115] . They have a spherical to elongated soma of 13–15 μm. Almost spine-free dendrites extend laterally and spread horizontally within layer I and superficial layer II. The horizontal extent can be up to 700 μm (own unpublished data). The noncollateralizing axon travels towards the deep layers to the hippocampus [110, 114, 115]. Horizontal neurons are GABAergic, in LEC some are positive for vasoactive intestinal polypeptide (VIP), whereas in MEC, the dendritic terminals can stain positive for cholecystokinin (CCK) [115–117].

Layer II

Layer II is mainly made up of densely packed, large and medium sized pyramidal and stellate cells. The most abundant cell type throughout layer II in MEC is the stellate cell, with their preferred location within superficial and middle layer II [118]. The soma of these cells is quite variable but their spiny dendritic tree is their defining characteristic. The dendritic arbor comprises multiple, roughly equally sized primary dendrites that branch widely (average extend of 497 $\pm$ 154 μm) and may cover about one half of the mediolateral extend of the MEC [118–121]. After reaching the pial surface, the dendrites curve and run parallel to it. The basal dendritic extent is smaller (average of 231 $\pm$ 69 μm) [118]. The relative thick axon of stellate cells courses straight towards the angular bundle from a primary dendrite or the base of the soma [120]. Up to 400 μm away from the start, the axon gives off very thin collaterals, branching repeatedly and reaching the superficial layers, forming a net that colocalizes with the entire dendritic tree, sometimes extending beyond [118]. Besides, the axon sends occasional collaterals into deep layers III–VI. In the angular bundle, it gives off one to three collaterals that travel into the subiculum, continuing to their main targets in the dentate gyrus and CA3 [122]. Most stellate cells are excitatory presumably using glutamate as their main transmitter [123–126] and some also stain positively for CB [107].

Stellate cells are less common in LEC than in MEC. In LEC, stellate cells are most likely replaced by a comparable cell type, called fan cells [120, 127]. They have large polygonal somata with multiple thick sparsely spiny primary dendrites that fan out from the soma mostly in the horizontal and ascending direction. This dendritic morphology is thus comparable to that of stellate cells in MEC. The morphological difference is that fan cells only have small descending dendrites but there are also physiological differences. The axons descend and can be followed into the angular bundle, sometimes giving of very thin ascending collaterals within layers II and III [127].

Aside from the stellate-like principal neurons, layer II contains a number of pyramidal-like cells that have medium sized triangular or ovoid shaped soma with a perpendicular elongation with respect to the pial surface. Most are located in the deep portion of layer II [110, 128, 129]. The majority of these cells have a prominent spiny thick apical dendrite branching at, or superficial to the border with layer I. The basal dendrites of all pyramidal types are spiny, thin, short and straight, with extensive branches within the most superficial portion of layer III. The maximal mediolateral expanse of the upper and lower dendritic fields in MEC is

around 184 ± 75 μm and is therefore smaller than that of stellate cells. The smooth and thin axons of the pyramidal-like cells originate from the soma, some follow a sinusoidal route within layers II and III, giving off collaterals that distribute in layers I–III [129] with an extend that can be larger than that of the dendritic tree (own unpublished data, Alonso et al., 1993). The distribution of the collaterals is comparable to that of stellate cells, but less profuse [118, 128]. Subtypes of pyramidal-like cells have been described including neurons with an obliquely oriented soma and dendrites, called horizontal pyramidal neurons that are mainly located in the superficial part of layer II [122].

Another pyramidal cell type described in LEC has a very thick and sparsely or nonspiny apical dendrite, which branches in layer II. Thin apical dendritic tufts reach layer I. The apical dendrite is not as frequently tilted as in MEC pyramidal neurons [127]. The neurons have thin sparsely spiny basal dendrites and an axon that has extensive collaterals within layers I–III with many varicosities. The main axon of these cells cannot always be followed until the angular bundle but only up to layer III [127, 130].

Interneurons within layer II are described as MPNs, bipolar, basket, and chandelier cells. MPNs have polygonal, fusiform, or round cell bodies with multiple, sparsely spiny dendrites, extending in all directions, reaching layer I and deep into layer III. It has been described that the axons of MPNs travel to the white matter but also form local synapses within layer II [127, 131]. Morphologically they seem to be comparable to stellate cells within the MEC but there are electrophysiological differences. The family of MPNs contains VIP, substance-P, CCK, SOM, ENK, or GABA and in the LEC also NPY [117]. The short-axis cylinder cells in layer III described by Lorento de Nó are comparable to these MPNs [29].

Sparsely spiny horizontal bipolar cells although considered to be local/interneurons project to the hippocampus [115, 119, 131]. The soma is located in layer II at the border to layer I. The dendrites are oriented horizontally along the border between layers I and II [131]. Vertically orientated bipolar cells have a spindle shaped perikaryon continuing into one smooth thin ascending and one descending primary dendrite that branch into thinner dendrites more distally [108]. CR, VIP, and the corticotrophin releasing factor (CRF) have been found in subpopulations of bipolar cells. In the LEC also ENK, CCK and NPY might be present in this class of neurons [115, 117, 119, 131].

Fast spiking basket-like cells have small spherical cell bodies with sparsely spiny dendrites that often ramify into layer I. The extensive axonal arbor is mainly confined to layer II. They form basket-like complexes mainly around the soma of other cells, preferably forming symmetric, inhibitory synapses with stellate or pyramidal cells [117, 132]. Basket cells are known to contain GAD and maybe CCK. Throughout the EC, PV positive axons have been found that form symmetric synapses with principal neurons in layers II and III. These terminals have a basket-like axosomatic configuration. Therefore, it is suggested that basket cells in the whole EC contain PV [117, 132, 133].

Chandelier or axo-axonic cells are characterized by vertical aggregations of axonal boutons, called candles, which preferably are located superficial to the cell body. The somata of chandelier cells are medium sized with different shapes. The almost nonspiny, poorly ramifying dendrites originate from the basal and apical poles of the somata, displaying a bipolar or bitufted arbor that often stays within layer II/III. Vertical chandelier cells that are restricted to MEC issue a vertically oriented axonal tree that is around 200–300 μm wide and 300–450 μm high with the main axonal branch dividing into several collaterals that form the characteristic vertical aggregations within the upper portion of layer II/III [134]. Horizontally organized chandelier cells are located in the MEC and LEC, and their axonal plexi are smaller (250–350 μm wide and 100–200 μm high) than that of vertically oriented chandelier cells. Chandelier cells are GABAergic, often PV-positive and form symmetric contacts with initial axon segments of principal cells [135–138].

Layer III

MEC and LEC layer III pyramidal neurons have comparable morphological as well as electrophysiological characteristics [28, 29, 127]. According to some authors, in MEC an anatomical distinction can be made between spiny and nonspiny pyramidal cells [114]. In the LEC, only sparsely spinous pyramidal cells exist that belong to the spiny pyramidal group [127]. The somata of spiny pyramidal cells (SPCs), which are located throughout layer III, give rise to a prominent apical dendrite that bifurcates, become spiny afterwards, and branch extensively. The spiny basal dendrites spread further in the horizontal direction 389 ± 36 μm compared to the vertical direction 203 ± 31 μm, allowing for widespread local connectivity [139]. Apical and basal dendrites together lead to a mean vertical extent of 410 ± 23 μm and a horizontal extent of 312 ± 37 μm. The main axon projects via the angular bundle to the subiculum [139]. Some axonal collaterals spread within layers III and II but also in the lamina dissecans and layer V, occasionally with a broader horizontal extent than the dendritic tree [110, 139, 140].

Nonspiny pyramidal cells (NSPCs), also called type 2 cells [139], have triangular to spherically shaped somata of different sizes. The nonspiny apical dendrite that, compared to SPC, branches significantly closer to the soma also branches frequently in the superficial layers, finally reaching the pia [139, 141]. The vertical dendritic extent of these neurons is comparable to that of SPCs, whereas the horizontal extent, specifically of the basal dendrites, is less [139]. NSPCs thus have a more circular basal dendritic tree around the soma than SPC. The axons of NSPCs travel towards the angular bundle. Collaterals leave the main axon close to the soma and may remain within the corresponding cell layer and/or distribute over all other layers of the entorhinal cortex [139]. The collaterals, which travel towards the superficial layers, sometimes form a net over the entire own dendritic extent and occasionally extending over an even larger domain [110, 139].

Layer III also contains stellate cells, in particular in the upper part of the layer. The somata of these neurons are

elongated, polygonal, or spherical. Cells belonging to the latter subgroup sometimes have evenly distributed spiny dendrites around the somata, whereas others have one or two spiny basal dendrites and a variety of ascending dendrites that branch in layer I. The axons reach the white matter, and collaterals are formed in layer III and the lamina dissecans [114].

Also located within layer III are principal MPN somata. These MPNs are either small and spherical, with laterally extending dendrites, or they are large. The largest MPNs are located in the outer half of layer III of the LEC with a conspicuous spatial lateral separation (500 μm) between each cell body. The cell body of large MPNs is 15–18 μm in diameter with multiple sparsely spiny dendrites that elongate in all directions showing moderate branching. The thickest dendrites face towards the superficial layers whereas the thinner ones radiate laterally towards the deep layers. The axons of MPNs reach the hippocampus via the white matter with collaterals distributed in the vicinity of the parent cell soma [114].

Multipolar local circuit neurons, mainly described in MEC, are characterized by wide-ranging apical dendrites that reach the cortical surface, multiple compact basal dendrites, and a prominent axonal arborization. The axon reaches layers I to III but rarely extends into the lamina dissecans or superficial layer V [139]. At least subgroups of MPNs contain GABA, CCK, SOM, substance-P and very rarely SRIF, VIP or ENK [113, 116, 142]. Another subgroup of inhibitory MPNs has sparsely spiny dendrites that extend with their multipolar dendritic arbor towards deep layers instead of superficial layers. In addition, these neurons have an axon extending locally with some collaterals projecting to and reaching layer I [143].

Interneurons resembling pyramidal cells, the so-called pyramidal looking interneurons (PLIs) have also been described as Type 3-(Gloveli) or Type 1-(Kumar) cells [139, 143]. PLIs have a pyramidal shaped cell body and non-spiny basal and apical dendrites branch extensively, forming a dense local network in superficial layers with a circular appearance [139]. The apical dendrites often do not reach the pia and have a vertical dendritic extent of 347 ± 73 μm and a horizontal extend of 269 ± 98 μm. The basal dendrites extend horizontally comparable to that of the apical dendrites. PLIs have a dense axonal plexus in the local vicinity surrounding the cell body, and extending superficially into layer II [143].

Bipolar cells have been described in layer III of MEC and LEC. They have a spindle-like perikaryon with one ascending and one descending smooth, thin and sometimes long dendrite. The ascending dendritic collaterals traverse throughout layer II, reaching layer I. The extent of the descending dendrites has not been described yet. The axon arises from the primary descending dendrite and extends into layer III and the lamina dissecans, deep to the parent cell body [108]. At least a subpopulation of bipolar cells is known to contain VIP or CR. The latter are more common in LEC than in MEC [108, 109].

Lamina dissecans (layer IV)

Occasionally, pyramidal-shaped neurons are located in the lamina dissecans, at the borders to layers III and V. These neurons have the morphological and physiological properties of either layer III or layer V pyramidal neurons, respectively (own unpublished data).

Furthermore, bipolar cells, whose dendrites grow horizontally instead of vertically to the pial surface, with axonal collaterals that can travel towards superficial layer III and deep layers, have been found in the lamina dissecans (unpublished data). It has been shown that bipolar cells might contain VIP, CCK, and CRF [117].

Layer V

There is no difference between layer V principal neurons in LEC and MEC [144, 145]. The apical dendrites as well as axon collaterals often travel towards superficial layers, sometimes even reaching the pial surface. The basal dendritic tree spreads mainly within deep layers. The main axon travels towards the angular bundle and the subiculum [144, 145]. In general, layer V consists of large pyramidal cells located immediately below the lamina dissecans, while the deeper part of layer V contains smaller cells. The somata of larger pyramidal cells can have different forms. Usually pyramidal formed somata are observed but sometimes also star-shaped cell bodies can be seen. All large pyramidal cells have one distinct large and spiny apical dendrite that often branches close to the soma with the main dendrite reaching the pial surface after branching into a tuft in superficial layers II and I. In case of large pyramidal neurons, spines occur on the dendrites after the first or second bifurcation [120]. The basal dendrites are thinner compared to the apical dendrites and can extent profusely in all directions within layers V and VI [146]. Compared to large pyramidal cells, small neurons have more basal dendrites that are also more densely occupied with spines. These basal dendrites of these smaller cells also extent further in the deep layers. The main axon of the pyramidal cells travels towards the angular bundle, eventually reaching the dentate gyrus via the subiculum [146]. Collaterals of these axons also split within layer V, forming collaterals which travel toward the lamina dissecans, reaching the vicinity of the soma [144, 145]. Some collaterals also travel towards superficial layers [110]. Some pyramidal cells in entorhinal cortex layer V contain SOM [117].

A second principal cell type described in layer V is generally referred to as a type of horizontal cell [29, 120, 144, 145]. Somata of these cells are polygonal rather than pyramidal in shape. A distinct, sparsely spiny, apical dendrite extends to the pial surface, branching extensively in layer I up to the lamina dissecans. In MEC, in contrast to LEC, the primary apical dendrite is not thicker than the other dendrites but is spinier. The characteristic, slightly spiny basal dendritic plexus extents horizontally sometimes up to 1mm from the soma within layers V and VI. Axons of horizontal cells travel to the angular bundle, giving off branches into layers V and VI [110, 144, 145].

A third type of principal neurons is polymorphic MPNs [144–146]. The somata of these cells are spherical to slightly pyramidal with average diameters of 13–24 μm. Instead of having a prominent apical dendrite, these neurons have a multipolar spiny dendritic arborization that extents for long

distances in all directions some even into the subiculum ([144–146]; own unpublished data). The axon branches within layer V but reaches the angular bundle and travels through the subiculum, finally reaching the dentate gyrus [146]. Members of the family of MPNs can express PV, SOM, NPY, and substance-P [116, 117].

Fusiform cells that project to the hippocampus were found in superficial layer V [120]. They also have a single ascending dendritic tree that sometimes even reaches the pia and one descending dendritic tree. The axon spreads locally but the main axon projects towards the hippocampus. Fusiform neurons can contain CR [108, 120].

Superficial layer V further harbours bipolar cells with a spindle-like soma having an average diameter along the short axis of around 12 μm [108, 120]. Dendrites originate from the apical and basal poles of the spindle shaped cell body. Except close to the soma, the dendrites are spiny and extend from the soma to the subiculum in one direction and to layer I in the other direction, extensively branching in layers II and I [120]. However, most dendrites are found within the deep layers. The main axon travels towards deep layers and perforates the subiculum, reaching the dentate gyrus [146]. Globular cells have very spiny and highly branched dendrites, originating radially from the soma [120]. Somata have a size of 19.5 μm and up to 12 dendrites that branch within layers III–V. The axon projects towards the angular bundle and within the layer V ([120] own unpublished data). It has been described that multipolar but not explicitly globular cells in the deep layers of the entorhinal cortex might contain SOM, substance-P, NPY, and GABA [117].

Layer VI

The multilaminated layer VI borders the white matter. MPNs are located throughout layer VI. They have a spherical soma with a diameter of approximately 14 μm. The spiny dendrites have multiple swellings and extend mainly within layer VI, parallel to the layering. The dendrites also extend towards the angular bundle and rarely to layer III [120]. We found MPNs with basal dendrites with no apical dendrite that surround the soma facing all directions. The axons and collaterals reach the subiculum, whereas other collaterals sometimes reach the superficial layers (own unpublished data).

The somata of classical pyramidal cells in the MEC are medium sized. Pyramidal cells in the LEC have not been described yet. The difference compared to layer V or III pyramidal cells is that the dominant dendrite does not always travel radially towards superficial layers but also either horizontally within layers VI and V or descends towards the angular bundle and the subiculum (own unpublished data). The basal dendrites and the widely spreading collaterals spread within layers VI and V. The axons of pyramidal cells travel towards the angular bundle and subiculum as well as towards superficial layers. Their axon collaterals are located within layers V, VI, the angular bundle, and the subiculum [110].

In conclusion, there are differences between cell types and the distribution of cell types in LEC and MEC (see Figure 2). In layers I and II, the differences between cell morphology and electrophysiology in the LEC compared to the MEC are more prominent than in layers III and V. We know for example that different subtypes of layer I MPNs neurons show a different distribution within layer I. The same holds for chandelier and basket cells in layer II. In addition, there are major differences in the distribution of for example PV- and CR-positive neurons and neuropil. This suggests that LEC and MEC are different with respect to the types of interneurons present. Furthermore, layer II principal neurons in LEC and MEC do not only have a somewhat different morphology but differ also electrophysiologically. Taken together these findings might be an indication that the microcircuits within layers I and II in the LEC and MEC are different. Layer III and V principal neurons of both LEC and MEC are more comparable regarding morphology as well as the electrophysiological properties. Having said this, we need to be aware of the fact that our understanding of the different cell types in the entorhinal cortex and how they are wired together is still rather fragmentary.

4.2. Intrinsic organization

The entorhinal cortex contains a substantial system of associational connections that are best described at two different levels. The first is that in all species studied, intraentorhinal fibers are organized in a limited number (generally three) of rostrocaudally oriented bands. Connections that link different transverse (or mediolateral) regions of the entorhinal cortex, thus providing connectivity between these bands, are rather sparse [147–151]. The associational connections within these bands originate in both superficial and deep layers. Results of anatomical tracing experiments have provided convincing evidence that projections originating from layers II and III tend to terminate mainly in the superficial layers, whereas projections originating from deep layers terminate both in the deep and superficial layers. The finding of rather extensive superficial to superficial connectivity seems at odds with results suggesting that there is only sparse collateral innervation among layer II principal cells but see Kumar and Buckmaster [143], who showed layer II to layer II excitatory connectivity with an up to 500 μm distance, and inhibitory connectivity (see also Figure 2). Among layer III principal cells, collateral innervation is more common [152]. One naturally has to take the nature of these local connections into account, and the anatomical results [147–149] do not indicate whether we are dealing with excitatory connections among principal cells or connections of principal cells with putative inhibitory interneurons or even with excitatory local neurons [108]. For example, the pyramidal-like interneurons in layer III or the multipolar interneuron at the border between layers II and III (see Figure 2) is likely candidates to contribute to these intrinsic associative networks, but this remains to be established.

The overall organization of the longitudinal intrinsic connections is best considered in relation to the organization of the reciprocal entorhinal connections with the hippocampal formation. Interconnected portions of the LEC and MEC close to the rhinal fissure, in rats referred to as the dorsolateral band of entorhinal cortex, are connected to

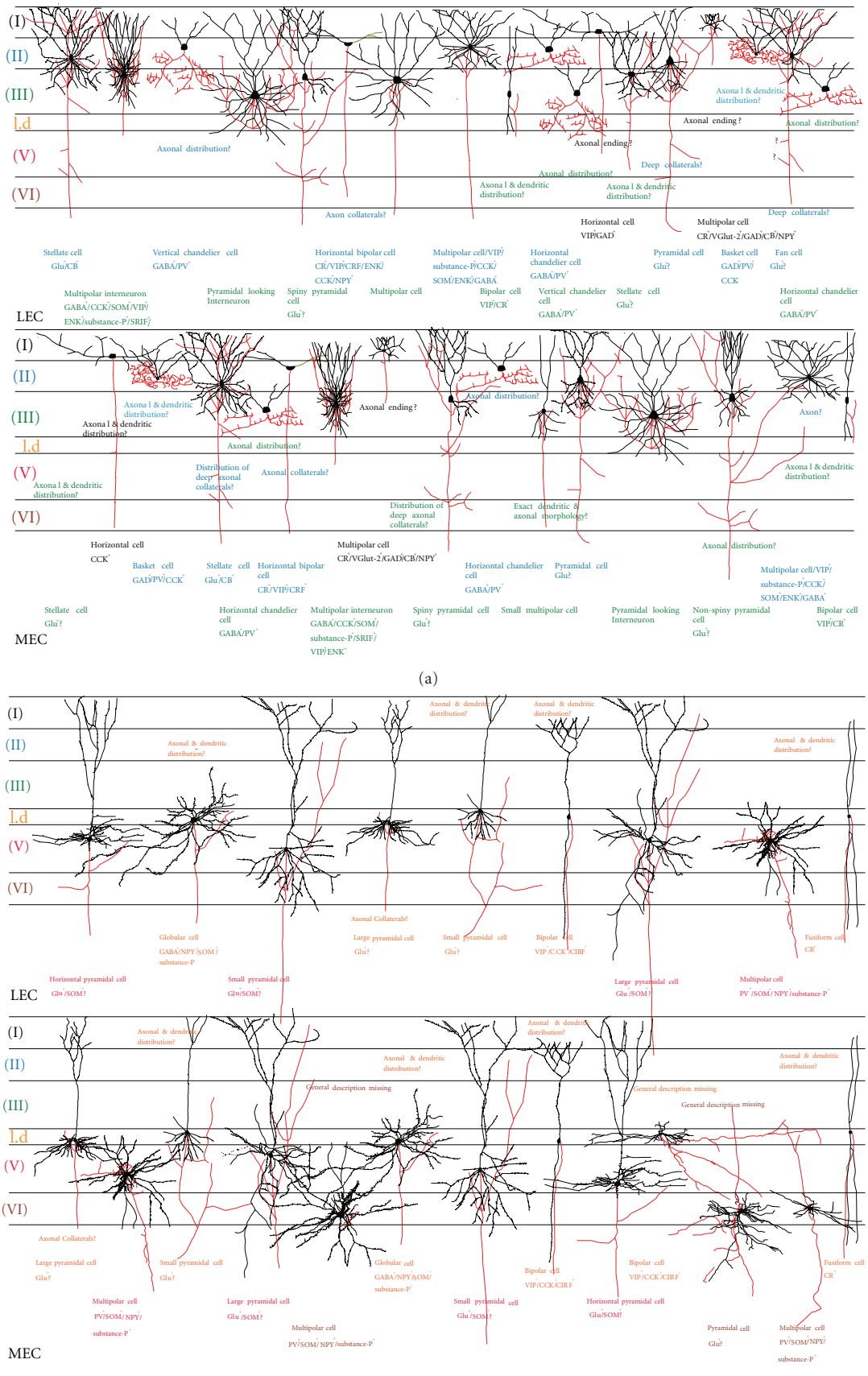

Figure 2: Summary diagram of the morphology of main cell types in LEC and MEC. (a) Cells in superficial layers I-III. (b) Cells in deep layers IV-VI. See text for more details.

the dorsal (nonprimate) or posterior (primate) part of the hippocampal formation (see Figures 1(c), 1(d)). Interconnected cells in the intermediate band, encompassing again parts of both LEC and MEC, connect to the intermediate hippocampal formation, whereas the most medially interconnected band of entorhinal cortex is mainly connected to the ventral (nonprimate) or anterior (primate) hippocampal formation. Cells located in each of these entorhinal bands thus give rise to associational connections to other cells in the same region, but not in any substantial way to portions of the entorhinal cortex that are connected with other levels of the hippocampal formation. Thus, the associational connections seem to be organized to integrate all of the information that targets a particular portion of the entorhinal cortex, and that portion of entorhinal cortex interacts selectively with a particular longitudinal level of the hippocampal formation [2, 147, 153, 154]. This implies that at the level of the entorhinal cortex integration across input modalities may occur and this is in line with reports that in the monkey entorhinal cortex, single neurons apparently respond to different types of sensory inputs [155]. It is still an open question whether these longitudinally organized associative intrinsic networks really support association between the two sets of inputs that reach MEC and LEC, respectively. It is also not known whether this network originates partially or completely from the same neurons that contribute to the more focal intrinsic connectivity that will be described subsequently.

The second organizational level deals with the local connectivity within and among layers of more restricted portions of the entorhinal cortex. As we know from the studies summarized above, neurons in different layers have very different inter- and intralaminar connectional patterns that include axon collaterals confined to the parent cell layer or spanning several layers. But not only the axonal distribution is of importance, the dendritic trees may also play an essential role in that they either span several layers or are more restricted to the parent cell layer. Although detailed information for quite a few of neuronal types in the entorhinal cortex is still lacking, it is safe to say that the entorhinal network, on the basis of its neuronal composition alone, cannot be properly described in terms of superficial and deep layers as more or less independent layers. All this may not come as a surprise since comparable concepts have been described with respect to the organization of the neocortex [156]. This second level of intrinsic organization has not yet been seriously incorporated into our working concept about entorhinal cortex. This is essential however in order to properly understand how inputs to the entorhinal cortex will be processed by the entorhinal network and what the eventual information is that will be conveyed to the hippocampal formation on the one hand and to other cortical and subcortical areas on the other hand. The following paragraphs will provide a description of recent most salient findings that may be related to this second level of the entorhinal intrinsic organization (see Figure 3).

One important anatomical observation already reported by Cajal [1, 28] is that neurons in the deep layers are connected to superficial layers by way of axonal projections

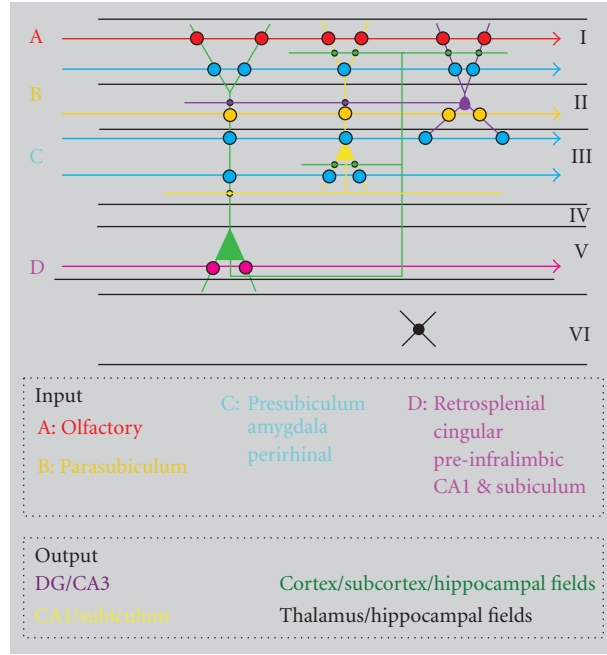

Figure 3: Schematic representation of laminar distribution and synaptic interactions between inputs and principle cells of the entorhinal cortex. Different inputs are represented by color-coded arrows; position of the arrows indicates the main laminar distribution. Circles indicate putative synaptic contacts between inputs and principle cells. Main output connectivity of principle cells is indicated as well. The figure emphasizes the integrative capacity of layer V cells.

([144, 145, 147–149, 157]; see also Figure 2: the small and large pyramidal cells in layer V of both LEC and MEC). These anatomical findings have been corroborated in a number of functional studies [158–162]. Recently, these connections have been studied in more detail in the rat with respect to projections from the subiculum, using both anatomical and electrophysiological techniques [50, 51, 157, 163]. The majority of the axons from deep to superficial layers are likely excitatory and target both interneurons as well as principal neurons in almost equal percentages [157]. This thus constitutes the substrate for powerful excitation as well as feedforward inhibition to neurons in the superficial layers. Stimulation of the subiculum in vivo, not only resulted in population activity in layers II and III of the entorhinal cortex, but subsequently activated the dentate gyrus and CA1 [50, 163]. Moreover, the transfer of activity from layer II to DG and from layer III to CA1 depended on the anesthetic used, suggesting that two functionally distinct parallel reentrant routes exist in the entorhinal-hippocampal system. Although it has not yet been established in freely moving animals whether these two parallel pathways function as separately controlled inputs to DG/CA3 on the one hand and CA1/subiculum on the other hand, the findings are of interest in relation to recently published ideas that DG, together with CA3, is preferentially involved in pattern separation whereas CA1 might be more relevant for pattern completion processes [164–167]. It should be mentioned

here that there is also convincing anatomical as well as electrophysiological evidence supporting the existence of connections between cells in layers III and II [114, 148, 149, 168–171] suggesting that they may function in concert as well.

As illustrated in Figure 2, all layers of both LEC and MEC, with the possible exception of layer VI where details are still lacking, contain neurons, mainly of the pyramidal type, with an apical dendrite that extends all the way up to layer I, quite often forming a dendritic tuft in layers II and I. This is a feature that is strikingly similar to what has been reported for the neocortex. Although the functional significance of this general pattern is still poorly understood, the commonality of it, even in evolutionary older parts of the cortex, must be an indication for its significance. In the neocortex, layer I is a main recipient of feedback projections and inputs from subcortical structures [156]. In contrast, in the entorhinal cortex, like in the hippocampus, layer I constitutes a major input layer; for example, the densest innervations from olfactory portions of the cortex, including the olfactory bulb, terminate in layer I [10, 111, 172, 173]. Likewise, in quite a few instances, inputs to the entorhinal cortex that densely terminate in layers II, III, or V have a component to the deep portion of layer I as well [2, 72]. In addition, the apical dendrites of entorhinal neurons not only receive synaptic inputs at their tufts in layer I, but in case of neurons in layer V of MEC, we have shown that they are among the postsynaptic targets of projections from the presubiculum [174]. Note that presubicular inputs to MEC, like those from the perirhinal cortex and some nuclei of the amygdaloid complex, densely terminate in layers III and deep I, almost avoiding layers II and V. Presubicular fibers contact neurons in layer III, and do so with a high density [175, 176]. Recent electrophysiological in vitro and in vivo data have corroborated that presubicular fibers synapse onto neurons in layers III and V, but also onto neurons in layer II [170, 171]. No data are available with respect to perirhinal and amygdale inputs to LEC, that show a similar laminar distribution, but in view of the overall similarity of the networks and cell types in both entorhinal areas, it is likely that for example inputs from perirhinal cortex and amygdale target neurons in layers II, III, and V. Data on inputs that specifically distribute to layer II of MEC, and to a lesser extent of LEC, such as fibers that originate in the parasubiculum, are not available. The potential for functionally relevant interaction between neurons in the deep layers of the entorhinal cortex and superficially terminating inputs has yet another dimension. It has been argued that hippocampal output that leads to firing of cells in layer V of the entorhinal cortex may result in back propagation into the superficial layers, along the dendrites of layer V cells. Back propagation has been documented in the neocortex and in CA1 and may occur in the entorhinal cortex as well. Back-propagating action potentials may increase the influence exerted by inputs to distal portions of the dendrite [163]. This combination of distally terminating inputs from local axon collaterals in layers II and III and back propagation along dendrites of layer V cells provides the most likely substrate for observations that activation of superficial entorhinal layers may lead to subsequent activation of deep layers of entorhinal cortex [158, 159]. Although axons of layers II and III occasionally send a collateral into deep layers of entorhinal cortex ([127]; own observations, illustrated in Figure 2), the overall direct connectivity from superficial to deep layers is rather sparse and therefore may not be sufficient to mediate this rather strong superficial to deep activation.

What then is the functional relevance of inputs from for example the medial prefrontal, cingular, and retrosplenial areas? Afferents from these areas preferentially, and in some instances even exclusively, terminate in the deep layers of the entorhinal cortex. Note that in the monkey, however, it has recently been reported that projections from the retrosplenial cortex densely innervate entorhinal layer I [78]. Do inputs to the deep layers of the entorhinal cortex modulate the transfer of hippocampal output to the cortex, interact with the integrative capacities of the entorhinal network, or both? These questions are relevant not only for our understanding of the functional relevance of the entorhinal cortex in relation to functions of the hippocampus but also since these cortical areas form part of the default mode network, implicated in higher-order cognitive functions [177–179].

5. PERSPECTIVES

The functional relevance of the organization of networks in the brain is often interpreted on the basis of a surprisingly restricted point of view. Debates on the functional organization of the hippocampal formation have been strongly influenced by the idea that the prevailing hippocampal circuitry is unidirectional. With regards to the entorhinal cortex, the breakthrough discovery, that deep entorhinal layers receive hippocampal output from CA1 and the subiculum on the one hand, and that these same layers are the origin of strong cortical projections, has biased our view towards the rather simple concept that the deep layers mediate hippocampal-to-cortical connectivity, similar to superficial layers providing the way in for cortical inputs to the hippocampal formation. If the entorhinal cortex is such an important hub, similar to the central station of a large city, and that is what all data seem to converge on, it is quite likely that it serves yet another role. In addition to serving simply to get into the city or leave the city, the station also provides the powerful potential for new interactions between and among incoming and outgoing people. This potential for "new" interactions has been grossly neglected in case of the entorhinal cortex. The potential of the entorhinal cortex to act as an interactive hub, contributing essentially to the functions of the cortico-hippocampal system instead of just transferring information, has been underscored not only by the recent finding of the unique spatial firing properties of grid cells in the entorhinal cortex [7–9], but also by reports that the spatial firing properties of CA1 cells likely depend on inputs from the entorhinal cortex [17–19]. More in particular, the findings that spatially tuned neurons are present in all layers of MEC, and that a clear relationship is apparent between closely associated portions of MEC across layers underscore the concept of the entorhinal cortex as an important higher-order association cortex where understanding the interactions between the

layers will provide us the key into its functional relevance [7, 20].

Similar to the yet unresolved mystery of the relevance of cortical inputs to deep layers of the entorhinal cortex, it remains to be established what the functional relevance is of LEC. The data summarized above indicate that with the exception of neurons in layer II, it is likely that both LEC and MEC are largely similar with respect to their intrinsic wiring, both in terms of neuronal elements that comprise the nodal points of the network as well as with respect to how these are wired together (see Figures 2, 3, [20]). What then accounts for the strikingly different features of LEC and MEC when spatially modulated neuronal firing is concerned? Most likely, differences in input and output characteristics will set the scene as eloquently summarized recently [5]. However, how convincing this may look, it may not be the complete story. Additional differences in modulatory connectivity from not only the septal complex, but also from the raphe nuclei, the ventral tegmental area, and locus coeruleus may turn out to be most relevant. Unfortunately, with the partial exception of inputs from the medial septum, very little detailed information is available regarding these inputs in terms of their overall distribution and topography in relation to both extrinsic and intrinsic wiring of the entorhinal cortex. Furthermore, detailed information of the postsynaptic targets of these modulatory inputs is largely missing. One final approach to further our understanding of the entorhinal cortex may be to make use of the striking involvement of the entorhinal cortex in an impressive list of brain diseases [35] and to focus on alterations in the circuitry that likely occur during development, ageing, and disease and their effect on entorhinal functioning.

ACKNOWLEDGMENTS

The preparation of this paper and the original research on entorhinal neurons are supported by the Kavli Foundation and a Centre of Excellence grant from the Norwegian Research Council. Cathrin B. Canto thanks the Department of Anatomy and Neurosciences, VU University medical center for the generous hospitality and warm atmosphere.

REFERENCES

[1] S. R. Y. Cajal, "Sobre un ganglio especial de la corteza esfeno-occipital," *Trabajos del Laboratorio de Investigaciones Biológicas de la Universidad de Madrid*, vol. 1, pp. 189–206, 1902.

[2] M. P. Witter, H. J. Groenewegen, F. H. Lopes da Silva, and A. H. Lohman, "Functional organization of the extrinsic and intrinsic circuitry of the parahippocampal region," *Progress in Neurobiology*, vol. 33, no. 3, pp. 161–253, 1989.

[3] P. A. Naber, M. Caballero-Bleda, B. Jorritsma-Byham, and M. P. Witter, "Parallel input to the hippocampal memory system through peri- and postrhinal cortices," *NeuroReport*, vol. 8, no. 11, pp. 2617–2621, 1997.

[4] M. P. Witter, F. G. Wouterlood, P. A. Naber, and T. van Haeften, "Anatomical organization of the parahippocampal-hippocampal network," *Annals of the New York Academy of Sciences*, vol. 911, no. 1, pp. 1–24, 2000.

[5] H. Eichenbaum, A. P. Yonelinas, and C. Ranganath, "The medial temporal lobe and recognition memory," *Annual Review of Neuroscience*, vol. 30, pp. 123–152, 2007.

[6] E. L. Hargreaves, G. Rao, I. Lee, and J. J. Knierim, "Major dissociation between medial and lateral entorhinal input to dorsal hippocampus," *Science*, vol. 308, no. 5729, pp. 1792–1794, 2005.

[7] F. Sargolini, M. Fyhn, T. Hafting, et al., "Conjunctive representation of position, direction, and velocity in entorhinal cortex," *Science*, vol. 312, no. 5774, pp. 758–762, 2006.

[8] M. Fyhn, S. Molden, M. P. Witter, E. I. Moser, and M.-B. Moser, "Spatial representation in the entorhinal cortex," *Science*, vol. 305, no. 5688, pp. 1258–1264, 2004.

[9] T. Hafting, M. Fyhn, S. Molden, M.-B. Moser, and E. I. Moser, "Microstructure of a spatial map in the entorhinal cortex," *Nature*, vol. 436, no. 7052, pp. 801–806, 2005.

[10] A. M. M. C. Habets, F. H. Lopes da Silva, and F. W. de Quartel, "Autoradiography of the olfactory-hippocampal pathway in the cat with special reference to the perforant path," *Experimental Brain Research*, vol. 38, no. 3, pp. 257–265, 1980.

[11] A. M. M. C. Habets, F. H. Lopes da Silva, and W. J. Mollevanger, "An olfactory input to the hippocampus of the cat: field potential analysis," *Brain Research*, vol. 182, no. 1, pp. 47–64, 1980.

[12] P. A. Naber, M. P. Witter, and F. H. Lopes da Silva, "Differential distribution of barrel or visual cortex. Evoked responses along the rostro-caudal axis of the peri- and postrhinal cortices," *Brain Research*, vol. 877, no. 2, pp. 298–305, 2000.

[13] R. D. Burwell, "The parahippocampal region: corticocortical connectivity," *Annals of the New York Academy of Sciences*, vol. 911, pp. 25–42, 2000.

[14] R. D. Burwell and D. G. Amaral, "Cortical afferents of the perirhinal, postrhinal, and entorhinal cortices of the rat," *The Journal of Comparative Neurology*, vol. 398, no. 2, pp. 179–205, 1998.

[15] K. M. Kerr, K. L. Agster, S. C. Furtak, and R. D. Burwell, "Functional neuroanatomy of the parahippocampal region: the lateral and medial entorhinal areas," *Hippocampus*, vol. 17, no. 9, pp. 697–708, 2007.

[16] H.-A. Steffenach, M. P. Witter, M.-B. Moser, and E. I. Moser, "Spatial memory in the rat requires the dorsolateral band of the entorhinal cortex," *Neuron*, vol. 45, no. 2, pp. 301–313, 2005.

[17] V. H. Brun, S. Leutgeb, H.-Q. Wu, et al., "Impaired spatial representation in CA1 after lesion of direct input from entorhinal cortex," *Neuron*, vol. 57, no. 2, pp. 290–302, 2008.

[18] V. H. Brun, M. K. Otnæss, S. Molden, et al., "Place cells and place recognition maintained by direct entorhinal-hippocampal circuitry," *Science*, vol. 296, no. 5576, pp. 2243–2246, 2002.

[19] T. Solstad, E. I. Moser, and G. T. Einevoll, "From grid cells to place cells: a mathematical model," *Hippocampus*, vol. 16, no. 12, pp. 1026–1031, 2006.

[20] M. P. Witter and E. I. Moser, "Spatial representation and the architecture of the entorhinal cortex," *Trends in Neurosciences*, vol. 29, no. 12, pp. 671–678, 2006.

[21] R. Insausti, T. Tunon, T. Sobreviela, A. M. Insausti, and L. M. Gonzalo, "The human entorhinal cortex: a cytoarchitectonic analysis," *The Journal of Comparative Neurology*, vol. 355, no. 2, pp. 171–198, 1995.

[22] R. Insausti, M. T. Herrero, and M. P. Witter, "Entorhinal cortex of the rat: cytoarchitectonic subdivisions and the

origin and distribution of cortical efferents," *Hippocampus*, vol. 7, no. 2, pp. 146–183, 1997.

[23] M. P. Witter and D. G. Amaral, "Hippocampal formation," in *The Rat Nervous System. 3*, G. Paxinos, Ed., chapter 21, pp. 635–704, Academic Press, San Diego, Calif, USA, 3rd edition, 2004.

[24] R. D. Burwell, M. P. Witter, and D. G. Amaral, "Perirhinal and postrhinal cortices of the rat: a review of the neuroanatomical literature and comparison with findings from the monkey brain," *Hippocampus*, vol. 5, no. 5, pp. 390–408, 1995.

[25] T. van Groen, P. Miettinen, and I. Kadish, "The entorhinal cortex of the mouse: organization of the projection to the hippocampal formation," *Hippocampus*, vol. 13, no. 1, pp. 133–149, 2003.

[26] H. Stephan, "Allocortex," in *Handbuch der Mikroskopischen Anatomie des Menschen*, W. Bargmann, Ed., pp. 1–998, Springer, Berlin, Germany, 1975.

[27] D. G. Amaral, R. Insausti, and W. M. Cowan, "The entorhinal cortex of the monkey. I. Cytoarchitectonic organization," *The Journal of Comparative Neurology*, vol. 264, no. 3, pp. 326–355, 1987.

[28] S. R. Y. Cajal, *Histologie du Système Nerveux de l'Homme et des Vertébrés*, Maloine, Paris, France, 1911.

[29] R. Lorente de Nó, "Studies on the structure of the cerebral cortex," *Journal für Psychologie und Neurologie*, vol. 45, no. 6, pp. 381–438, 1933.

[30] K. Brodmann, *Vergleichende Lokalisationslehre der Grosshirnrinde in ihren Prinzipien dargestellt auf Grund des Zellenbaues*, Barth, Leipzig, Germany, 1909.

[31] R. Insausti, D. G. Amaral, and W. M. Cowan, "The entorhinal cortex of the monkey. II. Cortical afferents," *The Journal of Comparative Neurology*, vol. 264, no. 3, pp. 356–395, 1987.

[32] R. Insausti, D. G. Amaral, and W. M. Cowan, "The entorhinal cortex of the monkey. III. Subcortical afferents," *The Journal of Comparative Neurology*, vol. 264, no. 3, pp. 396–408, 1987.

[33] A. Pitkänen, M. Pikkarainen, N. Nurminen, and A. Ylinen, "Reciprocal connections between the amygdala and the hippocampal formation, perirhinal cortex, and postrhinal cortex in rat," *Annals of the New York Academy of Sciences*, vol. 911, pp. 369–391, 2000.

[34] M. P. Witter, P. A. Naber, T. van Haeften, et al., "Cortico-hippocampal communication by way of parallel parahippocampal-subicular pathways," *Hippocampus*, vol. 10, no. 4, pp. 398–410, 2000.

[35] H. Braak and E. Braak, "The human entorhinal cortex: normal morphology and lamina-specific pathology in various diseases," *Neuroscience Research*, vol. 15, no. 1-2, pp. 6–31, 1992.

[36] L. deToledo-Morrell, T. R. Stoub, M. Bulgakova, et al., "MRI-derived entorhinal volume is a good predictor of conversion from MCI to AD," *Neurobiology of Aging*, vol. 25, no. 9, pp. 1197–1203, 2004.

[37] O. Steward, "Topographic organization of the projections from the entorhinal area to the hippocampal formation of the rat," *The Journal of Comparative Neurology*, vol. 167, no. 3, pp. 285–314, 1976.

[38] M. P. Witter, "The perforant path: projections from the entorhinal cortex to the dentate gyrus," *Progress in Brain Research*, vol. 163, pp. 43–61, 2007.

[39] M. P. Witter, G. W. van Hoesen, and D. G. Amaral, "Topographical organization of the entorhinal projection to the dentate gyrus of the monkey," *The Journal of Neuroscience*, vol. 9, no. 1, pp. 216–228, 1989.

[40] M. T. Shipley, "Presubiculum afferents to the entorhinal area and the Papez circuit," *Brain Research*, vol. 67, no. 1, pp. 162–168, 1974.

[41] M. T. Shipley, "The topographical and laminar organization of the presubiculum's projection to the ipsi- and contralateral entorhinal cortex in the guinea pig," *The Journal of Comparative Neurology*, vol. 160, no. 1, pp. 127–145, 1975.

[42] C. Köhler, "Morphological details of the projection from the presubiculum to the entorhinal area as shown with the novel PHA-L immunohistochemical tracing method in the rat," *Neuroscience Letters*, vol. 45, no. 3, pp. 285–290, 1984.

[43] P. Room and H. J. Groenewegen, "Connections of the parahippocampal cortex. I. Cortical afferents," *The Journal of Comparative Neurology*, vol. 251, no. 4, pp. 415–450, 1986.

[44] M. Caballero-Bleda and M. P. Witter, "Regional and laminar organization of projections from the presubiculum and parasubiculum to the entorhinal cortex: an anterograde tracing study in the rat," *The Journal of Comparative Neurology*, vol. 328, no. 1, pp. 115–129, 1993.

[45] D. G. Amaral, R. Insausti, and W. M. Cowan, "The commissural connections of the monkey hippocampal formation," *The Journal of Comparative Neurology*, vol. 224, no. 3, pp. 307–336, 1984.

[46] R. C. Saunders and D. L. Rosene, "A comparison of the efferents of the amygdala and the hippocampal formation in the rhesus monkey. I. Convergence in the entorhinal, prorhinal, and perirhinal cortices," *The Journal of Comparative Neurology*, vol. 271, no. 2, pp. 153–184, 1988.

[47] M. P. Witter, "Connections of the subiculum of the rat: topography in relation to columnar and laminar organization," *Behavioural Brain Research*, vol. 174, no. 2, pp. 251–264, 2006.

[48] M. P. Witter, "The perforant path: projections from the entorhinal cortex to the dentate gyrus," *Progress in Brain Research*, vol. 163, pp. 43–61, 2007.

[49] M. P. Witter, "Intrinsic and extrinsic wiring of CA3: indications for connectional heterogeneity," *Learning & Memory*, vol. 14, no. 11, pp. 705–713, 2007.

[50] F. Kloosterman, T. van Haeften, and F. H. Lopes da Silva, "Two reentrant pathways in the hippocampal-entorhinal system," *Hippocampus*, vol. 14, no. 8, pp. 1026–1039, 2004.

[51] F. Kloosterman, M. P. Witter, and T. van Haeften, "Topographical and laminar organization of subicular projections to the parahippocampal region of the rat," *The Journal of Comparative Neurology*, vol. 455, no. 2, pp. 156–171, 2003.

[52] L. Baks-te Bulte, F. G. Wouterlood, M. Vinkenoog, and M. P. Witter, "Entorhinal projections terminate onto principal neurons and interneurons in the subiculum: a quantitative electron microscopical analysis in the rat," *Neuroscience*, vol. 136, no. 3, pp. 729–739, 2005.

[53] N. L. Desmond, C. A. Scott, J. A. Jane Jr., and W. B. Levy, "Ultrastructural identification of entorhinal cortical synapses in CA1 stratum lacunosum-moleculare of the rat," *Hippocampus*, vol. 4, no. 5, pp. 594–600, 1994.

[54] R. Kajiwara, F. G. Wouterlood, A. Sah, A. J. Boekel, L. T. G. Baks-te Bulte, and M. P. Witter, "Convergence of entorhinal and CA3 inputs onto pyramidal neurons and interneurons in hippocampal area CA1—an anatomical study in the rat," *Hippocampus*, vol. 18, no. 3, pp. 266–280, 2008.

[55] M. P. Witter and D. G. Amaral, "Entorhinal cortex of the monkey. V. Projections to the dentate gyrus, hippocampus, and subicular complex," *The Journal of Comparative Neurology*, vol. 307, no. 3, pp. 437–459, 1991.

[56] T. Deller, A. Martinez, R. Nitsch, and M. Frotscher, "A novel entorhinal projection to the rat dentate gyrus: direct innervation of proximal dendrites and cell bodies of granule cells and GABAergic neurons," *The Journal of Neuroscience*, vol. 16, no. 10, pp. 3322–3333, 1996.

[57] M. P. Witter, "Organization of the entorhinal-hippocampal system: a review of current anatomical data," *Hippocampus*, vol. 3, pp. 33–44, 1993.

[58] D. G. Amaral, "Emerging principles of intrinsic hippocampal organization," *Current Opinion in Neurobiology*, vol. 3, no. 2, pp. 225–229, 1993.

[59] N. Tamamaki and Y. Nojyo, "Disposition of the slab-like modules formed by axon branches originating from single CA1 pyramidal neurons in the rat hippocampus," *The Journal of Comparative Neurology*, vol. 291, no. 4, pp. 509–519, 1990.

[60] D. G. Amaral, C. Dolorfo, and P. Alvarez-Royo, "Organization of CA1 projections to the subiculum: a PHA-L analysis in the rat," *Hippocampus*, vol. 1, no. 4, pp. 415–435, 1991.

[61] P. A. Naber, F. H. Lopes da Silva, and M. P. Witter, "Reciprocal connections between the entorhinal cortex and hippocampal fields CA1 and the subiculum are in register with the projections from CA1 to the subiculum," *Hippocampus*, vol. 11, no. 2, pp. 99–104, 2001.

[62] N. Tamamaki and Y. Nojyo, "Preservation of topography in the connections between the subiculum, field CA1, and the entorhinal cortex in rats," *The Journal of Comparative Neurology*, vol. 353, no. 3, pp. 379–390, 1995.

[63] W. M. Yee, D. M. Frim, and O. Isacson, "Relationships between stress protein induction and NMDA-mediated neuronal death in the entorhinal cortex," *Experimental Brain Research*, vol. 94, no. 2, pp. 193–202, 1993.

[64] N. L. M. Cappaert, W. J. Wadman, and M. P. Witter, "Spatiotemporal analyses of interactions between entorhinal and CA1 projections to the subiculum in rat brain slices," *Hippocampus*, vol. 17, no. 10, pp. 909–921, 2007.

[65] D. G. Amaral and P. Lavenex, "Hippocampal neuroanatomy," in *The Hippocampus Book*, P. Andersen, R. G. M. Morris, D. Amaral, T. Bliss, and J. O'Keefe, Eds., pp. 37–114, Oxford Univesity Press, Oxford, UK, 1st edition, 2006.

[66] K. G. Kjelstrup, T. Solstad, V. H. Brun, et al., "Very large place fields at the ventral pole of the hippocampal CA3 area," *Society for Neuroscience Abstracts*, vol. 33, 93.1, 2007.

[67] K. G. Kjelstrup, F. A. Tuvnes, H.-A. Steffenach, R. Murison, E. I. Moser, and M.-B. Moser, "Reduced fear expression after lesions of the ventral hippocampus," *Proceedings of the National Academy of Sciences of the United States of America*, vol. 99, no. 16, pp. 10825–10830, 2002.

[68] R. D. Burwell and D. G. Amaral, "Perirhinal and postrhinal cortices of the rat: interconnectivity and connections with the entorhinal cortex," *The Journal of Comparative Neurology*, vol. 391, no. 3, pp. 293–321, 1998.

[69] R. D. Burwell, "The parahippocampal region: corticocortical connectivity," *Annals of the New York Academy of Sciences*, vol. 911, pp. 25–42, 2000.

[70] R. D. Burwell and M. P. Witter, "Basic anatomy of the parahippocampal region in rats and monkeys," in *The Parahippocampal Region, Organization and Role in Cognitive Functions*, M. P. Witter and F. G. Wouterlood, Eds., pp. 35–60, Oxford University Press, Oxford, UK, 2002.

[71] S. C. Furtak, S.-M. Wei, K. L. Agster, and R. D. Burwell, "Functional neuroanatomy of the parahippocampal region in the rat: the perirhinal and postrhinal cortices," *Hippocampus*, vol. 17, no. 9, pp. 709–722, 2007.

[72] B. F. Jones and M. P. Witter, "Cingulate cortex projections to the parahippocampal region and hippocampal formation in the rat," *Hippocampus*, vol. 17, no. 10, pp. 957–976, 2007.

[73] G. W. van Hoesen, D. N. Pandya, and N. Butters, "Some connections of the entorhinal (area 28) and perirhinal (area 35) cortices of the rhesus monkey. II. Frontal lobe afferents," *Brain Research*, vol. 95, no. 1, pp. 25–38, 1975.

[74] G. W. van Hoesen and D. N. Pandya, "Some connections of the entorhinal (area 28) and perirhinal (area 35) cortices of the rhesus monkey. I. Temporal lobe afferents," *Brain Research*, vol. 95, no. 1, pp. 1–24, 1975.

[75] W. A. Suzuki and D. G. Amaral, "Topographic organization of the reciprocal connections between the monkey entorhinal cortex and the perirhinal and parahippocampal cortices," *The Journal of Neuroscience*, vol. 14, no. 3, pp. 1856–1877, 1994.

[76] Y. Kobayashi and D. G. Amaral, "Macaque monkey retrosplenial cortex. II. Cortical afferents," *The Journal of Comparative Neurology*, vol. 466, no. 1, pp. 48–79, 2003.

[77] J. M. Wyass and T. van Groen, "Connections between the retrosplenial cortex and the hippocampal formation in the rat: a review," *Hippocampus*, vol. 2, no. 1, pp. 1–11, 1992.

[78] Y. Kobayashi and D. G. Amaral, "Macaque monkey retrosplenial cortex. III. Cortical efferents," *The Journal of Comparative Neurology*, vol. 502, no. 5, pp. 810–833, 2007.

[79] L. W. Swanson and C. Köhler, "Anatomical evidence for direct projections from the entorhinal area to the entire cortical mantle in the rat," *The Journal of Neuroscience*, vol. 6, no. 10, pp. 3010–3023, 1986.

[80] P. Lavenex and D. G. Amaral, "Hippocampal-neocortical interaction: a hierarchy of associativity," *Hippocampus*, vol. 10, no. 4, pp. 420–430, 2000.

[81] F. Conde, E. Maire-Lepoivre, E. Audinat, and F. Crepel, "Afferent connections of the medial frontal cortex of the rat. II. Cortical and subcortical afferents," *The Journal of Comparative Neurology*, vol. 352, no. 4, pp. 567–593, 1995.

[82] G. E. Meredith, F. G. Wouterlood, and A. Pattiselanno, "Hippocampal fibers make synaptic contacts with glutamate decarboxylase-immunoreactive neurons in the rat nucleus accumbens," *Brain Research*, vol. 513, no. 2, pp. 329–334, 1990.

[83] S. Totterdell and G. E. Meredith, "Topographical organization of projections from the entorhinal cortex to the striatum of the rat," *Neuroscience*, vol. 78, no. 3, pp. 715–729, 1997.

[84] D. M. Finch, J. Gigg, A. M. Tan, and O. P. Kosoyan, "Neurophysiology and neuropharmacology of projections from entorhinal cortex to striatum in the rat," *Brain Research*, vol. 670, no. 2, pp. 233–247, 1995.

[85] P. F. Krayniak, R. C. Meibach, and A. Siegel, "A projection from the entorhinal cortex to the nucleus accumbens in the rat," *Brain Research*, vol. 209, no. 2, pp. 427–431, 1981.

[86] R. M. Beckstead, "Afferent connections of the entorhinal area in the rat as demonstrated by retrograde cell-labeling with horseradish peroxidase," *Brain Research*, vol. 152, no. 2, pp. 249–264, 1978.

[87] M. P. Witter, P. Room, H. J. Groenewegen, and A. H. M. Lohman, "Reciprocal connections of the insular and piriform claustrum with limbic cortex: an anatomical study in the cat," *Neuroscience*, vol. 24, no. 2, pp. 519–539, 1988.

[88] T. Eid, B. Jorritsma-Byham, R. Schwarcz, and M. P. Witter, "Afferents to the seizure-sensitive neurons in layer III of the medial entorhinal area: a tracing study in the rat," *Experimental Brain Research*, vol. 109, no. 2, pp. 209–218, 1996.

[89] J. Baizer, "Serotonergic innervation of the primate claustrum," *Brain Research Bulletin*, vol. 55, no. 3, pp. 431–434, 2001.

[90] A. Alonso and C. Köhler, "A study of the reciprocal connections between the septum and the entorhinal area using anterograde and retrograde axonal transport methods in the rat brain," *The Journal of Comparative Neurology*, vol. 225, no. 3, pp. 327–343, 1984.

[91] M.-M. Mesulam and E. J. Mufson, "Neural inputs into the nucleus basalis of the substantia innominata (Ch4) in the rhesus monkey," *Brain*, vol. 107, no. 1, pp. 253–274, 1984.

[92] F. T. Russchen, D. G. Amaral, and J. L. Price, "The afferennt connections of the substantia innominata in the monkey, *Macaca fascicularis*," *The Journal of Comparative Neurology*, vol. 242, no. 1, pp. 1–27, 1985.

[93] C. A. Kitt, S. J. Mitchell, M. R. DeLong, B. H. Wainer, and D. L. Price, "Fiber pathways of basal forebrain cholinergic neurons in monkeys," *Brain Research*, vol. 406, no. 1-2, pp. 192–206, 1987.

[94] A. J. McDonald, "Cortical pathways to the mammalian amygdala," *Progress in Neurobiology*, vol. 55, no. 3, pp. 257–332, 1998.

[95] L. Stefanacci and D. G. Amaral, "Topographic organization of cortical inputs to the lateral nucleus of the macaque monkey amygdala: a retrograde tracing study," *The Journal of Comparative Neurology*, vol. 421, no. 1, pp. 52–79, 2000.

[96] A. Pitkänen, J. L. Kelly, and D. G. Amaral, "Projections from the lateral, basal, and accessory basal nuclei of the amygdala to the entorhinal cortex in the macaque monkey," *Hippocampus*, vol. 12, no. 2, pp. 186–205, 2002.

[97] M. Pikkarainen, S. Rönkkö, V. Savander, R. Insausti, and A. Pitkänen, "Projections from the lateral, basal, and accessory basal nuclei of the amygdala to the hippocampal formation in rat," *The Journal of Comparative Neurology*, vol. 403, no. 2, pp. 229–260, 1999.

[98] J. P. Aggleton, R. Desimone, and M. Mishkin, "The origin, course, and termination of the hippocampothalamic projections in the macaque," *The Journal of Comparative Neurology*, vol. 243, no. 3, pp. 409–421, 1986.

[99] F. G. Wouterlood, E. Saldana, and M. P. Witter, "Projection from the nucleus reuniens thalami to the hippocampal region: light and electron microscopic tracing study in the rat with the anterograde tracer *Phaseolus vulgaris*-leucoagglutinin," *The Journal of Comparative Neurology*, vol. 296, no. 2, pp. 179–203, 1990.

[100] F. G. Wouterlood, "Innervation of entorhinal principal cells by neurons of the nucleus reuniens thalami. Anterograde PHA-L tracing combined with retrograde fluorescent tracing and intracellular injection with Lucifer yellow in the rat," *European Journal of Neuroscience*, vol. 3, no. 7, pp. 641–647, 1991.

[101] T. van Groen, I. Kadish, and J. M. Wyss, "Efferent connections of the anteromedial nucleus of the thalamus of the rat," *Brain Research Reviews*, vol. 30, no. 1, pp. 1–26, 1999.

[102] N. S. Canteras, R. B. Simerly, and L. W. Swanson, "Organization of projections from the ventromedial nucleus of the hypothalamus: a *Phaseolus vulgaris*-leucoagglutinin study in the rat," *The Journal of Comparative Neurology*, vol. 348, no. 1, pp. 41–79, 1994.

[103] M. J. Dolleman-Van der Weel, F. G. Wouterlood, and M. P. Witter, "Multiple anterograde tracing, combining *Phaseolus vulgaris* leucoagglutinin with rhodamine- and biotin-conjugated dextran amine," *Journal of Neuroscience Methods*, vol. 51, no. 1, pp. 9–21, 1994.

[104] F. T. Russchen, D. G. Amaral, and J. L. Price, "The afferent input to the magnocellular division of the mediodorsal thalamic nucleus in monkey, *Macaca fascicularis*," *The Journal of Comparative Neurology*, vol. 256, no. 2, pp. 175–210, 1987.

[105] R. P. Vertes, W. J. Fortin, and A. M. Crane, "Projections of the median raphe nucleus in the rat," *The Journal of Comparative Neurology*, vol. 407, no. 4, pp. 555–582, 1999.

[106] B. Berger and C. Alvarez, "Neurochemical development of the hippocampal region in the fetal rhesus monkey. II. Immunocytochemistry of peptides, calcium-binding proteins, DARPP-32, and monoamine innervation in the entorhinal cortex by the end of gestation," *Hippocampus*, vol. 4, no. 1, pp. 85–114, 1994.

[107] F. G. Wouterlood, "Spotlight on the neurones (I): cell types, local connectivity, microcircuits and distribution of markers," in *The Parahippocampal Region: Organization and Role in cognitive Function*, M. P. Witter and F. G. Wouterlood, Eds., pp. 61–88, Oxford University Press, Oxford, UK, 2002.

[108] F. G. Wouterlood, J. C. M. van Denderen, T. van Haeften, and M. P. Witter, "Calretinin in the entorhinal cortex of the rat: distribution, morphology, ultrastructure of neurons, and co-localization with γ-aminobutyric acid and parvalbumin," *The Journal of Comparative Neurology*, vol. 425, no. 2, pp. 177–192, 2000.

[109] M. Miettinen, A. Pitkänen, and R. Miettinen, "Distribution of calretinin-immunoreactivity in the rat entorhinal cortex: coexistence with GABA," *The Journal of Comparative Neurology*, vol. 378, no. 3, pp. 363–378, 1997.

[110] C. B. Canto, P. Ganter, E. I. Moser, M.-B. Moser, and M. P. Witter, "Neuron diversity in the medial entorhinal cortex of the rat," *Society for Neuroscience Abstracts*, vol. 32, 68.4, 2006.

[111] F. G. Wouterlood, E. Mugnaini, and J. Nederlof, "Projection of olfactory bulb efferents to layer I GABAergic neurons in the entorhinal area. Combination of anterograde degeneration and immunoelectron microscopy in rat," *Brain Research*, vol. 343, no. 2, pp. 283–296, 1985.

[112] D. M. Finch, A. M. Tan, and M. Isokawa-Akesson, "Feedforward inhibition of the rat entorhinal cortex and subicular complex," *The Journal of Neuroscience*, vol. 8, no. 7, pp. 2213–2226, 1988.

[113] F. G. Wouterlood and H. Pothuizen, "Sparse colocalization of somatostatin- and GABA-immunoreactivity in the entorhinal cortex of the rat," *Hippocampus*, vol. 10, no. 1, pp. 77–86, 2000.

[114] P. Germroth, W. K. Schwerdtfeger, and E. H. Buhl, "Morphology of identified entorhinal neurons projecting to the hippocampus. A light microscopical study combining retrograde tracing and intracellular injection," *Neuroscience*, vol. 30, no. 3, pp. 683–691, 1989.

[115] W. K. Schwerdtfeger, E. H. Buhl, and P. Germroth, "Disynaptic olfactory input to the hippocampus mediated by stellate cells in the entorhinal cortex," *The Journal of Comparative Neurology*, vol. 292, no. 2, pp. 163–177, 1990.

[116] C. Köhler and V. Chan-Palay, "Somatostatin and vasoactive intestinal polypeptide-like immunoreactive cells and terminals in the retrohippocampal region of the rat brain," *Anatomy and Embryology*, vol. 167, no. 2, pp. 151–172, 1983.

[117] C. Köhler, L. Eriksson, S. Davies, and V. Chan-Palay, "Neuropeptide Y innervation of the hippocampal region in the rat and monkey brain," *The Journal of Comparative Neurology*, vol. 244, no. 3, pp. 384–400, 1986.

[118] R. Klink and A. Alonso, "Morphological characteristics of layer II projection neurons in the rat medial entorhinal cortex," *Hippocampus*, vol. 7, no. 5, pp. 571–583, 1997.

[119] S. P. Schwartz and P. D. Coleman, "Neurons of origin of the perforant path," *Experimental Neurology*, vol. 74, no. 1, pp. 305–312, 1981.

[120] K. Lingenhohl and D. M. Finch, "Morphological characterization of rat entorhinal neurons in vivo: soma-dendritic structure and axonal domains," *Experimental Brain Research*, vol. 84, no. 1, pp. 57–74, 1991.

[121] R. Klink and A. Alonso, "Ionic mechanisms for the subthreshold oscillations and differential electroresponsiveness of medial entorhinal cortex layer II neurons," *Journal of Neurophysiology*, vol. 70, no. 1, pp. 144–157, 1993.

[122] N. Tamamaki and Y. Nojyo, "Projection of the entorhinal layer II neurons in the rat as revealed by intracellular pressure-injection of neurobiotin," *Hippocampus*, vol. 3, no. 4, pp. 471–480, 1993.

[123] M. Yoshida, M. Teramura, and M. Sakai, "Immunohistochemical visualization of glutamate- and aspartate-containing nerve terminal pools in the rat limbic structures," *Brain Research*, vol. 410, no. 1, pp. 169–173, 1987.

[124] M. P. Mattson, R. E. Lee, M. E. Adams, P. B. Guthrie, and S. B. Kater, "Interactions between entorhinal axons and target hippocampal neurons: a role for glutamate in the development of hippocampal circuitry," *Neuron*, vol. 1, no. 9, pp. 865–876, 1988.

[125] C.-W. Xie, J. F. McGinty, P. H. K. Lee, C. L. Mitchell, and J.-S. Hong, "A glutamate antagonist blocks perforant path stimulation-induced reduction of dynorphin peptide and prodynorphin mRNA levels in rat hippocampus," *Brain Research*, vol. 562, no. 2, pp. 243–250, 1991.

[126] W. F. White, J. V. Nadler, A. Hamberger, C. W. Cotman, and J. T. Cummins, "Glutamate as transmitter of hippocampal perforant path," *Nature*, vol. 270, no. 5635, pp. 356–357, 1977.

[127] B. Tahvildari and A. Alonso, "Morphological and electrophysiological properties of lateral entorhinal cortex layers II and III principal neurons," *The Journal of Comparative Neurology*, vol. 491, no. 2, pp. 123–140, 2005.

[128] A. Alonso and R. Klink, "Differential electroresponsiveness of stellate and pyramidal-like cells of medial entorhinal cortex layer II," *Journal of Neurophysiology*, vol. 70, no. 1, pp. 128–143, 1993.

[129] R. Klink and A. Alonso, "Muscarinic modulation of the oscillatory and repetitive firing properties of entorhinal cortex layer II neurons," *Journal of Neurophysiology*, vol. 77, no. 4, pp. 1813–1828, 1997.

[130] R. M. Empson, T. Gloveli, D. Schmitz, and U. Heinemann, "Electrophysiology and morphology of a new type of cell within layer II of the rat lateral entorhinal cortex in vitro," *Neuroscience Letters*, vol. 193, no. 3, pp. 149–152, 1995.

[131] P. Germroth, W. K. Schwerdtfeger, and E. H. Buhl, "Ultrastructure and aspects of functional organization of pyramidal and nonpyramidal entorhinal projection neurons contributing to the perforant path," *The Journal of Comparative Neurology*, vol. 305, no. 2, pp. 215–231, 1991.

[132] R. S. G. Jones and E. H. Buhl, "Basket-like interneurones in layer II of the entorhinal cortex exhibit a powerful NMDA-mediated synaptic excitation," *Neuroscience Letters*, vol. 149, no. 1, pp. 35–39, 1993.

[133] F. G. Wouterlood, W. Härtig, G. Brückner, and M. P. Witter, "Parvalbum-inimmunoreactive neurons in the entorhinal cortex of the rat: localization, morphology, connectivity and ultrastructure," *Journal of Neurocytology*, vol. 24, no. 2, pp. 135–153, 1995.

[134] E. Soriano, A. Martinez, I. Farinas, and M. Frotscher, "Chandelier cells in the hippocampal formation of the rat: the entorhinal area and subicular complex," *The Journal of Comparative Neurology*, vol. 337, no. 1, pp. 151–167, 1993.

[135] M. C. de Felipe, M. T. Molinero, and J. Del Río, "Long-lasting neurochemical and functional changes in rats induced by neonatal administration of substance P antiserum," *Brain Research*, vol. 485, no. 2, pp. 301–308, 1989.

[136] T. F. Freund, K. A. C. Martin, A. D. Smith, and P. Somogyi, "Glutamate decarboxylase-immunoreactive terminals of Golgi-impregnated axoaxonic cells and of presumed basket cells in synaptic contact with pyramidal neurons of the cat's visual cortex," *The Journal of Comparative Neurology*, vol. 221, no. 3, pp. 263–278, 1983.

[137] S. H. C. Hendry, E. G. Jones, P. C. Emson, D. E. M. Lawson, C. W. Heizmann, and P. Streit, "Two classes of cortical GABA neurons defined by differential calcium binding protein immunoreactivities," *Experimental Brain Research*, vol. 76, no. 2, pp. 467–472, 1989.

[138] P. Somogyi, "A specific 'axo-axonal' interneuron in the visual cortex of the rat," *Brain Research*, vol. 136, no. 2, pp. 345–350, 1977.

[139] T. Gloveli, D. Schmitz, R. M. Empson, T. Dugladze, and U. Heinemann, "Morphological and electrophysiological characterization of layer III cells of the medial entorhinal cortex of the rat," *Neuroscience*, vol. 77, no. 3, pp. 629–648, 1997.

[140] S. van der Linden, "Comparison of the electrophysiology and morphology of layers III and II neurons of the rat medial entorhinal cortex in vitro," *European Journal of Neuroscience*, vol. 10, no. 4, pp. 1479–1489, 1998.

[141] C. T. Dickson, A. R. Mena, and A. Alonso, "Electroresponsiveness of medial entorhinal cortex layer III neurons in vitro," *Neuroscience*, vol. 81, no. 4, pp. 937–950, 1997.

[142] C. Köhler, J.-Y. Wu, and V. Chan-Palay, "Neurons and terminals in the retrohippocampal region in the rat's brain identified by anti-γ-aminobutyric acid and anti-glutamic acid decarboxylase immunocytochemistry," *Anatomy and Embryology*, vol. 173, no. 1, pp. 35–44, 1985.

[143] S. S. Kumar and P. S. Buckmaster, "Hyperexcitability, interneurons, and loss of GABAergic synapses in entorhinal cortex in a model of temporal lobe epilepsy," *The Journal of Neuroscience*, vol. 26, no. 17, pp. 4613–4623, 2006.

[144] B. N. Hamam, D. G. Amaral, and A. A. Alonso, "Morphological and electrophysiological characteristics of layer V neurons of the rat lateral entorhinal cortex," *The Journal of Comparative Neurology*, vol. 451, no. 1, pp. 45–61, 2002.

[145] B. N. Hamam, T. E. Kennedy, A. Alonso, and D. G. Amaral, "Morphological and electrophysiological characteristics of layer V neurons of the rat medial entorhinal cortex," *The Journal of Comparative Neurology*, vol. 418, no. 4, pp. 457–472, 2000.

[146] T. Gloveli, T. Dugladze, D. Schmitz, and U. Heinemann, "Properties of entorhinal cortex deep layer neurons projecting to the rat dentate gyrus," *European Journal of Neuroscience*, vol. 13, no. 2, pp. 413–420, 2001.

[147] C. L. Dolorfo and D. G. Amaral, "Entorhinal cortex of the rat: organization of intrinsic connections," *The Journal of Comparative Neurology*, vol. 398, no. 1, pp. 49–82, 1998.

[148] C. Köhler, "Intrinsic connections of the retrohippocampal region in the rat brain. II. The medial entorhinal area," *The Journal of Comparative Neurology*, vol. 246, no. 2, pp. 149–169, 1986.

[149] C. Köhler, "Intrinsic connections of the retrohippocampal region in the rat brain. III. The lateral entorhinal area," *The Journal of Comparative Neurology*, vol. 271, no. 2, pp. 208–228, 1988.

[150] M. P. Witter, P. Room, H. J. Groenewegen, and A. H. M. Lohman, "Connections of the parahippocampal cortex in the cat. V. Intrinsic connections; comments on input/output connections with the hippocampus," *The Journal of Comparative Neurology*, vol. 252, no. 1, pp. 78–94, 1986.

[151] J. J. Chrobak and D. G. Amaral, "Entorhinal cortex of the monkey. VII. Intrinsic connections," *The Journal of Comparative Neurology*, vol. 500, no. 4, pp. 612–633, 2007.

[152] A. Dhillon and R. S. G. Jones, "Laminar differences in recurrent excitatory transmission in the rat entorhinal cortex in vitro," *Neuroscience*, vol. 99, no. 3, pp. 413–422, 2000.

[153] M. P. Witter, "Connectivity of the rat hippocampus," in *The Hippocampus: New Vistas*, V. Chan-Palay and C. Köhler, Eds., pp. 53–69, Allen R. Liss, New York, NY, USA, 1989.

[154] C. L. Dolorfo and D. G. Amaral, "Entorhinal cortex of the rat: topographic organization of the cells of origin of the perforant path projection to the dentate gyrus," *The Journal of Comparative Neurology*, vol. 398, no. 1, pp. 25–48, 1998.

[155] W. A. Suzuki, E. K. Miller, and R. Desimone, "Object and place memory in the macaque entorhinal cortex," *Journal of Neurophysiology*, vol. 78, no. 2, pp. 1062–1081, 1997.

[156] R. J. Douglas and K. A. C. Martin, "Mapping the matrix: the ways of neocortex," *Neuron*, vol. 56, no. 2, pp. 226–238, 2007.

[157] T. van Haeffen, L. Baks-te-Bulte, P. H. Goede, F. G. Wouterlood, and M. P. Witter, "Morphological and numerical analysis of synaptic interactions between neurons in deep and superficial layers of the entorhinal cortex of the rat," *Hippocampus*, vol. 13, no. 8, pp. 943–952, 2003.

[158] T. Iijima, M. P. Witter, M. Ichikawa, T. Tominaga, R. Kajiwara, and G. Matsumoto, "Entorhinal-hippocampal interactions revealed by real-time imaging," *Science*, vol. 272, no. 5265, pp. 1176–1179, 1996.

[159] R. Kajiwara, I. Takashima, Y. Mimura, M. P. Witter, and T. Iijima, "Amygdala input promotes spread of excitatory neural activity from perirhinal cortex to the entorhinal-hippocampal circuit," *Journal of Neurophysiology*, vol. 89, no. 4, pp. 2176–2184, 2003.

[160] R. S. G. Jones, "Synaptic and intrinsic properties of neurons of origin of the perforant path in layer II of the rat entorhinal cortex in vitro," *Hippocampus*, vol. 4, no. 3, pp. 335–353, 1994.

[161] R. Bartesaghi, T. Gessi, and L. Sperti, "Electrophysiological analysis of the hippocampal projections to the entorhinal area," *Neuroscience*, vol. 30, no. 1, pp. 51–62, 1989.

[162] T. Gloveli, D. Schmitz, R. M. Empson, and U. Heinemann, "Frequency-dependent information flow from the entorhinal cortex to the hippocampus," *Journal of Neurophysiology*, vol. 78, no. 6, pp. 3444–3449, 1997.

[163] F. Kloosterman, T. van Haeften, M. P. Witter, and F. H. Lopes da Silva, "Electrophysiological characterization of interlaminar entorhinal connections: an essential link for re-entrance in the hippocampal-entorhinal system," *European Journal of Neuroscience*, vol. 18, no. 11, pp. 3037–3052, 2003.

[164] S. Leutgeb, J. K. Leutgeb, A. Treves, M.-B. Moser, and E. I. Moser, "Distinct ensemble codes in hippocampal areas CA3 and CA1," *Science*, vol. 305, no. 5688, pp. 1295–1298, 2004.

[165] S. Leutgeb, J. K. Leutgeb, M.-B. Moser, and E. I. Moser, "Place cells, spatial maps and the population code for memory," *Current Opinion in Neurobiology*, vol. 15, no. 6, pp. 738–746, 2005.

[166] S. Leutgeb, J. K. Leutgeb, E. I. Moser, and M.-B. Moser, "Fast rate coding in hippocampal CA3 cell ensembles," *Hippocampus*, vol. 16, no. 9, pp. 765–774, 2006.

[167] A. Bakker, C. B. Kirwan, M. I. Miller, and C. E. Stark, "Pattern separation in the human hippocampal CA3 and dentate subfields," *Society for Neuroscience Abstracts*, vol. 33, 667.2, 2007.

[168] R. Bartesaghi, T. Gessi, and L. Sperti, "Electrophysiological analysis of the dorsal hippocampal commissure projections to the entorhinal area," *Neuroscience*, vol. 26, no. 1, pp. 55–67, 1988.

[169] R. Bartesaghi, V. Di Maio, and T. Gessi, "Topographic activation of the medial entorhinal cortex by presubicular commissural projections," *The Journal of Comparative Neurology*, vol. 487, no. 3, pp. 283–299, 2005.

[170] E. A. Tolner, F. Kloosterman, S. N. Kalitzin, F. H. Lopes da Silva, and J. A. Gorter, "Physiological changes in chronic epileptic rats are prominent in superficial layers of the medial entorhinal area," *Epilepsia*, vol. 46, supplement 5, pp. 72–81, 2005.

[171] E. A. Tolner, F. Kloosterman, E. A. van Vliet, M. P. Witter, F. H. Lopes da Silva, and J. A. Gorter, "Presubiculum stimulation in vivo evokes distinct oscillations in superficial and deep entorhinal cortex layers in chronic epileptic rats," *The Journal of Neuroscience*, vol. 25, no. 38, pp. 8755–8765, 2005.

[172] F. G. Wouterlood and J. Nederlof, "Terminations of olfactory afferents on layer II and III neurons in the entorhinal area: degeneration-Golgi-electron microscopic study in the rat," *Neuroscience Letters*, vol. 36, no. 2, pp. 105–110, 1983.

[173] P. Room, H. J. Groenewegen, and A. H. M. Lohmann, "Inputs from the olfactory bulb and olfactory cortex to the entorhinal cortex in the cat," *Experimental Brain Research*, vol. 56, no. 3, pp. 488–496, 1984.

[174] F. G. Wouterlood, T. van Haeften, M. Eijkhoudt, L. Baks-te-Bulte, P. H. Goede, and M. P. Witter, "Input from the presubiculum to dendrites of layer-V neurons of the medial entorhinal cortex of the rat," *Brain Research*, vol. 1013, no. 1, pp. 1–12, 2004.

[175] M. Caballero-Bleda and M. P. Witter, "Projections from the presubiculum and the parasubiculum to morphologically characterized entorhinal-hippocampal projection neurons in the rat," *Experimental Brain Research*, vol. 101, no. 1, pp. 93–108, 1994.

[176] T. van Haeften, F. G. Wouterlood, B. Jorritsma-Byham, and M. P. Witter, "GABAergic presubicular projections to the medial entorhinal cortex of the rat," *The Journal of Neuroscience*, vol. 17, no. 2, pp. 862–874, 1997.

[177] L. Q. Uddin, A. M. C. Kelly, B. B. Biswal, C. F. Xavier, and M. P. Milham, "Functional connectivity of default mode network components: correlation, anticorrelation, and causality," *Human Brain Mapping* (24 January 2008).

[178] J. S. Damoiseaux, C. F. Beckmann, E. J. S. Arigita, et al., "Reduced resting-state brain activity in the "default network" in normal aging," *Cerebral Cortex* (27 December 2007).

[179] C. Sorg, V. Riedl, M. Mühlau, et al., "Selective changes of resting-state networks in individuals at risk for Alzheimer's disease," *Proceedings of the National Academy of Sciences of the United States of America*, vol. 104, no. 47, pp. 18760–18765, 2007.

Hindawi Publishing Corporation
Neural Plasticity
Volume 2008, Article ID 258467, 8 pages
doi:10.1155/2008/258467

Review Article

Complementary Roles of Hippocampus and Medial Entorhinal Cortex in Episodic Memory

P. A. Lipton and H. Eichenbaum

Center for Memory and Brain, Department of Psychology, Boston University, 2 Cummington street, Boston, MA 02215, USA

Correspondence should be addressed to H. Eichenbaum, hbe@bu.edu

Received 30 December 2007; Revised 13 March 2008; Accepted 20 May 2008

Recommended by Min Jung

Spatial mapping and navigation are figured prominently in the extant literature that describes hippocampal function. The medial entorhinal cortex is likewise attracting increasing interest, insofar as evidence accumulates that this area also contributes to spatial information processing. Here, we discuss recent electrophysiological findings that offer an alternate view of hippocampal and medial entorhinal function. These findings suggest complementary contributions of the hippocampus and medial entorhinal cortex in support of episodic memory, wherein hippocampal networks encode sequences of events that compose temporally and spatially extended episodes, whereas medial entorhinal networks disambiguate overlapping episodes by binding sequential events into distinct memories.

Copyright © 2008 P. A. Lipton and H. Eichenbaum. This is an open access article distributed under the Creative Commons Attribution License, which permits unrestricted use, distribution, and reproduction in any medium, provided the original work is properly cited.

1. THE BRAIN'S GPS

Does hippocampal activity embody the cognitive map? One should expect the neural instantiation of Tolman's [1] cognitive map to contain units (neurons) that are fully allocentric, that is, identify places in the environment independent of the subject's perspective (egocentric direction) and ongoing behavior. Furthermore, one should expect that the neural ensemble composed of these units would be holistic; that is, all the neuronal representations should be tied to one another and change together between environments. And, if the map is to suit the purpose Tolman proposed in guiding behavior according to expectancies, the map should signal the locations of current goals.

Initially, hippocampal place cells seemed to satisfy key criteria for elements of Tolman's cognitive map. The first complete study characterized place cells as signaling an animal's location in the environment independent of egocentric direction and ongoing behavior, as would be expected of the units in an allocentric representation [2]. An expansive literature followed on the initial observations, and many interpreted the results as support for the claim that the neural substrate for the cognitive map lies in the circuitry of the hippocampus [3–9].

However, even in the early data there were loose ends. Location related hippocampal neuronal activity tells us only where the animal is, not where it plans to go, as is Tolman's intended function of a cognitive map [10]. Succeeding studies directly refuted the idea that the hippocampal network contains purely allocentric representations and a holistic map. Inconsistent with a holistic representation, simultaneously recorded place cells respond differently and independently to changes in environmental cues or task demands (e.g., [11–14]). Furthermore, inconsistent with allocentric representation, the activity of most hippocampal neurons is dependent on egocentric spatial parameters, including the direction and speed of the animal's movements [15]. Indeed, place cells reliably provide an allocentric signal only under highly constrained conditions where all perceptual cues, behaviors, and cognitive demands are held constant. In addition, hippocampal neuronal activity has been associated with a variety of nonspatial cues, behaviors, and task demands [16–27], consistent with additional findings showing a critical role for the hippocampus in nonspatial as well as spatial learning and memory [28–30]. Also, several recent studies have provided compelling evidence that so-called place cells are strongly influenced by nonspatial cognitive demands in animals performing

spatial memory tasks [31–37], and thus signal where the animal is only in particular circumstances associated with a behaviorally salient task.

In sum, place cells do identify where the animal is when important things happen. But place cells do not carry a reliable allocentric signal, and populations of place cells do not operate as a holistic representation of space or anticipate the locations of goals. Therefore, hippocampal neurons do not have the requisite properties to support Tolman's cognitive map. By contrast, the findings indicate that hippocampal neurons represent events in the places where they occur, consistent with current views of hippocampal involvement in episodic memory (e.g., [38, 39]).

The recent discovery of spatial firing patterns in the cortex immediately adjacent to the hippocampus has refocused the search for the cognitive map to a zone within the medial entorhinal area [36, 40–43]. A majority of the data describes the spatial firing patterns of principal neurons in the medial entorhinal cortex, and more specifically how a proportion of these neurons, the so-called "grid cells," exhibit an intriguing and unique spatial firing pattern with several interesting properties. First, the relative angles and densities of peaks within grids of neighboring cells remain invariant both across environments and in response to changes in local cues [41]. Second, while grid fields of medial entorhinal neurons remain stable in response to modest environmental manipulation, hippocampal CA3 neurons change their rate of firing ("rate remapping," [44]). In response to more significant environmental change, grid fields of local ensembles of medial entorhinal neurons rotate while maintaining relative geometric consistency, whereas CA3 neurons fire in a different location ("global remapping"), [44]. Thus, in response to environmental manipulation, changes in medial entorhinal activity are more systematic and predictable than corresponding hippocampal CA3 responses, and consequently more stable as sensory inputs change. Third, while lacking any obvious topographic organization of space, the relative size of medial entorhinal grid fields changes systematically along a dorsal-ventral axis [41]. Although medial entorhinal cells are influenced by egocentric parameters of head direction and velocity, [42], these findings modestly suggest that some version of the cognitive map may reside within the medial entorhinal cortex, rather than the immediately adjacent hippocampus. This interpretation will be argued in several other papers of the current volume. However, here we will suggest an alternate view driven by recent data that includes our own experiment wherein sensory cues were held constant throughout the experiment [36]—that spatial representations observed in medial entorhinal cortex may make a specific contribution to episodic memory.

2. EPISODIC MEMORY

2.1. Memory for order

The hippocampus is strongly implicated in spatial memory and navigation as evidenced by both behavioral and physiological studies. At the same time, a convergent stream of behavioral, physiological, and computational modeling data indicate that hippocampal processing is critical for episodic memory [45–57]. How can these two seemingly distinct lines of evidence be reconciled?

Current conceptions of episodic memory emphasize the temporal organization of sequences of events as they unfold over time and space [58]. Representations of events are composed as associations between specific objects, actions, and the locations where they occur. Complete episodes are composed of unique sequences of events [38]. Recent experiments have revealed a critical role of the hippocampus in memory for sequences of events that compose unique episodes [47, 59]. In addition, episodic memory also relies on the capacity to distinguish event sequences that share common elements [60]. This property of episodic memory is especially evident in spatial memories, for example, we are usually very good at remembering unique events that occur day by day as we take the same route to work each day. Computational models suggest that the ability to disambiguate overlapping elements from multiple experiences may be a critical feature of hippocampal function that contributes to episodic memory [53]. Consistent with this view, rats with hippocampal lesions fail on a sequence disambiguation task that involved two series of events that contain overlapping items [45].

Additional support for sequencing and disambiguation of serial events by hippocampal networks comes from analyses of hippocampal neuronal activity in animals performing spatial memory tasks. In one study, rats were trained on the classic spatial T-maze alternation task in which successful performance depends on distinguishing left- and right-turn episodes to guide each subsequent choice [37]. If hippocampal neurons encode each sequential behavioral event within one type of episode, then neuronal activity at locations that overlap in left- and right-turn trials should vary according to trial type. Indeed, virtually all cells that were active as the rat traversed these common locations were differentially active on left- versus right-turn trials. Despite modest differences in the proportion of neurons that exhibit this pattern of activity across studies—likely due to differences in training protocols—similar results have been observed in several versions of this task [31–35, 37, 61]. These findings suggest a reconciliation of the spatial and episodic memory views of hippocampal function: place cells represent the series of places where events occur in sequences that compose distinct episodic memories.

2.2. Temporal context

In order to correctly trigger a series of event representations within a particular episode, the hippocampus requires a mechanism to bind its representations of event sequences according to the appropriate episode they compose. One suggestion is that sequences are bound by a shared temporal context [49, 62] and that the mechanism for contextual binding involves context sensitive neurons that fire for prolonged periods to bridge sequences of events that occur within a particular context [63]. Here, we review evidence suggesting that the context sensitive neurons exist in the

medial entorhinal cortex and serve a function complementary to that of hippocampal place cells which encode discrete events.

Thus far, all observations of grid field activity patterns in medial entorhinal cortex are derived from animals foraging in random directions within an open field. In fact, Derdikman et al. [64] report that the grid structure breaks down when animals are constrained to make hairpin turns within the previously unconstrained open field. This is notable because in the standard, random foraging experimental protocol, spatial cues provide the only regularities and constraints. In contrast, what differed between the hairpin turn maze and the open field condition was the imposition of behavioral constraints; spatial cues were held constant. Importantly, it is only under the unconstrained open field condition that hippocampal cells display purely allocentric spatial firing patterns. Perhaps where stimulus or behavioral regularities are imposed, the activity of neurons in medial entorhinal cortex, like neurons in the hippocampus, might reflect the corresponding regularities embedded in the task protocol.

In a recent study, we adopted the same spatial memory task used previously [37] to compare the activity of hippocampal and medial entorhinal neurons in animals performing a continuous spatial alternation on a T-maze in which hippocampal neurons encode sequences of locations traversed and disambiguate overlapping routes [36]. Two important considerations are worth mentioning here. First, we were explicitly interested in comparing how medial entorhinal and hippocampal neurons uniquely represent aspects of the continuous spatial alternation, rather than in an analysis of grid cell properties. Our interpretation of our data therefore addresses the contribution of medial entorhinal cortex to episodic memory, not whether a grid field forms on a T-maze. Second, just as the expansive place cell literature relies almost exclusively on observations of hippocampal activity in situations that neither require any manner of hippocampal processing nor impose any memory demands, our experimental design exploited the capacity of medial entorhinal neurons to encode spatial information. Whether the task is hippocampal or entorhinal dependent is not relevant to our interpretations. Insofar as the continuous spatial alternation is not a hippocampal dependent-task, it is worth noting that hippocampal dependence is neither an operational definition of, nor a pre-requisite for, memory.

We trained rats to perform the spatial alternation task on a T-maze that included return arms that connected the end of each goal arm to the starting end of the central stem (Figure 1). A left-turn trial began as the animal departed the right goal area, ran down the return arm to the central stem, traversed the central stem, and made a left-turn into the left goal area to retrieve a water reward. Similarly, a right-turn trial began when the animal departed the left goal area, returned to and traversed the central stem, and made a right turn into the right goal area. Drawing on the model of episodic memory noted above, each left- or right-turn trial can be considered a unique episode, constructed by connecting sequential behavioral events identified by a series of loci along the maze. Areas that lie along the central stem

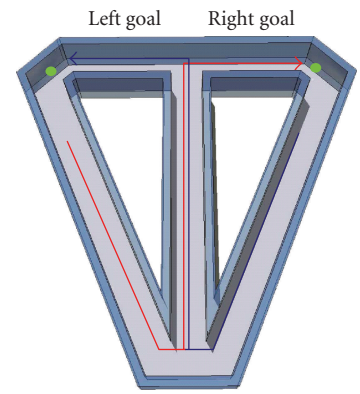

Figure 1: T-maze continuous alternation. Blue line indicates left-turn trial; red line indicates right-turn trial. Small green circles represent reward sites.

constitute overlapping elements of both types of episodes, and are indeed represented differently by hippocampal neurons depending on the ongoing episode (Figure 2, [36, 37]). Furthermore, consistent with previous reports [40, 65], activity of neurons in medial entorhinal cortex also signals an animal's position along the maze. Though we did not witness the development of a grid-like firing pattern on the T-maze, a proportion of our medial entorhinal neurons did exhibit a high degree of spatial specificity [36]. For example, the medial entorhinal cell shown in Figure 3 fired predominantly at the proximal end of the central stem during both left- and right-turn trials, while remaining largely silent through other regions of the maze.

Many of our medial entorhinal neurons that exhibited spatial specificity also exhibited differential firing along the central stem of the maze during left- and right-turn trials, similar to hippocampal neurons [36]. The patterns of neuronal activity illustrated in Figure 4 represent typical trial-type specific activity exhibited by medial entorhinal neurons. Some medial entorhinal cells fired selectively during the trial and distinguished left-turn and right-turn trials. For example, the cell shown in Figure 4(a) was selectively active when the rat was near the end of the central stem and fired at a higher rate during right-turn compared to left-turn trials. However, most medial entorhinal neurons showed only crude spatial specificity. For example, the cell shown in Figure 4(b) fired somewhat indiscriminately through different regions of the maze, and although active along the entire central stem, was significantly more active on left-turn trials. This pattern of activity was an exclusive feature of medial entorhinal neurons, such that we observed no hippocampal units with poorly localized, trial-type specific firing that extended the length of the central stem [36].

We used a two-way ANOVA and log-likelihood estimation to quantitatively compare the incidence and robustness of trial-type disambiguation in medial entorhinal and hippocampal neurons. Dividing the central stem into seven equal segments, we used a two-way ANOVA to compare the spatial firing patterns on segments of the central stem between left-turn and right-turn trial types for each cell [37]. We considered that a significant main effect of trial

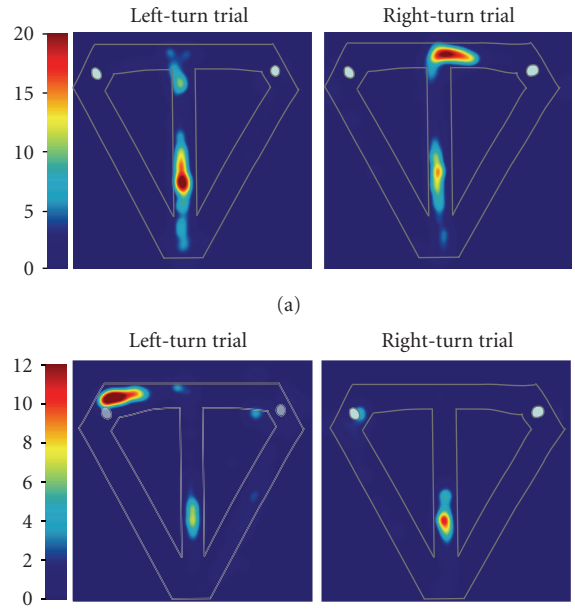

Figure 2: The activity of two example hippocampal neurons represented as false-color rate maps to illustrate differential firing on left- versus right-turn trials. (a). This unit was significantly more active on left-turn trials: significant main effect of segment ($F_{6,420} = 91.05$; $P < .00001$) and interaction ($F_{6,420} = 2.58$; $P < .02$); log-likelihood ratio = 0.2; $p_{\text{correct}} = 0.6$; $p_{\text{chance}} = 0.08$. (b). This unit was significantly more active on right-turn trials: significant main effect of segment $F_{6,252} = 68.3$; $P < .00001$) and interaction $F_{6,252} = 2.92$; $P = 0.009$); log-likelihood ratio = 1.22; $p_{\text{correct}} = 0.63$; $p_{\text{chance}} = 0.07$. Color bars indicate firing rate in Hz.

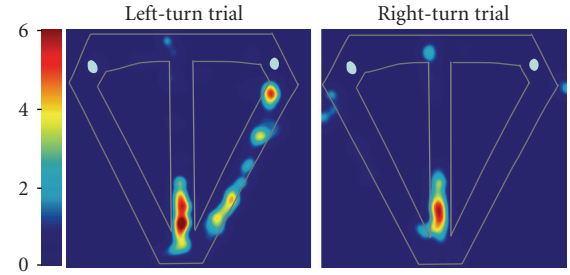

Figure 3: Location related firing of a medial entorhinal neuron that did not fire differentially on left- versus right-turn trials. Significant main effect of segment ($F_{6,238} = 44.43$; $P < .00001$); loglikelihood ratio = 2.5; $p_{\text{correct}} = 0.72$; $p_{\text{chance}} = 0.006$. Color bars indicate firing rate in Hz.

type or a trial type by segment interaction qualified a cell as differentiating left- from right-turn trials. A significant main effect of segment without a significant main effect of trial type or trial type by segment interaction denoted location-specific activity only. The log-likelihood ratio [66], on the other hand, represented the degree to which firing patterns on left-turn and right-turn trials differed, and thus allowed us to measure the difference in the firing patterns across trial types, rather than knowing simply that they

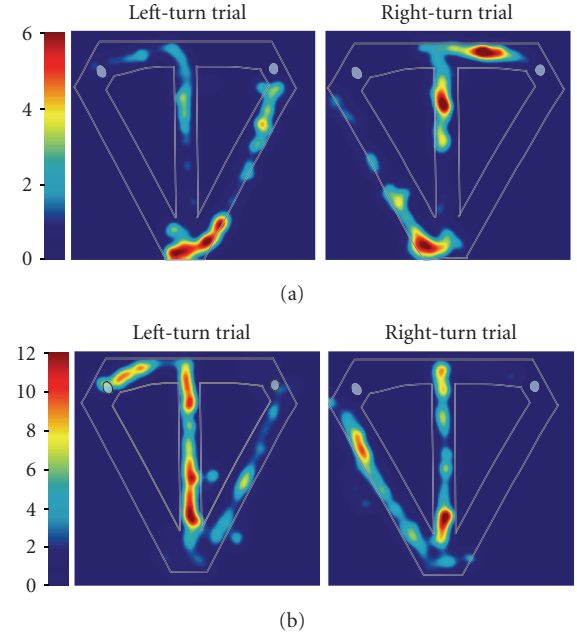

Figure 4: Firing patterns of two representative medial entorhinal neurons that reflect both trial disambiguation and a low degree of spatial specificity. (a). This unit was significantly more active on right-turn trials: significant main effect of segment ($F_{6,392} = 11.73$; $P < .00001$), trial type ($F_{1,392} = 7.32$; $P < .00071$) and interaction ($F_{6,392} = 2.22$; $P < .04$); log-likelihood ratio = 4.62; $p_{\text{correct}} = 0.67$; $p_{\text{chance}} = 0.006$. (b). This unit was significantly more active on left-turn trials: significant main effect of segment ($F_{6,280} = 3.83$; $P < .0011$), trial type ($F_{1,280} = 4.87$; $P < .03$) and interaction ($F_{6,280} = 1.83$; $P < .09$); log-likelihood ratio = 1.29; $p_{\text{correct}} = 0.71$; $p_{\text{chance}} = 0.004$. Color bars indicate firing rate in Hz.

differed. The log-likelihood ratio was calculated as follows: $1np[r \mid L, x]/p[r \mid R, x]$, where $p[r \mid L, x]$ is the probability density function of left-turn (L) trials at position x, evaluated at the observed firing rate r, and $p[r \mid R, x]$ is the equivalent function for right-turn (R) trials [66]. For each cell, log-likelihood ratios were summed over all central stem bins for each trial. Where the log-likelihood sum is greater than zero, maximum likelihood analysis predicts that the data came from a left-turn trial; otherwise, a right-turn trial is predicted. We calculated the average absolute value of the summed log-likelihood ratio, such that larger values of this term indicate firing-rate patterns that are statistically more distinct (for a more detailed description, see [36]).

Using the two-way ANOVA, we identified neurons in the hippocampus and medial entorhinal area that distinguished trial type as animals traversed the central stem. Based on the two-way ANOVA, 56% of medial entorhinal neurons (23/41 with place fields on the central stem) were significantly more active on either right- or left-turn trials, whereas 33% (16/48) of hippocampal neurons exhibited differential firing on the central stem. Moreover, the log-likelihood estimation revealed that medial entorhinal neurons more robustly distinguished left- from right-turn trials than did hippocampal neurons, such that the average log-likelihood ratio for medial entorhinal neurons was significantly greater

than for hippocampal neurons (MEC, 2.82; Hippocampus, 1.7; Wilcoxon rank-sum test, $P < .003$). In other words, firing patterns of medial entorhinal neurons were on average more distinct on either left- or right-turn trials than were hippocampal neurons.

Two additional measures were applied to describe how the patterns of activity in hippocampal and medial entorhinal neurons differed along the central stem during left- and right-turn trials [36]. The first measure, p_{correct}, is based on a maximum-likelihood guess performed for each trial compared against the actual outcome of that trial, and thus describes how accurate the log-likelihood estimate is for each trial type. To calculate p_{correct}, we performed a maximum likelihood analysis using the conditional density functions as described above. p_{correct} represents the number of times that prediction was correct, divided by the total number of trials. Therefore, p_{correct} is the average trial-by-trial probability that the log-likelihood analysis gives the correct answer for each trial type: a population that more consistently and significantly differentiates left- from right-turn trials will have a higher p_{correct}. The second measure, p_{chance}, is the average probability that firing patterns across left- and right-turn trials arose by chance, given a p_{correct} of 0.5 (i.e., the firing rate contains no trial-specific information, which is necessary to avoid biasing the calculation). To calculate p_{chance}, we evaluated the following formula: $\text{Pnk} = n!/k!/(n-k)!(0.5^k)0.5^{(1-k)}$, where n is the number of trials, and k is the number of apparently correct answers from maximal likelihood analysis. To get p_{chance}, we summed Pnk for all values of k greater than or equal to the number associated with our measured value of p_{correct}. A $p_{\text{chance}} = 0.05$ determined that a cell could successfully distinguish trial type.

Again, medial entorhinal neurons had a significantly higher mean p_{correct} than hippocampal neurons (MEC, 70%; Hippocampus, 63%; Wilcoxon rank-sum test, $P < .0001$), indicating that the activity of medial entorhinal neurons along the central stem more successfully predicted trial type than hippocampal neurons. Correspondingly, the difference in firing among left- and right-turn trials of medial entorhinal neurons was on average less likely to have occurred by chance than that of hippocampal neurons (p_{chance} equal to or less than 0.05: 90% MEC; 50% Hippocampus).

While the ANOVA and log-likelihood estimation did not always agree on specific units, together they converged on the same conclusion; just as hippocampal units did not exclusively encode information about space, medial entorhinal neurons likewise exhibited location-related firing modulated by mnemonic demands. Furthermore, medial entorhinal neurons performed better than hippocampal neurons at distinguishing trial type on our version of the continuous spatial alternation [36].

Conversely, hippocampal neurons showed greater spatial specificity than medial entorhinal neurons, as is evident by directly comparing the spatial firing patterns displayed in Figures 3 and 4. Our visual observations were bolstered by three quantitative measures—performed on all hippocampal and medial entorhinal units with a firing field somewhere on the maze—meant to assess spatial selectivity: place field size, spatial tuning, and spatial information rate. On all three measures hippocampal and medial entorhinal activity differed significantly. For example, average hippocampal place field size for all units with location related activity on the maze was significantly smaller than that of medial entorhinal neurons ($256.8\,\text{cm}^2$ versus $330.8\,\text{cm}^2$, resp.; Wilcoxon rank-sum test, $P < .0003$). The degree of spatial tuning, or the ratio of firing inside versus outside a place field, for hippocampal neurons was on average significantly higher than for medial entorhinal neurons (11.5 versus 3.0, resp.; Wilcoxon rank-sum test, $P < 8.8\text{E}{-16}$). The amount of spatial information conveyed by hippocampal neurons also was significantly greater than that of medial entorhinal neurons (2.02 bits/second versus 0.89 bits/second, resp.; Wilcoxon rank-sum test, $P < .00001$).

Together the results of this study suggest that disambiguation of overlapping experiences occurs prior to the hippocampus, and that hippocampal and medial entorhinal circuits play distinct and complementary roles in the continuous spatial alternation. Medial entorhinal neurons more successfully distinguished task related episodes in the context of left- versus right-turn trial type, whereas hippocampal neurons provided a greater degree of spatial specificity. Together both regions supply requisite elements of a neural code for particular events as they occur within unique episodes.

Since the neural circuitry among these brain regions constitutes a series of loops [67], it is difficult to positively attribute specific functions to individual brain regions. However, very recent evidence from observations of CA1 neuronal activity in animals with lesions to layer III of medial entorhinal cortex offers crucial support [68]. The results demonstrate that precise spatial coding of CA1 neurons is more dependent on this direct entorhinal input than on projections from CA3 which provide indirect input from layer II of medial entorhinal cortex [68], indicating that the manner of spatial information processing most commonly observed in CA1 is the result of a clear progression from medial entorhinal cortex to hippocampus.

3. HOW DOES THE MEDIAL ENTORHINAL CORTEX CONTRIBUTE TO EPISODIC MEMORY?

Our recent experimental results confirm that medial entorhinal neurons carry a spatial signal. However, as noted above, most of these neurons do not fire at discrete locations associated with particular trial events, as do hippocampal neurons. Instead, many medial entorhinal cells show strong context sensitivity, outperforming hippocampal neurons in distinguishing left-turn and right-turn trials. Furthermore, the prolonged firing periods of medial entorhinal cells are consistent with the characterization of context sensitive neurons that could bind a series of hippocampal representations of punctate events [63].

A growing body of evidence supports the notion that the medial entorhinal area is part of the parahippocampal region that processes contextual representations. This evidence is derived from knowledge about the anatomical pathways of the hippocampal system and from recent functional imaging

studies [39]. Inputs to the hippocampus arrive via the surrounding cortical areas that compose the parahippocampal region [67]. This region can be subdivided into the perirhinal cortex, the parahippocampal cortex (called postrhinal cortex in rodents), and the entorhinal cortex. Most neocortical inputs to the perirhinal cortex are derived from association areas that process unimodal sensory information about qualities of objects (i.e., "what" information), whereas most of the neocortical inputs to the parahippocampal cortex (called postrhinal cortex in rats) originate in areas that process polymodal spatial (where) information.

Subsequently, the "what" and "where" streams of processing remain largely segregated as the perirhinal cortex projects primarily to the lateral entorhinal area, whereas the parahippocampal cortex projects mainly to the medial entorhinal area. While there are also some connections between the perirhinal and parahippocampal cortices and between the entorhinal areas, the "what" and "where" information mainly converge within the hippocampus. Hippocampal efferents back to the cortex involve feedback connections from the hippocampus successively back to the parahippocampal region and thence to neocortical areas from which the inputs originated. This anatomical evidence suggests that, during encoding, "what" information carried in the perirhinal-lateral entorhinal stream is combined with "where" information carried in the parahippocampal-medial entorhinal stream and the hippocampus associates items and their spatial context. When an item is subsequently presented as a memory cue, the hippocampus completes the full pattern and mediates a recovery of the contextual representation in the parahippocampal cortex and medial entorhinal area, and the recovery of context constitutes the experience of episodic recollection.

In support of this model, evidence from functional imaging studies in humans indicates that the parahippocampal cortex component of the "where" stream represents spatial context. One line of evidence comes from the work of Kanwisher and colleagues, showing that the parahippocampal region is activated when people view spatial scenes and not objects or faces [69]. The other line of evidence comes from work of Bar and colleagues, showing that the parahippocampal cortex is activated when people view objects that have strong spatial contextual associations (e.g., a refrigerator, a roulette wheel, [70]). Similarly, a cellular (fos) imaging study indicates that the postrhinal cortex also is activated in rats by novel spatial arrangements of cues [71]. In addition, Aminoff et al. [72] reported that adjacent components of the parahippocampal cortex are activated by spatial context, and that this activity emerges as people view abstract patterns that were elements of newly learned spatial patterns or simply temporally associated. These findings extend the potential role of the parahippocampal cortex to temporal contextual representations as well as spatial context. Such a view is consistent with the frequent observation that the parahippocampal region is activated when humans recollect items in the context in which they were learned (reviewed in [39]).

We lack studies that compare response properties of the parahippocampal cortex and the medial entorhinal area. However, the combined data from functional imaging of the parahippocampal cortex in humans and animals and our recent study of spatial firing properties of medial entorhinal neurons suggest that both the parahippocampal cortex and medial entorhinal area components of the "where" pathway may be specialized for the processing of spatial and temporal context in humans and animals. Much work remains to be done to test this hypothesis. However, we believe there is sufficient evidence to consider the medial entorhinal area as part of a contextual representation system rather than the embodiment of a cognitive map that guides spatial navigation.

ACKNOWLEDGMENT

This work was supported by National Institute of Mental Health Grants MH51570 and MH071702 and National Science Foundation Science of Learning Center grant SBE-0354378.

REFERENCES

[1] E. C. Tolman, "Cognitive maps in rats and men," *Psychological Review*, vol. 55, no. 4, pp. 189–208, 1948.

[2] J. O'Keefe, "Place units in the hippocampus of the freely moving rat," *Experimental Neurology*, vol. 51, no. 1, pp. 78–109, 1976.

[3] R. Muller, "A quarter of a century of place cells," *Neuron*, vol. 17, no. 5, pp. 813–822, 1996.

[4] R. U. Muller and J. L. Kubie, "The effects of changes in the environment on the spatial firing of hippocampal complex-spike cells," *Journal of Neuroscience*, vol. 7, no. 7, pp. 1951–1968, 1987.

[5] J. O'Keefe and A. Speakman, "Single unit activity in the rat hippocampus during a spatial memory task," *Experimental Brain Research*, vol. 68, no. 1, pp. 1–27, 1987.

[6] J. O'Keefe, "Do hippocampal pyramidal cells signal non-spatial as well as spatial information?" *Hippocampus*, vol. 9, no. 4, pp. 352–364, 1999.

[7] J. O'Keefe and L. Nadel, *The Hippocampus as a Cognitive Map*, Clarendon Press, Oxford, UK, 1978.

[8] G. J. Quirk, R. U. Muller, J. L. Kubie, and J. B. Ranck Jr., "The positional firing properties of medial entorhinal neurons: description and comparison with hippocampal place cells," *Journal of Neuroscience*, vol. 12, no. 5, pp. 1945–1963, 1992.

[9] L. T. Thompson and P. J. Best, "Long-term stability of the place-field activity of single units recorded from the dorsal hippocampus of freely behaving rats," *Brain Research*, vol. 509, no. 2, pp. 299–308, 1990.

[10] R. G. M. Morris, "Does the hippocampus play a disproportionate role in spatial memory?" *Discussions in Neuroscience*, vol. 6, pp. 39–45, 1990.

[11] M. L. Shapiro, H. Tanila, and H. Eichenbaum, "Cues that hippocampal place cells encode: dynamic and hierarchical representation of local and distal stimuli," *Hippocampus*, vol. 7, no. 6, pp. 624–642, 1997.

[12] R. E. Hampson, D. R. Byrd, J. K. Konstantopoulos, T. Bunn, and S. A. Deadwyler, "Hippocampal place fields: relationship between degree of field overlap and cross-correlations within ensembles of hippocampal neurons," *Hippocampus*, vol. 6, no. 3, pp. 281–293, 1996.

[13] P. A. Hetherington and M. L. Shapiro, "Hippocampal place fields are altered by the removal of single visual cues in a distance-dependent manner," *Behavioral Neuroscience*, vol. 111, no. 1, pp. 20–34, 1997.

[14] W. E. Skaggs and B. L. McNaughton, "Spatial firing properties of hippocampal CA1 populations in an environment containing two visually identical regions," *Journal of Neuroscience*, vol. 18, no. 20, pp. 8455–8466, 1998.

[15] B. L. McNaughton, C. A. Barnes, and J. O'Keefe, "The contributions of position, direction, and velocity to single unit activity in the hippocampus of freely-moving rats," *Experimental Brain Research*, vol. 52, no. 1, pp. 41–49, 1983.

[16] S. A. Deadwyler, T. Bunn, and R. E. Hampson, "Hippocampal ensemble activity during spatial delayed-nonmatch-to-sample performance in rats," *Journal of Neuroscience*, vol. 16, no. 1, pp. 354–372, 1996.

[17] H. Eichenbaum, M. Kuperstein, A. Fagan, and J. Nagode, "Cue-sampling and goal-approach correlates of hippocampal unit activity in rats performing an odor-discrimination task," *Journal of Neuroscience*, vol. 7, no. 3, pp. 716–732, 1987.

[18] M. D. McEchron and J. F. Disterhoft, "Sequence of single neuron changes in CA1 hippocampus of rabbits during acquisition of trace eyeblink conditioned responses," *Journal of Neurophysiology*, vol. 78, no. 2, pp. 1030–1044, 1997.

[19] R. E. Hampson, C. J. Heyser, and S. A. Deadwyler, "Hippocampal cell firing correlates of delayed-match-to-sample performance in the rat," *Behavioral Neuroscience*, vol. 107, no. 5, pp. 715–739, 1993.

[20] T. Otto and H. Eichenbaum, "Neuronal activity in the hippocampus during delayed non-match to sample performance in rats: evidence for hippocampal processing in recognition memory," *Hippocampus*, vol. 2, no. 3, pp. 323–334, 1992.

[21] Y. Sakurai, "Hippocampal cells have behavioral correlates during the performance of an auditory working memory task in the rat," *Behavioral Neuroscience*, vol. 104, no. 2, pp. 253–263, 1990.

[22] Y. Sakurai, "Involvement of auditory cortical and hippocampal neurons in auditory working memory and reference memory in the rat," *Journal of Neuroscience*, vol. 14, no. 5, part 1, pp. 2606–2623, 1994.

[23] Y. Sakurai, "Hippocampal and neocortical cell assemblies encode memory processes for different types of stimuli in the rat," *Journal of Neuroscience*, vol. 16, no. 8, pp. 2809–2819, 1996.

[24] C. G. Wible, R. L. Findling, M. Shapiro, E. J. Lang, S. Crane, and D. S. Olton, "Mnemonic correlates of unit activity in the hippocampus," *Brain Research*, vol. 399, no. 1, pp. 97–110, 1986.

[25] S. I. Wiener, C. A. Paul, and H. Eichenbaum, "Spatial and behavioral correlates of hippocampal neuronal activity," *Journal of Neuroscience*, vol. 9, no. 8, pp. 2737–2763, 1989.

[26] E. R. Wood, P. A. Dudchenko, and H. Eichenbaum, "The global record of memory in hippocampal neuronal activity," *Nature*, vol. 397, no. 6720, pp. 613–616, 1999.

[27] B. J. Young, G. D. Fox, and H. Eichenbaum, "Correlates of hippocampal complex-spike cell activity in rats performing a nonspatial radial maze task," *Journal of Neuroscience*, vol. 14, no. 11, part 1, pp. 6553–6563, 1994.

[28] G. Winocur, "Anterograde and retrograde amnesia in rats with dorsal hippocampal or dorsomedial thalamic lesions," *Behavioural Brain Research*, vol. 38, no. 2, pp. 145–154, 1990.

[29] M. Bunsey and H. Eichenbaum, "Selective damage to the hippocampal region blocks long-term retention of a natural and nonspatial stimulus-stimulus association," *Hippocampus*, vol. 5, no. 6, pp. 546–556, 1995.

[30] M. Bunsey and H. Eichenbaum, "Conservation of hippocampal memory function in rats and humans," *Nature*, vol. 379, no. 6562, pp. 255–257, 1996.

[31] M. R. Bower, D. R. Euston, and B. L. McNaughton, "Sequential-context-dependent hippocampal activity is not necessary to learn sequences with repeated elements," *Journal of Neuroscience*, vol. 25, no. 6, pp. 1313–1323, 2005.

[32] J. Ferbinteanu and M. L. Shapiro, "Prospective and retrospective memory coding in the hippocampus," *Neuron*, vol. 40, no. 6, pp. 1227–1239, 2003.

[33] L. M. Frank, E. N. Brown, and M. Wilson, "Trajectory encoding in the hippocampus and entorhinal cortex," *Neuron*, vol. 27, no. 1, pp. 169–178, 2000.

[34] A. L. Griffin, H. Eichenbaum, and M. E. Hasselmo, "Spatial representations of hippocampal CA1 neurons are modulated by behavioral context in a hippocampus-dependent memory task," *Journal of Neuroscience*, vol. 27, no. 9, pp. 2416–2423, 2007.

[35] I. Lee, A. L. Griffin, E. A. Zilli, H. Eichenbaum, and M. E. Hasselmo, "Gradual translocation of spatial correlates of neuronal firing in the hippocampus toward prospective locations," *Neuron*, vol. 51, no. 5, pp. 639–650, 2006.

[36] P. A. Lipton, J. A. White, and H. Eichenbaum, "Disambiguation of overlapping experiences by neurons in the medial entorhinal cortex," *Journal of Neuroscience*, vol. 27, no. 21, pp. 5787–5795, 2007.

[37] E. R. Wood, P. A. Dudchenko, R. J. Robitsek, and H. Eichenbaum, "Hippocampal neurons encode information about different types of memory episodes occurring in the same location," *Neuron*, vol. 27, no. 3, pp. 623–633, 2000.

[38] H. Eichenbaum, "Hippocampus: cognitive processes and neural representations that underlie declarative memory," *Neuron*, vol. 44, no. 1, pp. 109–120, 2004.

[39] H. Eichenbaum, A. P. Yonelinas, and C. Ranganath, "The medial temporal lobe and recognition memory," *Annual Review of Neuroscience*, vol. 30, pp. 123–152, 2007.

[40] M. Fyhn, S. Molden, M. P. Witter, E. I. Moser, and M.-B. Moser, "Spatial representation in the entorhinal cortex," *Science*, vol. 305, no. 5688, pp. 1258–1264, 2004.

[41] T. Hafting, M. Fyhn, S. Molden, M.-B. Moser, and E. I. Moser, "Microstructure of a spatial map in the entorhinal cortex," *Nature*, vol. 436, no. 7052, pp. 801–806, 2005.

[42] F. Sargolini, M. Fyhn, T. Hafting, et al., "Conjunctive representation of position, direction, and velocity in entorhinal cortex," *Science*, vol. 312, no. 5774, pp. 758–762, 2006.

[43] H.-A. Steffenach, M. Witter, M.-B. Moser, and E. I. Moser, "Spatial memory in the rat requires the dorsolateral band of the entorhinal cortex," *Neuron*, vol. 45, no. 2, pp. 301–313, 2005.

[44] M. Fyhn, T. Hafting, A. Treves, M.-B. Moser, and E. I. Moser, "Hippocampal remapping and grid realignment in entorhinal cortex," *Nature*, vol. 446, no. 7132, pp. 190–194, 2007.

[45] K. L. Agster, N. J. Fortin, and H. Eichenbaum, "The hippocampus and disambiguation of overlapping sequences," *Journal of Neuroscience*, vol. 22, no. 13, pp. 5760–5768, 2002.

[46] A. A. Chiba, R. P. Kesner, and A. M. Reynolds, "Memory for spatial location as a function of temporal lag in rats: role of hippocampus and medial prefrontal cortex," *Behavioral and Neural Biology*, vol. 61, no. 2, pp. 123–131, 1994.

[47] N. J. Fortin, K. L. Agster, and H. B. Eichenbaum, "Critical role of the hippocampus in memory for sequences of events," *Nature Neuroscience*, vol. 5, no. 5, pp. 458–462, 2002.

[48] M. E. Hasselmo, "What is the function of hippocampal theta rhythm?—Linking bahavioral data to phasic properties of field potential and unit recording data," *Hippocampus*, vol. 15, no. 7, pp. 936–949, 2005.

[49] M. E. Hasselmo and H. Eichenbaum, "Hippocampal mechanisms for the context-dependent retrieval of episodes," *Neural Networks*, vol. 18, no. 9, pp. 1172–1190, 2005.

[50] J. S. Holdstock, A. R. Mayes, C. L. Isaac, Q. Gong, and N. Roberts, "Differential involvement of the hippocampus and temporal lobe cortices in rapid and slow learning of new semantic information," *Neuropsychologia*, vol. 40, no. 7, pp. 748–768, 2002.

[51] M. W. Howard, M. S. Fotedar, A. V. Datey, and M. E. Hasselmo, "The temporal context model in spatial navigation and relational learning: toward a common explanation of medial temporal lobe function across domains," *Psychological Review*, vol. 112, no. 1, pp. 75–116, 2005.

[52] R. P. Kesner and J. M. Novak, "Serial position curve in rats: role of the dorsal hippocampus," *Science*, vol. 218, no. 4568, pp. 173–175, 1982.

[53] W. B. Levy, "A sequence predicting CA3 is a flexible associator that learns and uses context to solve hippocampal-like tasks," *Hippocampus*, vol. 6, no. 6, pp. 579–590, 1996.

[54] G. O'Kane, E. A. Kensinger, and S. Corkin, "Evidence for semantic learning in profound amnesia: an investigation with patient H.M," *Hippocampus*, vol. 14, no. 4, pp. 417–425, 2004.

[55] E. Tulving and H. J. Markowitsch, "Episodic and declarative memory: role of the hippocampus," *Hippocampus*, vol. 8, no. 3, pp. 198–204, 1998.

[56] F. Vargha-Khadem, D. G. Gadian, K. E. Watkins, A. Connelly, W. Van Paesschen, and M. Mishkin, "Differential effects of early hippocampal pathology on episodic and semantic memory," *Science*, vol. 277, no. 5324, pp. 376–380, 1997.

[57] M. Verfaellie, P. Koseff, and M. P. Alexander, "Acquisition of novel semantic information in amnesia: effects of lesion location," *Neuropsychologia*, vol. 38, no. 4, pp. 484–492, 2000.

[58] E. Tulving, "Episodic memory: from mind to brain," *Annual Review of Psychology*, vol. 53, pp. 1–25, 2002.

[59] R. P. Kesner, P. E. Gilbert, and L. A. Barua, "The role of the hippocampus in memory for the temporal order of a sequence of odors," *Behavioral Neuroscience*, vol. 116, no. 2, pp. 286–290, 2002.

[60] M. L. Shapiro and D. S. Olton, "Hippocampal function and interference," in *Memory Systems*, E. Tulving and D. L. Schacter, Eds., pp. 87–117, MIT Press, Cambridge, Mass, USA, 1994.

[61] J. A. Ainge, M. Tamosiunaite, F. Woergoetter, and P. A. Dudchenko, "Hippocampal CA1 place cells encode intended destination on a maze with multiple choice points," *Journal of Neuroscience*, vol. 27, no. 36, pp. 9769–9779, 2007.

[62] M. E. Hasselmo, L. M. Giocomo, and E. A. Zilli, "Grid cell firing may arise from interference of theta frequency membrane potential oscillations in single neurons," *Hippocampus*, vol. 17, no. 12, pp. 1252–1271, 2007.

[63] G. V. Wallenstein, H. Eichenbaum, and M. E. Hasselmo, "The hippocampus as an associator of discontiguous events," *Trends in Neurosciences*, vol. 21, no. 8, pp. 317–323, 1998.

[64] D. Derdikman, M. Fyhn, T. Hafting, M.-B. Moser, and E. I. Moser, "Breaking up the entorhinal grid in a hairpin maze," Program No. 68.10. 2006. Neuroscience Meeting Planner. Atlanta, GA: Society for Neuroscience, 2006. Online.

[65] E. L. Hargreaves, G. Rao, I. Lee, and J. J. Knierim, "Neuroscience: major dissociation between medial and lateral entorhinal input to dorsal hippocampus," *Science*, vol. 308, no. 5729, pp. 1792–1794, 2005.

[66] P. Dayan and L. F. Abbott, *Theoretical Neuroscience: Computational and Mathematical Modeling of Neural Systems*, MIT Press, Cambridge, Mass, USA, 2001.

[67] R. D. Burwell, "The parahippocampal region: corticocortical connectivity," *Annals of the New York Academy of Sciences*, vol. 911, pp. 25–42, 2000.

[68] V. H. Brun, S. Leutgeb, H.-Q. Wu, et al., "Impaired spatial representation in CA1 after lesion of direct input from entorhinal cortex," *Neuron*, vol. 57, no. 2, pp. 290–302, 2008.

[69] R. Epstein and N. Kanwisher, "A cortical representation of the local visual environment," *Nature*, vol. 392, no. 6676, pp. 598–601, 1998.

[70] M. Bar and E. Aminoff, "Cortical analysis of visual context," *Neuron*, vol. 38, no. 2, pp. 347–358, 2003.

[71] H. Wan, J. P. Aggleton, and M. W. Brown, "Different contributions of the hippocampus and perirhinal cortex to recognition memory," *Journal of Neuroscience*, vol. 19, no. 3, pp. 1142–1148, 1999.

[72] E. Aminoff, N. Gronau, and M. Bar, "The parahippocampal cortex mediates spatial and nonspatial associations," *Cerebral Cortex*, vol. 17, no. 7, pp. 1493–1503, 2007.

Hindawi Publishing Corporation
Neural Plasticity
Volume 2008, Article ID 595282, 8 pages
doi:10.1155/2008/595282

Review Article

The Role of the Entorhinal Cortex in Extinction: Influences of Aging

Lia R. M. Bevilaqua,[1,2] Janine I. Rossato,[1] Juliana S. Bonini,[1] Jociane C. Myskiw,[1] Julia R. Clarke,[1] Siomara Monteiro,[1] Ramón H. Lima,[1] Jorge H. Medina,[1,3] Martín Cammarota,[1] and Iván Izquierdo[1]

[1] *Centro de Memória, Instituto de Pesquisas Biomédicas, Pontifícia Universidade Católica do Rio Grande do Sul, Avenue Ipiranga 6690, 2nd floor, 90610-000 Porto Alegre, RS, Brazil*
[2] *Centro Universitário IPA, Rua Cel. Joaquim Pedro Salgado 80, 90420-060 Porto Alegre, RS, Brazil*
[3] *Departamento de Fisiologia, Facultad de Medicina, Universidad de Buenos Aires, Paraguay 2155, 7th floor, 1121 Buenos Aires, Argentina*

Correspondence should be addressed to Iván Izquierdo, izquier@terra.com.br

Received 2 January 2008; Accepted 23 May 2008

Recommended by Min Jung

The entorhinal cortex is perhaps the area of the brain in which neurofibrillary tangles and amyloid plaques are first detectable in old age with or without mild cognitive impairment, and very particularly in Alzheimer's disease. It plays a key role in memory formation, retrieval, and extinction, as part of circuits that include the hippocampus, the amygdaloid nucleus, and several regions of the neocortex, in particular of the prefrontal cortex. Lesions or biochemical impairments of the entorhinal cortex hinder extinction. Microinfusion experiments have shown that glutamate NMDA receptors, calcium and calmodulin-dependent protein kinase II, and protein synthesis in the entorhinal cortex are involved in and required for extinction. Aging also hinders extinction; it is possible that its effect may be in part mediated by the entorhinal cortex.

Copyright © 2008 Lia R. M. Bevilaqua et al. This is an open access article distributed under the Creative Commons Attribution License, which permits unrestricted use, distribution, and reproduction in any medium, provided the original work is properly cited.

1. INTRODUCTION

Since extinction is perceived as the waning of a CR, it might be taken for the expression of forgetting [1]. However, real forgetting involves the actual disappearance of memories. Instead, contrarily to this, extinguished responses usually recover spontaneously with the passage of time [2]; in addition, upon retraining, they recover very rapidly [3–5]. This is usually taken to indicate that extinguished memories do not disappear but are just made less available for retrieval (Milad, 2006). Therefore, the most widely accepted view is that extinction is just one more form of learning, in which the CS is dissociated from the former unconditioned stimulus (US) and reassociated with a new US which consists precisely in the absence of the former US [2]. In other words, a new CS-no US association is formed which supersedes the former CS-US association [2, 6], and a new conditioned response (CR) develops, usually the omission of a formerly learned response. Gale et al. (2004) have in fact produced evidence that the basolateral amygdala stores fear memories for a rat's lifetime.

Some recent evidence, however, raises the alternative possibility that extinction may involve the actual erasure of a memory trace. Extinction can be made more intense by increasing the time that rats are exposed to the absence of a footshock US in an inhibitory avoidance conditioning paradigm. In these conditions, spontaneous recovery may not be (readily) seen, and the reinstallment of the original avoidance response requires again gene expression and protein synthesis in the hippocampus [6], as it would be if it were a new response [7]. Very importantly, two different groups [8, 9] have found that if conditioned startle (a mild form of conditioned fear) is extinguished 10 to 60 minutes or less after the original training, there is no spontaneous recovery; if, instead, extinction is carried out 24 or 72 hours after training, there is rapid reinstatement of the original response. Mao et al. also observed that intra-amygdala D-cycloserine administration not only enhanced extinction, but also, in addition, reversed a GluR1 increase caused by the original training. The findings of Myers et al. and Mao et al. might be important for therapeutic purposes. There has been a search for drugs or treatments that may effectively

erase a fearsome memory. Most findings have been negative. However, some reports indicate that two of these treatments, the β-adrenergic antagonist, propranolol (see [10]), and the gaseous anesthetic sevofluorane [11] can produce selective amnesia for emotional memories if administered at the time of encoding, but usually not later. The pretest administration of β blockers into entorhinal cortex, hippocampus, amygdala, or anterior cingulate cortex hinders retrieval (Barros et al., 2000). Retrieval often triggers a reconsolidation of learned responses [12]. Postretrieval propranolol hinders further recollection of traumatic memories in humans [13]. The potential usefulness of this finding is obvious. As said, many forms of learning that cannot be readily qualified as CRs can also be extinguished, and this is in fact why it is widely used in the psychotherapy of learned fear. It was originally advocated for the treatment of phobias by Freud in 1920s, but he gave it another name (habituation), which is a different form of learning [3, 14] (see below). Extinction has been also given other names when used for psychotherapeutic purposes [15], such as exposure therapy [16] or flooding [17, 18]. But it consists in all cases of what Pavlov [3], Konorski [4], and Rescorla [2] called extinction [19, 20].

2. EXTINCTION IS NOT HABITUATION

There are similarities and differences between extinction and habituation. As defined by Pavlov [3] and by hundreds of others after him [4, 14, 21], habituation consists in the gradual reduction of the natural, unlearned response to an unassociated stimulus or constellation of stimuli; that is, of the response to novelty. "As we sit by a highway we often quickly come to ignore the sounds of passing automobiles" [21]. The same can be said of exploration of a new environment [14], of smelling the same odor for a long time, and so forth. The response to novelty or to a novel stimulus or set of stimuli is remarkably similar across species and stimuli, and involves arousal and movements of the eyes, ears, head, or body toward the source of the stimuli; it is called the "orienting" [22] or "what is it?" reflex [3]. The hippocampal molecular correlates of the response to a novel stimulus have been studied only recently. It involves the activation of different protein kinases in the hippocampus [23–25], and by the phosphorylation of the constitutive transcription factor CREB (cAMP response element binding protein) [26, 27]. This sequence of events underlies the effects of novelty on the formation of long-term memories, as part of a process of behavioral tagging [28]. Like extinction, habituation results from the repetition of a stimulus; but of a novel stimulus rather than one that had been used to form a previous association [3]. However, unlike extinction [2, 6], habituation is widely viewed as nonassociative. Also unlike extinction, habituation must be differentiated from fatigue. Pavlov [3] considered both habituation and extinction as forms of "internal inhibition", as opposed to the stimuli that cause distraction and eventually may induce dishabituation, which he and his followers considered as examples of "external inhibition." A major difference between both forms of "inhibition" is that whereas the "internal" type leads to diminished arousal levels, and even eventually to sleep, external inhibition causes an enhancement of arousal or alertness [3, 4]. Dishabituation has been more recently viewed as another form of learning [29], separate from [30] or linked to sensitization [31].

3. EXTINCTION IS NOT FORGETTING

Real forgetting involves the actual erasure of learned information. It may rely on the atrophy and eventual disappearance of synapses by disuse, as described by Eccles (1955). Indeed, we forget the face of people we saw just once or twice and then never again, unless they were highly arousing or emotionally important [32, 33]. Memories are believed to be formed and stored in synapses since Cajal [34] (see [33, 35]). In contrast, extinguished responses, knowledge, or behavior are reinstated immediately after a presentation of the US even if unassociated with the cue [36]. Relearning after extinction is usually much quicker than the original learning [5]. In addition, it may occur even if the US is presented out of context; without pairing with the CS or even outside of the training apparatus (i.e., the so-called "reminder foot-shock", [37]). As commented above, it might be possible to proceed to the formal disappearance of a memory through an extinction procedure [6, 8, 9], see; [19]. Further indirect evidence for this is suggested by Lin et al. (2003a,b) who reported that, in the amygdala, the phosphatase calcineurin may weaken memory traces originally built by phosphatidylinositol 3-kinase mediated phosphorylation, and thereby generate extinction. In addition, recent results indicate that extinction reverses conditioning-induced enhancement of surface expression of AMPA receptor subunits in synaptsomes prepared from the lateral amygdala [38]. However, in none of the experiments which suggest that extinction may involve trace erasure is there sufficient evidence to go beyond the demonstration of a formal erasure, not of a real and incontrovertible erasure of a trace. There might always be a fragment or a hidden or otherwise strongly inhibited (repressed?) component of the memory trace thought to be lost somewhere in the brain, and it may reappear unexpectedly long after it was thought to be forgotten. One must bear in mind that the most widely used forms of psychotherapy are based precisely on this premise (see [39]).

4. BRAIN CIRCUITS IN EXTINCTION

Several fMRI studies show an activation of prefrontal areas, notably the ventromedial prefrontal cortex (vmPFC), together with reduced blood flow in the basolateral amygdala (BLA) [40–42] and/or the hippocampus (Milad et al., 2006); [43], in the extinction of conditioned fear responses. Importantly, the data fit with the previous evidence for a crucial role for the vmPFC ([44–47], but see also [48, 49]), and with important roles for the BLA [50, 51] and the hippocampus in retrieval and in extinction [52, 53]. Circuits linking the vmPFC with the amygdala [40] and the hippocampus (Sotres-Bayon et al., 2007), [42] in extinction have been proposed. A separate role for each of these two

pathways in extinction has been envisaged by Corcoran and Quirk [54]. Circuits linking the vmPFC and as well as the dorsolateral PFC with the hippocampus have also been recently described for memory consolidation [55]; the vmPFC-hippocampus link has actually been viewed as obligatory both for consolidation and reconsolidation [41]. In more than one respect, the physiology of extinction learning is similar to that of the noninhibitory, or "regular" forms of learning; that is, the acquisition and storage of the "original" tasks that are later to be extinguished [56]. This of course agrees with the now widely accepted notion that extinction is just one more form of learning [2]. Localized brain microinfusion studies have shown that, depending on the task, the hippocampus [36, 52], the BLA [50, 51], the vmPFC (in conditioned taste aversion), and the insular cortex [56] are involved in, and are necessary for, extinction. The sequence of molecular events involved most of these regions includes glutamate N-methyl-D-aspartate (NMDA) receptors, protein kinase A, and protein synthesis in all areas studied (Vianna et al., 2004), calcium and calmodulin-dependent protein kinase II (CaMKII) in some [52, 57], and the extracellular signal regulated kinases (ERKs) in others [51]. Overall, these molecular requirements are analogous to those of memory consolidation of the original tasks [33], which further stresses the point that extinction is indeed a form of learning. In all cases, the molecular findings on extinction were determined by the use of receptor antagonists (AP5), inhibitors of CaMKII (KN62 or KN93), PKA inhibitors (Rp-cAMPs, KT5720 or others), ERK1/2 inhibitors, and protein synthesis inhibitors or inhibitors of gene expression. In the case of NMDA receptors, the partial allosteric agonist D-cycloserine has also been studied (see below). Even though all brain areas that participate in extinction in one or other task have been found to use signaling pathways and involve protein synthesis (see above), the signaling of gene expression by protein kinase cascades must surely be different across tasks and across brain areas [57–59]. For example, the ERKs are involved in extinction of auditory fear conditioning in amygdala [60] and in the extinction of contextual fear conditioning [59] and of inhibitory avoidance in hippocampus [52] but not in entorhinal cortex [57]. The extinction of conditioned taste aversion has different molecular requirements in the insula [56] and the amygdala (Bahar et al., 2003), and both are different to those reported in amygdala, hippocampus, entorhinal, or medial prefrontal cortex in other tasks (see above).

5. THE ENTORHINAL CORTEX: A ROLE IN LEARNING AND A ROLE IN EXTINCTION

Several early studies using localized brain lesion or stimulation techniques [61–64] and one recent pharmacological study [57] point to a crucial role of the entorhinal cortex (EC) in extinction, mostly of aversive tasks. Lesions of the entorhinal cortex inhibit not only various forms of extinction in rats but also some forms of habituation [65, 66]. Indeed, the best and most illustrative source of evidence in favor of a fundamental role of the entorhinal cortex in extinction, and indeed in all forms of learning, is human pathology: from the analysis of the famous amnestic patient H.M. [67, 68] to that of humans with mild cognitive impairment and/or with early Alzheimer's disease ([69], see below). A few studies of lesions of the EC in animals have failed to produce any result on extinction [70–72]. But some of these negative studies have also failed to detect influences of EC lesions on acquisition and retention [70] and simple discrimination [72], which disagrees with the vast majority of papers on the role of the EC in learning (see above, and [57, 69, 73] for references). In several of the negative results with entorhinal lesions, these were incomplete or encompassed other areas as well. Both the lesion and the stimulation techniques that were in vogue 20 or more years ago often gave artifactual results attributable to spread to neighboring physiologically unrelated areas [74]. In many cases, those results have not been confirmed by the more selective and circumscribed imaging, histo- or neurochemical results of the last decade or so. No doubt the entorhinal cortex must be a key component of any circuit that includes the vmPFC, the BLA, and the hippocampus, particularly one that links the former to the latter two, as has been suggested for extinction [54] (see above). First, a very large number of afferent and efferent connections between the vmPFC and the hippocampus and amygdala relay in the entorhinal cortex [75]. Second, the entorhinal cortex is the afferent and efferent relay for BLA and hippocampal connections with other regions of the rest of the cerebral cortex, all of which are connected to the entorhinal cortex [76]. Van Hoesen [76] has in fact stated that "it is clear that the entorhinal cortices receive potentially a significant portion of the sensory output generated by forebrain structures and this includes both interoceptive and exteroceptive information. In structural terms, it could be argued that the entorhinal cortex would be privy to or receive a digest of nearly all neural reactions and many of the combinations or permutations that may result. Third, the entorhinal cortex probably plays an active learning role rather than a role as a mere relay in extinction, as microneuropharmacological studies suggest. Fourth, and perhaps very importantly, medial EC neurons display positional firing properties that are somewhat different from, but related to, that of hippocampal place cells [77, 78]. Importantly, short-term memory lasting up to 3 or 4 hours is known to be processed mainly by the entorhinal cortex [23, 24, 33] and does not have extinction (Cammarota et al., 2006). Short-term memory is in charge of cognitive processing while long-term memory is being slowly built-up (Izquierdo et al., 1978), [33]. By the nature of its function, it should not have extinction (Izquierdo et al., 1978), [53], and indeed it does not leave biochemically identifiable traces [23, 33].

6. MOLECULAR BASIS OF THE ROLE OF THE ENTORHINAL CORTEX IN EXTINCTION

The molecular basis of inhibitory avoidance [33] and other forms of learning [58] has been studied in detail in recent years. In the case of extinction, it was studied in the ventromedial prefrontal cortex (vmPFC), the basolateral amygdala (BLA), the CA1 region of the hippocampus, the

insular cortex (for conditioned taste aversion), and in the entorhinal cortex. The area of the brain in which the biological basis of extinction has been studied in most tasks is the vmPFC (see above). This area connects to the BLA and the hippocampus in order to regulate extinction, and this connection is through the entorhinal cortex [75, 76]. The dorsal hippocampus has been studied in relation to extinction very extensively, but almost exclusively in one trial step-down inhibitory avoidance [36], (Vianna et al., 2004), [6, 52, 79]. This is the task in which the molecular basis of consolidation is best known [33]. Extinction of this form of learning is indeed susceptible to the deleterious effect of the glutamate NMDA receptor blocker, 2-amino-5-phosphono pentanoate (AP5), the CaMKII inhibitor, KN93, and the protein synthesis inhibitor, anisomycin, infused into the entorhinal cortex at the time of the first of a series of retrieval sessions [57]. NMDA receptors, CaMKII, and protein synthesis are crucial for the formation of a new memory and, of course, for consolidation of this task in the hippocampus [33]. Therefore, both lesion and microinfusion experiments support a role for the entorhinal cortex in extinction; which was predictable from anatomical knowledge [76].

7. AGING AND EXTINCTION

It is widely agreed that aging is accompanied by a cognitive decline both in laboratory animals and in humans. Behavioral and molecular aspects of this decline have been studied extensively in the last two decades (see [80]). Recent studies have specifically demonstrated a decline of the capacity to extinguish in aged rats [81–84]. Perhaps the first to study this systematically in laboratory animals was Schneider-Rivas and his group. The decline of extinction seen in old rats correlates with changes in brain serotonin and 5-hydroxy-indole acetic acid in neocortex, hippocampus, thalamus, and dorsal raphe nucleus compatible with predictions from the serotonin hypothesis of depression, as well as with other brain neurochemical correlates ([82], see also [84, 85]). Others have reported an abnormality of forced extinction in aged rats submitted to removal of the escape platform in a water maze ([83, 86–88], see also [89]). In aged rats, this procedure quickly leads to immobility, which the authors have termed "despair" behavior by analogy with "learned helplessness" paradigms, and which they view as a model of depression [87, 88]. The immobility is accompanied by a number of symptoms of anxiety, and by a large number of neurotransmitter changes both in striatum and in hippocampus [86, 88]. The immobility triggered by forced extinction in aged rats can be reduced by chronic desimipramine, but is actually enhanced by chronic fluoxetine, however [87]. In the forced extinction experiments in the water maze, the animals find themselves all of a sudden without the regular escape that they had learned to attain, which surely is traumatic and should cause despair. Forced extinction might happen as a result of the losses suffered by the aged, which have been so often cited as triggers of depressive episodes. When the aging person loses friends or family, or is forced to retire, or finds to have lost sensory, mental or physical powers, (s)he automatically suffers the forced extinction of a rich and large variety of responses. The cues are there: objects, pictures, remembrances, smells, sounds pertaining to the elements lost; but the response is prevented from happening because the elements themselves are gone forever. This usually occurs with pain and often with despair; and may be viewed as a nonadaptive form of extinction. The picture can be very distressing and thus lead the way to posttraumatic stress [16, 20]. The deficit of extinction in aging reported by most authors may have serious consequences, such as a proneness to perform dangerous behaviors and therefore be exposed to genuine fear situations (Izquierdo et al., 2004), ([90], see [47]).

8. AGING AND THE ENTORHINAL CORTEX

Perhaps the region of the brain which ages more rapidly is the entorhinal cortex. Normal aging has been known for many years to be accompanied by a reduction of neuron and synapse counts in many regions of the cerebral cortex, particularly the entorhinal cortex and then the hippocampus. The earliest occurrence of prototypical lesions in Alzheimer's disease is usually considered to be in the entorhinal cortex ([69], Jellinger et al., 1991, see [91, 92]). However, in a sizable proportion of normal aged persons lesions typical of Alzheimer's disease such as neurofibrillary tangles and neuritic plaques are also seen (Jellinger et al., 1991), [93–96], together, of course, with computerized tomography or other imaging changes suggestive of a degree of brain atrophy [91, 96, 97]. The question has been asked whether the mild cognitive impairment often seen in the aged correlates with a larger number of such lesions than that seen in the normal aged subjects, and/or with a peculiar concentration of them in the hippocampus and entorhinal cortex [96, 98]. Recent findings indicate that the answer to both questions is positive [99, 100]. Years ago it was suggested that the early atrophy of the hippocampus and particularly the entorhinal cortex could be an early marker of Alzheimer's disease [91, 92]. This correlates with the high incidence of lesions viewed as typical of Alzheimer's in the entorhinal cortex and in the hippocampus, in that order of importance in that disease [69], (Jellinger et al., 1991). Recent observations are somewhat more cautious [100, 101] and suggest that the combined use of imaging techniques plus that of cerebrospinal fluid biomarkers [101] are more likely to yield an adequate monitoring of the preclinical diagnosis of Alzheimer's in as much as the occurrence of lesions and of imaging changes in the normal and the demented elderly overlaps perhaps more than was originally thought [96, 101]. However, many studies indicate that cortical losses in the hippocampus and entorhinal cortex of elderly patients do predict mild cognitive impairment [102]. This prediction is more consistent than that of the eventual conversion of mild cognitive impairment into full-fledged Alzheimer symptomatology [103]. The dissociation of hippocampal and entorhinal memory functions has been difficult and fraught with pitfalls in as much as there is such a close interconnection between the two [75] and

lesions of both structures cause very large and complete memory losses in animals (see [73]). There has been one purportedly successful attempt to dissociate the contribution of hippocampus and entorhinal cortex to different aspects of memory function in the elderly; namely, conscious recollection and familiarity-based judgments [104]; but this should be complemented by observations on other forms of memory. To be sure, aging-related changes have not only been described in the entorhinal cortex and the hippocampus, but also in other regions of the brain involved in learning and in extinction. In a very careful study, Burgmans et al. [105] reported that prefrontal cortex atrophy (particularly of the orbital region) is seen in elderly patients with cognitive impairment and more intensely in those with dementia, and is a better predictor of the latter over a 6-year period than medial temporal lobe atrophy. In the rat basolateral amygdala, a hypertrophy of the dendritic tree independent of sex was seen in aged (20–24-month old) animals as compared with 3–5-month old animals (Rubinow et al., 2007). How does this hypertrophy relate to the atrophy described in the prefrontal cortex and in the medial temporal lobe de-scribed in aging mammals, including humans, it is hard to tell.

9. CONCLUSIONS

The entorhinal cortex plays a key role in cognition. It contributes to, and processes, information that the rest of the cortex, particularly the prefrontal areas, sends to it in order to be relayed to the hippocampus and amygdala, as part of the acquisition, retrieval, or extinction of many forms of learning. In addition, the entorhinal cortex also processes information generated by the hippocampus and sends it to the neocortex, and interconnects the hippocampus with its main regulatory nucleus complex, the amygdala. Thus the entorhinal cortex is crucially involved in all aspects of learning. Its role in extinction has been best studied in aversive tasks. The entorhinal cortex on one hand and extinction on the other suffer severe losses with aging. The changes are more marked in humans with mild cognitive impairment, and much worse in Alzheimer's disease, in which the entorhinal losses are diagnostic at early stages. The impairment of extinction seen in old age may be related in part to entorhinal cortex damage.

ACKNOWLEDGMENTS

Work supported by grants from the National Research Council of Brazil (CNPq) for the study of aging to L. R. M. Bevilaqua, M. Cammarota, and I. Izquierdo. L. R. M. Bevilaqua, M. Cammarota, and I. Izquierdo are CNPq Research Fellows. J. H. Medina is a CAPES Visiting Research Fellow at Programa de Pós-graduação em Ciências Médicas, PUCRS.

REFERENCES

[1] T. Tsumoto, "Long-term depression in cerebral cortex: a possible substrate of "forgetting" that should not be forgotten," *Neuroscience Research*, vol. 16, no. 4, pp. 263–270, 1993.

[2] R. A. Rescorla, "Retraining of extinguished Pavlovian stimuli," *Journal of Experimental Psychology: Animal Behavior Processes*, vol. 27, no. 2, pp. 115–124, 2001.

[3] I. P. Pavlov, *Conditioned Reflexes: An Investigation of the Physiological Activity of the Cerebral Cortex*, Oxford University Press, London, UK, 1927.

[4] J. Konorski, *Conditioned Reflexes and Neuron Organization*, Cambridge University Press, Cambridge, UK, 1948.

[5] I. Izquierdo, W. Wyrwicka, G. Sierra, and J. P. Segundo, "Établissement de reflexes conditionnés de trace pendant le sommeil naturel chez le chat," *Actual Neurophysiol*, vol. 6, pp. 277–296, 1965.

[6] M. Cammarota, L. R. M. Bevilaqua, D. Kerr, J. H. Medina, and I. Izquierdo, "Inhibition of mRNA and protein synthesis in the CA1 region of the dorsal hippocampus blocks reinstallment of an extinguished conditioned fear response," *The Journal of Neuroscience*, vol. 23, no. 3, pp. 737–741, 2003.

[7] L. M. Igaz, M. R. M. Vianna, J. H. Medina, and I. Izquierdo, "Two time periods of hippocampal mRNA synthesis are required for memory consolidation of fear-motivated learning," *The Journal of Neuroscience*, vol. 22, no. 15, pp. 6781–6789, 2002.

[8] S.-C. Mao, Y.-H. Hsiao, and P.-W. Gean, "Extinction training in conjunction with a partial agonist of the glycine site on the NMDA receptor erases memory trace," *The Journal of Neuroscience*, vol. 26, no. 35, pp. 8892–8899, 2006.

[9] K. M. Myers, K. J. Ressler, and M. Davis, "Different mechanisms of fear extinction dependent on length of time since fear acquisition," *Learning & Memory*, vol. 13, no. 2, pp. 216–223, 2006.

[10] S. P. Orr, M. R. Milad, L. J. Metzger, N. B. Lasko, M. W. Gilbertson, and R. K. Pitman, "Effects of beta blockade, PTSD diagnosis, and explicit threat on the extinction and retention of an aversively conditioned response," *Biological Psychology*, vol. 73, no. 3, pp. 262–271, 2006.

[11] M. T. Alkire, R. Gruver, J. Miller, J. R. McReynolds, E. L. Hahn, and L. Cahill, "Neuroimaging analysis of an anesthetic gas that blocks human emotional memory," *Proceedings of the National Academy of Sciences of the United States of America*, vol. 105, no. 5, pp. 1722–1727, 2008.

[12] N. C. Tronson and J. R. Taylor, "Molecular mechanisms of memory reconsolidation," *Nature Reviews Neuroscience*, vol. 8, no. 4, pp. 262–275, 2007.

[13] A. Brunet, S. P. Orr, J. Tremblay, K. Robertson, K. Nader, and R. K. Pitman, "Effect of post-retrieval propranolol on psychophysiologic responding during subsequent script-driven traumatic imagery in post-traumatic stress disorder," *Journal of Psychiatric Research*, vol. 42, no. 6, pp. 503–506, 2008.

[14] M. R. M. Vianna, M. Alonso, H. Viola, et al., "Role of hippocampal signaling pathways in long-term memory formation of a nonassociative learning task in the rat," *Learning & Memory*, vol. 7, no. 5, pp. 333–340, 2000.

[15] B. O. Rothbaum and M. Davis, "Applying learning principles to the treatment of post-trauma reactions," *Annals of the New York Academy of Sciences*, vol. 1008, pp. 112–121, 2003.

[16] W. S. Beckett, "Post-traumatic stress disorder," *New England Journal of Medicine*, vol. 346, no. 19, pp. 1495–1498, 2002.

[17] J. Difede, J. Cukor, N. Jayasinghe, et al., "Virtual reality exposure therapy for the treatment of posttraumatic stress disorder following September 11, 2001," *Journal of Clinical Psychiatry*, vol. 68, no. 11, pp. 1639–1647, 2007.

[18] M. Sijbrandij, M. Olff, J. B. Reitsma, I. V. E. Carlier, M. H. de Vries, and B. P. R. Gersons, "Treatment of acute

posttraumatic stress disorder with brief cognitive behavioral therapy: a randomized controlled trial," *American Journal of Psychiatry*, vol. 164, no. 1, pp. 82–90, 2007.

[19] M. Barad, "Is extinction of fear erasure or inhibition? why both, of course," *Learning & Memory*, vol. 13, no. 2, pp. 108–109, 2006.

[20] M. Davis, K. Ressler, B. O. Rothbaum, and R. Richardson, "Effects of D-cycloserine on extinction: translation from preclinical to clinical work," *Biological Psychiatry*, vol. 60, no. 4, pp. 369–375, 2006.

[21] H. Harlow, J. L. McGaugh, and R. F. Thompson, *Psychology*, Albion, San Francisco, Calif, USA, 1971.

[22] E. N. Sokolov, N. I. Nezlina, V. B. Polyanskii, and D. V. Evtikhin, "The orientating reflex: the "targeting reaction" and "searchlight of attention"," *Neuroscience and Behavioral Physiology*, vol. 32, no. 4, pp. 347–362, 2002.

[23] L. A. Izquierdo, D. M. Barros, J. H. Medina, and I. Izquierdo, "Novelty enhances retrieval of one-trial avoidance learning in rats 1 or 31 days after training unless the hippocampus is inactivated by different receptor antagonists and enzyme inhibitors," *Behavioural Brain Research*, vol. 117, no. 1-2, pp. 215–220, 2000.

[24] L. A. Izquierdo, D. M. Barros, P. G. Ardenghi, et al., "Different hippocampal molecular requirements for short- and long-term retrieval of one-trial avoidance learning," *Behavioural Brain Research*, vol. 111, no. 1-2, pp. 93–98, 2000.

[25] H. Viola, M. Furman, L. A. Izquierdo, et al., "Phosphorylated cAMP response element-binding protein as a molecular marker of memory processing in rat hippocampus: effect of novelty," *The Journal of Neuroscience*, vol. 20, no. 23, p. RC112, 2000.

[26] M. Winograd and H. Viola, "Detection of novelty, but not memory of spatial habituation, is associated with an increase in phosphorylated cAMP response element-binding protein levels in the hippocampus," *Hippocampus*, vol. 14, no. 1, pp. 117–123, 2004.

[27] D. Moncada and H. Viola, "Phosphorylation state of CREB in the rat hippocampus: a molecular switch between spatial novelty and spatial familiarity?" *Neurobiology of Learning and Memory*, vol. 86, no. 1, pp. 9–18, 2006.

[28] D. Moncada and H. Viola, "Induction of long-term memory by exposure to novelty requires protein synthesis: evidence for a behavioral tagging," *The Journal of Neuroscience*, vol. 27, no. 28, pp. 7476–7481, 2007.

[29] C. H. Rankin and T. J. Carew, "Development of learning and memory in Aplysia. II. Habituation and dishabituation," *The Journal of Neuroscience*, vol. 7, no. 1, pp. 133–143, 1987.

[30] C. H. Rankin and T. J. Carew, "Dishabituation and sensitization emerge as separate processes during development in Aplysia," *The Journal of Neuroscience*, vol. 8, no. 1, pp. 197–211, 1988.

[31] R. D. Hawkins, T. E. Cohen, and E. R. Kandel, "Dishabituation in Aplysia can involve either reversal of habituation or superimposed sensitization," *Learning & Memory*, vol. 13, no. 3, pp. 397–403, 2006.

[32] L. Cahill, "Similar neural mechanisms for emotion-induced memory impairment and enhancement," *Proceedings of the National Academy of Sciences of the United States of America*, vol. 100, no. 23, pp. 13123–13124, 2003.

[33] I. Izquierdo, L. R. M. Bevilaqua, J. I. Rossato, J. S. Bonini, J. H. Medina, and M. Cammarota, "Different molecular cascades in different sites of the brain control memory consolidation," *Trends in Neurosciences*, vol. 29, no. 9, pp. 496–505, 2006.

[34] S. R. Y. Cajal, "Neue Darstellung vom histologischen Bau des Zentralnervösen System," *Archiv für Anatomie und Physiologie*, pp. 319–428, 1893.

[35] J. C. Eccles, *The Physiology of Synapses*, Springer, Berlin, Germany, 1963.

[36] M. R. M. Vianna, G. Szapiro, J. L. McGaugh, J. H. Medina, and I. Izquierdo, "Retrieval of memory for fear-motivated training initiates extinction requiring protein synthesis in the rat hippocampus," *Proceedings of the National Academy of Sciences of the United States of America*, vol. 98, no. 21, pp. 12251–12254, 2001.

[37] A. M. Schneider, P. E. Gold, J. W. Haycock, and J. L. McGaugh, "Retrograde amnesia and the "reminder effect"," *Science*, vol. 186, no. 4169, pp. 1135–1136, 1974.

[38] J. Kim, S. Lee, K. Park, et al., "Amygdala depotentiation and fear extinction," *Proceedings of the National Academy of Sciences of the United States of America*, vol. 104, no. 52, pp. 20955–20960, 2007.

[39] M. C. Anderson, K. N. Ochsner, B. Kuhl, et al., "Neural systems underlying the suppression of unwanted memories," *Science*, vol. 303, no. 5655, pp. 232–235, 2004.

[40] E. A. Phelps, M. R. Delgado, K. I. Nearing, and J. E. LeDoux, "Extinction learning in humans: role of the amygdala and vmPFC," *Neuron*, vol. 43, no. 6, pp. 897–905, 2004.

[41] I. Akirav and M. Maroun, "Ventromedial prefrontal cortex is obligatory for consolidation and reconsolidation of object recognition memory," *Cerebral Cortex*, vol. 16, no. 12, pp. 1759–1765, 2006.

[42] I. Akirav and M. Maroun, "The role of the medial prefrontal cortex-amygdala circuit in stress effects on the extinction of fear," *Neural Plasticity*, vol. 2007, Article ID 30873, 11 pages, 2007.

[43] R. Kalisch, E. Korenfeld, K. E. Stephan, N. Weiskopf, B. Seymour, and R. J. Dolan, "Context-dependent human extinction memory is mediated by a ventromedial prefrontal and hippocampal network," *The Journal of Neuroscience*, vol. 26, no. 37, pp. 9503–9511, 2006.

[44] A. Burgos-Robles, I. Vidal-Gonzalez, E. Santini, and G. J. Quirk, "Consolidation of fear extinction requires NMDA receptor-dependent bursting in the ventromedial prefrontal cortex," *Neuron*, vol. 53, no. 6, pp. 871–880, 2007.

[45] M. R. Milad, G. J. Quirk, R. K. Pitman, S. P. Orr, B. Fischl, and S. L. Rauch, "A role for the human dorsal anterior cingulate cortex in fear expression," *Biological Psychiatry*, vol. 62, no. 10, pp. 1191–1194, 2007.

[46] G. J. Quirk and J. S. Beer, "Prefrontal involvement in the regulation of emotion: convergence of rat and human studies," *Current Opinion in Neurobiology*, vol. 16, no. 6, pp. 723–727, 2006.

[47] G. J. Quirk and D. Mueller, "Neural mechanisms of extinction learning and retrieval," *Neuropsychopharmacology*, vol. 33, no. 1, pp. 56–72, 2008.

[48] M. A. Morgan, J. Schulkin, and J. E. LeDoux, "Ventral medial prefrontal cortex and emotional perseveration: the memory for prior extinction training," *Behavioural Brain Research*, vol. 146, no. 1-2, pp. 121–130, 2003.

[49] R. Garcia, C.-H. Chang, and S. Maren, "Electrolytic lesions of the medial prefrontal cortex do not interfere with long-term memory of extinction of conditioned fear," *Learning & Memory*, vol. 13, no. 1, pp. 14–17, 2006.

[50] K. M. Myers and M. Davis, "Behavioral and neural analysis of extinction," *Neuron*, vol. 36, no. 4, pp. 567–584, 2002.

[51] K. M. Myers and M. Davis, "Mechanisms of fear extinction," *Molecular Psychiatry*, vol. 12, no. 2, pp. 120–150, 2007.

[52] G. Szapiro, M. R. M. Vianna, J. L. McGaugh, J. H. Medina, and I. Izquierdo, "The role of NMDA glutamate receptors, PKA, MAPK, and CAMKII in the hippocampus in extinction of conditioned fear," *Hippocampus*, vol. 13, no. 1, pp. 53–58, 2003.

[53] M. Cammarota, L. R. M. Bevilaqua, J. I. Rossato, M. Ramirez, J. H. Medina, and I. Izquierdo, "Relationship between short- and long-term memory and short- and long-term extinction," *Neurobiology of Learning and Memory*, vol. 84, no. 1, pp. 25–32, 2005.

[54] K. A. Corcoran and G. J. Quirk, "Recalling safety: cooperative functions of the ventromedial prefrontal cortex and the hippocampus in extinction," *CNS Spectrums*, vol. 12, no. 3, pp. 200–206, 2007.

[55] L. A. Izquierdo, D. M. Barros, J. C. da Costa, et al., "A link between role of two prefrontal areas in immediate memory and in long-term memory consolidation," *Neurobiology of Learning and Memory*, vol. 88, no. 2, pp. 160–166, 2007.

[56] D. E. Berman and Y. Dudai, "Memory extinction, learning anew, and learning the new: dissociations in the molecular machinery of learning in cortex," *Science*, vol. 291, no. 5512, pp. 2417–2419, 2001.

[57] L. R. M. Bevilaqua, J. S. Bonini, J. I. Rossato, L. A. Izquierdo, M. Cammarota, and I. Izquierdo, "The entorhinal cortex plays a role in extinction," *Neurobiology of Learning and Memory*, vol. 85, no. 2, pp. 192–197, 2006.

[58] G. Riedel and B. Platt, *From Messengers to Molecules: Memories are Made of These*, Kluwer Academic Publishers, New York, NY, USA, 2004.

[59] A. Fischer, M. Radulovic, C. Schrick, F. Sananbenesi, J. Godovac-Zimmermann, and J. Radulovic, "Hippocampal Mek/Erk signaling mediates extinction of contextual freezing behavior," *Neurobiology of Learning and Memory*, vol. 87, no. 1, pp. 149–158, 2007.

[60] C. Herry, P. Trifilieff, J. Micheau, A. Lüthi, and N. Mons, "Extinction of auditory fear conditioning requires MAPK/ERK activation in the basolateral amygdala," *European Journal of Neuroscience*, vol. 24, no. 1, pp. 261–269, 2006.

[61] M. Gauthier and C. Destrade, "Late post-learning effect of entorhinal cortex electrical stimulation persists despite destruction of the perforant path," *Brain Research*, vol. 310, no. 1, pp. 174–179, 1984.

[62] T. N. Oniani, N. G. Nachkebia, A. Y. Nachkebia, E. V. Chkhartishvili, and L. T. Oniani, "The influence of electrocoagulation of the septum and section of the entorhinal cortex on general behaviour and memory in cats," *Acta Physiologica Hungarica*, vol. 74, no. 1, pp. 9–25, 1989.

[63] A. Ueki, C. Miwa, and K. Miyoshi, "Impairment in the acquisition of passive and active avoidance learning tasks due to bilateral entorhinal cortex lesions," *Journal of the Neurological Sciences*, vol. 125, no. 1, pp. 14–21, 1994.

[64] J. H. Freeman Jr., A. Weible, J. Rossi, and M. Gabriel, "Lesions of the entorhinal cortex disrupt behavioral and neuronal responses to context change during extinction of discriminative avoidance behavior," *Experimental Brain Research*, vol. 115, no. 3, pp. 445–457, 1997.

[65] C. Köhler and H. Sundberg, "Locomotor activity and exploratory behavior after medial entorhinal cortex lesions in the albino rat," *Behavioral Biology*, vol. 20, no. 4, pp. 419–432, 1977.

[66] C. Köhler and H. Sundberg, "Orienting and habituation after lesions of the medial entorhinal cortex in the albino rat," *Behavioral and Neural Biology*, vol. 27, no. 3, pp. 276–293, 1979.

[67] S. Corkin, D. G. Amaral, R. G. González, K. A. Johnson, and B. T. Hyman, "H. M.'s medial temporal lobe lesion: findings from magnetic resonance imaging," *The Journal of Neuroscience*, vol. 17, no. 10, pp. 3964–3979, 1997.

[68] D. H. Salat, A. J. W. van der Kouwe, D. S. Tuch, et al., "Neuroimaging H.M.: a 10-year follow-up examination," *Hippocampus*, vol. 16, no. 11, pp. 936–945, 2006.

[69] H. Braak and E. Braak, "Neurofibrillary changes confined to the entorhinal region and an abundance of cortical amyloid in cases of presenile and senile dementia," *Acta Neuropathologica*, vol. 80, no. 5, pp. 479–486, 1990.

[70] H. Sundberg and C. Köhler, "One way active avoidance after angular bundle and entorhinal cortex lesions in the albino rat," *Behavioral Biology*, vol. 19, no. 3, pp. 371–379, 1977.

[71] B. K. Yee, J. Feldon, and J. N. P. Rawlins, "Cytotoxic lesions of the retrohippocampal region attenuate latent inhibition but spare the partial reinforcement extinction effect," *Experimental Brain Research*, vol. 115, no. 2, pp. 247–256, 1997.

[72] I. Daum, S. Channon, and J. A. Gray, "Classical conditioning after temporal lobe lesions in man: sparing of simple discrimination and extinction," *Behavioural Brain Research*, vol. 52, no. 2, pp. 159–165, 1992.

[73] L. R. Squire, *Memory and Brain*, Oxford University Press, New York, NY, USA, 1992.

[74] I. Izquierdo and J. H. Medina, "On brain lesions, the milkman and sigmunda," *Trends in Neurosciences*, vol. 21, no. 10, pp. 423–426, 1998.

[75] B. T. Hyman, G. W. Van Hoesen, and A. R. Damasio, "Memory-related neural systems in Alzheimer's disease: an anatomic study," *Neurology*, vol. 40, no. 11, pp. 1721–1730, 1990.

[76] G. W. Van Hoesen, "Neural systems of the non-human primate forebrain implicated in memory," *Annals of the New York Academy of Sciences*, vol. 444, no. 1, pp. 97–112, 1985.

[77] G. J. Quirk, R. U. Muller, J. L. Kubie, and J. B. Ranck Jr., "The positional firing properties of medial entorhinal neurons: description and comparison with hippocampal place cells," *The Journal of Neuroscience*, vol. 12, no. 5, pp. 1945–1963, 1992.

[78] T. Hafting, M. Fyhn, S. Molden, M.-B. Moser, and E. I. Moser, "Microstructure of a spatial map in the entorhinal cortex," *Nature*, vol. 436, no. 7052, pp. 801–806, 2005.

[79] M. Cammarota, D. M. Barros, M. R. M. Vianna, et al., "The transition from memory retrieval to extinction," *Anais da Academia Brasileira de Ciencias*, vol. 76, no. 3, pp. 573–582, 2004.

[80] M. Barad, "Later developments: molecular keys to age-related memory impairment," *Alzheimer Disease and Associated Disorders*, vol. 17, no. 3, pp. 168–176, 2003.

[81] S. Schneider-Rivas, S. Rivas-Arancibia, F. Vazquez-Pereyra, R. Vázquez-Sandoval, and G. Borgonio-Pérez, "Modulation

of long-term memory and extinction responses induced by growth hormone (GH) and growth hormone releasing hormone (GHRH) in rats," *Life Sciences*, vol. 56, no. 22, pp. PL433–PL441, 1995.

[82] S. Schneider-Rivas, C. Paredes-Carbajal, D. Mascher, et al., "Effects of testosterone and growth hormone on long-term retention and extinction of a passive avoidance response in young and aged rats," *International Journal of Neuroscience*, vol. 117, no. 10, pp. 1443–1456, 2007.

[83] B. Topic, E. Dere, D. Schulz, et al., "Aged and adult rats compared in acquisition and extinction of escape from the water maze: focus on individual differences," *Behavioral Neuroscience*, vol. 119, no. 1, pp. 127–144, 2005.

[84] I. F. Oliveira-Silva, L. Pinto, S. R. C. Pereira, et al., "Age-related deficit in behavioural extinction is counteracted by long-term ethanol consumption: correlation between 5-HIAA/5HT ratio in dorsal raphe nucleus and cognitive parameters," *Behavioural Brain Research*, vol. 180, no. 2, pp. 226–234, 2007.

[85] R. G. W. Pires, S. R. C. Pereira, F. M. Carvalho, I. F. Oliveira-Silva, V. P. Ferraz, and A. M. Ribeiro, "Correlation between phosphorylation level of a hippocampal 86 kDa protein and extinction of a behaviour in a model of Wernicke-Korsakoff syndrome," *Behavioural Brain Research*, vol. 180, no. 1, pp. 102–106, 2007.

[86] D. Schulz, B. Topic, M. A. De Souza Silva, and J. P. Huston, "Extinction-induced immobility in the water maze and its neurochemical concomitants in aged and adult rats: a possible model for depression?" *Neurobiology of Learning and Memory*, vol. 82, no. 2, pp. 128–141, 2004.

[87] D. Schulz, T. Buddenberg, and J. P. Huston, "Extinction-induced "despair" in the water maze, exploratory behavior and fear: effects of chronic antidepressant treatment," *Neurobiology of Learning and Memory*, vol. 87, no. 4, pp. 624–634, 2007.

[88] D. Schulz, J. P. Huston, T. Buddenberg, and B. Topic, ""Despair" induced by extinction trials in the water maze: relationship with measures of anxiety in aged and adult rats," *Neurobiology of Learning and Memory*, vol. 87, no. 3, pp. 309–323, 2007.

[89] C. Bellebaum and I. Daum, "Effects of age and awareness on eyeblink conditional discrimination learning," *Behavioral Neuroscience*, vol. 118, no. 6, pp. 1157–1165, 2004.

[90] S. L. Rauch, M. R. Milad, S. P. Orr, B. T. Quinn, B. Fischl, and R. K. Pitman, "Orbitofrontal thickness, retention of fear extinction, and extraversion," *NeuroReport*, vol. 16, no. 17, pp. 1909–1912, 2005.

[91] M. J. de Leon, A. E. George, L. A. Stylopoulos, G. Smith, and D. C. Miller, "Early marker for Alzheimer's disease: the atrophic hippocampus," *The Lancet*, vol. 2, no. 8664, pp. 672–673, 1989.

[92] M. J. de Leon, J. Golomb, A. E. George, et al., "The radiologic prediction of Alzheimer disease: the atrophic hippocampal formation," *American Journal of Neuroradiology*, vol. 14, no. 4, pp. 897–906, 1993.

[93] J. P. Kesslak, O. Nalcioglu, and C. W. Cotman, "Quantification of magnetic resonance scans for hippocampal and parahippocampal atrophy in Alzheimer's disease," *Neurology*, vol. 41, no. 1, pp. 51–54, 1991.

[94] B. T. Hyman, P. V. Arriagada, and G. W. Van Hoesen, "Pathologic changes in the olfactory system in aging and Alzheimer's disease," *Annals of the New York Academy of Sciences*, vol. 640, pp. 14–19, 1991.

[95] P. V. Arriagada, K. Marzloff, and B. T. Hyman, "Distribution of Alzheimer-type pathologic changes in nondemented elderly individuals matches the pattern in Alzheimer's disease," *Neurology*, vol. 42, no. 9, pp. 1681–1688, 1992.

[96] M. J. de Leon, A. Convit, A. E. George, et al., "In vivo structural studies of the hippocampus in normal aging and in incipient Alzheimer's disease," *Annals of the New York Academy of Sciences*, vol. 777, no. 1, pp. 1–13, 1996.

[97] M. Gado, C. P. Hughes, W. Danziger, and D. Chi, "Aging, dementia, and brain atrophy: a longitudinal computed tomographic study," *American Journal of Neuroradiology*, vol. 4, no. 3, pp. 699–702, 1983.

[98] B. Reisberg, S. H. Ferris, A. Kluger, E. Franssen, J. Wegiel, and M. J. de Leon, "Mild cognitive impairment (MCI): a historical perspective," *International Psychogeriatrics*, vol. 20, no. 1, pp. 18–31, 2008.

[99] S. Bell-McGinty, O. L. Lopez, C. C. Meltzer, et al., "Differential cortical atrophy in subgroups of mild cognitive impairment," *Archives of Neurology*, vol. 62, no. 9, pp. 1393–1397, 2005.

[100] D. P. Devanand, G. Pradhaban, X. Liu, et al., "Hippocampal and entorhinal atrophy in mild cognitive impairment: prediction of Alzheimer disease," *Neurology*, vol. 68, no. 11, pp. 828–836, 2007.

[101] M. J. de Leon, L. Mosconi, K. Blennow, et al., "Imaging and CSF studies in the preclinical diagnosis of Alzheimer's disease," *Annals of the New York Academy of Sciences*, vol. 1097, pp. 114–145, 2007.

[102] C. D. Smith, H. Chebrolu, D. R. Wekstein, et al., "Brain structural alterations before mild cognitive impairment," *Neurology*, vol. 68, no. 16, pp. 1268–1273, 2007.

[103] T. Tapiola, C. Pennanen, M. Tapiola, et al., "MRI of hippocampus and entorhinal cortex in mild cognitive impairment: a follow-up study," *Neurobiology of Aging*, vol. 29, no. 1, pp. 31–38, 2008.

[104] A. P. Yonelinas, K. Widaman, D. Mungas, B. Reed, M. W. Weiner, and H. C. Chui, "Memory in the aging brain: doubly dissociating the contribution of the hippocampus and entorhinal cortex," *Hippocampus*, vol. 17, no. 11, pp. 1134–1140, 2007.

[105] S. Burgmans, M. P. J. van Boxtel, F. Smeets, et al., "Prefrontal cortex atrophy predicts dementia over a six-year period," *Neurobiology of Aging*. In press.

Hindawi Publishing Corporation
Neural Plasticity
Volume 2008, Article ID 814815, 12 pages
doi:10.1155/2008/814815

Research Article

Differential Induction of Long-Term Potentiation in the Horizontal versus Columnar Superficial Connections to Layer II Cells of the Entorhinal Cortex

Li Ma,[1,2] Angel Alonso,[1] and Clayton T. Dickson[2,3,4]

[1] *Department of Neurology and Neurosurgery, McGill University and Montreal Neurological Institute, Montreal, PQ, Canada H3A 2B4*
[2] *Department of Psychology, University of Alberta, Edmonton, AB, Canada T6G 2E9*
[3] *Department of Physiology, University of Alberta, Edmonton, AB, Canada T6G 2H7*
[4] *Centre for Neuroscience, University of Alberta, Edmonton, AB, Canada T6G 2H7*

Correspondence should be addressed to Clayton T. Dickson, clayton.dickson@ualberta.ca

Received 11 April 2008; Accepted 20 May 2008

Recommended by Min Jung

The entorhinal cortex (EC) is a nodal and independent mnemonic element of the medial temporal lobe memory circuit as it forms a bidirectional interface between the neocortex and hippocampus. Within the EC, intra- and inter-lamellar associational connections occur via horizontal and columnar projections, respectively. We undertook a comparative study of these two inputs as they converge upon EC layer II cells using whole-cell patch techniques in an adult rat EC horizontal slice preparation in which the deepest layers (V-VI) had been dissected out. Electrical stimulation of layers I and III during GABA blockade allowed us to study excitatory synaptic properties and plasticity in the horizontal and columnar fibre systems, respectively. Both pathways exhibited AMPA- and NMDA-receptor mediated transmission and both exhibited long-term potentiation (LTP) after high-frequency (tetanic) stimulation. LTP in the horizontal, but not in the columnar pathway, was blocked by NMDA receptor antagonism. Intriguingly, LTP in both appeared to be mediated by post synaptic increases in Ca^{2+} that may be coupled to differing second messenger pathways. Thus, the superficial excitatory horizontal and columnar associative pathways to layer II have divergent mechanisms for LTP which may endow the EC with even more complex and dynamic processing characteristics than previously thought.

Copyright © 2008 Li Ma et al. This is an open access article distributed under the Creative Commons Attribution License, which permits unrestricted use, distribution, and reproduction in any medium, provided the original work is properly cited.

1. INTRODUCTION

The entorhinal cortex (EC) is a prominent component of the medial temporal lobe memory system. The superficial layers (II and III) of the EC receive an extensive input from multimodal sensory associational areas of neocortex and, in turn, project to all subregions of the hippocampal formation. Output stations of the hippocampus, including CA1 and subiculum, project back to the deep layers of entorhinal cortex (VI & V), reciprocating the input channels [1, 2]. Therefore, the EC serves as a bidirectional interface between the neocortex and hippocampal formation and as such forms a nodal part of the cortico-hippocampo-cortical loop that is the brain's hardware for the formation of declarative memories.

The importance of the EC in memory processing, however, is thought to go beyond just its interconnections with the hippocampus. One suggestion is that the EC and other parahippocampal regions serve as a temporary memory store that is critical to normal hippocampal-dependent memory processing [3]. Behavioral studies have suggested that lesions involving the EC are followed by learning and memory deficits in mammals (reviewed in [4]). Indeed, early stage tissue from Alzheimer's patients in which memory impairments are just subclinical demonstrates neurodegeneration in the superficial layers of the EC specifically [5, 6]. Still other work has shown that embryonic entorhinal transplants partially ameliorate the deficits in spatial memory in adult rats with EC lesions [7]. Perhaps the strongest evidence for an independent role of the EC in memory is that a number

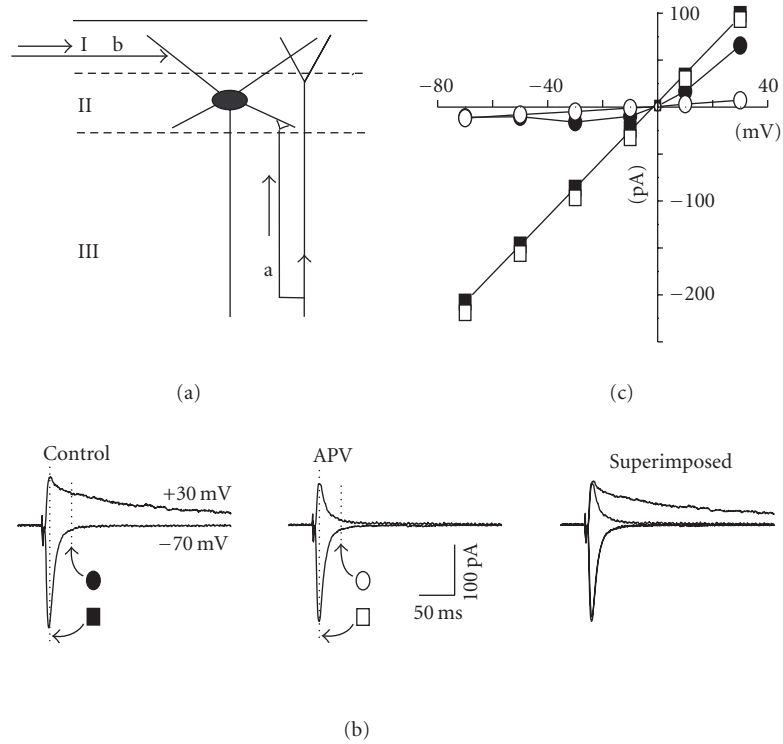

Figure 1: Properties of evoked EPSCs in EC layer II neurons. (a) Schematic diagram of the ascending columnar (arrow a) and the horizontal (arrow b) inputs converging on a layer II cell in entorhinal cortex (I, II, and III refer to the superficial layers of the EC). (b) Stimulation of layer III evoked excitatory postsynaptic currents that had different profiles at hyperpolarized (−70 mV) versus depolarized (+30 mV) potentials and sensitivity to APV. For these experiments, 130 mM CsGluconate and 0.8 mM QX314-Cl were substituted for KGluconate in the recording pipette. Corrections were made for the liquid junction potential. In control conditions (leftmost panel), EPSCs demonstrated only a fast decay component at −70 mV, but showed a slower decay component at +30 mV. In the presence of 50 μM DL-APV (middle panel), only the fast component was observed at both holding potentials (a direct comparison is shown in the superimposed traces in the rightmost panel). (c) I-V relationship for EPSC components measured at peak and 30 milliseconds post peak for the same cell (see dotted lines in (b)). The peak amplitude (closed square plots) showed a linear relationship across the full range of membrane potentials tested (−70 to +30 mV). This was unchanged following application of APV (open square plots). In control conditions, the amplitude measured 30 milliseconds following the peak (filled circles) was lower and showed a negative slope region at depolarized membrane potentials levels (−60 to −20 mV) but became nearly linear thereafter. In the presence of APV (open circles), the negative slope region was abolished and the resultant plot was linear across the full range of membrane potentials.

of entorhinal cells demonstrate persistent activity in the delay phase of memory tasks which correlates to the retention of information necessary to perform during a subsequent go phase [8, 9]. Indeed, entorhinal cells also demonstrate intrinsic "memory-like" persistent firing properties dependent upon associative convergence of excitatory inputs and cholinergic neuromodulation [10].

Synaptic plasticity of excitatory glutamatergic responses, via long-term potentiation (LTP), has been proposed as a mechanism underlying learning and memory. The most commonly studied form involves an NMDA-receptor dependent process whereby postsynaptic Ca^{2+} influx through this ligand-gated channel induces changes via a series of intracellular second messengers (typically beginning with the calcium/calmodulin-dependent kinase: CaMKII) that result in the enhancement of neurotransmission [11]. It has also been shown that LTP can occur through non-NMDA dependent triggers such as activation of either voltage-dependent calcium channels or metabotropic glutamatergic receptors which can also lead to increases in Ca^{2+} influx and LTP via potentially overlapping intracellular mechanisms [12–14]. In addition, non-CaMKII-dependent processes have also been elucidated [11, 15, 16]. Although perhaps differing in their cellular induction mechanisms, all of the above are thought to express their effects mainly through postsynaptic changes to AMPA-type receptors that result in an enhancement of glutamate responsiveness. Changes to presynaptic release (due to growth of new contacts and enhancement of release machinery) have also been suggested to play a role (reviewed in [11, 15]).

A different form of LTP exists that appears to involve a completely different induction and expression mechanisms. This form, first elucidated in the mossy fibre input to CA3 pyramidal neurons in the hippocampus, does not require either NMDA receptor activation or an increase in postsynaptic Ca^{2+} [17]. The locus of induction and expression of this form of LTP is presynaptic [18–20], involving no changes in postsynaptic receptivity. This presumed increase

in neurotransmitter release is accompanied by a marked and long-lasting decrease in the paired-pulse facilitation ratio [18].

The cellular mechanisms underlying LTP in the EC remain understudied. Field recordings of LTP phenomenon have been reported in layer II and some interesting differences between deep and superficial associational pathways have been reported [21, 22]. To date, no studies have assessed, in the same superficial layer II cells, the differential properties of LTP in these two important pathways. Here, using whole-cell-recording technique, we investigated the physiology, pharmacology, and plasticity of both horizontal and columnar associative inputs to layer II cells using whole cell techniques in an in vitro slice preparation. These results have been previously published in abstract form [23].

2. MATERIALS AND METHODS

2.1. General

Brain slices were prepared from male Long-Evans rats (100–200 g) using standard procedures [24]. All methods used conformed to the guidelines established by the Canadian Council on Animal Care and the Society for Neuroscience. Animals were quickly decapitated, and the brain was rapidly removed, blocked, and placed in a cold (4–6°C) oxygenated normal Ringer's solution containing (in mM): 124 NaCl, 5 KCl. 1.3 NaH_2PO_4, 2.0 $CaCl_2$, 2.0 $MgSO_4$, 26 $NaHCO_3$, and 10 glucose (pH 7.4, by gaseous saturation with 95% O_2 & 5% CO_2). Horizontal slices from the retrohippocampal region were cut at a thickness of 400 μm using a vibratome (Pelco, Redding, Calif, USA). After at least an hour recovery period during which they were submerged in normal Ringer's at room temperature (23°C–25°C), individual slices were transferred to a recording chamber located on the stage of an upright, fixed-stage microscope (Axioskop, Zeiss). Slices were submerged and perfused continuously with a saturated (95% O_2 + 5% CO_2) solution containing (in mM) 126 NaCl, 2.5 KCl, 1.3 NaH_2PO_4, 2.4 $CaCl_2$, 1.4 $MgSO_4$, 26 $NaHCO_3$, 10 glucose, and 0.05 picrotoxin (a $GABA_A$ receptor antagonist) at room temperature. Before being transferred, a cut was made between layer III and layer V regions of entorhinal cortex to prevent the propagation of epileptiform activity. The microscope was equipped with a water immersion objective (40–63X: long-working distance), Nomarski optics, and a near-infrared charge-coupled device (CCD) camera (Sony XC-75). With this equipment, individual cells in layer II could be visualized via video microscopy and targeted for recording [25].

2.2. Recording

Somatic whole-cell voltage-clamp recordings [26] were made under visual control using 4–7 MΩ electrodes. The whole-cell solution contained (in mM): 130 K-Gluconate, 5 NaCl, 2 $MgCl_2$, 10 Hepes, 0.5 EGTA, 2 ATP, 0.4 GTP (pH 7.2–7.4 with 1 M KOH; osmolarity: 290–300 mOsm). In experiments designed to chelate intracellular Ca^{2+}, 10 mM BAPTA was substituted for equimolar K-Gluconate. To investigate properties of evoked EPSCs at varying membrane potentials, 130 mM Cs-Gluconate and 0.8 mM QX314-Cl were used in the whole-cell solution in place of K-Gluconate. The liquid junction potential was estimated using the method of Neher (1992) and was found to be 8 mV. No correction of transmembrane potential was applied for the liquid junction potential unless indicated otherwise.

Whole cell voltage clamp recordings were made using an Axoclamp2A or Axopatch200B amplifier (Axon Instruments, Foster City, Calif, USA). The low-pass filter (−3 dB) was set to 1 kHz, and the resulting current trace was digitized to computer at 2 kHz using a Digidata 1320 A-D converter driven by Pclamp7 (Axon Instruments).

Cells were held at −60 to −70 mV during recordings unless indicated otherwise. Series resistance was measured automatically using Pclamp7 software and those with values higher than 30 MΩ in whole-cell configuration were discarded. In the remainder, series resistance was compensated >40% with the amplifier's built-in compensation circuitry. Input resistance of cells (averaging 169.67 ± 5.67 MΩ, N = 171) was calculated by measuring current deflections in response to 5 mV hyperpolarizing voltage pulses from the holding potential and was monitored through each recording. A short-duration hyperpolarizing voltage step (−5 mV, 250 millisecods) was always applied to each sweep just prior to stimulation to monitor any change in input resistance and series resistance. Cells exhibiting detectible changes in the elicited current process to the hyperpolarization during recording were discarded.

2.3. Stimulation and experimental protocol

Electrical stimulation of afferent pathways to layer II was conducted through bipolar, stainless steel electrodes insulated except at their tips. These were positioned on the surface of the slice in layers I/II or III (see diagram in Figure 1(a)). Afferent inputs were activated in this way by passing short (100 μs) current pulses of 0.5–4.0 mA using a pulse generator (PG-4000 Cygnus Tech, NY) coupled to a stimulus isolation/constant current generator (Model A395 WPI). EPSCs were evoked once every 30 seconds, and the basal amplitude of EPSCs was set to 100–200 pA by adjusting the stimulation intensity. EPSCs were accepted as being monosynaptic if they exhibited short and consistent latencies that did not change with increasing stimulus intensity.

Following at least 5 minutes of stable baseline recording, LTP was elicited using a high-frequency (tetanic) stimulation train (HFS: 100 Hz; 1 second) at the same intensity used for baseline recording. Typically, HFS was delivered no more than approximately 15 minutes following the formation of whole cell configuration. Little to no potentiation was observed if HFS was applied at times greater than 30 minutes after achieving whole cell mode. Successful LTP was evaluated statistically in comparison to baseline values at a time point 30 minutes following HFS for each experiment.

Paired pulse facilitation protocols were used in order to assess any changes in presynaptic release mechanisms. The two pathways were stimulated either singly or alternatively at short intervals (50–70 milliseconds). PPF ratio was

computed by dividing the peak amplitude of the second EPSC by the peak amplitude of the first in each experiment.

Application of drugs was conducted by adding stock solutions directly to the superfusion medium to make appropriate final concentrations. DL-APV (Tocris) and CNQX (Tocris) were made up as a 10 mM stock solution in an equivalent volume mix of 1M NaOH and dimethyl sulfoxide. These were pipetted at smaller volumes into centrifuge tubes and stored frozen (-20°) until used. Picrotoxin and BAPTA were purchased from "Sigma (St. Louis, Mo)."

2.4. Data analysis

The amplitude of EPSCs was measured offline using Clampfit 6 (Axon Instruments), by calculating the difference between the peak deflections relative to the average holding current level computed for the 10 milliseconds preceding the stimulus. Average traces as shown in figure insets represented means of 5–10 individual EPSC sweeps. Peak amplitudes or paired-pulse facilitation (PPF) ratios were computed from these averages. Potentiation of EPSC amplitudes or PPF ratios following the application of HFS was expressed by normalizing amplitudes to the baseline values pre-HFS. Reported values reflect arithmetic means ± standard error of the mean (SEM), and statistical significance was determined by paired and unpaired Student's t-tests.

3. RESULTS

3.1. Characterization of EPSCs in layer II cells

Application of electrical stimulation to either lateral positions in layers I/II or deep positions in layer III evoked pure excitatory postsynaptic currents (EPSCs) in layer II cells under our recording and superfusion conditions (with added 50 μM picrotoxin). These EPSCs were routinely characterized as monosynaptic but occasionally polysynaptic or even antidromic responses were observed. In these latter cases, the stimulation electrode was physically adjusted or even moved on the surface of the slice until it evoked a pure monosynaptic response. The latency of responses was 4.01 ± 0.13 milliseconds (layer I stimulation) and 3.85 ± 0.11 milliseconds (layer III stimulation). These responses were completely blocked by TTX (1 μM), cadmium (200 μM), and the nonspecific glutamate antagonist, kynurenic acid (0.5 mM) (not shown).

To characterize the basic properties of the evoked EPSCs, we recorded the response over a broad range of membrane potentials (see Figures 1(b), 1(c)—layer III stimulation in this case). EPSCs displayed only a fast decay component when the membrane potential was held at -70 mV. A slow decay component became apparent as the holding potential was depolarized (see Figure 1(b), $n = 6$). These fast and slow decay components of EPSC appeared similar to AMPA- and NMDA-receptor mediated currents in other parts of the central nervous system. In order to examine this possibility in further detail, we constructed the current-voltage (I-V) relation of the EPSC response measured at the peak and 30 milliseconds after the peak (see dashed lines in Figure 1(b)). The peak I-V relation (filled squares in Figure 1(c)) was linear over the entire voltage range with a reversal potential of 0 mV whereas the I-V relation measured 30 milliseconds after the peak (filled circles in Figure 1(c)) was nonlinear with a region of negative slope resistance in the range of -60 to -20 mV. This nonlinear I-V behavior is typical for NMDA-receptor mediated EPSCs. Indeed, bath application of the NMDA receptor antagonist DL-APV (50 μM) abolished the slow decaying component of the EPSC at depolarized potentials without any significant effect on the early component (see Figures 1(b), 1(c)). In consequence, in the presence of DL-APV the peak I-V relation remained unchanged (open squares in Figure 1(c)). A small synaptic current could still be measured at 30 milliseconds but this displayed a completely linear I-V relation (open circles in Figure 1(c)) and was thus due to the late phase of the fast EPSC. In contrast to DL-APV, the selective non-NMDA receptor blocker CNQX (10 μM) completely abolished the EPSC at hyperpolarized potentials (not shown). These data suggest that the properties of EPSCs evoked by stimulation of both horizontal and columnar afferents in EC layer II cells are similar to their glutamatergic counterparts in the hippocampus, or indeed, in other parts of the central nervous system.

3.2. Independence of the horizontal and vertical associational pathways

In order to assure that our stimulation conditions evoked activity in independent sets of inputs converging in layer II, we used homosynaptic and heterosynaptic paired pulse facilitation (PPF) protocols. The two pathways were stimulated independently or alternatively at short intervals (50–70 milliseconds) and we measured whether the amplitude of EPSCs evoked by the second stimulation pulse was increased following the first. Since PPF reflects an increase in neurotransmitter release based on prior activity in the same synapse, any facilitation observed across different site stimulation would reflect the activation of overlapping synapses. Consistent with this idea, each pathway could independently demonstrate PPF (see Figures 2(a), 2(b): left panels). In contrast, heterosynaptic stimulation protocols (either layer I followed by layer III or vice versa) failed to show any PPF (see Figures 2(a), 2(b): right panels). Using the same protocol in a total of three cells, we obtained similar results which indicated that the two converging pathways were indeed independent.

3.3. LTP of the horizontal associational pathway

Previous work using both field and intracellular methods have demonstrated that the inputs to layer II activated by stimulation of layer I (which include horizontal association fibres from layer II and extraentorhinal afferent fibre systems) exhibit homosynaptic LTP [21, 27]. We confirmed this in our own whole cell recording conditions using HFS protocols. Posttetanic potentiation (PTP) was observed in all recorded cells following the application of high-frequency stimulation (100 Hz, 1 second) to layer I at sites lateral to

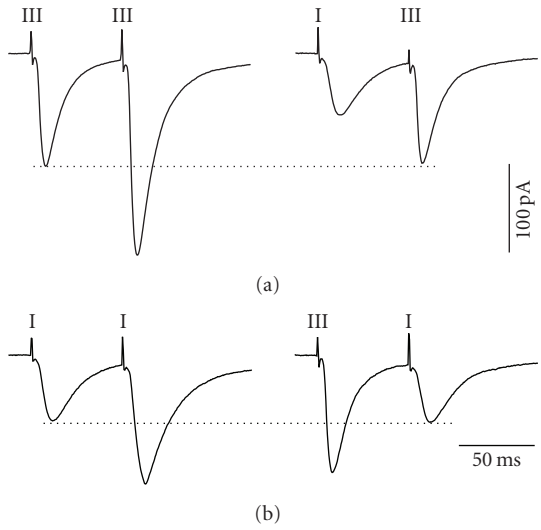

Figure 2: Afferent independence between the ascending columnar and horizontal associational pathways. The two pathways were stimulated repetitively (left panels) or alternatively (right panels) using a short interpulse interval (60 milliseconds). Each trace represents an average of 16 sweeps. Although paired-pulse facilitation (PPF) was observed in both (a) the ascending and (b) horizontal pathways when stimulated independently (right panels), no facilitation was observed when stimulating each alternatively (left panels). Dotted lines indicate the maximum amplitude to the first pulse in each case.

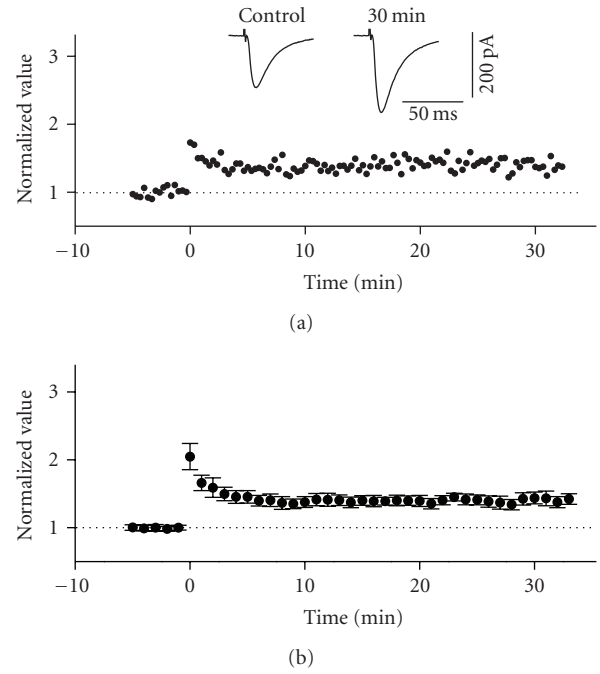

Figure 3: LTP in the horizontal associative pathway of the superficial entorhinal cortex. The stimulation electrode was positioned on the surface of layer I, lateral to the recording electrode. (a) Normalized scaled amplitude of peak EPSCs evoked by test pulses in a layer II cell is plotted against time. HFS at time zero led to an immediate and long-lasting potentiation of EPSCs. The inset shows two traces reflecting averaged EPSCs at baseline (pre-HFS) and at 30 minutes post-HFS. (b) Average normalized scaled amplitude of peak EPSCs across 15 cells. The value at 30 minutes post-HFS (1.401 ± 0.087) is significantly different from baseline ($P < .01$).

the recording electrode position (see Figure 3(a)). LTP of EPSCs following PTP was observed in 65% of cells tested (15 of 23) and lasted for more than 30 minutes following HFS. The average normalized value of peak EPSCs in these cells increased by a factor of 1.401 ± 0.087 of baseline values at 30 minutes following HFS (see Figure 3(b)). This value was significantly different from baseline ($n = 15$, $P < .01$).

To determine whether induction of LTP in this pathway required NMDA receptor activation, we tested slices treated with the NMDA receptor antagonist DL-APV ($50\,\mu$M). Under these conditions, HFS to lateral sites in layer I only produced a short term (PTP) facilitation of EPSCs in all cells tested. These values returned to baseline levels within 10 minutes following HFS (see Figure 4(a)). The average normalized value of peak EPSCs was 0.979 ± 0.095 at 30 minutes after HFS in the presence of APV which was not significantly different from baseline values ($n = 6$, $P > .01$, see Figure 4(b)).

To determine if HFS-induced LTP was also dependent upon a rise in postsynaptic Ca^{2+}, we tested the effects of dialysing the fast chelator BAPTA (10 mM) into the postsynaptic cell. As in NMDA blockade conditions, HFS of lateral layer I led to a short term facilitation of EPSCs only. This facilitation returned to baseline levels in slightly less than 10 minutes following the application of HFS (see Figure 5(a)). The average increase in the amplitude of EPSCs at 30 minutes post-HFS (1.008 ± 0.068) was not significantly different from baseline ($n = 5$, $P > .01$, see Figure 5(b)).

In order to assess if the expression of LTP in the horizontal associative pathway was solely dependent on postsynaptic mechanisms, we investigated any changes in PPF ratio. HFS to lateral layer I led to an immediate and obvious decrease in PPF which soon returned to stable (and near-baseline) levels within 5 minutes (see Figure 6(a)). PPF ratio at 30 and 50 minutes post-HFS was 0.917 ± 0.084 and 0.938 ± 0.062, respectively, which were both slightly, but significantly, less than baseline ($n = 8$, $P < .01$, see Figure 6(b)). Thus, while the primary component of LTP in this pathway appeared to be postsynaptic in expression, a small component also appeared to involve a presynaptic locus.

3.4. LTP of the ascending columnar associational pathway

Application of HFS to afferent fibres in layer III caused an immediate and long-lasting potentiation of EPSCs in 79% of cells tested (23 of 29) which lasted for the duration of the recording situation (>30 minutes post-HFS). Short-term posttetanic potentiation (PTP) was a consistent feature of this facilitation and lasted for just less than 5 minutes following HFS (see Figure 7(a)). The average normalized value of peak EPSCs increased by a factor of 1.65 ± 0.102 and 1.68 ± 0.128 of baseline (pre-HFS values) at 30 and 50

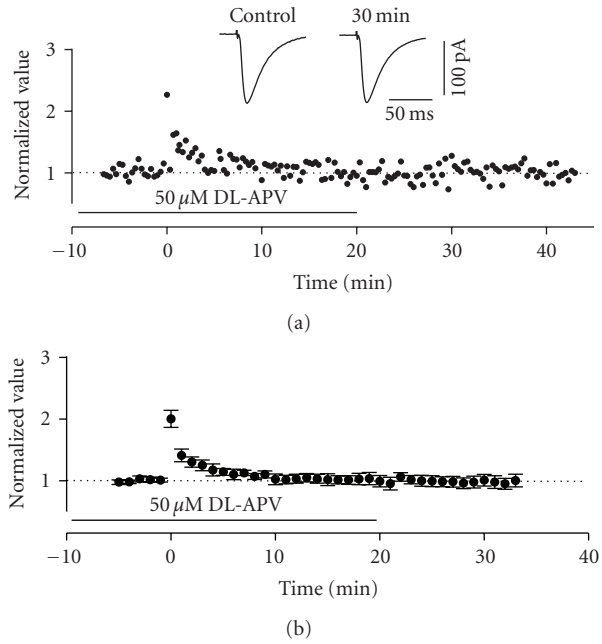

Figure 4: Induction of LTP in the horizontal pathway required activation of NMDA-receptors. (a) Normalized scaled amplitude of peak EPSCs evoked by test pulses in a layer II cell is plotted against time. Time point of application of 50 μM DL-APV is indicated by the line. HFS at time zero led to short-term (PTP) but not long-term potentiation. The inset shows two traces reflecting averaged EPSCs at baseline (pre-HFS) and at 30 minutes post-HFS. (b) Average normalized scaled amplitude of peak EPSCs across 6 cells in the presence of APV as indicated by the line. The value at 30 minutes post-HFS (0.979 ± 0.095) was not significantly different from baseline ($P > .05$).

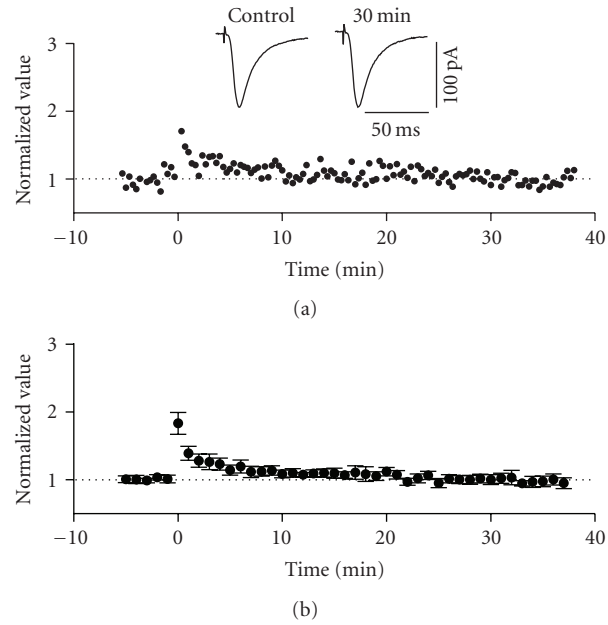

Figure 5: Induction of LTP in the horizontal pathway required an increase in postsynaptic calcium. (a) Normalized scaled amplitude of peak EPSCs evoked by test pulses in a layer II cell loaded with 10 mM BAPTA is plotted against time. HFS was routinely applied about 15 minutes after formation of whole-cell mode to ensure adequate BAPTA diffusion. The inset shows two traces reflecting averaged EPSCs at baseline (pre-HFS) and at 30 minutes post-HFS. (b) Average normalized scaled amplitude of peak EPSCs across 5 BAPTA-loaded cells. HFS at time zero induced only short-term (PTP) but not long-term potentiation. The value at 30 minutes post-HFS (1.008 ± 0.068) was not significantly different from baseline ($P > .05$).

minutes, respectively, following HFS (see Figure 7(b)). Both values were significantly different from baseline ($n = 23$, $P < .01$).

To determine whether induction of LTP in this pathway required NMDA receptor activation, we tested slices treated with the NMDA receptor antagonist DL-APV (50 μM). Surprisingly, both the induction and maintenance of LTP appeared unaffected by this manipulation even though slices were superfused for at least 10 minutes prior to HFS and in some cases, constantly during the entire experimental protocol. Results for both washout (10 to 20 minutes following high-frequency stimulation) and constant perfusion conditions were pooled together for statistic analysis since no difference was observed between these conditions. As in control conditions, enhancement of EPSCs in APV-treated slices became stable and long lasting after short-term PTP (see Figure 8(a)). The average normalized value of peak EPSCs in the presence of APV increased by a factor of 1.695 ± 0.145 and 1.707 ± 0.19 of baseline (pre-HFS) values at 30 and 50 minutes, respectively, values that were 1 significantly different from baseline values ($n = 10$, $P < .01$) and 2 not significantly different from increases found in control conditions ($P > .05$, see Figure 8(b)). In an additional two experiments, we also tested the effects of a higher concentration of APV (100 μM), but both the induction and expression of LTP were still unaffected (data not shown).

Given that calcium flux arising from activation of either postsynaptic calcium channels or metabotropic glutamate receptors can also induce synaptic plasticity independently of NMDA receptor activation, we tested whether fast chelation of free intracellular calcium with BAPTA would block LTP in this pathway. High-frequency stimulation was applied 15 minutes after whole cell configuration to allow for full intracellular dialysis of BAPTA to occur. With 10 mM BAPTA in the pipette solution, the amplitude of LTP was markedly reduced although PTP was consistently induced. Under this condition (see Figure 9(a)), the average increase in the normalized peak value of EPSCs was only 1.427 ± 0.092 30 minutes post-HFS, a value reflecting a significant reduction (to 86%) of synaptic enhancement from control experiments (see Figure 9(b); $n = 5$). When we included 20 mM BAPTA in the recording pipette we could completely abolish LTP (but not PTP: $n = 7$). However, this manipulation also significantly decreased the input resistance of the postsynaptic cell by an average of 20% (data not shown).

The above data, though not completely conclusive, suggest that postsynaptic calcium entry may partially play a role in LTP induction in the layer II-II pathway. Since NMDA

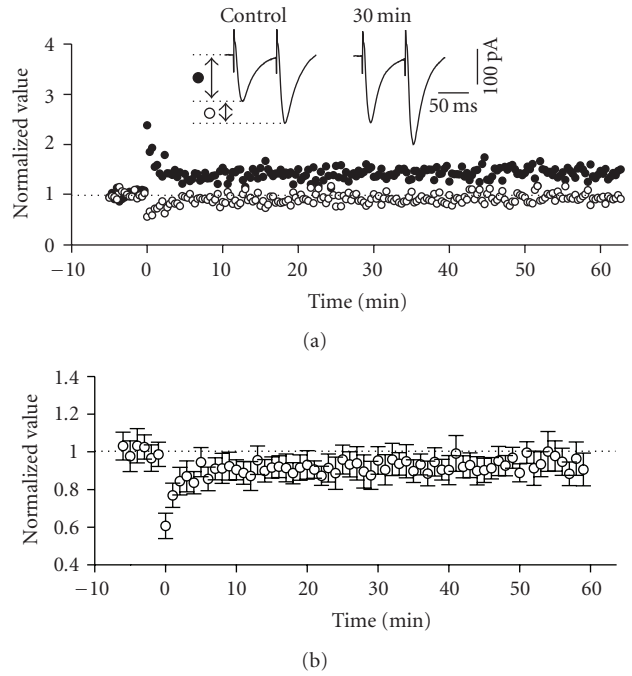

Figure 6: Expression of LTP in the horizontal pathway was associated with a slight change in paired-pulse facilitation (PPF) ratio. (a) Normalized scaled amplitude of the peak EPSCs evoked by the first of a pair of test pulses separated by 60 milliseconds (filled circles) and the normalized paired pulse facilitation ratio (open circles) in a layer II cell is plotted against time. The inset shows two traces reflecting averaged paired EPSCs at baseline (pre-HFS) and at 30 minutes post-HFS. PPF ratio was calculated as the amplitude of the peak of the second EPSC divided by the first. (b) Average normalized scaled amplitude of PPF ratio in 10 cells. HFS at time zero induced a short-term decrease which decayed back to near baseline levels. The values at 30 and 50 minutes after HFS, however, (0.944 ± 0.065 and 0.966 ± 0.068, resp.) were significantly different from baseline ($P < .01$).

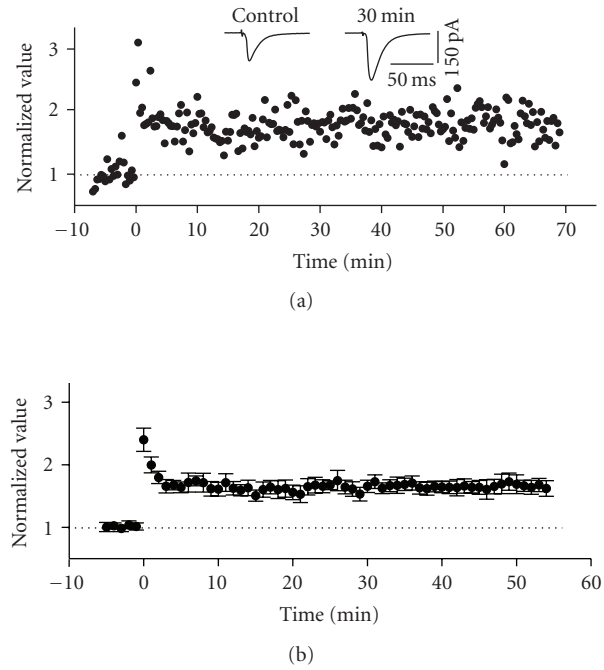

Figure 7: LTP in the columnar associative (ascending) pathway of superficial entorhinal cortex. The stimulation electrode was positioned on the surface of layer III, just deep to the recording electrode. (a) Normalized scaled amplitude of peak EPSCs evoked by test pulses in a layer II cell is plotted against time. Application of HFS delivered at time zero led to an immediate and long-lasting increase in the amplitude of EPSCs. This posttetanic potentiation lasted less than 5 minutes before it reached a stable and potentiated level. The inset shows two traces reflecting averaged EPSCs at baseline (pre-HFS) and at 30 minutes post-HFS. (b) Average normalized scaled amplitude of peak EPSCs across 11 cells. The values at 30 and 50 minutes post-HFS (1.65 ± 0.102 and 1.68 ± 0.128, resp.) were significantly different from baseline ($P < .01$).

receptor-channels were obviously not the source of this calcium, we then explored two other possibilities: (1) calcium entry via voltage-gated Ca^{2+} channels and (2) calcium entry via metabotropic glutamate receptors (mGluRs). To assess the first possibility we attempted to induce LTP by pairing low-frequency presynaptic stimulation (0.05–01 HZ) with large amplitude postsynaptic depolarizing voltage-clamp steps (200 milliseconds at −20 mV) which have been shown to elicit LTP in other systems. However, this protocol did not cause any significant change in the amplitude of the baseline EPSC (not shown, $P > .05$, $n = 5$). To assess the second possibility, we blocked mGluRs with the broad spectrum antagonist MCPG (100 μM). However, in 5 neurons tested, HFS continued to induce LTP to a similar extent as in control conditions (not shown).

Previous findings using field potential recordings [22] have shown that LTP in the ascending layer V to layer associative pathway of the EC is partially NMDA-independent. By measuring changes in paired-pulse facilitation (PPF), these researchers suggested that this non-NMDA component of LTP reflected an increase in presynaptic transmitter release. To assess whether LTP in the layer III input to layer II cells was expressed presynaptically, we computed changes in the PPF ratio before and after expression of LTP. PPF from the intrinsic ascending layer III pathway was observed in 77% cells (17 of 23 cells) during control (pre-HFS) conditions in the presence of 2.4 mM extracellular Ca^{2+}. The range of ratios observed was between 1.08 and 1.96, with an average value of 1.36 ± 0.081. Only cells displaying both PPF and LTP were examined (see Figure 10(a)). Directly following (1 minute post) HFS (i.e., during the expression of PTP) the normalized PPF ratio was reduced by a factor of 0.64 ± 0.048 compared to baseline values ($n = 10$, see Figure 10(b)). This decrease, however, was only transient since PPF values showed an initial quick and later slow increase which brought them back to near baseline (unity) values (see Figure 10(b)). The average normalized PPF ratio measured 30 and 50 minutes after application of HFS was 0.944 ± 0.065 and 0.966 ± 0.068, respectively, which were only slightly, but significantly, different from that during baseline period ($P <$ .01). Thus, it would appear that only a small component of

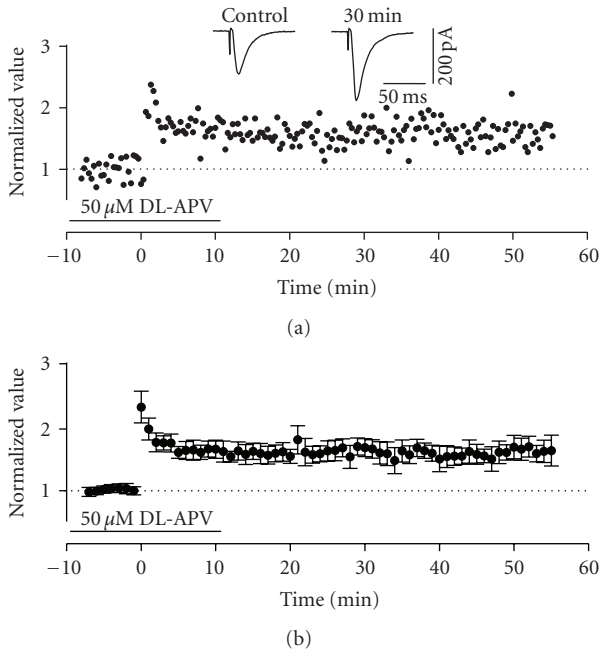

Figure 8: Induction of LTP in the ascending pathway did not require activation of NMDA-receptors. (a) Normalized scaled amplitude of peak EPSCs evoked by test pulses in a layer II cell is plotted against time. Time point of application of 50 μM DL-APV is indicated by the line (note, all experiments involved superfusions of APV for more than 10 minutes before application of HFS at time zero). HFS led to both short-term (PTP) and long-term potentiation. The inset shows two traces reflecting averaged EPSCs at baseline (pre-HFS) and at 30 minutes post-HFS. (b) Average normalized scaled amplitude of peak EPSCs across 10 cells in the presence of APV as indicated by the line. The value 30 and 50 minutes after was 1.695 ± 0.145 and 1.707 ± 0.19, respectively, which were both significantly different from baseline values ($P < .01$).

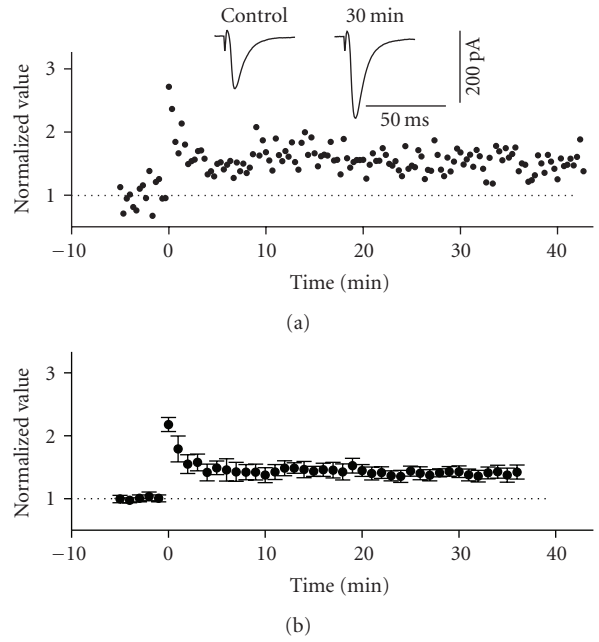

Figure 9: Induction of LTP in the ascending pathway was not blocked by sequestering of free postsynaptic calcium. (a) Normalized scaled amplitude of peak EPSCs evoked by test pulses in a layer II cell loaded with 10 mM BAPTA is plotted against time. HFS was routinely applied about 15 minutes after formation of whole-cell mode to ensure adequate BAPTA diffusion. The inset shows two traces reflecting averaged EPSCs at baseline (pre-HFS) and at 30 minutes post-HFS. HFS-induced enhancement of EPSCs was still observed. (b) Average normalized scaled amplitude of peak EPSCs across 5 BAPTA-loaded cells. HFS at time zero induced both short-term (PTP) and long-term potentiation. The value at 30 minutes post-HFS (1.427 ± 0.092) was slightly reduced compared to control conditions but significantly different from baseline ($P < .05$).

the LTP expressed in this pathway reflected an increase in neurotransmitter release.

3.5. Molecular mechanistic differences in LTP of the horizontal and columnar associative pathways

Based on the differences in induction properties of LTP in the two pathways examined, we sought to evaluate their potential differential dependence on independent second-messenger pathways. We first tested the effect of the widely-used CamKII specific inhibitor, KN62. KN62 (3.8 μM) was applied to slices though bath perfusion for more than 10 minutes before HFS was delivered. This compound had differential effects on LTP expressed in the horizontal versus the columnar associative pathways. HFS of layer I in the presence of KN62 failed to elicit LTP in layer II cells (see Figure 11). The normalized average of EPSC amplitude at 30 minutes post-HFS was 0.8998 ± 0.0545, which was actually significantly reduced with respect to baseline values ($n = 6$, $P < .05$). In contrast, HFS of layer III in the presence of KN62 was still able to produce LTP in all layer II cells tested (see Figure 12), although in two cells it did suppress the expression of PTP. The normalized average of EPSC amplitude at 30 minutes after HFS was 1.656 ± 0.124, a value which reflected a significant facilitation ($n = 11$, $P < .01$) and which was not significantly different from the degree of potentiation expressed in control conditions (unpaired t-test, $P > .05$).

Since LTP in the ascending pathway did not appear to be dependent on CaMKII, we next tested its dependence on PKA signalling. To inhibit PKA activity, we used bath applications of the catalytic subunit inhibitor KT5720 (250 nM). This manipulation, applied for 10 minutes before HFS, did not completely block LTP in layer II cells but did significantly suppress it (see Figure 13). The normalized average of EPSC amplitude at 30 minutes post-HFS was 1.338 ± 1.016 ($n = 8$) which was significantly smaller than that shown in control conditions (unpaired t-test, $P < .01$,). Thus, at least part of the LTP expressed in this pathway appears to depend upon PKA signalling.

4. DISCUSSION

In this study, we investigated the basic characteristics of synaptic communication and plasticity in two independent

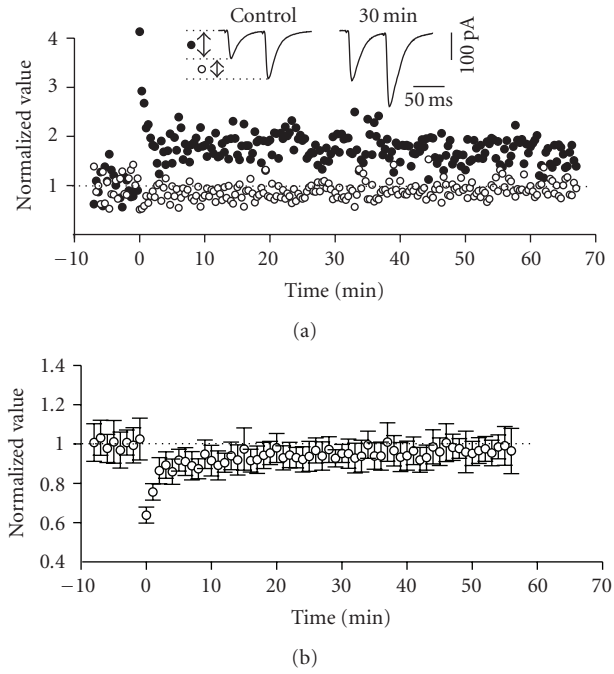

Figure 10: Expression of LTP in the ascending pathway was associated with a slight change in PPF ratio. (a) Normalized scaled amplitude of the peak EPSCs evoked by the first of a pair of test pulses separated by 60 milliseconds (filled circles), and the normalized PPF ratio (open circles) in a layer II cell is plotted against time. The inset shows two traces reflecting averaged paired EPSCs at baseline (pre-HFS) and at 30 minutes post-HFS. PPF ratio was calculated as the amplitude of the peak of the second EPSC divided by the first. (b) Average normalized scaled amplitude of PPF ratio in 8 cells. HFS at time zero induced a short-term decrease of PPF which decayed back to near baseline levels. The values at 30 and 50 minutes after HFS, however, (0.917 ± 0.084 and 0.938 ± 0.062, resp.) were significantly different from baseline ($P < .01$).

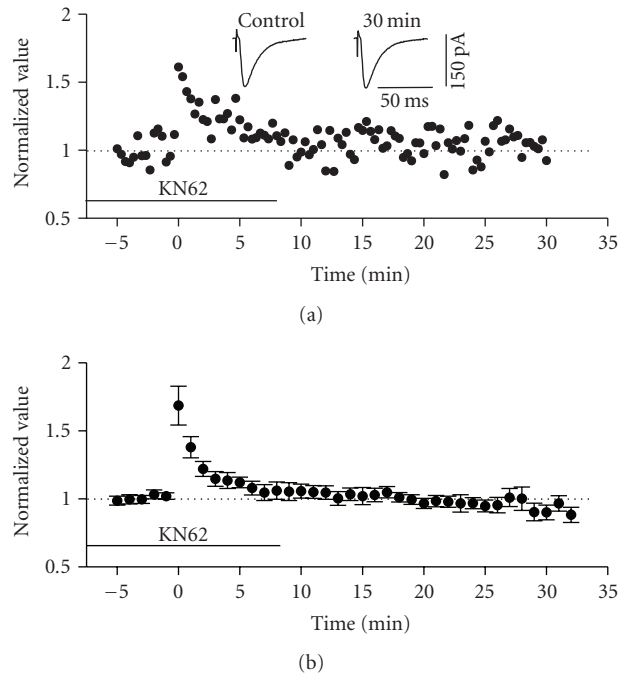

Figure 11: Induction of LTP in the horizontal pathway required intact CaMKII signalling. (a) Normalized scaled amplitude of peak EPSCs evoked by test pulses in a layer II cell is plotted against time. Time point of application of 3.8 μM KN62 is indicated by the line. HFS at time zero led to a slight short-term potentiation (PTP) but no long-term potentiation. The inset shows two traces reflecting averaged EPSCs at baseline (pre-HFS) and at 30 minutes post-HFS. (b) Average normalized scaled amplitude of peak EPSCs across 6 cells in the presence of KN62 as indicated by the line. The value at 30 minutes post-HFS (0.8998 ± 0.0545) was significantly reduced from baseline ($P < .05$).

pathways converging on EC layer II principal neurons, the horizontal input (containing cortical afferents and intralaminar associative connections between cells of layer II), and the ascending columnar (interlaminar) layer III input, respectively. Although prior work has been conducted on the properties of LTP in the superficial layers of the EC, few have focussed on cellular mechanisms and none has compared the superficial associative pathways that converge upon layer II. Indeed, a recent whole-cell investigation of plasticity in EC layer II stellates concluded that only LTD is present in conditions similar to those reported here [28].

Our results demonstrated that both associational pathways within the EC were independent and had basic physiological and pharmacological characteristics similar to other glutamatergic synapses in the central nervous system. In addition, both displayed robust LTP evoked by HFS that was accompanied by small decreases in paired pulse facilitation ratio. Importantly, we confirmed that the induction mechanisms of LTP in these two convergent pathways demonstrated some important differences in terms of their dependence upon NMDA receptors and on their dependence upon postsynaptic calcium. This difference may reflect a differential dependence on second-messenger systems. While this is not the first direct demonstration of differential plasticity in independent pathways that terminate in the superficial layers of the EC, it is the first cellular investigation of this type. This confirms that the intrinsic circuit dynamics of the EC are highly complex.

4.1. Physiology of the horizontal and ascending excitatory inputs to EC layer II

The projection cells of EC layer II are important components of the medial temporal lobe memory circuit since they receive highly processed neocortical information and provide the hippocampus with its most massive input via the perforant path. Through feedforward excitatory (and presumably inhibitory) collaterals, these cells also form part of a rich autoassociative network [29] whereby neighbouring neurons can influence and entrain each other [30]. As well, the activity of these cells is influenced by inputs which derive from laminae located deeper to it [1, 2, 31, 32]. The functional significance of convergent horizontal and ascending pathways in layer II is unclear although it could be relevant in order to compare the results of processing in deeper layers to that conducted in the most superficial.

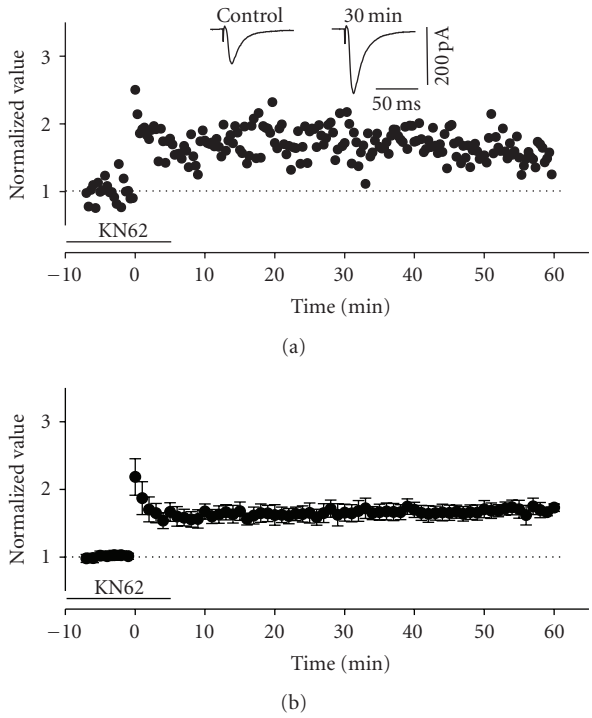

Figure 12: Induction of LTP in the ascending pathway was not dependent upon intact CaMKII signalling. (a) Normalized scaled amplitude of peak EPSCs evoked by test pulses in a layer II cell is plotted against time. Time point of application of 3.8 μM KN62 is indicated by the line. HFS led to only a slight short-term potentiation (PTP) but a prominent long-term potentiation. The inset shows two traces reflecting averaged EPSCs at baseline (pre-HFS) and at 30 minutes post-HFS. (b) Average normalized scaled amplitude of peak EPSCs across 10 cells in the presence of KN62 as indicated by the line. The value 30 minutes after HFS was 1.656 ± 0.124 which was significantly different from baseline values ($P < .01$) and no different from LTP in control conditions ($P > .05$).

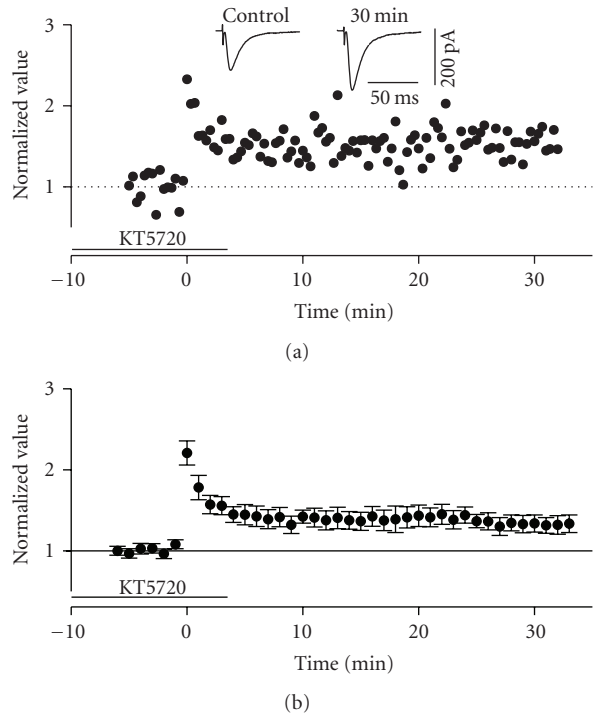

Figure 13: Induction of LTP in the ascending pathway was partially dependent upon intact PKA signalling. (a) Normalized scaled amplitude of peak EPSCs evoked by test pulses in a layer II cell is plotted against time. Time point of application of 250 nM KT5720 is indicated by the line. HFS led to intact short-term potentiation (PTP) but the degree of long-term potentiation was slightly decreased although still intact. The inset shows two traces reflecting averaged EPSCs at baseline (pre-HFS) and at 30 minutes post-HFS. (b) Average normalized scaled amplitude of peak EPSCs across 10 cells in the presence of KT5720 as indicated by the line. The value 30 minutes after HFS was 1.338 ± 1.016 which was significantly different from baseline values ($P < .01$) but was also significantly reduced in comparison to control conditions ($P < .01$).

We have demonstrated in the present study that excitatory feedforward interlaminar communication is not only a feature of the traditional hippocampal input and output laminae of the EC (i.e., the most deep and the most superficial) but is also a feature of the independent superficial laminae (III and II) which comprise the cells of origin of the temporal ammonic and perforant pathways, respectively. As well, we demonstrated that both the horizontal and ascending associative pathways have properties consistent with excitatory glutamatergic synapses at a variety of locations in the central nervous system. Both demonstrated NMDA and non-NMDA (presumably AMPA) components. Indeed, pharmacological manipulations using both APV and CNQX completely abolished excitatory synaptic responses.

Also similar to other glutamatergic synapses throughout the nervous system, both the horizontal and ascending associative pathways exhibited LTP. These results are in stark contrast to those of Deng and Lei [28] who failed to show LTP in either the horizontal or ascending (layer V) inputs to EC layer II stellate cells using a variety of stimulation paradigms including HFS. The only apparent differences between our conditions was their inclusion of QX-314 (0.2 mM) in the whole-cell pipette (in order to suppress action potential generation) and their baseline periods used (>30 minutes) in order to attain stable series resistances following whole cell dialysis. Although we found that complete whole-cell dialysis over this time periods greater than 30 minutes appeared to negatively affect the probability of achieving LTP, Deng and Lei were also unable to demonstrate LTP using perforated patch methods. Thus, whole-cell washout is presumably not the cause of the discrepancy. However, we do note that both field and sharp-electrode intracellular recording methods have consistently demonstrated LTP in the superficial EC [21, 22, 27, 33–35]. Interestingly, Alonso et al. [27] suggested that the intrinsic rhythmic properties of EC layer II stellates, brought about by the interaction of I_h and I_{Nap} [25], may play a pivotal role in the induction of plasticity of afferent inputs. Since QX-314 blocks both these currents and suppresses resonant and oscillatory behavior [36], this manipulation may indeed be relevant.

We did not test if the expression of LTP in the layer I input was NMDA or non-NMDA dependent [33, 35] although

with continued perfusions of APV in some experiments we continued to observe LTP in the layer III pathway, showing that it is presumably mediated by non-NMDA glutamate receptors.

4.2. Differential plasticity of the horizontal and ascending excitatory inputs to EC layer II

Although both pathways demonstrated intact NMDA receptor mediated transmission, only the induction of LTP in the horizontal pathway required NMDA signalling. As well, the calcium dependence of LTP in the layer III to II inputs did not appear to be as critical as that in the horizontal pathway. This suggests that the second-messenger systems mediating LTP in the two different input pathways are quite different and potentially independent. This makes layer II cells similar to other CNS neurons (such as CA3 pyramids in the hippocampus) in which different afferent inputs demonstrate NMDA- dependent and -independent LTP simultaneously [18]. A major difference is that the bulk of the LTP in EC layer II neurons in both pathways appears to be expressed via postsynaptic changes. Similar differences have been observed in LTP mechanisms in early postnatal (<P9) cortex and hippocampus [37, 38]. However, this is the first report to our knowledge showing this kind of difference in two independent pathways to the same sets of neurons in adult (>P27) brain.

ACKNOWLEDGMENTS

This work was supported by grants from the Medical Research Council/Canadian Institutes of Health Research and the Human Frontiers in Science Program to A. Alonso and the Natural Sciences and Engineering Research Council (RGPIN 249861) to C. T Dickson. A. Alonso was an MNI Killam Scholar and C. T Dickson is an Alberta Heritage Medical Scholar.

REFERENCES

[1] D. G. Amaral and M. P. Witter, "Hippocampal formation," in *The Rat Nervous System*, G. Paxinos, Ed., pp. 443–449, Academic Press, New York, NY, USA, 2nd edition, 1995.

[2] M. P. Witter, F. G. Wouterlood, P. A. Naber, and T. van Haeften, "Anatomical organization of the parahippocampal-hippocampal network," *Annals of the New York Academy of Sciences*, vol. 911, pp. 1–24, 2000.

[3] H. Eichenbaum, "A cortical-hippocampal system for declarative memory," *Nature Reviews Neuroscience*, vol. 1, no. 1, pp. 41–50, 2000.

[4] R. Schwarcz and M. P. Witter, "Memory impairment in temporal lobe epilepsy: the role of entorhinal lesions," *Epilepsy Research*, vol. 50, no. 1-2, pp. 161–177, 2002.

[5] B. T. Hyman, G. W. Van Hoesen, A. R. Damasio, and C. L. Barnes, "Alzheimer's disease: cell-specific pathology isolates the hippocampal formation," *Science*, vol. 225, no. 4667, pp. 1168–1170, 1984.

[6] G. W. Van Hoesen, J. C. Augustinack, J. Dierking, S. J. Redman, and R. Thangavel, "The parahippocampal gyrus in Alzheimer's disease. Clinical and preclinical neuroanatomical correlates," *Annals of the New York Academy of Sciences*, vol. 911, pp. 254–274, 2000.

[7] W. Zhou, D. Jiang, G. Raisman, and C. Zhou, "Embryonic entorhinal transplants partially ameliorate the deficits in spatial memory in adult rats with entorhinal cortex lesions," *Brain Research*, vol. 792, no. 1, pp. 97–104, 1998.

[8] B. J. Young, T. Otto, G. D. Fox, and H. Eichenbaum, "Memory representation within the parahippocampal region," *The Journal of Neuroscience*, vol. 17, no. 13, pp. 5183–5195, 1997.

[9] W. A. Suzuki and H. Eichenbaum, "The neurophysiology of memory," *Annals of the New York Academy of Sciences*, vol. 911, pp. 175–191, 2000.

[10] A. V. Egorov, B. N. Hamam, E. Fransén, M. E. Hasselmo, and A. Alonso, "Graded persistent activity in entorhinal cortex neurons," *Nature*, vol. 420, no. 6912, pp. 173–178, 2002.

[11] T. V. P. Bliss and G. L. Collingridge, "A synaptic model of memory: long-term potentiation in the hippocampus," *Nature*, vol. 361, no. 6407, pp. 31–39, 1993.

[12] J. G. Gu, C. Albuquerque, C. J. Lee, and A. B. MacDermott, "Synaptic strengthening through activation of Ca^{2+}-permeable AMPA receptors," *Nature*, vol. 381, no. 6585, pp. 793–796, 1996.

[13] L. M. Grover and T. J. Teyler, "Two components of long-term potentiation induced by different patterns of afferent activation," *Nature*, vol. 347, no. 6292, pp. 477–479, 1990.

[14] L. M. Grover and T. J. Teyler, "Different mechanisms may be required for maintenance of NMDA receptor-dependent and independent forms of long-term potentiation," *Synapse*, vol. 19, no. 2, pp. 121–133, 1995.

[15] R. C. Malenka and M. F. Bear, "LTP and LTD: an embarrassment of riches," *Neuron*, vol. 44, no. 1, pp. 5–21, 2004.

[16] P. V. Nguyen and N. H. Woo, "Regulation of hippocampal synaptic plasticity by cyclic AMP-dependent protein kinases," *Progress in Neurobiology*, vol. 71, no. 6, pp. 401–437, 2003.

[17] R. A. Nicoll and R. C. Malenka, "Contrasting properties of two forms of long-term potentiation in the hippocampus," *Nature*, vol. 377, no. 6545, pp. 115–118, 1995.

[18] R. A. Zalutsky and R. A. Nicoll, "Comparison of two forms of long-term potentiation in single hippocampal neurons," *Science*, vol. 248, no. 4963, pp. 1619–1624, 1990.

[19] H. Katsuki, S. Kaneko, A. Tajima, and M. Satoh, "Separate mechanisms of long-term potentiation in two input systems to CA3 pyramidal neurons of rat hippocampal slices as revealed by the whole-cell patch-clamp technique," *Neuroscience Research*, vol. 12, no. 3, pp. 393–402, 1991.

[20] M. G. Weisskopf, P. E. Castillo, R. A. Zalutsky, and R. A. Nicoll, "Mediation of hippocampal mossy fiber long-term potentiation by cyclic AMP," *Science*, vol. 265, no. 5180, pp. 1878–1882, 1994.

[21] S. H. Yun, I. Mook-Jung, and M. W. Jung, "Variation in effective stimulus patterns for induction of long-term potentiation across different layers of rat entorhinal cortex," *The Journal of Neuroscience*, vol. 22 RC214, pp. 1–5, 2002.

[22] S. Yang, D. S. Lee, C. H. Chung, M. Y. Cheong, C.-J. Lee, and M. W. Jung, "Long-term synaptic plasticity in deep layer-originated associational projections to superficial layers of rat entorhinal cortex," *Neuroscience*, vol. 127, no. 4, pp. 805–812, 2004.

[23] L. Ma, C. T. Dickson, and A. Alonso, "Long-term potentiation in the intrinsic ascending pathways of the entorhinal cortex," *Society for Neuroscience Abstracts*, vol. 25, p. 461, 1999.

[24] A. Alonso and R. Klink, "Differential electroresponsiveness of stellate and pyramidal-like cells of medial entorhinal cortex

layer II," *Journal of Neurophysiology*, vol. 70, no. 1, pp. 128–143, 1993.

[25] C. T. Dickson, J. Magistretti, M. H. Shalinsky, E. Fransén, M. E. Hasselmo, and A. Alonso, "Properties and role of I_h in the pacing of subthreshold oscillations in entorhinal cortex layer II neurons," *Journal of Neurophysiology*, vol. 83, no. 5, pp. 2562–2579, 2000.

[26] M. G. Blanton, J. J. Lo Turco, and A. R. Kriegstein, "Whole cell recording from neurons in slices of reptilian and mammalian cerebral cortex," *Journal of Neuroscience Methods*, vol. 30, no. 3, pp. 203–210, 1989.

[27] A. Alonso, M. de Curtis, and R. R. Llinás, "Postsynaptic Hebbian and non-Hebbian long-term potentiation of synaptic efficacy in the entorhinal cortex in slices and in the isolated adult guinea pig brain," *Proceedings of the National Academy of Sciences of the United States of America*, vol. 87, no. 23, pp. 9280–9284, 1990.

[28] P.-Y. Deng and S. Lei, "Long-term depression in identified stellate neurons of juvenile rat entorhinal cortex," *Journal of Neurophysiology*, vol. 97, no. 1, pp. 727–737, 2007.

[29] R. Klink and A. Alonso, "Morphological characteristics of layer II projection neurons in the rat medial entorhinal cortex," *Hippocampus*, vol. 7, no. 5, pp. 571–583, 1997.

[30] C. T. Dickson, G. Biella, and M. de Curtis, "Evidence for spatial modules mediated by temporal synchronization of carbachol-induced gamma rhythm in medial entorhinal cortex," *The Journal of Neuroscience*, vol. 20, no. 20, pp. 7846–7854, 2000.

[31] C. T. Dickson and A. Alonso, "Muscarinic induction of synchronous population activity in the entorhinal cortex," *The Journal of Neuroscience*, vol. 17, no. 17, pp. 6729–6744, 1997.

[32] F. Kloosterman, T. van Haeften, M. P. Witter, and F. H. Lopes da Silva, "Electrophysiological characterization of interlaminar entorhinal connections: an essential link for re-entrance in the hippocampal-entorhinal system," *European Journal of Neuroscience*, vol. 18, no. 11, pp. 3037–3052, 2003.

[33] M. de Curtis and R. R. Llinás, "Entorhinal cortex long-term potentiation evoked by theta-patterned stimulation of associative fibers in the isolated in vitro guinea pig brain," *Brain Research*, vol. 600, no. 2, pp. 327–330, 1993.

[34] H.-Y. Jung, T. Mickus, and N. Spruston, "Prolonged sodium channel inactivation contributes to dendritic action potential attenuation in hippocampal pyramidal neurons," *The Journal of Neuroscience*, vol. 17, no. 17, pp. 6639–6646, 1997.

[35] S. H. Yun, K. Huh, and M. W. Jung, "Selective enhancement of non-NMDA receptor-mediated responses following induction of long-term potentiation in entorhinal cortex," *Synapse*, vol. 35, no. 1, pp. 1–7, 2000.

[36] B. Hutcheon, R. M. Miura, and E. Puil, "Subthreshold membrane resonance in neocortical neurons," *Journal of Neurophysiology*, vol. 76, no. 2, pp. 683–697, 1996.

[37] A. Kirkwood, A. Silva, and M. F. Bear, "Age-dependent decrease of synaptic plasticity in the neocortex of αCaMKII mutant mice," *Proceedings of the National Academy of Sciences of the United States of America*, vol. 94, no. 7, pp. 3380–3383, 1997.

[38] H. Yasuda, A. L. Barth, D. Stellwagen, and R. C. Malenka, "A developmental switch in the signaling cascades for LTP induction," *Nature Neuroscience*, vol. 6, no. 1, pp. 15–16, 2003.

Hindawi Publishing Corporation
Neural Plasticity
Volume 2008, Article ID 646919, 9 pages
doi:10.1155/2008/646919

Research Article

Effect of Prenatal Protein Malnutrition on Long-Term Potentiation and BDNF Protein Expression in the Rat Entorhinal Cortex after Neocortical and Hippocampal Tetanization

Alejandro Hernández,[1] Héctor Burgos,[2] Mauricio Mondaca,[3] Rafael Barra,[3] Héctor Núñez,[3] Hernán Pérez,[3] Rubén Soto-Moyano,[3] Walter Sierralta,[3] Victor Fernández,[4] Ricardo Olivares,[5] and Luis Valladares[3]

[1] *Department of Biology, Faculty of Chemistry and Biology, University of Santiago of Chile, 3363 Avenida Alameda Bernardo O'Higgins, 9170022 Santiago, Chile*
[2] *School o f Psychology, Las Americas University, 1 Oriente Mall Marina Arauco, 2541362 Viña del Mar, Chile*
[3] *Institute of Nutrition and Food Technology (INTA), University of Chile, 5540 Avenida Macul, 7830489 Santiago, Chile*
[4] *Montessori Study Center, 2865 Avenida Duble Alméyda, 7750169 Santiago, Chile*
[5] *Department of Animal Biological Sciences, Faculty of Veterinary Sciences, University of Chile, 11735 Avenida Santa Rosa, 8820808 Santiago, Chile*

Correspondence should be addressed to Alejandro Hernández, ahernand@lauca.usach.cl

Received 5 February 2008; Accepted 30 May 2008

Recommended by C. Andrew Chapman

Reduction of the protein content from 25 to 8% casein in the diet of pregnant rats results in impaired neocortical long-term potentiation (LTP) of the offspring together with lower visuospatial memory performance. The present study was aimed to investigate whether this type of maternal malnutrition could result in modification of plastic capabilities of the entorhinal cortex (EC) in the adult progeny. Unlike normal eutrophic controls, 55–60-day-old prenatally malnourished rats were unable to develop LTP in the medial EC to tetanizing stimulation delivered to either the ipsilateral occipital cortex or the CA1 hippocampal region. Tetanizing stimulation of CA1 also failed to increase the concentration of brain-derived neurotrophic factor (BDNF) in the EC of malnourished rats. Impaired capacity of the EC of prenatally malnourished rats to develop LTP and to increase BDNF levels during adulthood may be an important factor contributing to deficits in learning performance having adult prenatally malnourished animals.

Copyright © 2008 Alejandro Hernández et al. This is an open access article distributed under the Creative Commons Attribution License, which permits unrestricted use, distribution, and reproduction in any medium, provided the original work is properly cited.

1. INTRODUCTION

Both human and animal studies indicate that maternal protein malnutrition alters various maturational events in the brain resulting in behavioral abnormalities, altered cognitive functioning, and disturbances in learning and memory (for review, see [1]). Alterations extend into the postnatal period and continue into adulthood. For example, on reaching adulthood prenatally malnourished rats on a 6% prenatal/25% postnatal casein diet exhibit learning disturbances, such as deficits in execution of spatial alternation tasks [2] as well as impaired visual discrimination learning [3]. In addition, on reaching adulthood, rats born from 8% case in-restricted mothers showed decreased visuo-spatial memory performance [4].

One of the principal hypotheses in the malnutrition field relates to the issue that decreases in synaptic plasticity may be a critical brain mechanism underlying learning deficits observed as a result of nutritional insults to the developing brain. In this regard, it has been shown that it is difficult to induce and maintain hippocampal [5, 6] and neocortical [4] long-term potentiation (LTP) in brains of prenatally malnourished rats. Whether prenatal malnutrition could affect synaptic plasticity in brain regions other than the hippocampus and cerebral neocortex is unknown at present. The entorhinal cortex (EC) is well situated to play a key role in the bidirectional interactions between the neocortex and the hippocampus, and is thought to be critically involved in the formation of declarative (or explicit) memory—the ability to recollect everyday events and factual knowledge.

Potentially, prenatal malnutrition could alter at this level the bidirectional communication between the neocortex and the hippocampus, thereby disturbing some types of cognitive processes. However, the effects of prenatal malnutrition on EC neuroplastic mechanisms have not still been explored. The superficial layers (I–III) of the EC are regarded as "input layers" since terminations of the projections from perirhinal and parahippocampal cortices—the recipients of cortical association areas—occur primarily in these layers [7–11]. Information processed in the hippocampus and subiculum is then returned to the deep layers (V-VI) of the EC via projections from the CA1 field and subiculum [11–14], and these layers in turn project to forebrain structures [15–17]. Accordingly, the deep layers are regarded as "output layers," and therefore functionally segregated from the superficial layers. Similar to other brain regions, the EC has been shown to express N-methyl-D-aspartate (NMDA) receptor-dependent LTP [18–20] and long-term depression [20–24], both in in vitro and in vivo experimental paradigms.

The present study was aimed to investigate whether mild reduction of the protein content of the diet of pregnant rats can modify plastic capabilities of the EC in vivo. In contrast to severe forms of maternal malnutrition, mild reduction of the casein content in the diet of pregnant rats from 25 to 8%, calorically compensated for by carbohydrates, results in apparently normal in utero development of fetuses, as assessed by normal maternal weight gain during pregnancy and normal body and brain weights of pups at birth [25]. However, this insidious form of protein maternal malnutrition, so-called "hidden" prenatal malnutrition [25], results in altered noradrenergic function in the neocortex of the offspring together with impaired neocortical LTP and lower visuospatial memory performance [4, 26–28]. The present results provide evidence that mild prenatal malnutrition in rats leads to impaired long-term synaptic potentiation together with decreased expression of brain-derived neurotrophic factor (BDNF) in the EC of adult animals; a neurotropin plays a major role in regulating induction and maintenance of LTP [29, 30].

2. MATERIALS AND METHODS

2.1. Animals and diets

The experimental protocol and animal management were in accordance with the NIH Guide for the Care and Use of Laboratory Animals [31], and was approved by the Committee for the Ethical Use of Experimental Animals, INTA, University of Chile. Female Sprague-Dawley rats were fed isocaloric purified diets containing either normal (25% casein, providing 22.5% protein) or low (8% casein, providing 7.2% protein) amounts of protein. The other components of the purified diets were as follows. (i) Normal diet: carbohydrate, 50.2%; fat, 15.0%; vitamin mix, 1.0%; salt mix, 4.7%; water, 1.7%; cellulose, 4.2%; L-methionine, 0.4%. (ii) Low protein diet: carbohydrate, 66.5%; fat, 15.0%; vitamin mix, 1.0%; salt mix, 4.7%; water, 1.0%; cellulose, 4.2%; L-methionine, 0.4%. Both diets provide about 4.3 Kcal/g. The dietary paradigm was started 1 day after mating and continued throughout pregnancy. The body weight gain of the pregnant mothers was controlled daily. At birth, all pups were weighed and litters were culled to 8 pups (4 males, 4 females). Afterwards, pups born from mothers fed the 7.2% protein diet were fostered to well-nourished dams (22.5% protein diet) giving birth on that day. Pups born from mothers receiving the 22.5% protein diet were also fostered to well-nourished dams in order to equalize among groups other factors that may depend on the rearing conditions (i.e., stress due to cross-fostering). After weaning, at 22 days of age, all pups were fed a standard laboratory diet providing 22.5% protein.

2.2. LTP determinations in the medial EC

Experiments were carried out in 16 normal and 16 malnourished rats of 55–60 days of age. Rats were weighed, anesthetized with 1.5 g/kg i.p. urethane, and placed in a stereotaxic apparatus under artificial ventilation. Reinforcement of anesthesia during the experiments was not necessary since surgical procedures and recordings lasted no longer than 3 hours and, in our experience, 1.5 g/kg i.p. urethane induces profound anesthesia lasting more than 6 hours. Animals never regained consciousness and no changes in heart rate in response to stimulation were detected throughout the experiments.

Field responses were evoked in the left medial EC by electrical stimulation of either the ipsilateral occipital cortex or the ipsilateral ventral CA1 hippocampal region, in an alternated fashion. After exposure of the left occipital lobe, electrical stimulation of the occipital cortex and the ventral CA1 hippocampal region was carried out by means of two independent bipolar side-by-side electrodes composed each by two glued, parylen-insulated, 50-μm-diameter tungsten wires with a 0.8-mm tip separation. One stimulating electrode was positioned in the left occipital cortex at coordinates $A = -5.8$, $L = -3.5$, in mm, in such a way that the longer tip penetrated the cortex by 1.0 mm. The other stimulating electrode was advanced to the ventral CA1 region at coordinates $A = -5.5$, $L = -5.0$, $V = 7.0$, in mm. As has pointed out recently, progressively more ventral CA1 regions innervate progressively more medial regions of the medial entorhinal areas [32], which in turn receive more strong visual input through the parahippocampal cortex (postrhinal cortex in the rat [7]).

Field responses were recorded from the left medial EC with another bipolar side-by-side electrode (two glued, parylen-insulated, 50-μm-diameter tungsten wires with a 0.8-mm tip separation) positioned at coordinates $A = -7.5$, $L = -5.0$, $V = 6.5$, the longer tip being 0.1-0.2 mm above the ventral brain surface. Configuration and positioning of the recording electrode pair into the EC allowed one tip of the bipolar electrode was into layer II-III and the other tip near layer V. Although bipolar electrode arrangement does not allow performing laminar analysis of potential reversal, it maximizes field recordings corresponding to depolarization of neurons (active inward current or sink) situated near to one electrode tip, while minimizing those produced in distant current generators affecting rather similarly the

two electrode tips. Thus, bipolar electrodes seem especially appropriate for focalized recording from laminar cortical structures such as the EC, where differential activation of neurons of layers II-III by neocortical-EC pathways, or layer V by CA1-EC afferents, will create, respectively, superficial and deep current sinks. Rostrocaudal (A) and lateral (L) coordinates were relative to bregma, while vertical (V) coordinates were relative to the cortical surface, all taken from Paxinos and Watson [33]. Figure 1 shows a scheme of two coronal planes of the rat brain illustrating the positions of the stimulating electrodes in the occipital cortex and ventral CA1 region of the left hemisphere, as well as the location of the recording electrode in the ipsilateral EC. Test stimuli, alternately applied to either the occipital cortex (during 2.5 minutes) or the ventral CA1 region (during 2.5 minutes), consisted of 100 microseconds duration square-wave pulses at 0.2 Hz generated by means of a Grass S11 stimulator in conjunction with a Grass SIU-5 stimulus isolation unit and a Grass CCU 1A constant current unit (Astro-Med Inc., West Warwick, RI, USA). Bipolar recording of EC field responses to occipital cortex stimulation consisted of a bigger upward negative wave followed by a downward positive component. Surface negative responses have been already recorded in vivo from the EC of rats during stimulation of the piriform cortex [34]. In turn, EC field responses to CA1 stimulation begin with a marked downward surface positive deflection followed by a late upward surface negative wave of smaller amplitude. In vivo recording of surface positive field responses from the EC of rats during CA1 stimulation has recently been reported [35–37]. Thus, only the negative first-wave of occipital cortex-EC responses and the positive first-wave of CA1-EC responses were measured in the present experiments. Before beginning each experiment, two full input-output series, one for the occipital cortex and the other for CA1, were performed at stimulus intensities of 200–1200 μA. Test stimuli with a stimulation intensity yielding EC responses with first-wave peak amplitude of 50% of the maximum were used for the remainder of the experiment. Thus, test stimuli applied to the occipital cortex were similar in frequency and duration to those applied to CA1, but rather different in intensity. EC responses evoked from the occipital cortex and from the CA1 region were also subjected to a 10-pulse, 30 Hz stimulus in order to test the ability of the response to follow repetitive stimulation. As showed elsewhere [34, 38], polysynaptic components usually fail at frequencies <40–50 Hz, whereas monosynaptic components should follow frequencies near 100 Hz. After a 30-minute stabilization period of alternated occipital cortex and CA1 stimulation with test stimuli, a 2.5-minute control period of EC basal responses (30 averaged responses) evoked from the occipital cortex was recorded, followed by another 2.5-minute control period of EC basal responses (30 averaged responses) evoked from the CA1 region. Thereafter, LTP was induced in the medial EC by applying tetanizing stimulation either to the occipital cortex (8 normal and 8 malnourished rats) or to the ventral CA1 region (8 additional normal and 8 additional malnourished rats). The tetanizing stimulus consisted of three high-frequency trains (100 microseconds square-wave pulses at 312 Hz) of 500 milliseconds duration each, applied every 30 seconds with intensity 50% higher than the respective test stimuli. Such a stimulating protocol has been shown to induce saturating LTP in the EC, at least when activating the EC from the piriform cortex in awake rats, meaning that subsequent application of additional trains fails to induce further increments of field responses [34]. A closely similar stimulating protocol (3 trains of stimuli for 200 milliseconds at 250 Hz with intertrain interval of 30 seconds) applied to the CA1 hippocampal region has been reported to produce reliable LTP induction in the EC of uretanized rats [37].

Recordings were amplified by a Grass P-511 preamplifier (0.8–1000 Hz bandwidth), and displayed and averaged on a Philips PM 3365A digital oscilloscope. They were also digitized at a rate of 10000/second by an A/D converter interfaced to an Acer PC, and stored for retrieval and offline analysis. In all experiments, body temperature and expired CO_2 were monitored and remained within normal limits. Peak latency and peak amplitude of the early component of averaged field responses were measured using time and voltage cursors provided in the digital oscilloscope. Slope was determined as the amplitude/time ratio on the nearest sample to the 10% and the 90% level between cursors set on the beginning and the peak of the early negative or positive wave (see Figure 1, first and second arrow, resp., in recordings (A and C)). The efficacy of the tetanizing train to potentiate cortical evoked responses was evaluated by measuring both the peak amplitude and the maximal slope increases. The results were similar but the former procedure led to lower variability of means (as revealed by statistical variance), so amplitudes were used for analyses of the experiments.

Two hours after occipital cortex or CA1 tetanization, once the electrophysiological experiments were finished, the animals were sacrificed by decapitation, the brain rapidly removed and weighed, and the left and right ECs dissected out. The average weight of dissected entorhinal area (averaged without taking into consideration left or right hemisphere origin) was 5.77 ± 0.61 for normal rats and 5.30 ± 0.50 for malnourished animals (mean $\pm$ SEM). These samples were stored at -80°C before use. Afterwards, the tissues were examined for expression of BDNF protein level by ELISA.

2.3. Determination of BDNF in the EC

Whole samples of EC were homogenized in ice-cold lysis buffer, containing 137 mM NaCl, 20 mM Tris-HCl (pH 8.0), 1% Triton X-100, 10% glycerol, and 2 μL/mL protease inhibitor cocktail P8340 (Sigma-Aldrich, St. Louis, MO, USA). The tissue homogenate solutions were centrifuged at 14000 x g for 5 minutes at 4°C. The supernatants were collected and diluted 1/5 in buffer DPBS and then acidified in 1 N HCl. They were then incubated for 15 minutes at room temperature and neutralized with 1 N NaOH until pH 7.6. BDNF was assessed using the E-Max ImmunoAssay system ELISA kit (Promega, Co., Madison, Wis, USA). Briefly, standard 96-well flat-bottom NUNC-immuno maxisorp ELISA plates were incubated overnight at 4°C with a monoclonal

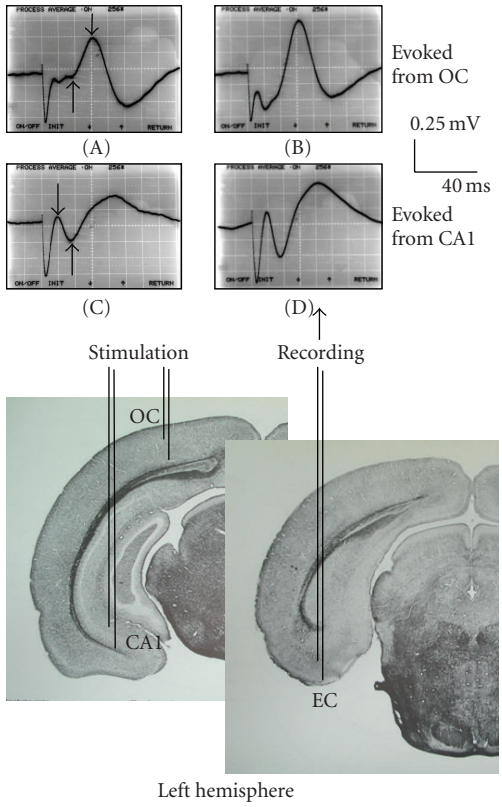

(a)

	Onset latency	Peak latency
Evoked from OC	18.7 ± 2.2	30.6 ± 1.8
Evoked from CA1	9.6 ± 0.7	17.9 ± 0.8

(b)

Figure 1: (a) Scheme of two coronal planes of the rat brain illustrating the positions of the stimulating electrodes in the occipital cortex (OC) and ventral CA1 region of the left hemisphere, as well as the location of the recording electrode in the ipsilateral entorhinal cortex EC. In the upper part are shown representative examples of the average of 30 successive responses evoked in the medial EC of one rat by ipsilateral stimulation of the occipital cortex (A and B) or the ventral CA1 hippocampal region (C and D) at 0.2 Hz, obtained before (A and C) and after (B and D) tetanization. Calibration bars are indicated. Upward potential deflection is negative. First and second arrows indicate, respectively, the beginning and the peak of the early negative (A) or early positive (C) wave, which served to calculate peak amplitude or slope (amplitude/time ratio on the nearest sample to the 10% and the 90% level) of the early component. (b) Onset and peak latencies (values are means ± SEM, in millisecond) of the early component of EC responses to test stimulus applied to either the OC or CA1 region before tetanization.

anti-BDNF antibody. The plates were blocked by incubation for 1 hour at room temperature (RT) with a 1x block and sample buffer. Serial dilutions of known amounts of BDNF ranging from 0 to 500 pg/mL were performed in duplicate for standard curve determination. Wells containing the standard curves and supernatants of brain tissue homogenates were incubated at room temperature for 2 hours, as specified by the protocol. They were then incubated with a secondary antihuman BDNF polyclonal antibody for 2 hours at room temperature, as specified by the protocol. A species-specific antibody conjugated to horseradish peroxidase was used for tertiary reaction for 1 hour at room temperature following this incubation step. TMB one solution was used to develop color in the wells. This reaction was terminated with 1 N hydrochloric acid at a specific time (10 minutes) at room temperature, and absorbance was then recorded at 450 nm in a microplate reader within 40 minutes of stopping the reaction. The neurotrophin values were determined by comparison with the regression line for BDNF and expressed as pg BDNF/mg wet weight. Using this kit, BDNF can be quantified in the range of 7.8–500 pg/mL.

2.4. Statistical analyses

All statistical analyses were performed with GraphPad Instat version 3.00 (GraphPad Software, Inc., San Diego, Calif, USA). For the effect of dietary treatments on body and brain weights, intergroup comparisons were made using unpaired Student's t-test. For the analysis of the time-course in LTP studies, a one-way ANOVA was performed for intragroup comparisons followed by Dunnett's multiple comparisons post-hoc test. For analyzing results of BDNF protein expression, intergroup comparisons between normal and malnourished groups were made using unpaired Student's t-test, while the effect of tetanization was assessed using nonparametric ANOVA (Kruskal-Wallis test) followed by Dunn's multiple comparisons post-hoc test.

3. RESULTS

3.1. Effect of dietary treatment on body and brain weights

Body and brain weights measurements revealed that there were no significant differences in body weight gain of pregnant mothers receiving 7.2% or 22.5% protein diet (data not shown). Full data on the effects of this dietary treatment on maternal weight gain during the first, second, and third weeks of pregnancy was published elsewhere [26]. At days 1, 8, and 55–60 of postnatal life, no significant differences in body and brain weights were found between rats born from mothers receiving 7.2% or 22.5% protein diet (Table 1).

3.2. LTP in vivo in the medial EC

In rats of 55–60 days of age, bipolar recording of basal EC field responses to occipital cortex stimulation consisted of a prominent upward negative wave followed by a positive component. This is consistent with the arrangement of the side-by-side bipolar electrode located into the EC, where the longer tip is expected to be recording an early superficial sink generated by depolarization of stellate and pyramidal principal neurons within input layers II-III (in relation to rather silent deep layers). In contrast, basal EC responses to CA1 stimulation began with a marked downward surface

Table 1: Body and brain weights of normal and prenatally malnourished rats. Values are means ± SEM. $N = 16$ rats in each group. No statistically significant differences (NS) were found when comparing body and brain weights of normal and malnourished groups of same ages (unpaired Student's t-test).

	Body weight (g)			Brain weight (mg)
Age	Day 1	Day 8	Day 55	Day 55–60
Normal	7.3 ± 0.07	18.9 ± 0.37	235 ± 10	1322.0 ± 16.1
Malnourished	7.2 ± 0.09	19.1 ± 0.45	229 ± 12	1318.6 ± 15.7
P	NS	NS	NS	NS

positive deflection followed by a late surface negative wave, which is consistent with the recording through the shorter tip of an early deep sink resulting from depolarization of pyramidal cells within output layer V. Figure 1(a) shows typical recordings of basal (A and C) and potentiated (B and D) averaged EC field responses evoked by stimulation of the occipital cortex (A and B) or the CA1 region (C and D). In normal eutrophic rats, the onset and peak latencies of the early negative component of basal EC responses evoked from the occipital cortex were 18.7 ± 2.2 and 30.6 ± 1.8 milliseconds, respectively, while the onset and peak latencies of the early positive wave in basal responses evoked from CA1 were 9.6 ± 0.7 and 17.9 ± 0.8 milliseconds (Figure 1(b)). For both type of responses, the differences in latency before and after potentiation were not statistically significant (paired Student's t-test, $N = 8$). Shape, latencies, and wave amplitudes of basal field responses evoked in the EC of prenatally malnourished rats, either from the occipital cortex or the CA1 area, did not differ from those of normal eutrophic rats (unpaired Student's t-test, $N = 8$ in each group). Frequency testing showed that the early component of the EC potential evoked from the occipital cortex declined rapidly with a stimulus frequency of 30 Hz, thus suggesting a polysynaptic nature of the response. In contrast, the early component of the EC response elicited from CA1 was able to follow 30 Hz stimulation frequency with decreasing amplitude of less than 20%, which is characteristic of monosynaptic responses.

In normal animals, tetanizing stimulation applied to either the occipital cortex or the CA1 hippocampal region produced a significant increase in peak amplitude of the early component evoked in the ipsilateral medial EC, which remained unchanged throughout the recording period (Figure 2). After tetanizing the occipital cortex, the early negative wave to occipital cortex test stimuli was potentiated to neocortical test stimuli in all blocks over the time-course (ranging from 107 to 136%, Dunnett's multiple comparisons test) excepting for block 2.5–5 minutes, while no significant potentiation to CA1 stimuli was observed in the early component of EC responses (Dunnett's multiple comparisons test); however, a transient but complete inhibition was early observed on block 0–2.5 minutes. After tetanizing the ventral CA1, the early positive wave of EC responses to CA1 test stimuli was potentiated in all blocks over the time-course (ranging from 59 to 72%, Dunnett's multiple comparisons test) excepting for block 2.5–5 minutes, while no significant potentiation to occipital cortex stimulation was observed.

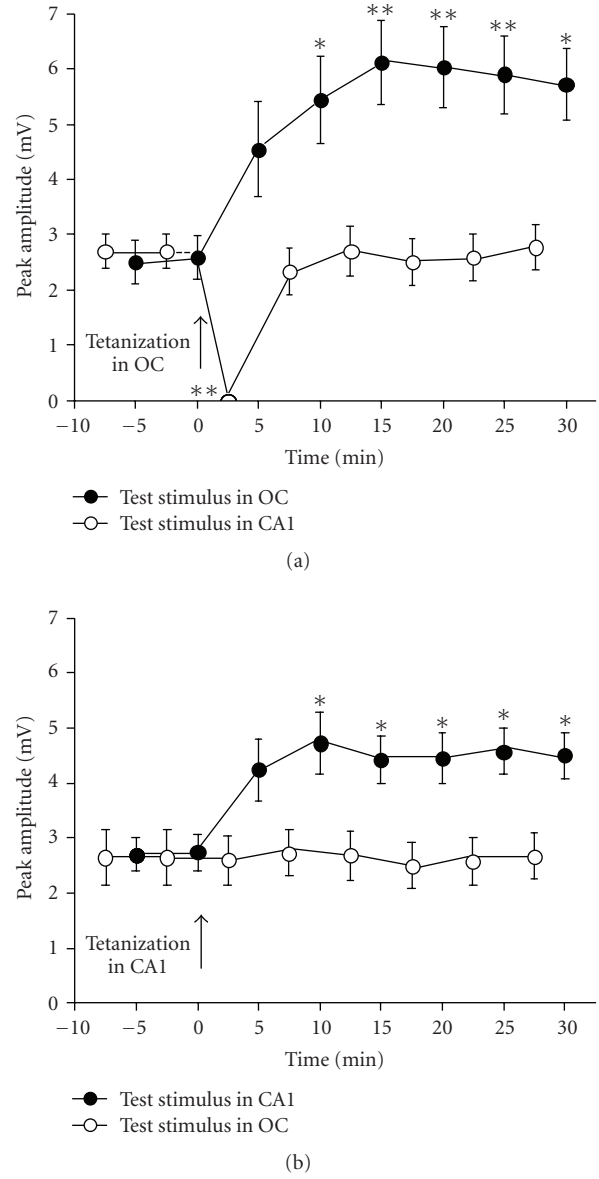

Figure 2: Time-course of LTP induced in the medial entorhinal cortex of 55–60-day-old normal eutrophic rats by applying tetanizing stimulation to the occipital cortex (a) or to the ventral CA1 hippocampal region (b). The arrow indicates time of application of the tetanizing stimulus. $N = 8$ rats in all groups. Values are means ± SEM of peak-to-peak amplitudes, 30 responses averaged per rat. Note the occurrence of homosynaptic, but not heterosynaptic potentiation. One-way ANOVA followed by Dunnett's multiple comparisons test indicated significant intragroup differences in peak-to-peak amplitudes ($^*P < .05$, $^{**}P < .01$) when comparing post-tetanizing values with the last pretetanizing basal point (at 0 minute), excepting for block 2.5–5 minutes (a), where significant inhibition ($^{**}P < .01$) occurred.

In contrast to that occurred in normal controls, no significant increase of the early component of EC field responses evoked from the occipital cortex or from the CA1 region ($P > .05$ for all blocks, Dunnett's multiple comparisons test) was

observed in malnourished animals after applying neocortical or hippocampal tetanizing stimulation (Figure 3).

3.3. BDNF expression in the EC

Serial dilutions of known amounts of BDNF ranging from 0 to 500 pg/mL allowed to determine a standard curve demonstrating a direct relationship between optical density and BDNF concentration ($r^2 = 0.9106$).

Table 2 shows that application of tetanizing stimulation to the left CA1 region in normal rats resulted in a significant increase of BDNF concentration in the ipsilateral EC ($P < .05$, Dunn's multiple comparisons test) two hours after tetanization, while application of tetanizing stimuli to the left occipital cortex did not significantly modify the BDNF level in the ipsilateral EC. In contrast, tetanizing stimulation applied to either the occipital cortex or the CA1 hippocampal region in malnourished rats was ineffective in modifying the BDNF concentration in the ipsilateral EC. Table 2 also shows that on days 55–60 of postnatal life, malnourished rats exhibited significant lower concentration of BDNF protein in the right medial EC (corresponding to the nonstimulated cerebral hemisphere) than that observed in normal animals of same ages ($P < .05$, unpaired Student's t-test).

4. DISCUSSION

Mild reduction of the protein content of the maternal diet of pregnant rats did not significantly alter body and brain weights of pups at birth, indicating that protein deficiency in the 7.2% protein group was masked by caloric compensation with carbohydrates, leading to apparently normal fetal development as assessed by body and brain weights at birth. A similar result has been reported elsewhere [25, 39]. As discussed by others [25, 39], fetal growth retardation and reductions in brain weight after prenatal malnutrition are only produced by severe protein restriction, that is, reduction of the protein content of the maternal diet to less than 6%.

The foregoing electrophysiological data show that the medial EC of normal eutrophic rats can develop LTP in vivo to tetanization of both the occipital cortex and the CA1 hippocampal region. This is consistent with previous data showing that the EC could express LTP to tetanizing stimulation of some cortical and hippocampal regions in in vivo conditions. For example, Chapman and Racine [34] have reported a surface negative response that could be evoked in vivo in the EC of rats by stimulation of the piriform cortex, and that these responses undergo LTP to high-frequency stimulation of the piriform cortex. However, Ivanco and Racine [35] found that stimulation of the motor cortex failed to elicit EC responses. On the other hand, surface positive field responses have been elicited in vivo in the EC of rats by stimulation of CA1 [35–37]. In all these studies, the early positive component of the EC response supported LTP to high frequency stimulation.

The present results also suggest that the early negative response evoked in the entorhinal cortex (EC) by occipital cortex stimulation is apparently polysynaptic, since it had slow onset and peak latencies and it was very sensitive

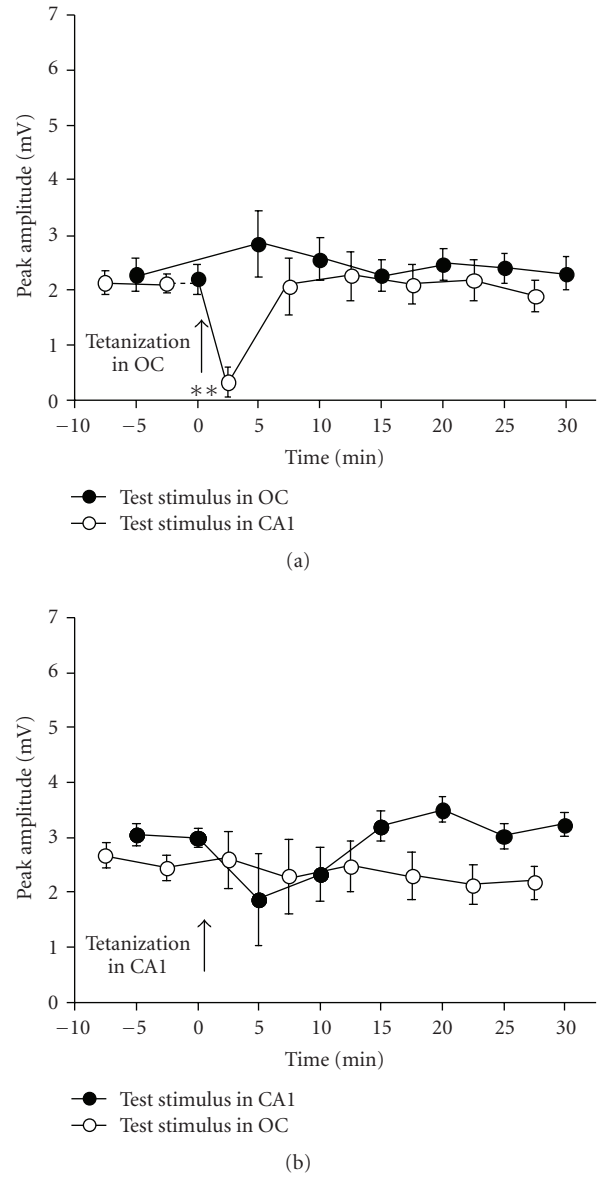

Figure 3: Failure of tetanizing stimulation applied to the occipital cortex (a) or to the ventral CA1 hippocampal region (b) to induce LTP in the medial entorhinal cortex of 55–60-day-old prenatally malnourished rats. The arrow indicates time of application of the tetanizing stimulus. $N = 8$ rats in all groups. Values are means ± SEM of peak-to-peak amplitudes, 30 responses averaged per rat. It can be noted that neither homosynaptic nor heterosynaptic potentiation occurred in the EC of malnourished animals. One-way ANOVA followed by Dunnett's multiple comparisons test indicated no significant intragroup differences in peak-to-peak amplitudes when comparing posttetanizing values with the last pretetanizing basal point (at 0 minute), excepting for block 2.5–5 minutes (a) where significant inhibition ($^{**}P < .01$) occurred.

to 30 Hz stimuli. As reported previously, these inputs are synaptically relayed within the perirhinal and/or parahippocampal cortices before to reach the superficial layers of the EC [7–11]. Polysynaptic LTP often involves local circuits within the recipient brain region, but sometimes is synaptically relayed by brain intermediate regions that are

Table 2: Changes in BDNF expression (pg/mg wet tissue) in the left entorhinal cortex (EC) of 55–60-day-old normal and prenatally malnourished rats two hours after applying ipsilateral tetanizing stimulation to the occipital cortex (OC) or the CA1 hippocampal region, as compared to BDNF levels in the right EC. Values are means ± SEM. The number of samples in each group is shown in parentheses. BDNF concentrations in right EC samples after tetanizing the left OC or left CA1 did not significantly differ between them, and were therefore pooled. Comparisons of BDNF levels between normal and malnourished groups were made using unpaired Student's t-test, and P_{NC} is the probability level for comparisons related to the nutritional condition (NS = not significant). Comparisons between basal BDNF levels (right EC) with those obtained after OC or CA1 tetanization (left EC) were made using nonparametric ANOVA (Kruskal-Wallis test) followed by Dunn's multiple comparisons post-hoc test, and P_T is the probability level for comparisons between right and left EC samples (different superscripts indicate a significant difference, $P < .05$; NS = not significant).

	Pooled OC + CA1 tetanization (right EC)	OC tetanization (left EC)	CA1 tetanization (left EC)	P_T
Normal	$15.7 \pm 3.5^a(8)$	$14.4 \pm 2.6^a(4)$	$25.1 \pm 2.2^b(4)$	<0.05
Malnourished	9.5 ± 0.82 (8)	11.4 ± 2.0 (4)	8.1 ± 1.6 (4)	NS
P_{NC}	<0.05	NS	<0.001	

more distant from the recipient zone thus involving long axonmediated connections. Regarding the present results, it is not possible to directly known if potentiation occurred in neurons of the final recipient entorhinal region or in intermediate perirhinal neurons relaying the response (or in both) and, therefore, the site of LTP occurrence remains rather unresolved. In contrast, the early positive response evoked in the entorhinal cortex (EC) by CA1 stimulation is apparently monosynaptic since it had shorter onset and peak latencies and followed a stimulus frequency of 30 Hz without showing a significant amplitude decrease. As mentioned previously, direct projections from the CA1 field to the deep V-VI layers of the EC have already been reported [15–17].

The fact that tetanization of the occipital cortex or the CA1 region only potentiates the responses driven by the tetanized region confirms that the early component of EC responses to either occipital cortex or CA1 stimulation represents the activation of two distinct set of neurons (presumably located in superficial layers II-III and deep layer V, resp.). Nevertheless, prenatally malnourished adult rats were unable to develop LTP in the medial EC, at least when submitted to a similar tetanizing stimulation protocol to that applied to the occipital neocortex or the ventral CA1 region in normal eutrophic animals, thus suggesting that mild prenatal malnutrition impairs some neural substrate involved in the generation and/or maintenance of EC plasticity. Previous reports have shown that it is difficult to induce and maintain hippocampal [5, 6] and neocortical [4] LTP in brains of prenatally malnourished rats, but the underlying cellular/molecular mechanisms are still unresolved. Reduced plastic response in the hippocampus of prenatally malnourished rats seems to be related to significant increases in GABAergic inhibition in the dentate gyrus [1, 40], while in neocortex it may be correlated with decreased noradrenaline release due to enhanced α_{2C} adrenoceptor expression [4, 28]. However, the effect of prenatal malnutrition on neuroplastic mechanisms operating in the EC had not yet been explored.

Interestingly, the medial EC of normal eutrophic rats showed increased BDNF concentration two hours after delivering tetanizing stimulation to the ipsilateral CA1, whereas the same stimulatory protocol failed in modifying the BDNF level in the EC of prenatally malnourished rats. As has previously been reported, high-frequency stimulation inducing LTP evokes significant increases in BDNF mRNA expression [41–44] and BDNF release [45] in the hippocampus, although changes in hippocampal BDNF protein levels after LTP induction, have not still been evaluated. In addition, released BDNF activates distinct mechanisms to regulate the induction, early maintenance, and late maintenance phases of hippocampal LTP [29, 30]. Curiously, LTP induced by unilateral perforant path stimulation seems to produce bilateral induction of BDNF mRNA, although limited to the dentate gyrus [42–46]. A more detailed study addressing this aspect was carried out by Bramham et al. [47], who demonstrated that unilateral LTP induction in the dentate gyrus of awake rats led to highly selective ipsilateral (trkB and NT-3 mRNA) or bilateral (trkC, BDNF, and nerve growth factor mRNA) increases in gene expression, indicating that LTP triggers an interhemispheric communication manifested as selective, bilateral increases in gene expression at multiple sites in the hippocampal network. Whether changes in BDNF concentration occurred bilaterally in the medial EC after unilateral tetanization of CA1 could not be assessed in the present study, because of the BDNF level in the EC of the nonstimulated right side served as control for the BDNF value obtained in the EC of the left stimulated side. Nevertheless, despite the inexistence of a proper control taken from nontetanized rats, the present data show that there was a significant difference in BDNF concentration when values from right (nonstimulated) ECs were compared with those from left (stimulated) ECs in normal eutrophic rats, whereas such a difference was not present in entorhinal tissue from malnourished animals. Failure of tetanizing stimulus in modifying BDNF levels in the ipsilateral EC of prenatally malnourished rats (so-called "instructive mechanisms" [29, 30], those initiated in response to high-frequency stimulation and required for subsequent development of LTP) clearly match the inability of the medial EC to induce LTP in malnourished animals, but caution must be exercised regarding this issue because this observation reveals a correlational but not causal relationship. Additionally, malnourished animals had significantly lower concentration of BDNF in the right EC (supposedly "basal" levels in the nonstimulated side) than

normal ones, thus suggesting a possible additional deficit in "permissive mechanisms" of BDNF (those that make synapses competent for LTP [29, 30]).

Why application of tetanizing stimulation to the occipital cortex of normal eutrophic rats resulted in potentiation of ipsilateral evoked EC responses, but not in increased BDNF concentration in the same EC, is presently unclear. One plausible explanation is that occipital cortex tetanization really increased BDNF expression but solely in some restricted layers of the EC and therefore they were not detected by staining the whole EC. Alternatively, it is possible that this type of polysynaptic LTP did not actually lead to increased BDNF expression. Then, this negative result in the occipital cortex-EC pathway should be interpreted with caution as the analysis performed is quite preliminary. Comparable tetanizing stimulation of the occipital cortex in malnourished rats did not induce either LTP or BDNF protein enhancement in the ipsilateral EC. Furthermore, high-frequency stimulation of the occipital cortex gave rise to a short period (about 5 minutes) of depression (or even irresponsiveness) of ipsilateral EC neurons to CA1 stimulation, both in normal and malnourished animals (see Figures 2(a) and 3(a)). Whether this transient presumably intra-EC inhibitory activity resulted from a feedforward inhibitory mechanism [48] or from a feedback mechanism triggered by the returning CA1 output into deep layers of the EC (see Craig and Commins [36]) remains to be determined. Also, the possibility that the complete loss of the CA1-evoked EC response after tetanizing the OC could be the result of generating local spreading depression cannot be discarded. In this regard, spreading depression-like episodies that were confined to the first 5 minutes after tetanizing the perforant path-granule cell pathway have been reported in anesthetized rats [49].

In summary, the present data show that mild prenatal protein malnutrition resulted in impaired ability of the EC to undergo LTP and to increase BDNF levels in response to tetanizing stimulation of the ipsilateral ventral CA1 hippocampal region during postnatal life. On the basis that EC is part of a circuit underlying networked representations of previous experiences via bidirectional connections between the neocortex with the hippocampus, impaired EC plasticity may be an important factor contributing to deficits in explicit learning having adult, prenatally malnourished animals.

ACKNOWLEDGMENT

This work was supported by Grant no. 1070028 from FONDECYT.

REFERENCES

[1] P. J. Morgane, D. J. Mokler, and J. R. Galler, "Effects of prenatal protein malnutrition on the hippocampal formation," *Neuroscience & Biobehavioral Reviews*, vol. 26, no. 4, pp. 471–483, 2002.

[2] J. Tonkiss and J. R. Galler, "Prenatal protein malnutrition and working memory performance in adult rats," *Behavioural Brain Research*, vol. 40, no. 2, pp. 95–107, 1990.

[3] J. Tonkiss, J. R. Galler, B. Shukitt-Hale, and F. J. Rocco, "Prenatal protein malnutrition impairs visual discrimination learning in adult rats," *Psychobiology*, vol. 19, no. 3, pp. 247–250, 1991.

[4] R. Soto-Moyano, L. Valladares, W. Sierralta, et al., "Mild prenatal protein malnutrition increases α_{2C}- adrenoceptor density in the cerebral cortex during postnatal life and impairs neocortical long-term potentiation and visuo-spatial performance in rats," *Journal of Neurochemistry*, vol. 93, no. 5, pp. 1099–1109, 2005.

[5] K. B. Austin, J. Bronzino, and P. J. Morgane, "Prenatal protein malnutrition affects synaptic potentiation in the dentate gyrus of rats in adulthood," *Brain Research*, vol. 394, no. 2, pp. 267–273, 1986.

[6] J. D. Bronzino, R. J. Austin La France, P. J. Morgane, and J. R. Galler, "Diet-induced alterations in the ontogeny of long-term potentiation," *Hippocampus*, vol. 6, no. 2, pp. 109–117, 1996.

[7] R. D. Burwell and D. G. Amaral, "Perirhinal and postrhinal cortices of the rat: interconnectivity and connections with the entorhinal cortex," *The Journal of Comparative Neurology*, vol. 391, no. 3, pp. 293–321, 1998.

[8] D. C. McIntyre, M. E. Kelly, and W. A. Staines, "Efferent projections of the anterior perirhinal cortex in the rat," *The Journal of Comparative Neurology*, vol. 369, no. 2, pp. 302–318, 1996.

[9] P. A. Naber, M. Caballero-Bleda, B. Jorritsma-Byham, and M. P. Witter, "Parallel input to the hippocampal memory system through peri- and postrhinal cortices," *NeuroReport*, vol. 8, no. 11, pp. 2617–2621, 1997.

[10] W. A. Suzuki and D. G. Amaral, "Topographic organization of the reciprocal connections between the monkey entorhinal cortex and the perirhinal and parahippocampal cortices," *The Journal of Neuroscience*, vol. 14, no. 3, pp. 1856–1877, 1994.

[11] M. P. Witter, F. G. Wouterlood, P. A. Naber, and T. Van Haeften, "Anatomical organization of the parahippocampal-hippocampal network," *Annals of the New York Academy of Sciences*, vol. 911, pp. 1–24, 2000.

[12] C. Köhler, "Intrinsic projections of the retrohippocampal region in the rat brain. I. The subicular complex," *The Journal of Comparative Neurology*, vol. 236, no. 4, pp. 504–522, 1985.

[13] N. Tamamaki and Y. Nojyo, "Preservation of topography in the connections between the subiculum, field CA1, and the entorhinal cortex in rats," *The Journal of Comparative Neurology*, vol. 353, no. 3, pp. 379–390, 1995.

[14] T. van Groen and J. M. Wyss, "Extrinsic projections from area CA1 of the rat hippocampus: olfactory, cortical, subcortical, and bilateral hippocampal formation projections," *The Journal of Comparative Neurology*, vol. 302, no. 3, pp. 515–528, 1990.

[15] H. Barbas, "Organization of cortical afferent input to orbitofrontal areas in the rhesus monkey," *Neuroscience*, vol. 56, no. 4, pp. 841–864, 1993.

[16] B. Delatour and M. P. Witter, "Projections from the parahippocampal region to the prefrontal cortex in the rat: evidence of multiple pathways," *European The Journal of Neuroscience*, vol. 15, no. 8, pp. 1400–1407, 2002.

[17] R. J. Morecraft, C. Geula, and M.-M. Mesulam, "Cytoarchitecture and neural afferents of orbitofrontal cortex in the brain of the monkey," *The Journal of Comparative Neurology*, vol. 323, no. 3, pp. 341–358, 1992.

[18] A. Alonso, M. de Curtis, and R. R. Llinás, "Postsynaptic Hebbian and non-Hebbian long-term potentiation of synaptic efficacy in the entorhinal cortex in slices and in the isolated adult guinea pig brain," *Proceedings of the National Academy*

of Sciences of the United States of America, vol. 87, no. 23, pp. 9280–9284, 1990.

[19] M. de Curtis and R. R. Llinás, "Entorhinal cortex long-term potentiation evoked by theta-patterned stimulation of associative fibers in the isolated in vitro guinea pig brain," *Brain Research*, vol. 600, no. 2, pp. 327–330, 1993.

[20] S. Yang, D. S. Lee, C. H. Chung, M. Y. Cheong, C.-J. Lee, and M. W. Jung, "Long-term synaptic plasticity in deep layer-originated associational projections to superficial layers of rat entorhinal cortex," *Neuroscience*, vol. 127, no. 4, pp. 805–812, 2004.

[21] R. Bouras and C. A. Chapman, "Long-term synaptic depression in the adult entorhinal cortex in vivo," *Hippocampus*, vol. 13, no. 7, pp. 780–790, 2003.

[22] S. Kourrich and C. A. Chapman, "NMDA receptor-dependent long-term synaptic depression in the entorhinal cortex in vitro," *Journal of Neurophysiology*, vol. 89, no. 4, pp. 2112–2119, 2003.

[23] J. Solger, C. Wozny, D. Manahan-Vaughan, and J. Behr, "Distinct mechanisms of bidirectional activity-dependent synaptic plasticity in superficial and deep layers of rat entorhinal cortex," *European The Journal of Neuroscience*, vol. 19, no. 7, pp. 2003–2007, 2004.

[24] Y.-D. Zhou, C. D. Acker, T. I. Netoff, K. Sen, and J. A. White, "Increasing Ca^{2+} transients by broadening postsynaptic action potentials enhances timing-dependent synaptic depression," *Proceedings of the National Academy of Sciences of the United States of America*, vol. 102, no. 52, pp. 19121–19125, 2005.

[25] O. Resnick, P. J. Morgane, R. Hasson, and M. Miller, "Overt and hidden forms of chronic malnutrition in the rat and their relevance to man," *Neuroscience & Biobehavioral Reviews*, vol. 6, no. 1, pp. 55–75, 1982.

[26] R. Soto-Moyano, S. Alarcón, J. Belmar, et al., "Prenatal protein restriction alters synaptic mechanisms of callosal connections in the rat visual cortex," *International Journal of Developmental Neuroscience*, vol. 16, no. 2, pp. 75–84, 1998.

[27] R. Soto-Moyano, V. Fernández, M. Sanhueza, et al., "Effects of mild protein prenatal malnutrition and subsequent postnatal nutritional rehabilitation on noradrenaline release and neuronal density in the rat occipital cortex," *Developmental Brain Research*, vol. 116, no. 1, pp. 51–58, 1999.

[28] W. Sierralta, A. Hernández, L. Valladares, H. Pérez, M. Mondaca, and R. Soto-Moyano, "Mild prenatal protein malnutrition increases α_{2C}-adrenoceptor expression in the rat cerebral cortex during postnatal life," *Brain Research Bulletin*, vol. 69, no. 5, pp. 580–586, 2006.

[29] C. R. Bramham and E. Messaoudi, "BDNF function in adult synaptic plasticity: the synaptic consolidation hypothesis," *Progress in Neurobiology*, vol. 76, no. 2, pp. 99–125, 2005.

[30] J. Soulé, E. Messaoudi, and C. R. Bramham, "Brain-derived neurotrophic factor and control of synaptic consolidation in the adult brain," *Biochemical Society Transactions*, vol. 34, no. 4, pp. 600–604, 2006.

[31] National Research Council, *Guide for the Use and Care of Laboratory Animals*, Publication no. 85–23 (rev.), National Institutes of Health, Bethesda, Md, USA, 1985.

[32] L. A. Cenquizca and L. W. Swanson, "Spatial organization of direct hippocampal field CA1 axonal projections to the rest of the cerebral cortex," *Brain Research Reviews*, vol. 56, no. 1, pp. 1–26, 2007.

[33] G. Paxinos and C. Watson, *The Rat Brain in Stereotaxic Coordinates*, Academic Press, San Diego, Calif, USA, 1998.

[34] C. A. Chapman and R. J. Racine, "Converging inputs to the entorhinal cortex from the piriform cortex and medial septum: facilitation and current source density analysis," *Journal of Neurophysiology*, vol. 78, no. 5, pp. 2602–2615, 1997.

[35] T. L. Ivanco and R. J. Racine, "Long-term potentiation in the reciprocal corticohippocampal and corticocortical pathways in the chronically implanted, freely moving rat," *Hippocampus*, vol. 10, no. 2, pp. 143–152, 2000.

[36] S. Craig and S. Commins, "Plastic and metaplastic changes in the CA1 and subicular projections to the entorhinal cortex," *Brain Research*, vol. 1147, no. 1, pp. 124–139, 2007.

[37] S. Craig and S. Commins, "Interaction between paired-pulse facilitation and long-term potentiation in the projection from hippocampal area CA1 to the entorhinal cortex," *Neuroscience Research*, vol. 53, no. 2, pp. 140–146, 2005.

[38] C. A. Chapman, C. Trepel, T. L. Ivanco, D. J. Froc, K. Wilson, and R. J. Racine, "Changes in field potentials and membrane currents in rat sensorimotor cortex following repeated tetanization of the corpus callosum in vivo," *Cerebral Cortex*, vol. 8, no. 8, pp. 730–742, 1998.

[39] P. J. Morgane, M. Miller, T. Kemper, et al., "The effects of protein malnutrition on the developing central nervous system in the rat," *Neuroscience & Biobehavioral Reviews*, vol. 2, no. 3, pp. 137–230, 1978.

[40] P. J. Morgane, R. J. Austin La France, J. Bronzino, et al., "Prenatal malnutrition and development of the brain," *Neuroscience & Biobehavioral Reviews*, vol. 17, no. 1, pp. 91–128, 1993.

[41] S. L. Patterson, L. M. Grover, P. A. Schwartzkroin, and M. Bothwell, "Neurotrophin expression in rat hippocampal slices: a stimulus paradigm inducing LTP in CA1 evokes increases in BDNF and NT-3 mRNAs," *Neuron*, vol. 9, no. 6, pp. 1081–1088, 1992.

[42] M. Dragunow, E. Beilharz, B. Mason, P. Lawlor, W. Abraham, and P. Gluckman, "Brain-derived neurotrophic factor expression after long-term potentiation," *Neuroscience Letters*, vol. 160, no. 2, pp. 232–236, 1993.

[43] K. Morimoto, K. Sato, S. Sato, N. Yamada, and T. Hayabara, "Time-dependent changes in neurotrophic factor mRNA expression after kindling and long-term potentiation in rats," *Brain Research Bulletin*, vol. 45, no. 6, pp. 599–605, 1998.

[44] P. R. Lee, J. E. Cohen, K. G. Becker, and R. D. Fields, "Gene expression in the conversion of early-phase to late-phase long-term potentiation," *Annals of the New York Academy of Sciences*, vol. 1048, pp. 259–271, 2005.

[45] V. Lessmann, K. Gottmann, and M. Malcangio, "Neurotrophin secretion: current facts and future prospects," *Progress in Neurobiology*, vol. 69, no. 5, pp. 341–374, 2003.

[46] E. Castrén, M. Pitkänen, J. Sirviö, et al., "The induction of LTP increases BDNF and NGF mRNA but decreases NT-3 mRNA in the dentate gyrus," *NeuroReport*, vol. 4, no. 7, pp. 895–898, 1993.

[47] C. R. Bramham, T. Southard, J. M. Sarvey, M. Herkenham, and L. S. Brady, "Unilateral LTP triggers bilateral increases in hippocampal neurotrophin and trk receptor mRNA expression in behaving rats: evidence for interhemispheric communication," *The Journal of Comparative Neurology*, vol. 368, no. 3, pp. 371–382, 1996.

[48] D. M. Finch, A. M. Tan, and M. Isokawa-Akesson, "Feedforward inhibition of the rat entorhinal cortex and subicular complex," *The Journal of Neuroscience*, vol. 8, no. 7, pp. 2213–2226, 1988.

[49] C. R. Bramham and B. Srebro, "Induction of long-term depression and potentiation by low- and high-frequency stimulation in the dentate area of the anesthetized rat: magnitude, time course and EEG," *Brain Research*, vol. 405, no. 1, pp. 100–107, 1987.

Hindawi Publishing Corporation
Neural Plasticity
Volume 2008, Article ID 840374, 9 pages
doi:10.1155/2008/840374

Research Article

Postsynaptic Signals Mediating Induction of Long-Term Synaptic Depression in the Entorhinal Cortex

Saïd Kourrich,[1,2] Stephen D. Glasgow,[1] Douglas A. Caruana,[1] and C. Andrew Chapman[1]

[1] *Center for Studies in Behavioral Neurobiology, Department of Psychology, Concordia University, Montréal, QC, Canada H4B 1R6*
[2] *Departments of Neuroscience and Psychology and the Institute of Human Genetics, University of Minnesota, Minneapolis, MN 55455, USA*

Correspondence should be addressed to C. Andrew Chapman, andrew.chapman@concordia.ca

Received 17 December 2007; Accepted 24 April 2008

Recommended by Roland S. G. Jones

The entorhinal cortex receives a large projection from the piriform cortex, and synaptic plasticity in this pathway may affect olfactory processing. In vitro whole cell recordings have been used here to investigate postsynaptic signalling mechanisms that mediate the induction of long-term synaptic depression (LTD) in layer II entorhinal cortex cells. To induce LTD, pairs of pulses, using a 30-millisecond interval, were delivered at 1 Hz for 15 minutes. Induction of LTD was blocked by the NMDA receptor antagonist APV and by the calcium chelator BAPTA, consistent with a requirement for calcium influx via NMDA receptors. Induction of LTD was blocked when the FK506 was included in the intracellular solution to block the phosphatase calcineurin. Okadaic acid, which blocks activation of protein phosphatases 1 and 2a, also prevented LTD. Activation of protein phosphatases following calcium influx therefore contributes to induction of LTD in layer II of the entorhinal cortex.

Copyright © 2008 Saïd Kourrich et al. This is an open access article distributed under the Creative Commons Attribution License, which permits unrestricted use, distribution, and reproduction in any medium, provided the original work is properly cited.

1. INTRODUCTION

The mechanisms that mediate the induction of long-term synaptic potentiation (LTP) [1, 2] and depression (LTD) [3–5] have been studied intensively within the hippocampus, but less is known about the signalling mechanisms for LTP and LTD in the entorhinal cortex. Because the entorhinal cortex receives highly processed inputs from sensory and association cortices and also provides the hippocampal region with much of its sensory input [6, 7], lasting changes in the strength of synaptic inputs to the entorhinal cortex could alter the manner in which multimodal cortical inputs are integrated, modulate the strength of transmission of specific patterns of sensory input within the hippocampal formation, and contribute to mnemonic function [8–11]. Determining the effective stimulation parameters and the intracellular signals that mediate synaptic plasticity in the entorhinal cortex should allow insight into basic mechanisms that contribute to the cognitive functions of the parahippocampal region.

Long-term potentiation of cortical inputs to the superficial layers of the entorhinal cortex has been described in vivo [11–14] and in vitro [15, 16]. Stimulation patterns required to induce LTP tend to be more intense in the entorhinal cortex than in the hippocampus [12, 14], and we have also found that induction of LTD in the entorhinal cortex requires intense low-frequency stimulation [17, 18]. In the hippocampus, conventional 1 Hz stimulation trains have been most effective in slices taken from juvenile animals [19, 20] but are generally ineffective in adult slices [21–23] and in intact animals ([31, 32], see also [33]). Similarly, 1 Hz stimulation induces entorhinal LTD in slices from young animals [28, 29] but is not effective in vivo [17] or in slices from older animals [18]. Repeated stimulation using pairs of pulses separated by a short 25- to 50-millisecond interval can induce LTD more effectively in both the CA1 ([24–26], but see [27]) and entorhinal cortex [17, 18, 33, 34]. In the CA1, the LTD induced by this stimulation pattern is NMDA receptor-dependent, but it also depends upon activation of local inhibitory mechanisms by the pulse-pairs [30, 31]. In the entorhinal cortex, however, repeated paired-pulse stimulation using a 10-millisecond interval that evokes maximal paired-pulse inhibition does not induce LTD, and LTD is induced when a 30-millisecond interval is used that evokes maximal paired-pulse *facilitation* [17]. The LTD can also be enhanced when $GABA_A$ transmission

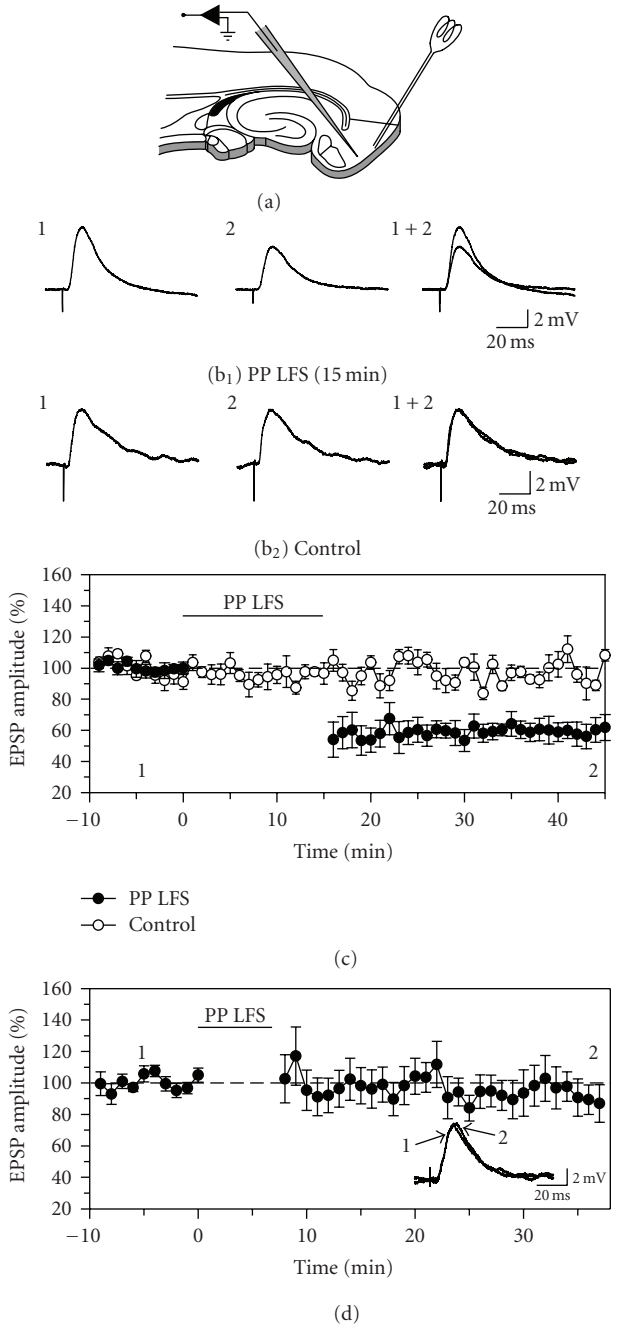

Figure 1: Prolonged, low-frequency stimulation induces long-term depression of EPSPs in neurons in layer II of the entorhinal cortex. (a) The location of stimulating and recording electrodes in acute slices containing the entorhinal cortex. (b) and (c) Long-term depression was induced by repetitive delivery of pairs of stimulation pulses at a rate of 1 Hz for 15 minutes (PP-LFS). The amplitude of synaptic responses remained stable in control cells that did not receive conditioning stimulation. Traces in (b) compare responses recorded during the baseline period (1) and during the follow-up period (2) in a neuron that received low-frequency stimulation (b_1) and in a control cell (b_2). Responses were obtained at the times indicated in (c). Averaged points in (b) indicate the mean ±1 SEM in this and subsequent figures. (d) Long-term depression was not reliably induced when low-frequency stimulation was delivered for only 7.5 minutes rather than 15 minutes, indicating that induction of LTD requires prolonged stimulation.

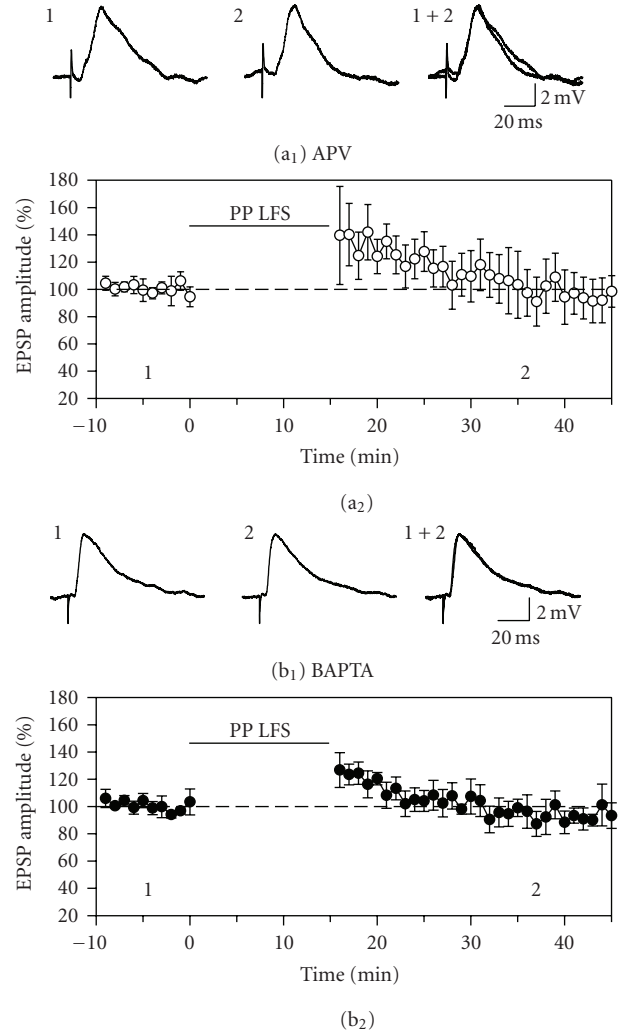

Figure 2: The induction of long-term depression is dependent on activation of NMDA glutamate receptors and on increases in postsynaptic calcium. (a) Constant bath application of the NMDA receptor antagonist APV (50 μM) blocked the induction of long-term depression by 15 minutes of paired-pulse low-frequency stimulation (PP LFS). (b) Blocking increases in postsynaptic calcium by including the calcium chelator BAPTA (10 mM) in the recording electrode solution also blocked the induction of LTD. The transient facilitation of EPSPs immediately following stimulation was significant for the BAPTA condition but not the APV condition, and responses were at baseline levels at the end of the recording periods. The block of lasting depression suggests that calcium influx via NMDA receptors is required for induction of LTD.

is reduced with bicuculline [18]. This further suggests that LTD in the entorhinal cortex does not require activation of local inhibitory mechanisms but rather requires prolonged stimulation patterns that are strong enough to overcome local inhibition and lead to NMDA receptor activation. Strong local inhibition in the entorhinal cortex [8, 35] may thus place a restraint on activity-dependent synaptic modification. Consistent with this idea is the finding that the same pairing stimulation protocol that induces LTP in hippocampus leads to LTD in entorhinal cortex [28].

Signalling mechanisms that mediate LTD in the superficial layers of the entorhinal cortex share some similarities with NMDA receptor-dependent LTD in the hippocampus. Long-term depression of superficial layer inputs to layer II is dependent on NMDA receptor activation both in vivo and in vitro [17, 18, 28, 33] but does not require activation of group I/II metabotropic glutamate receptors ([18, 28], see [36, 37]). In the hippocampus, moderate and prolonged influx of calcium via NMDA receptors activates calmodulin which leads to LTD via activation of the protein phosphatase calcineurin (PP2b). Calcineurin increases the activity of protein phosphatase 1 by reducing the activity of inhibitor 1, and this can cause rapid reductions in AMPA-mediated responses [2, 38, 39]. Hippocampal LTD is expressed partly through the reduced conductance of AMPA receptors caused by dephosphorylation of the GluR1 subunit by PP1 [2, 4], but careful study has shown that calcineurin-dependent LTD in deep layer inputs to layer II neurons in the young entorhinal cortex is not associated with a reduced AMPA conductance, but rather involves internalization of AMPA receptors and their proteosome-mediated degradation [28].

In the present study, the early postsynaptic signalling mechanisms that mediate LTD in layer I inputs to layer II neurons of the medial entorhinal cortex have been investigated using recordings of whole cell excitatory postsynaptic potentials. Long-term depression was induced using a prolonged paired-pulse stimulation pattern that was previously found to be effective for induction of NMDA-receptor-dependent LTD [18]. Pharmacological agents applied to the bathing medium or intracellular solution were used to assess the dependence of LTD on calcium-dependent signalling mechanisms including the phosphatases calcineurin and PP1/PP2a.

2. EXPERIMENTAL PROCEDURES

2.1. Slices and whole cell recordings

Experiments were performed on slices from male Long-Evans rats (4 to 8 weeks old). Animals were anesthetized with halothane and brains were rapidly removed and cooled (4°C) in oxygenated artificial cerebrospinal fluid (ACSF). ACSF consisted of (in mM) 124 NaCl, 5 KCl, 1.25 NaH_2PO_4, 2 $MgSO_4$, 2 $CaCl_2$, 26 $NaHCO_3$, and 10 dextrose and was saturated with 95% O_2–5% CO_2. All chemicals were obtained from Sigma (St. Louis, Mo, USA) unless otherwise indicated. Horizontal slices (300 μm) were cut with a vibratome (WPI, Vibroslice NVSL, Sarasota, Fla, USA) and were allowed to recover for at least one hour before recordings. Slices were maintained in a recording chamber with oxygenated ACSF at a rate of 2.0 mL/min, and a temperature from 22 to 24°C was used to minimize metabolic demands on slices [18, 28]. Neurons were viewed with an upright microscope (Leica DML-FS, Wetzlar, Germany) equipped with a 40x objective, differential interference contrast optics, and an infrared video camera (Cohu, 4990 series, San Diego, Calif, USA).

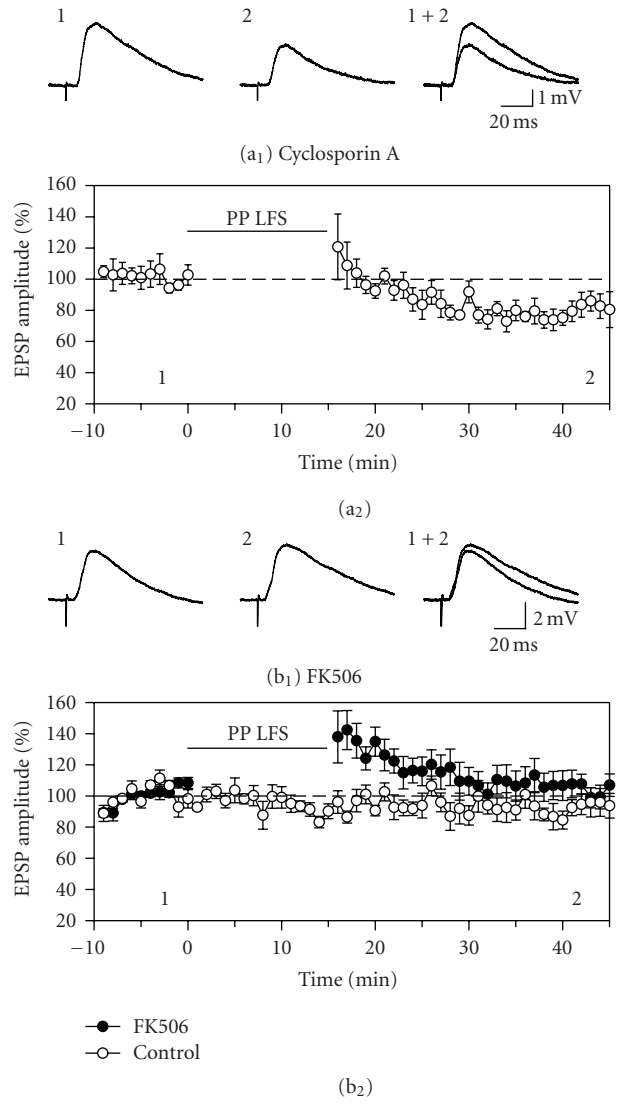

Figure 3: Long-term depression is dependent on activation of the calmodulin-dependent protein phosphatase calcineurin. Although LTD was only partially inhibited by pre-exposure to cyclosporin A, it was completely blocked when FK506 was included in the recording electrode solution. (a) Pre-exposure of slices to the calcineurin inhibitor cyclosporin A (250 μM) for 1.5 to 3 hours resulted in a partial block of LTD by repeated paired-pulse stimulation. The amount of LTD induced was smaller than in control ACSF and was close to statistical significance ($n = 6$, $P = .07$). (b) Including the FK506 in the recording electrode solution to directly block postsynaptic calcineurin prevented the induction of LTD. Analysis of group responses showed a significant increase in responses during the baseline period, but responses in control cells indicate that this increase is transient and unlikely to have affected measurement of LTD. Inhibition of postsynaptic calcineurin therefore prevents induction of LTD in layer II cells of the entorhinal cortex.

Whole-cell current clamp recordings were obtained using patch pipettes pulled from borosilicate glass (1.0 mm OD, 4–7 MΩ) using a horizontal puller (Sutter Instr., P-97, Novato, Calif, USA) and filled with a solution containing (in mM)

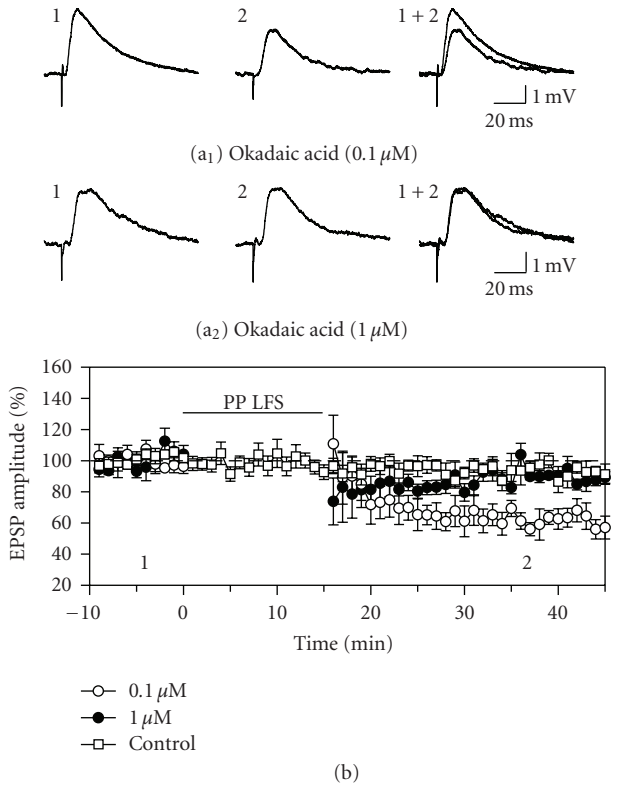

Figure 4: The induction of LTD was blocked in a dose-dependent manner by including okadaic acid in the recording electrode solution to block activation of protein phosphatase 1 (PP1). (a) and (b) A low concentration of 0.1 μM okadaic acid failed to block LTD induction, but raising the concentration to 1.0 μM resulted in a block of LTD induction (compare traces in A_1 versus A_2). Responses in control cells filled with 1.0 μM okadaic acid that did not receive conditioning stimulation remained stable. The block of LTD by okadaic acid suggests that activation of PP1 mediates LTD in the entorhinal cortex.

140 K-gluconate, 5 NaCl, 2 $MgCl_2$, 10 HEPES, 0.5 EGTA, 2 ATP-tris, 0.4 GTP-tris (pH adjusted to 7.25 with KOH). Tight seals (>1 GΩ) between the pipette and soma of cells in layer II of the medial entorhinal cortex were obtained in voltage-clamp, and whole-cell configuration was obtained using suction. Synaptic responses were evoked with a bipolar stimulating electrode constructed from two fine tungsten electrodes (1 MΩ; Frederick Haer & Co., Bowdoin, Me, USA) placed in layer I of the medial entorhinal cortex, 0.4 to 0.8 mm rostral to the recording electrode. Constant current pulses (0.1 millisecond, 60–250 μA) were delivered using a pulse generator (WPI, Model A300) and stimulus isolator (WPI, A360). Responses to synaptic activation and intracellular current injection were obtained with an Axopatch 200B amplifier (Axon Instr., Sunnyvale, Calif, USA), filtered (10 kHz low-pass), displayed on a digital oscilloscope (Gould 1602), and digitized at 20 kHz (Axon Instr., Digidata 1322A) for storage on computer hard disc using the software package Clampex 8.2 (Axon Instr.). Series and input resistances were monitored regularly using −100 pA pulses. Recordings were accepted if the series resistance was <35 MΩ, and if input resistance and resting membrane potential were stable.

2.2. LTD Induction and pharmacology

Whole-cell current clamp recordings of EPSPs were monitored 10 minutes before and 30 minutes after LTD induction by delivering test-pulses every 20 seconds. Intensity was adjusted to evoke EPSPs that were approximately 3 to 4 mV in amplitude, and cells were held 5 mV below threshold when necessary to prevent the occurrence of spikes in response to EPSPs. Stimulus parameters for LTD induction were based on those used previously in vivo and in vitro [17, 18]. The induction of LTD was tested using pairs of stimulation pulses (30-millisecond interpulse interval) delivered at a frequency of 1 Hz for either 7.5 or 15 minutes [18]. Control cells received test-pulses throughout the recording period and did not receive conditioning stimulation.

Signalling mechanisms mediating the induction of LTD were tested using stock solutions of pharmacological agents that were stored frozen and diluted on the day of use. NMDA glutamate receptors were blocked by constant bath application of 50 μM DL-2-amino-5-phosphonovalerate (APV). The calcium chelator 1,2-bis(2-aminophenoxy)-ethane-N,N,N′N′-tetraacetic acid (BAPTA, 10 mM) was included in the recording electrode solution to block increases in intracellular calcium. To block activation of the calmodulin-dependent protein phosphatase calcineurin (PP2b) slices were pre-exposed to 250 μM cyclosporin A (Toronto Research Chemicals Inc., North York, Ontario, Canada) for 1.5 to 3 hours [39]. In other experiments, FK506 (50 μM) was included in the recording electrode solution to block calcineurin [39, 40]. In other experiments, okadaic acid (0.1 or 1.0 μM) was included in the recording solution to block activation of protein phosphatases 1 and 2a [40, 41]. Control recordings without paired-pulse stimulation were used to verify the stability of recordings in cells filled with FK506 and 1.0 μM okadaic acid.

2.3. Data analysis

Synaptic responses and electrophysiological properties of layer II neurons were analyzed using the program Clampfit 8.2 (Axon Instr.). Data were standardized to the mean of baseline responses for plotting and were expressed as the mean ±SEM. Changes in EPSP amplitude were assessed using mixed-design ANOVAs and Neuman-Keuls tests that compared the average responses during the baseline period, 5 minutes after conditioning stimulation, and during the last 5 minutes of the recording period.

Layer II neurons were classified as putative stellate or nonstellate neurons based on electrophysiological characteristics described by Alonso and Klink [42]. Stellate neurons were characterized by the presence of low-frequency subthreshold membrane potential oscillations, a depolarizing afterpotential following spikes, and prominent inward rectification in response to hyperpolarizing current pulses. Both pyramidal and stellate neurons in layer II can show

inward rectifying sag responses [43]. Here, neurons recorded were clearly in layer II, usually near the border with layer I, and a proportion of these neurons did not show clear sag and were classified as pyramidal neurons. Input resistance was determined from the peak voltage response to −100 pA current pulses (500-millisecond duration), and rectification ratio was quantified by expressing peak input resistance as a proportion of the steady-state resistance at the end of the current pulse.

3. RESULTS

Stable recordings were obtained from 57 putative stellate neurons and 21 putative nonstellate cells. Peak input resistance was similar in stellate and pyramidal neurons (stellate, 95 ± 6 MΩ; pyramidal, 96 ± 10 MΩ) but there was a much larger sag in voltage responses to hyperpolarizing current injection in stellate cells (rectification ratio 1.37 ± 0.04 in stellate cells versus 1.06 ± 0.01 in pyramidal cells). The amplitude of baseline synaptic responses evoked by layer I stimulation was similar in stellate (3.9 ± 0.2 mV) and pyramidal cells (3.7 ± 0.4 mV), and the amount of depression induced was also similar for recording conditions in which significant LTD was obtained (71.2 ± 5.6% in 14 stellate and 76.8 ± 7.6% in 6 pyramidal cells).

3.1. LTD induction

To determine if a relatively brief LTD induction protocol could be used to induce LTD in whole-cell recordings, the first tests attempted to induce LTD using paired-pulse delivery at 1 Hz for 7.5 minutes ($n = 10$) which can induce moderate LTD of field potentials in a gas-fluid interface recording chamber [18]. Paired-pulse stimulation for 7.5 minutes did not induce depression of EPSPs relative to control cells (93.0 ± 10.0% of baseline after 30 minutes; $F_{2,28} = 0.09$, $P = .92$). We previously observed stronger LTD of field potentials in the interface recording chamber after 15 minutes versus 7.5 minutes of paired-pulse stimulation [18], and prolonged paired-pulse stimulation for 15 minutes also reliably induced LTD of whole-cell EPSPs ($n = 7$, Figure 1). EPSP amplitude was reduced to 56.3 ± 9.5% of baseline levels 5 minutes after the conditioning stimulation, and remained at 58.6 ± 6.1% of baseline levels at the end of the 30 minutes follow-up period ($F_{2,22} = 14.2$, $P < .001$). Responses in control cells were stable ($n = 6$), and remained at 99.6 ± 2.6% of baseline levels at the end of the recording period (Figures 1(b_2), 1(c)).

3.2. NMDA receptors and postsynaptic calcium

The NMDA receptor antagonist MK-801 blocks induction of LTD in the entorhinal cortex in vivo [17] and the NMDA receptor blocker APV has been shown to prevent LTD of field potentials and EPSPs in entorhinal cortex slices [18, 28, 33]. We therefore tested for the NMDA receptor-dependence of LTD of EPSPs in the current preparation using constant bath application of APV (50 μM). Induction of LTD by 15 minutes of paired-pulse stimulation was blocked by APV ($n = 6$, Figure 2(a)). There was a tendency for responses to be potentiated immediately following conditioning stimulation, but this variable effect was not statistically significant, and responses were close to baseline levels at the end of the recording period (96.7 ± 13.2% of baseline; $F_{2,10} = 2.99$, $P = .09$).

The role of postsynaptic calcium in LTD induction was tested by recording from cells in which the calcium chelator BAPTA (10 mM) was included in the recording electrode solution (10 mM, $n = 6$, Figure 2(b)). Cells filled with BAPTA had longer-duration action potentials than control cells (6.1 ± 0.7 versus 3.3 ± 0.1 milliseconds measured at the base; $t_{1,9} = 3,57$, $P < .01$) consistent with a reduction in calcium-dependent potassium conductances. The induction of LTD was blocked in cells loaded with BAPTA. There was a significant increase in the amplitude of EPSPs immediately following paired-pulse stimulation (to 122.3 ± 6.0% of baseline; $F_{2,10} = 5.46$, $P < .05$; N–K, $P < .05$), but responses returned to baseline levels within 10 minutes and were at 94.8 ± 7.1% of baseline levels after 30 minutes (N–K, $P = 0.50$, Figure 2(b)). An increase in postsynaptic calcium is therefore required for induction of LTD in layer II neurons of the entorhinal cortex.

3.3. Protein phosphatases

The role of the calmodulin-dependent protein phosphatase calcineurin (PP2b) in LTD in layer II neurons was tested using either pre-exposure to 250 μM cyclosporin A in the bathing medium [39], or by including 50 μM FK506 postsynaptically in the recording electrode solution. In cells pre-exposed to cyclosporin A, paired-pulse stimulation was followed by a depression in EPSP amplitude that reached 82.4 ± 7.5% of baseline levels after 30 minutes (Figure 3(a)). Although the depression in the cyclosporin group was not statistically significant ($F_{2,10} = 3.51$, $P = 0.07$, $n = 6$), the depression obtained was also not significantly less than that observed in control ACSF ($F_{1,11} = 3.79$, $P = .08$). The result was therefore ambiguous with respect to the role of calcineurin in LTD. To test the involvement of calcineurin more definitively and to avoid potential presynaptic effects, the calcineurin blocker FK506 was included in the recording electrode solution for additional groups of cells [40]. Responses in cells filled with FK506 showed a significant potentiation immediately following paired-pulse stimulation ($n = 8$), but there was no lasting change in response amplitudes in comparison to control cells filled with FK506 that did not receive conditioning stimulation ($n = 7$). Responses were increased to 134.9 ± 10.5% of baseline levels immediately following paired-pulse stimulation, ($F_{2,26} = 7.71$, $P < .01$; N–K, $P < .001$; $n = 8$) but returned to 102.2 ± 6.1% of baseline levels after 30 minutes (Figure 3(b)).

Inspection of averaged responses suggested that there was an initial increase in responses during the baseline period among cells filled with FK506, and comparison of responses recorded during the first and last minutes of the baseline period showed that the increase was significant

($t_{14} = 3.09$, $P < .01$). Interestingly, then, interfering with calcineurin function can lead to enhanced basal synaptic transmission in entorhinal neurons. This increase is not likely to have affected measures of LTD in conditioned cells, however, because control responses showed only a transient increase after which responses remained stable.

Protein phosphatase 1 is thought to contribute directly to suppression of hippocampal EPSPs during LTD by dephosphorylation of the GluR1 AMPA receptor subunit. The involvement of PP1 to LTD in the entorhinal cortex was therefore tested by including okadaic acid in the recording electrode solution. In early experiments, a low concentration of 0.1 μM okadaic acid [41] did not block LTD induction, and responses were depressed to 72.7 ± 8.7% of baseline levels at the end of the recording period ($F_{2,24} = 4.65$, $P < .05$; N–K, $P < .001$; $n = 8$). However, increasing the concentration of okadaic acid to 1.0 μM [40] blocked the induction of LTD. There was a variable and nonsignificant reduction in responses immediately following conditioning stimulation (to 89.0 ± 14.9% of baseline) and responses were also near baseline levels after 30 minutes (96.0 ± 6.6% of baseline 30; $F_{2,22} = 0.18$, $P = .84$; $n = 7$; Figure 4). Activation of PP1 is therefore likely to contribute to mechanisms of LTD in the entorhinal cortex.

4. DISCUSSION

The current paper has used prolonged repetitive paired-pulse stimulation to induce LTD in layer I inputs to layer II neurons of the medial entorhinal cortex and has determined the early postsynaptic signals that mediate LTD in these cells. Consistent with previous observations, the LTD observed here was obtained in both putatively identified stellate [28] and pyramidal [44] cells. The induction of LTD was blocked by the NMDA glutamate receptor antagonist APV, and by the calcium chelator BAPTA, indicating that calcium influx via NMDA receptors is required for LTD. The induction of LTD was also blocked by the calcineurin inhibitor FK506, and by okadaic acid which blocks activation of protein phosphatases 1 and 2a. Calcineurin is required for LTD of deep layer inputs to layer II stellate cells [28], and calcineurin-dependent activation of PP1 contributes to NMDA receptor-dependent LTD of AMPA responses in the hippocampus [2, 4].

The dependence of LTD in the entorhinal cortex on activation of NMDA receptors has been a consistent finding in vivo and in slices. It has been observed following stimulation protocols including 1 Hz trains, pairing of presynaptic stimulation at 0.33 Hz with postsynaptic depolarization [28], repeated paired-pulse stimulation [18, 33], and spike-timing-dependent induction of LTD [44]. Long-term depression was blocked by including the calcium chelator BAPTA in the recording electrode solution (Figure 2) [28], and this is consistent with calcium influx via NMDA receptors as a critical trigger for entorhinal LTD. Metabotropic glutamate receptor activation and release of calcium from intracellular stores can contribute to LTD in the hippocampus [2, 36, 37, 45], but activation of metabotropic glutamate receptors is not required for entorhinal LTD [18, 28]. Calcium influx through voltage-gated calcium channels can contribute to spike-timing-dependent LTD in the entorhinal cortex, however. Cells with broadened action potentials that result in larger calcium transients show greater NMDA receptor-dependent spike-timing-dependent LTD in layer II-III cells [44]. Calcium influx through voltage-gated channels also mediates bidirectional spike-timing-dependent plasticity of inhibitory synapses in entorhinal cortex [46]. A form of long-term depression on layer V-VI neurons, expressed presynaptically through reduced transmitter release, is also dependent on activation of voltage-dependent calcium channels [33]. Calcium signalling mediated by voltage-gated channels therefore plays a number of roles in modulating synaptic plasticity in the entorhinal cortex.

The contribution of the calmodulin-dependent protein phosphatase calcineurin to LTD was tested by incubating slices in cyclosporin A or by including FK506 in the recording electrode solution. Cyclosporin A appeared to cause a partial block of LTD, and responses were reduced to 82.4% of baseline as compared to 58.6% in untreated cells (compare Figures 1(c) and 3(a)), but the sizes of these LTD effects were not statistically different. We obtained a more conclusive result with FK506, however, and LTD was completely blocked by including FK506 in the recording electrode solution. Including FK506 in the bathing medium has been used to block calcineurin-dependent depression effects in entorhinal cortex [28], and in excitatory [47] and inhibitory [48] synapses of the CA1 region. Here, we have loaded FK506 into the recording electrode solution to avoid possible presynaptic effects of the drug and to ensure that FK506 could act on calcineurin [39, 40, 49, 50]. The block of LTD by FK506 indicates that LTD is dependent on calcineurin, and this suggests that cyclosporin A resulted in only a partial block of calcineurin activity.

Calcineurin is thought to mediate expression of LTD in part by dephosphorylating inhibitor 1 and thereby increasing the activity of PP1 [2, 4, 39]. The PP1/PP2a inhibitor okadaic acid blocks LTD in the CA1 region [38, 40], and we have shown here that the induction of LTD in the entorhinal cortex was blocked by including okadaic acid in the recording electrode solution. This is the first report of LTD in the entorhinal cortex dependent on PP1/PP2a. Protein phosphatases can regulate synaptic function through a variety of mechanisms [51] that include dephosphorylation of the ser-845 residue on the AMPA GluR1 subunit, and LTD in the entorhinal cortex may be expressed partly through this mechanism. In addition, the work of Deng and Lei [28] has found entorhinal LTD to be associated with a reduction in the number of postsynaptic AMPA receptors, with no change in AMPA receptor conductance, and has shown that this effect is dependent on proteosomes that degrade AMPA receptors internalized through ubiquitinization. As in the hippocampus, therefore, entorhinal LTD can be expressed through mechanisms involving trafficking of AMPA receptors [52].

Long-term depression was induced here using strong repetitive paired-pulse stimulation which we have used previously to induce LTD in the entorhinal cortex in vivo and in slices ([17, 18], see also [33, 34]). LTD was induced following 15 minutes, but not 7.5 minutes of paired-pulse

stimulation; this is consistent with a requirement for prolonged activation of calcium-dependent signalling mechanisms, and is also consistent with the possibility that NMDA receptor-dependent metaplastic changes early in the train may promote LTD induced by stimuli that occurred later in the 15-minute duration trains [53]. We previously found 1 Hz stimulation to be ineffective in vivo and in slices from Long-Evans rats [17, 18], but deep layer inputs to stellate neurons in slices from 2 to 3 week-old Sprague-Dawley rats express NMDA receptor-dependent LTD following 15 minutes of 1 Hz stimulation, or following low-frequency stimulation paired with postsynaptic depolarization [28]. Thus, there may be developmental, strain-related, or pathway-specific factors that affect the ability of 1 Hz stimulation to activate these signalling mechanisms.

The entorhinal cortex is embedded within the temporal lobe through an extensive array of anatomical connections [7] and has been linked behaviorally to a variety of sensory and cognitive functions (e.g., [9, 10]). Lasting synaptic plasticity in the entorhinal cortex is therefore likely to serve a variety of functions depending on the synaptic pathways involved. Synaptic depression effects are generally thought to complement synaptic potentiation during the formation of memory [45, 54–56], and it is possible that depression effects contribute to short and/or long-term memory processing. However, the laminar architecture of the entorhinal cortex, with superficial layers mediating much of the cortical input to the hippocampal formation, suggests that long-term depression of synaptic transmission in layer II may lead to long-term reductions in the salience of particular elements or patterns of cortical input and may thus lead to lasting changes in the multimodal inputs processed by the hippocampal formation. Similarly, the general resistance of the entorhinal cortex to induction of LTD could serve to maintain relatively stable information processing and integration of multimodal sensory inputs within the medial entorhinal cortex.

ACKNOWLEDGMENTS

This research was funded by grants to C. A. Chapman from the Natural Sciences and Engineering Research Council of Canada and the Canada Foundation for Innovation, and by a postdoctoral fellowship to S.K. from Fondation Fyssen (France). C.A. Chapman is a member of the Center for Studies in Behavioral Neurobiology funded by the Fonds pour la Recherche en Santé du Québec.

REFERENCES

[1] R. C. Malenka and R. A. Nicoll, "Long-term potentiation—a decade of progress?" *Science*, vol. 285, no. 5435, pp. 1870–1874, 1999.

[2] R. C. Malenka and M. F. Bear, "LTP and LTD: an embarrassment of riches," *Neuron*, vol. 44, no. 1, pp. 5–21, 2004.

[3] M. F. Bear and W. C. Abraham, "Long-term depression in hippocampus," *Annual Review of Neuroscience*, vol. 19, pp. 437–462, 1996.

[4] N. Kemp and Z. I. Bashir, "Long-term depression: a cascade of induction and expression mechanisms," *Progress in Neurobiology*, vol. 65, no. 4, pp. 339–365, 2001.

[5] P. V. Massey and Z. I. Bashir, "Long-term depression: multiple forms and implications for brain function," *Trends in Neurosciences*, vol. 30, no. 4, pp. 176–184, 2007.

[6] R. D. Burwell and D. G. Amaral, "Cortical afferents of the perirhinal, postrhinal, and entorhinal cortices of the rat," *Journal of Comparative Neurology*, vol. 398, no. 2, pp. 179–205, 1998.

[7] K. M. Kerr, K. L. Agster, S. C. Furtak, and R. D. Burwell, "Functional neuroanatomy of the parahippocampal region: the lateral and medial entorhinal areas," *Hippocampus*, vol. 17, no. 9, pp. 697–708, 2007.

[8] M. de Curtis and D. Paré, "The rhinal cortices: a wall of inhibition between the neocortex and the hippocampus," *Progress in Neurobiology*, vol. 74, no. 2, pp. 101–110, 2004.

[9] C. Barry, R. Hayman, N. Burgess, and K. J. Jeffery, "Experience-dependent rescaling of entorhinal grids," *Nature Neuroscience*, vol. 10, no. 6, pp. 682–684, 2007.

[10] P. A. Lipton, J. A. White, and H. Eichenbaum, "Disambiguation of overlapping experiences by neurons in the medial entorhinal cortex," *The Journal of Neuroscience*, vol. 27, no. 21, pp. 5787–5795, 2007.

[11] D. A. Caruana, S. J. Reed, D. J. Sliz, and C. A. Chapman, "Inhibiting dopamine reuptake blocks the induction of long-term potentiation and depression in the lateral entorhinal cortex of awake rats," *Neuroscience Letters*, vol. 426, no. 1, pp. 6–11, 2007.

[12] R. J. Racine, N. W. Milgram, and S. Hafner, "Long-term potentiation phenomena in the rat limbic forebrain," *Brain Research*, vol. 260, no. 2, pp. 217–231, 1983.

[13] C. A. Chapman and R. J. Racine, "Converging inputs to the entorhinal cortex from the piriform cortex and medial septum: facilitation and current source density analysis," *Journal of Neurophysiology*, vol. 78, no. 5, pp. 2602–2615, 1997.

[14] C. A. Chapman and R. J. Racine, "Piriform cortex efferents to the entorhinal cortex in vivo: kindling-induced potentiation and the enhancement of long-term potentiation by low-frequency piriform cortex or medial septal stimulation," *Hippocampus*, vol. 7, no. 3, pp. 257–270, 1997.

[15] A. Alonso, M. de Curtis, and R. Llinás, "Postsynaptic Hebbian and non-Hebbian long-term potentiation of synaptic efficacy in the entorhinal cortex in slices and in the isolated adult guinea pig brain," *Proceedings of the National Academy of Sciences of the United States of America*, vol. 87, no. 23, pp. 9280–9284, 1990.

[16] S. H. Yun, I. Mook-Jung, and M. W. Jung, "Variation in effective stimulus patterns for induction of long-term potentiation across different layers of rat entorhinal cortex," *The Journal of Neuroscience*, vol. 22, no. 5, RC214, pp. 1–5, 2002.

[17] R. Bouras and C. A. Chapman, "Long-term synaptic depression in the adult entorhinal cortex in vivo," *Hippocampus*, vol. 13, no. 7, pp. 780–790, 2003.

[18] S. Kourrich and C. A. Chapman, "NMDA receptor-dependent long-term synaptic depression in the entorhinal cortex in vitro," *Journal of Neurophysiology*, vol. 89, no. 4, pp. 2112–2119, 2003.

[19] S. M. Dudek and M. F. Bear, "Homosynaptic long-term depression in area CA1 of hippocampus and effects of *N*-methyl-D-aspartate receptor blockade," *Proceedings of the National Academy of Sciences of the United States of America*, vol. 89, no. 10, pp. 4363–4367, 1992.

[20] R. M. Mulkey and R. C. Malenka, "Mechanisms underlying induction of homosynaptic long-term depression in area CA1 of the hippocampus," *Neuron*, vol. 9, no. 5, pp. 967–975, 1992.

[21] S. M. Dudek and M. F. Bear, "Bidirectional long-term modification of synaptic effectiveness in the adult and immature hippocampus," *The Journal of Neuroscience*, vol. 13, no. 7, pp. 2910–2918, 1993.

[22] J. J. Wagner and B. E. Alger, "GABAergic and developmental influences on homosynaptic LTD and depotentiation in rat hippocampus," *The Journal of Neuroscience*, vol. 15, no. 2, pp. 1577–1586, 1995.

[23] N. Kemp, J. McQueen, S. Faulkes, and Z. I. Bashir, "Different forms of LTD in the CA1 region of the hippocampus: role of age and stimulus protocol," *European Journal of Neuroscience*, vol. 12, no. 1, pp. 360–366, 2000.

[24] M. L. Errington, T. V. Bliss, G. Richter-Levin, K. Yenk, V. Doyere, and S. Laroche, "Stimulation at 1–5 Hz does not produce long-term depression or depotentiation in the hippocampus of the adult rat in vivo," *Journal of Neurophysiology*, vol. 74, no. 4, pp. 1793–1799, 1995.

[25] C. A. Doyle, W. K. Cullen, M. J. Rowan, and R. Anwyl, "Low-frequency stimulation induces homosynaptic depotentiation but not long-term depression of synaptic transmission in the adult anaesthetized and awake rat hippocampus in vivo," *Neuroscience*, vol. 77, no. 1, pp. 75–85, 1997.

[26] U. Staubli and J. Scafidi, "Studies on long-term depression in area CA1 of the anesthetized and freely moving rat," *The Journal of Neuroscience*, vol. 17, no. 12, pp. 4820–4828, 1997.

[27] A. J. Heynen, W. C. Abraham, and M. F. Bear, "Bidirectional modification of CA1 synapses in the adult hippocampus in vivo," *Nature*, vol. 381, no. 6578, pp. 163–166, 1996.

[28] P.-Y. Deng and S. Lei, "Long-term depression in identified stellate neurons of juvenile rat entorhinal cortex," *Journal of Neurophysiology*, vol. 97, no. 1, pp. 727–737, 2007.

[29] M. Y. Cheong, S. H. Yun, I. Mook-Jung, Y. Kang, and M. W. Jung, "Induction of homosynaptic long-term depression in entorhinal cortex," *Brain Research*, vol. 954, no. 2, pp. 308–310, 2002.

[30] E. Thiels, G. Barrionuevo, and T. W. Berger, "Excitatory stimulation during postsynaptic inhibition induces long-term depression in hippocampus in vivo," *Journal of Neurophysiology*, vol. 72, no. 6, pp. 3009–3016, 1994.

[31] V. Doyère, M. L. Errington, S. Laroche, and T. V. Bliss, "Low-frequency trains of paired stimuli induce long-term depression in area CA1 but not in dentate gyrus of the intact rat," *Hippocampus*, vol. 6, no. 1, pp. 52–57, 1996.

[32] E. Thiels, X. Xie, M. F. Yeckel, G. Barrionuevo, and T. W. Berger, "NMDA receptor-dependent LTD in different subfields of hippocampus in vivo and in vitro," *Hippocampus*, vol. 6, no. 1, pp. 43–51, 1996.

[33] J. Solger, C. Wozny, D. Manahan-Vaughan, and J. Behr, "Distinct mechanisms of bidirectional activity-dependent synaptic plasticity in superficial and deep layers of rat entorhinal cortex," *European Journal of Neuroscience*, vol. 19, no. 7, pp. 2003–2007, 2004.

[34] J. Solger, U. Heinemann, and J. Behr, "Electrical and chemical long-term depression do not attenuate low-Mg^{2+}-induced epileptiform activity in the entorhinal cortex," *Epilepsia*, vol. 46, no. 4, pp. 509–516, 2005.

[35] G. L. Woodhall, S. J. Bailey, S. E. Thompson, D. I. P. Evans, and R. S. G. Jones, "Fundamental differences in spontaneous synaptic inhibition between deep and superficial layers of the rat entorhinal cortex," *Hippocampus*, vol. 15, no. 2, pp. 232–245, 2005.

[36] A. M. Watabe, H. J. Carlisle, and T. J. O'Dell, "Postsynaptic induction and presynaptic expression of group 1 mGluR-dependent LTD in the hippocampal CA1 region," *Journal of Neurophysiology*, vol. 87, no. 3, pp. 1395–1403, 2002.

[37] N. Kemp and Z. I. Bashir, "Induction of LTD in the adult hippocampus by the synaptic activation of AMPA/kainate and metabotropic glutamate receptors," *Neuropharmacology*, vol. 38, no. 4, pp. 495–504, 1999.

[38] R. M. Mulkey, C. E. Herron, and R. C. Malenka, "An essential role for protein phosphatases in hippocampal long-term depression," *Science*, vol. 261, no. 5124, pp. 1051–1055, 1993.

[39] R. M. Mulkey, S. Endo, S. Shenolikar, and R. C. Malenka, "Involvement of a calcineurin/inhibitor-1 phosphatase cascade in hippocampal long-term depression," *Nature*, vol. 369, no. 6480, pp. 486–488, 1994.

[40] W. Morishita, H. Marie, and R. C. Malenka, "Distinct triggering and expression mechanisms underlie LTD of AMPA and NMDA synaptic responses," *Nature Neuroscience*, vol. 8, no. 8, pp. 1043–1050, 2005.

[41] S.-N. Yang, "Ceramide-induced sustained depression of synaptic currents mediated by ionotropic glutamate receptors in the hippocampus: an essential role of postsynaptic protein phosphatases," *Neuroscience*, vol. 96, no. 2, pp. 253–258, 2000.

[42] A. Alonso and R. Klink, "Differential electroresponsiveness of stellate and pyramidal-like cells of medial entorhinal cortex layer II," *Journal of Neurophysiology*, vol. 70, no. 1, pp. 128–143, 1993.

[43] S. van der Linden, "Comparison of the electrophysiology and morphology of layers III and II neurons of the rat medial entorhinal cortex in vitro," *European Journal of Neuroscience*, vol. 10, no. 4, pp. 1479–1489, 1998.

[44] Y.-D. Zhou, C. D. Acker, T. I. Netoff, K. Sen, and J. A. White, "Increasing Ca^{2+} transients by broadening postsynaptic action potentials enhances timing-dependent synaptic depression," *Proceedings of the National Academy of Sciences of the United States of America*, vol. 102, no. 52, pp. 19121–19125, 2005.

[45] B. R. Christie, D. S. Kerr, and W. C. Abraham, "Flip side of synaptic plasticity: long-term depression mechanisms in the hippocampus," *Hippocampus*, vol. 4, no. 2, pp. 127–135, 1994.

[46] J. S. Haas, T. Nowotny, and H. D. I. Abarbanel, "Spike-timing-dependent plasticity of inhibitory synapses in the entorhinal cortex," *Journal of Neurophysiology*, vol. 96, no. 6, pp. 3305–3313, 2006.

[47] M.-H. Kang-Park, M. A. Sarda, K. H. Jones, et al., "Protein phosphatases mediate depotentiation induced by high-intensity theta-burst stimulation," *Journal of Neurophysiology*, vol. 89, no. 2, pp. 684–690, 2003.

[48] Y. M. Lu, I. M. Mansuy, E. R. Kandel, and J. Roder, "Calcineurin-mediated LTD of GABAergic inhibition underlies the increased excitability of CA1 neurons associated with LTP," *Neuron*, vol. 26, no. 1, pp. 197–205, 2000.

[49] S.-T. Li, K. Kato, K. Tomizawa, et al., "Calcineurin plays different roles in group II metabotropic glutamate receptor- and NMDA receptor-dependent long-term depression," *The Journal of Neuroscience*, vol. 22, no. 12, pp. 5034–5041, 2002.

[50] H. Yasuda, H. Higashi, Y. Kudo, et al., "Imaging of calcineurin activated by long-term depression-inducing synaptic inputs in living neurons of rat visual cortex," *European Journal of Neuroscience*, vol. 17, no. 2, pp. 287–297, 2003.

[51] I. M. Mansuy and S. Shenolikar, "Protein serine/threonine phosphatases in neuronal plasticity and disorders of learning and memory," *Trends in Neurosciences*, vol. 29, no. 12, pp. 679–686, 2006.

[52] D. S. Bredt and R. A. Nicoll, "AMPA receptor trafficking at excitatory synapses," *Neuron*, vol. 40, no. 2, pp. 361–379, 2003.

[53] B. Mockett, C. Coussens, and W. C. Abraham, "NMDA receptor-mediated metaplasticity during the induction of long-term depression by low-frequency stimulation," *European Journal of Neuroscience*, vol. 15, no. 11, pp. 1819–1826, 2002.

[54] M. F. Bear, "A synaptic basis for memory storage in the cerebral cortex," *Proceedings of the National Academy of Sciences of the United States of America*, vol. 93, no. 24, pp. 13453–13459, 1996.

[55] L. F. Abbott and S. B. Nelson, "Synaptic plasticity: taming the beast," *Nature Neuroscience*, vol. 3, pp. 1178–1183, 2000.

[56] K.-H. Braunewell and D. Manahan-Vaughan, "Long-term depression: a cellular basis for learning?" *Reviews in the Neurosciences*, vol. 12, no. 2, pp. 121–140, 2001.

Hindawi Publishing Corporation
Neural Plasticity
Volume 2008, Article ID 872456, 13 pages
doi:10.1155/2008/872456

Research Article

The Role of NMDA Receptor Subtypes in Short-Term Plasticity in the Rat Entorhinal Cortex

Sophie E. L. Chamberlain, Jian Yang, and Roland S. G. Jones

Department of Pharmacy and Pharmacology, University of Bath, Claverton Down, Bath BA2 7AY, UK

Correspondence should be addressed to Roland S. G. Jones, r.s.g.jones@bath.ac.uk

Received 27 May 2008; Accepted 24 July 2008

Recommended by C. Andrew Chapman

We have previously shown that spontaneous release of glutamate in the entorhinal cortex (EC) is tonically facilitated via activation of presynaptic NMDA receptors (NMDAr) containing the NR2B subunit. Here we show that the same receptors mediate short-term plasticity manifested by frequency-dependent facilitation of evoked glutamate release at these synapses. Whole-cell patch-clamp recordings were made from layer V pyramidal neurones in rat EC slices. Evoked excitatory postsynaptic currents showed strong facilitation at relatively low frequencies (3 Hz) of activation. Facilitation was abolished by an NR2B-selective blocker (Ro 25-6981), but unaffected by NR2A-selective antagonists (Zn^{2+}, NVP-AAM077). In contrast, postsynaptic NMDAr-mediated responses could be reduced by subunit-selective concentrations of all three antagonists. The data suggest that NMDAr involved in presynaptic plasticity in layer V are exclusively NR1/NR2B diheteromers, whilst postsynaptically they are probably a mixture of NR1/NR2A, NR1/NR2B diheteromers and NR1/NR2A/NR2B triheteromeric receptors.

Copyright © 2008 Sophie E. L. Chamberlain et al. This is an open access article distributed under the Creative Commons Attribution License, which permits unrestricted use, distribution, and reproduction in any medium, provided the original work is properly cited.

1. INTRODUCTION

A huge amount of research has been devoted to the study of the physiology, pharmacology, function, and pathology of NMDA receptors (NMDAr). This has been extensively reviewed elsewhere (e.g., [1–6]). Native NMDAr are heteromeric structures, and consist of NR1 subunits, which are obligatory, in combination with one or more of four subtypes of NR2 subunit (NR2A-D). Functional receptors are tetramers, comprising two NR1 subunits and two NR2 subunits, where the functional unit is probably an NR1/NR2 heterodimer. The functional properties of NMDAr, such as single channel conductance, the degree of voltage-dependent Mg^{2+} block, and deactivation kinetics depend on which of the four NR2 subunits is assembled in the receptor. For example, NR2A and NR2B-containing channels have a high single channel conductance (40–50 pS) whereas NR2C and NR2D are lower (15–35 pS). NR2A-containing receptors display fast decay kinetics (around 100 milliseconds), whereas NR2B and C are much slower (250 milliseconds), and NR2D slower still (4 seconds) [5, 7]. In addition to functional differences, various subunit combinations display pharmacological differences in susceptibility to antagonists and regulatory mechanisms (such as sensitivity to H^+, Zn^{2+}, polyamines).

Synaptic transmission is a highly dynamic and plastic process, modified on-demand by a myriad of instantaneous, short, intermediate, and long-term regulatory mechanisms. Much attention has been devoted to the study of the role of NMDAr in synaptic plasticity, particularly in long-term potentiation (LTP) and depression (LTD). These studies have largely focussed on NMDAr at postsynaptic sites. However, dynamic regulation of synaptic strength can also involve receptors on presynaptic terminals, which provide a powerful, synapse-delimited control of transmitter release, and the existence of presynaptic NMDAr (preNMDAr) is now firmly established. Neurochemical [8–11] and immunolocalization studies [12–15] provided early indications for preNMDAr. We provided the first clear functional demonstration of preNMDAr, showing that the competitive antagonist, 2-AP5, could reduce the frequency of spontaneous excitatory postsynaptic currents (sEPSCs) at glutamate synapse in the rat entorhinal cortex (EC), indicating a tonic facilitatory effect of preNMDAr on glutamate release [16]. PreNMDAr

are now known to modify both glutamate and GABA release in a wide variety of locations and tissues [17–33].

Increasing attention is being paid to the role of preNMDAr as mediators of both long-term alterations in synaptic strength, and in moment-to-moment and short-term activity-dependent changes in transmitter release. For example, a role of preNMDAr in LTD has been demonstrated in cerebellum [34], visual [22, 33], and somatosensory [17] cortex. Conversely, involvement of preNMDAr in LTP has been demonstrated in amygdala [26, 32]. More intermediate forms of potentiation of glutamate [30] and GABA transmission [23], over a time scale of minutes, may also involve preNMDAr. As noted above, we found that preNMDAr are tonically activated by ambient glutamate [17, 35], providing instantaneous control over the level of glutamate release at EC synapses. Similar results have been reported for other areas [22, 27, 28, 33]. In addition, we found that preNMDAr are activated after action potential-driven synaptic release of glutamate, increasing the probability of subsequent release and allowing them to mediate short-term, frequency-dependent facilitation of glutamate transmission [16, 35].

We have also demonstrated that the tonic facilitatory effect of preNMDAr on spontaneous glutamate release is likely to be predominantly mediated by NR2B-containing NMDAr, since the increase induced by 2-AP5 was mimicked [35, 36] by relatively specific blockers of the NR2B subunit, ifenprodil [37], and Ro 25-6981 [38]. In addition, an antagonist with some specificity (albeit weak) for the NR2A subunits, NVP-AAM077 [39] had little effect. Others have also concluded that preNMDAr are likely to be predominantly NR2B-containing [27, 33, 40]. Postsynaptically, both NR2A and NR2B contribute to glutamate transmission, although there is controversy over whether diheteromeric NR1/NR2A and NR1/NR2B coexist at the postsynaptic density, or are segregated between synaptic and extrasynaptic locations, or even in a synapse-specific way [3]. The contribution of triheteromeric NR1/NR2A/NR2B receptors is also still a matter of debate [3, 41].

In the present study, we have extended our studies in the EC to examine the contribution of NR2A and NR2B receptors to short-term plasticity of glutamate transmission, by examining the effects of relatively specific blockers on the preNMDAr mediated, frequency-dependent facilitation of evoked glutamate release. In addition, we have used the same agents to determine whether postsynaptic NMDAr may differ from those on presynaptic terminals.

2. METHODS

2.1. Slice preparation

Experiments were performed in accordance with the U.K. Animals (Scientific Procedures) Act 1986, European Communities Council Directive 1986 (86/609/EEC), and the University of Bath ethical review document. Slices containing EC and hippocampus were prepared from male Wistar rats (P28–35), which were anaesthetized with an intramuscular injection of ketamine (120 mg/kg) plus xylazine (8 mg/kg) and decapitated. The brain was rapidly removed and immersed in oxygenated artificial cerebrospinal fluid (aCSF) chilled to 4°C. Slices (350–400 μm) were cut using a Vibroslice, and stored in aCSF bubbled with 95% O_2/5% CO_2, at room temperature. Following recovery for at least 1 hour, individual slices were transferred to a recording chamber mounted on the stage of a Zeiss Axioskop FS or an Olympus BX50WI microscope. The chamber was perfused (2.0 ml/min) with oxygenated aCSF (pH 7.4) at 31–33°C. The aCSF contained (in mM) NaCl (126), KCl (3), NaH_2PO_4 (1.4), $NaHCO_3$ (19), $MgSO_4$ (2), $CaCl_2$ (2), and D-glucose (10). Neurones were visualized using differential interference contrast optics and an infrared video camera.

2.2. Electrophysiological recording

Patch pipettes were pulled from borosilicate glass on a Flaming/Brown microelectrode puller. For recording spontaneous (sEPSCs) or evoked (eEPSCs) excitatory postsynaptic currents, pipettes were filled with a Cs-gluconate-based solution containing (in mM) D-Gluconate (100), HEPES (40), QX-314 (1), EGTA (0.6), NaCl (2), $MgCl_2$ (5), TEA-Cl (1), phosphocreatinine (5); ATP-Na (4), GTP-Na (0.3), MK-801 (2). Solutions were adjusted to 290 mOsmol, and to pH 7.3 with CsOH. Whole-cell voltage clamp recordings (holding potential −60 mV unless otherwise stated) were made from neurones in layer V of the medial division of the EC, using an Axopatch 200B amplifier (Molecular Devices, Calif., USA). Series resistance compensation was not employed, but access resistance (10–30 MΩ) was monitored at regular intervals throughout each recording and cells were discarded from analysis if it changed by more than ±10%. Liquid junction potential (12.3 mV) was estimated using the Junction Potential Calculator included in pClamp-8 software (Molecular Devices, Calif., USA), and compensated for in the holding potentials.

eEPSCs were elicited by electrical stimulation (bipolar pulses, 10–50 V, 0.02 millisecond duration) via a bipolar tungsten electrode placed on the surface of the slice in layer V of the lateral EC. The stimulation intensity was adjusted to give submaximal (approx. 50–60% maximum amplitude) responses.

2.3. Monitoring presynaptic NMDAr activity

In all these experiments, MK-801 (2 mM) was included in the patch pipette solution to block postsynaptic NMDAr. This allowed us to record AMPA-receptor mediated responses in isolation, and to monitor activity at preNMDAr uncontaminated by postsynaptic receptor effects. This approach was developed by us [16, 35, 42], and has been used successfully by others to block postsynaptic NMDAr in the recorded neurone [17, 27, 28, 32, 33, 40]. When whole-cell access was gained, neurones were voltage clamped at 0 mV, and synaptic stimulation was delivered at 2 Hz for 30–40 seconds to allow blockade of postsynaptic NMDAr by MK-801 dialyzed into the cell via the patch pipette solution. Membrane potential was then clamped at −60 mV and single shock stimulation delivered at low frequency (0.05 Hz) to

evoke AMPAr mediated EPSCs. At 2 or 3 minute intervals, the single shock was replaced with stimulation at 3 Hz for 10 seconds. Such stimulation results in a frequency-dependent facilitation of the AMPAr-mediated EPSC, which we have shown previously to be dependent on activation of preNMDAr [35]. We used the degree of frequency-dependent facilitation of AMPAr-mediated eEPSCs as a quantitative measure of preNMDAr activation.

2.4. Monitoring postsynaptic NMDAr activity

In these experiments, MK-801 was omitted from the patch pipette solution. When whole-cell access was gained, control eEPSCs were recorded at a holding potential of −60 mV, before addition of the AMPAr antagonist, NBQX, and the $GABA_A$r-antagonist, bicuculline to the bath perfusion. After 10–12 minutes, the holding potential was changed to +40 mV to record isolated NMDAr-mediated EPSCs as positive going currents. These were evoked at low frequency (0.05 Hz) until stable amplitudes were recorded, before addition of antagonists to the bath.

2.5. Data analysis

Data were recorded to computer hard disk using Axoscope software. Minianalysis (Synaptosoft, Decatur, Ga, USA) was used for analysis of EPSCs offline. In the studies of preNMDAr, the average peak amplitude of the 8 responses before each episode of 3 Hz stimulation was determined. During the period of 3 Hz stimulation, the amplitude of the 8 largest events was determined and normalized to the average amplitude of the preceding low-frequency events to obtain a quantitative measure of frequency-dependent facilitation in the presence and absence of antagonists. In these studies, we also analyzed AMPAr-mediated sEPSCs, by determining interevent interval (IEI), amplitude, rise (10–90%), and decay times. sEPSCs were detected automatically using a threshold-crossing algorithm. Threshold varied from neurone to neurone but was always maintained at a constant level in any given recording. At least 200 events were sampled during a continuous recording period for each neurone under each condition. Cumulative probability distributions of IEI were compared using the Kolmogorov-Smirnoff test. In experiments on postsynaptic NMDAr, responses were quantified by measuring mean peak amplitudes of at least 5 NMDAr-mediated eEPSCs evoked at low frequency at intervals throughout the study. In these studies, the vast majority of sEPSCs were blocked, as recordings were conducted in the presence of NBQX. Occasional slow sEPSCs mediated by NMDAr were recorded, their frequency was very low (2-3 per minute) and precluded meaningful analysis.

2.6. Materials

Salts used in preparation of aCSF were "Analar" grade and purchased from Merck/BDH or Fisher Scientific (Dorset, UK). All drugs were applied by bath perfusion. MK-801, NMDA, NBQX, D-2-AP5, bicuculline methiodide, and Ro 25-6981 ((αR,βS)-α-(4-hydroxyphenyl)-β-methyl-4-(phenylmethyl)-1-piperidinepropanol hydrochloride) were obtained from Tocris (Bristol, UK). TPEN (N,N,N′, N′-Tetrakis-(2-pyridylmethyl)-Ethylenediamine) was obtained from Sigma (UK). UBP302 ((S)-1-(2-amino-2-carboxyethyl)-3-(2-carboxybenzyl) pyrimidine-2,4-dione) was a kind gift from Dr. Dave Jane, University of Bristol, and NVP-AAM077 ((R)-[(S)-1-(4-bromo-phenyl)-ethylamino]-(2,3-dioxo-1,2,3,4-tetrahydroquinoxalin-5-yl)-methyl]-phosphonic acid) was a gift from Dr. Yve Auberson at Novartis (Basel, Switzerland).

3. RESULTS

3.1. Presynaptic NMDAar

Figure 1(a) shows eEPSCs evoked in a layer V neurone at 3 Hz, with postsynaptic NMDAr blocked by internally dialyzed MK-801. The first 6 responses evoked during a train of 30 at 3 Hz are shown and demonstrate the facilitation seen at this relatively low frequency. As reported previously [35], the facilitation of the AMPAr-mediated eEPSCs was entirely dependent on presynaptic NMDAar activation, since it could be abolished by 2-AP5 ($n = 5$, Figure 1(b)). Likewise, the NMDAr channel blocker, MK-801, also abolished frequency facilitation ($n = 10$, Figure 1(b)). In some neurones, facilitation was replaced by a weak frequency-dependent depression of eEPSCs in the presence of the blockers. This can be seen as a reduction in mean amplitude of eEPSCs in the presence of the blockers (e.g., Figure 1(b)). In a further 5 neurones, we confirmed the specificity of the effect by testing the effects of GluR5 subunit specific antagonist of kainate receptors (UBP 302, 20 μM), since we have recently shown that these receptors mediate a similar short-term facilitation of glutamate transmission at 3–5 Hz in layer III of the EC (Chamberlain S.E.L and Jones R.S.G. unpublished). UBP 302 had no effect on facilitation in layer V (not shown) confirming its dependence on NMDAar. Interestingly, 2-AP5 had no effect on frequency facilitation in layer III of the EC (not shown), so although similar short-term plasticity is seen in both layers, its underlying mechanism is lamina-specific.

Since neither 2-AP5 nor MK-801 has selectivity for NR2A v NR2B subunits [5], the data do not indicate the subunit composition of NMDAr responsible for short-term frequency-facilitation. To determine the receptor involved, we have examined the effect of more specific antagonists. First, we tested the effects of Ro 25-6981. This is an allosteric inhibitor of NMDA receptors, which binds to a site on the N-terminal domain of the NR2 subunit, with a high degree of selectivity (>3000 fold) for NR2B over NR2A [38]. Figure 2(a) shows that Ro 25-6981 at 500 nM abolished the frequency facilitation of eEPSCs, again revealing a weak depression. A lower concentration (200 nM, $n = 3$) of Ro 25-6981 resulted in a mean maximal reduction in frequency-facilitation of 69 ± 7%. At these concentrations, the drug should have little or no effect on NR2A subunits [38], strongly suggesting that NR2B-containing receptors are primarily responsible for this form of short-term plasticity at layer V synapses. This would agree with previous studies that have shown the tonic facilitatory effect on spontaneous

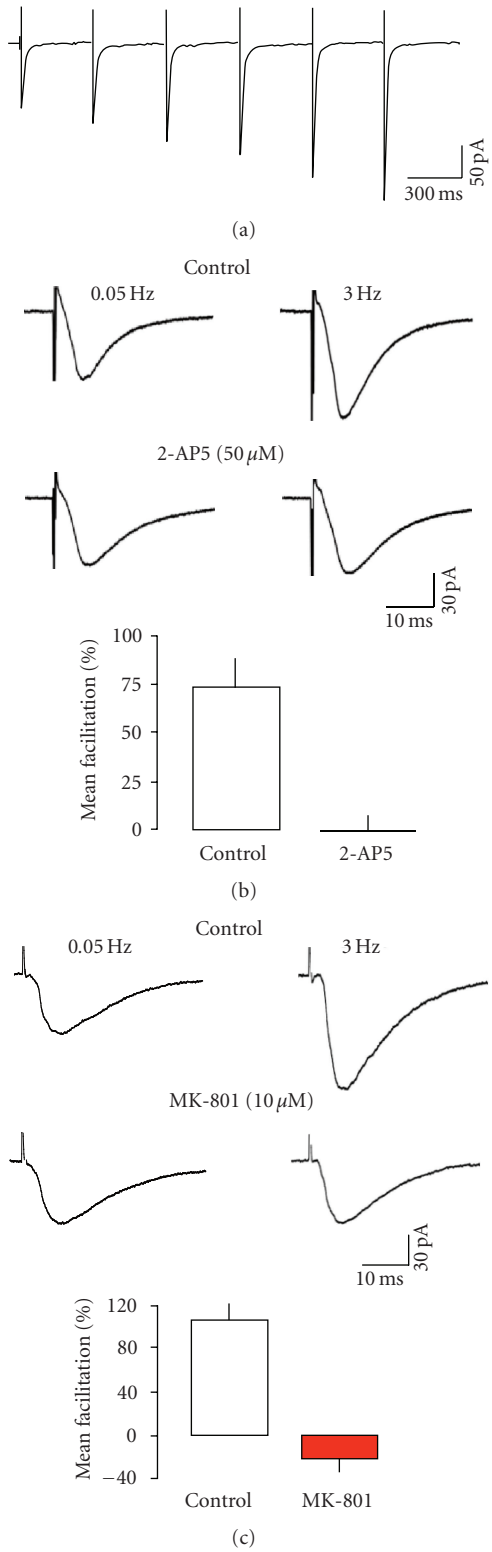

Figure 1: Short-term facilitation is mediated by presynaptic NMDA receptors. (a) First 6 responses evoked by a train of stimuli (3 Hz, 20 seconds) averaged from 3 neurones. (b) Responses ($n = 8$) were averaged at low frequency and during 3 Hz stimulation. In the presence of 2-AP5, low-frequency responses were unaltered, but facilitation was abolished. The bar graphs show the mean results from 5 neurones. (c) Similar results were seen with MK-801. Stimulation artifacts have been partially blanked for clarity.

release is likely to be NR2B-mediated [16, 35, 43]. Accordingly, Ro 25-6981 resulted in a substantial increase in IEI of sEPSCs from 277 ± 82 milliseconds (5.5 ± 1.9 Hz) to 764 ± 261 milliseconds (2.1 ± 0.7 Hz) recorded in the same neurones (cf. [36, 43]). KS analysis of cumulative probability distributions confirmed a highly significant change. There was no concurrent change in mean amplitude, rise, or decay time (not shown).

Next, we examined the effect of NVP-AAM077 in 5 neurones. This is a competitive antagonist that shows some selectivity for receptors containing the NR2A subtype. Initial reports indicated a greater than 100 fold selectivity of the compound for NR2A over NR2B [39, 44]. However, recently, it has been suggested that the selectivity is closer to 10 fold when the affinity of the two subtypes for glutamate is accounted for ([41], see also [45, 46]). Thus, at the concentration employed here (400 nM), we might expect almost complete blockade of NR2A receptors, but it is possible that substantial inhibition of NR2B would also occur [41]. Nevertheless, NVP-AAM077 did not significantly affect the frequency-dependent facilitation of eEPSCs (see Figure 2(b)). If anything, the facilitation was slightly (although not significantly) increased. These data suggest that NVP-AAM077 may have reasonable selectivity for the NR2A receptor in our preparation, but that these receptors are not involved in presynaptic short-term plasticity at layer V synapses. Further support for this was obtained from analysis of sEPSCs. The mean IEI in control was 443 ± 230 milliseconds (4.0 ± 0.9 Hz), and this decreased slightly to 377 ± 180 milliseconds (4.5 Hz) with the addition of NVP-AAM077. Likewise, there was no change in amplitude, rise, or decay times of sEPSCs (not shown).

In view of the controversy over the selectivity of NVP-AAM077, we also tested ($n = 5$) the effects of Zn^{2+}, which has been shown to discriminate between NR2A and NR2B receptors. Like Ro 25-6981 at NR2B subunits, Zn^{2+} binds to the N-terminal domain of the NR2A subunit to exert a voltage-independent inhibition with >100 fold selectivity over NR2B [47–49]. However, as with NVP-AAM077, a relatively high concentration of Zn^{2+} (300 nM) failed to alter frequency-dependent facilitation of eEPSCs (see Figure 2(c)). In addition, it had little effect on the IEI (200 ± 150 *v* 298 ± 170 milliseconds, see Figure 2(d)), amplitude (17.7 ± 3.4 *v* 15.4 ± 2.2 pA), rise (1.9 ± 0.3 *v* 2.1 ± 0.4 milliseconds), or decay times (24.6 ± 1.6 *v* 27.3 ± 1.3 milliseconds) of sEPSCs (cf. [43]). Thus, the data from both NVP-AAM077 and Zn^{2+} studies militate strongly against a role for NR2A receptors in presynaptic frequency-dependent facilitation in layer V of the EC. The ability of Ro 25-6981 to block facilitation strongly indicates that presynaptic plasticity at these synapses is dependent only on NR2B-containing receptors.

A recent paper [50] suggested that activation of postsynaptic NR2B-containing receptors at a similar frequency (3.3 Hz) to that employed by us to elicit frequency-dependent facilitation induced a long-term depression of the NMDAr-mediated currents themselves (primarily by decreasing fractional Ca^{2+} currents carried by the receptors). We were interested to see if the repetitive activation of the

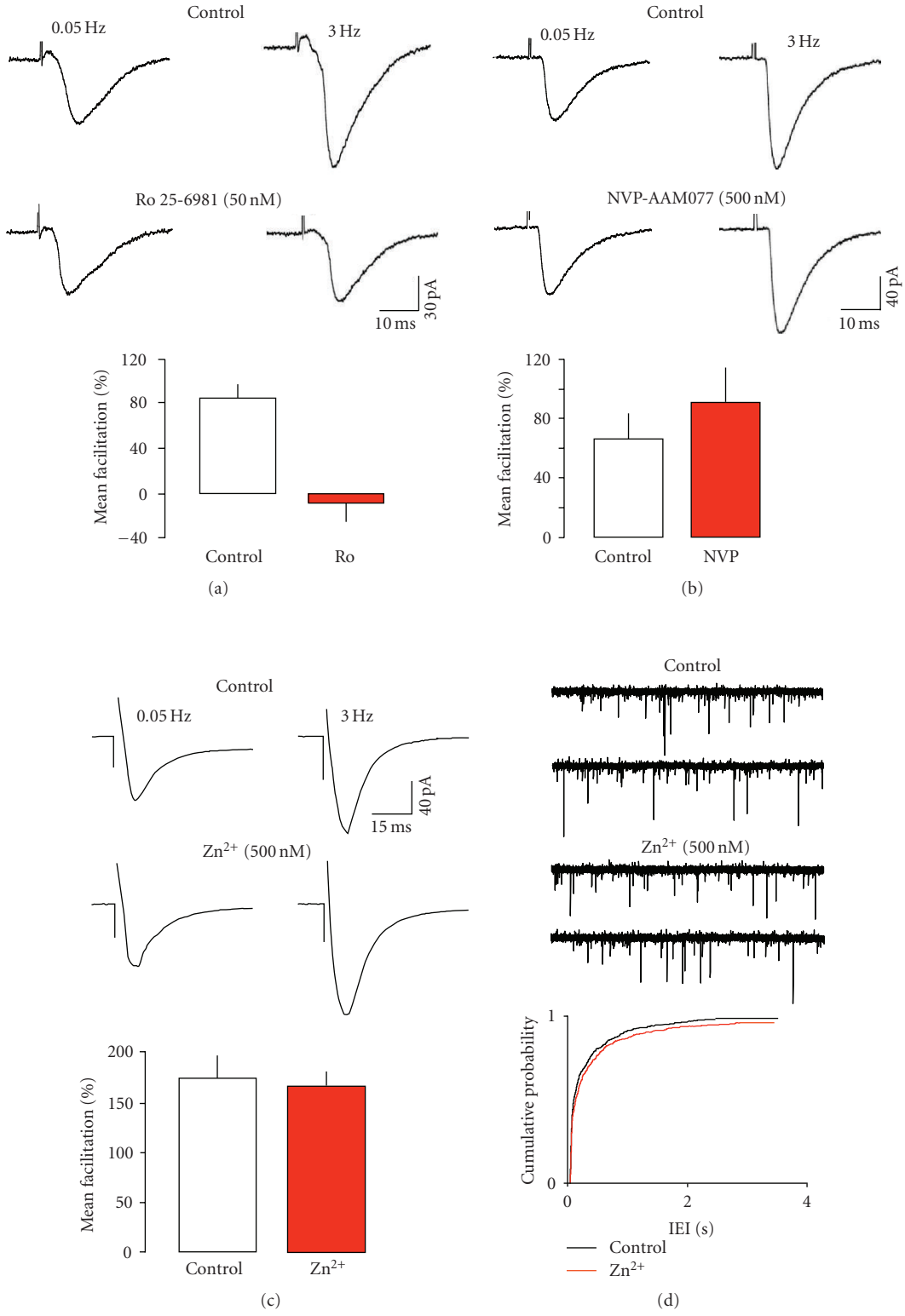

Figure 2: Effects of subunit selective antagonists. (a) Ro 25-6981 abolished frequency-dependent facilitation. In contrast, neither NVP-AAM077 (b) nor Zn^{2+} (c) had any significant effect. (d) Zn^{2+} also had little effect on sEPSCs. The records show consecutive sweeps of baseline recording of sEPSCs and in the presence of Zn^{2+}. The cumulative probability plots show pooled data from 6 neurones, with 200 events from each neurone in the presence and absence of the blocker. There was a small shift to the right in the presence of Zn^{2+}, but this failed to reach significance (KS test).

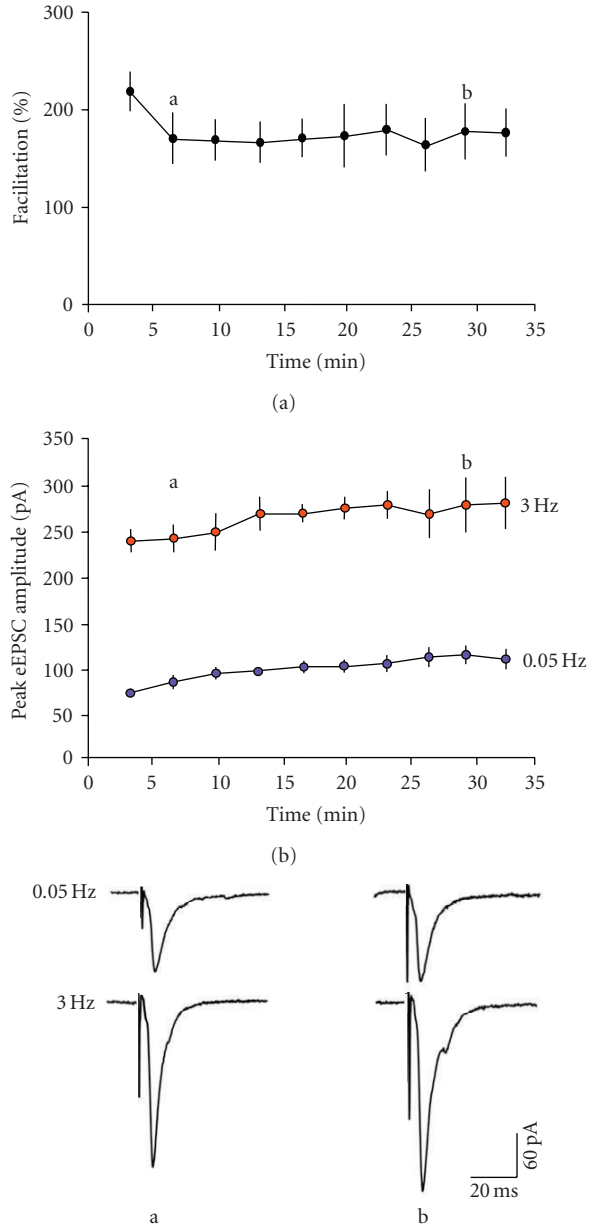

Figure 3: Progressive changes associated with repeated episodes of stimulation at 3 Hz in the absence of NMDAr blockers. Each point is the degree of facilitation recorded during a 30-second period of stimulation and is the average from 5 neurones. (a) After an initial decline in the degree of facilitation, it remained stable throughout the subsequent 30 minutes of recording. (b) Mean amplitude of responses recorded at low and high frequency used to assess the facilitation in the neurones shown in (a). There was a progressive, albeit small increase in amplitude of responses in both cases. Representative records from one neurone, sampled at the times indicated, are shown below.

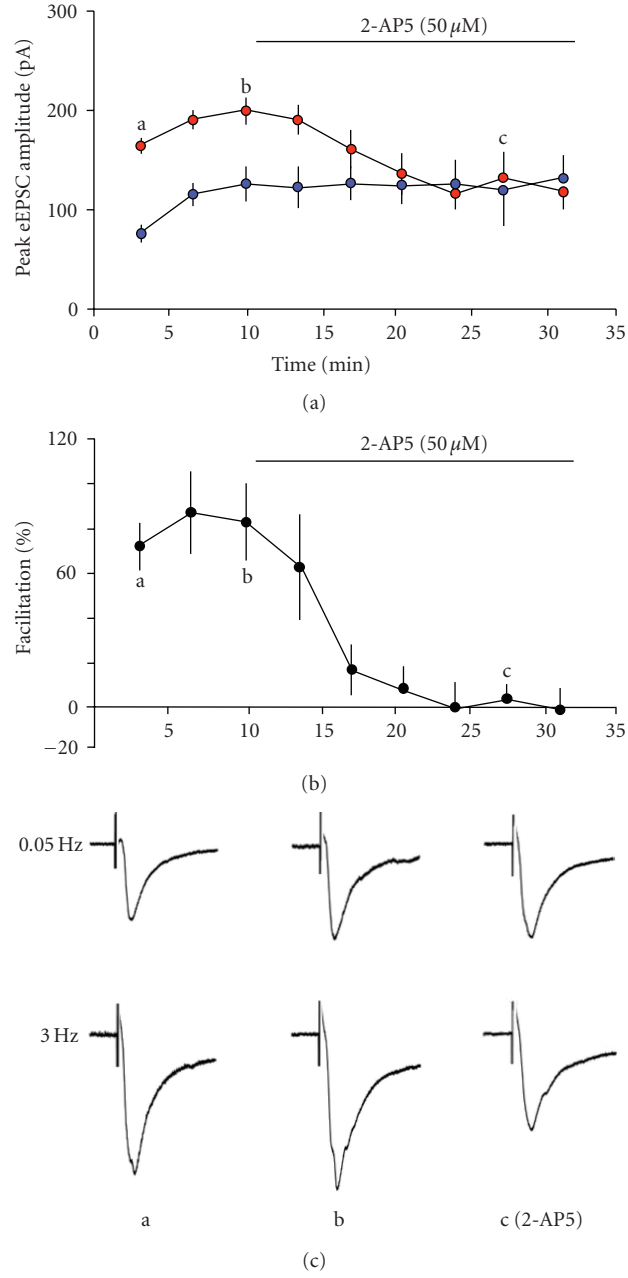

Figure 4: Time course of the effect of 2-AP5 on eEPSC amplitude and facilitation. (a) The progressive increase in both low- and high-frequency responses was prevented by the addition of 2-AP5 (n = 5 neurones). The responses at high frequency were progressively reduced to control levels, in parallel with the degree of facilitation (b). (c) Representative responses recorded in one neurone at the times indicated.

presynaptic NR2B-containing receptors would induce any decrement in frequency facilitation at layer V synapses. In 5 neurones, we induced facilitation of eEPSCs and monitored the degree of facilitation but without the addition of any blockers. Overall there was an initial decrease in the degree of facilitation of AMPAr-mediated eEPSCs from the first to second episode, but thereafter it was remarkably consistent (see Figure 3(a)). However, when we looked at absolute amplitude of eEPSCs, there was a small, but consistent, increase over the course of the studies. This applied to events evoked at both low and high frequencies (see Figure 3(b)). We also examined the time course of these changes in the neurones tested with 2-AP5 (see Figure 4). The antagonist appeared to prevent the progressive increase in amplitude

of the low-frequency events at the same time as blocking the frequency-dependent facilitation. This limited protocol may suggest the short-term frequency-dependent facilitation could underlie a longer-term enhancement of glutamate transmission. As the postsynaptic NMDAr were already blocked (by internal MK-801), this is likely to involve the presynaptic, NR2B-containing receptors.

3.2. Postsynaptic NMDAr

We now wished to determine the contribution of NR2A/B subunits to NMDAr at postsynaptic sites in layer V of the EC, so we tested the same antagonists used in the presynaptic experiments for effects on isolated NMDAr-mediated eEPSCs. As expected, the nonspecific blockers 2-AP5 ($n = 5$) and MK-801 ($n = 9$) both abolished the slow eEPSCs recorded at +40 mV in the presence of NBQX and bicuculline (not shown). Ro 25-6981 ($n = 5$) also elicited a concentration dependent reduction in postsynaptic NMDAr responses at concentrations that would be expected to retain selectivity for NR2B-containing receptors (see Figure 5(a)). The slow eEPSCs were essentially abolished by Ro 25-6981 at 500 nM. This suggests that NR1/NR2B receptors dominate at postsynaptic sites as they do presynaptically. However, when we tested NVP-AAM077 ($n = 6$), we again found a concentration-related reduction in postsynaptic responses with around 80% inhibition at 500 nM (see Figure 5(b)). Comparison with the data of Neyton and Paoletti [41] suggests that the effect of NVP-AAM077 could be explained by blockade of both NR2B and NR2A receptors since 500 nM was sufficient to abolish NR2A responses in oocytes, but also to exert around 60% block of NR2B. However, this is at odds with its failure to alter preNMDAr-dependent facilitation, which is clearly an NR2B-mediated response. Studies with Zn^{2+} ($n = 6$) failed to substantially clarify the situation. The divalent cation also elicited a concentration-dependent reduction in slow eEPSCs (see Figure 5(c)). The concentrations employed exert around an 80% voltage-independent block of NR2A receptors expressed in oocytes, but retain a considerable degree of selectivity with regard to block of NR2B receptors [47, 49]. These data do suggest a role for NR2A receptors at postsynaptic sites, but it is puzzling that Ro 25-6981 essentially also abolished NMDAr EPSC, when it would be expected to have little effect on NR2A receptors.

We performed two more sets of experiments to look at this question further. In 5 neurones, we first perfused a low concentration of Ro 25-6981 (200 nM), to partially block the NMDAr EPSC. We then added a low concentration of Zn^{2+} (100 nM). In these neurones, Ro 25-6981 resulted in inhibition of around 45%, and with the addition of Zn^{2+} there was a further reduction to around 90–100%, which clearly indicates a role of both NR2A and NR2B in mediating the postsynaptic response (see Figure 5(d)). Finally, there is evidence that under control conditions, NR2A-containing receptors may be substantially blocked by Zn^{2+}, present in the ACSF as a result of contamination of other salts used in its preparation [47]. Although addition of Zn^{2+} clearly reduced slow eEPSCs in our experiments, we also examined whether there was significant blockade of the NR2A receptor in control recordings by testing the effect of the Zn^{2+}-chelator, TPEN (2 μM), in 3 neurones. This had no effect on the mean amplitude of NMDAr eEPSCs (125.3 ± 25.1 *v* 111.9 ± 26.1 pA) suggesting that our results with antagonists were unlikely to be confounded by Zn^{2+}-contamination.

Finally, as noted above, relatively low frequency, repetitive activation of NR2B receptors has been shown to induce a depression of postsynaptic NMDA responses per se [50]. In 7 neurones, we determined the effects of a brief period of repetitive stimulation (3 Hz, 40 seconds) on postsynaptic NMDAr eEPSCs in 5 neurones. Overall, during the repetitive stimulation there was a small (15%), progressive decrease in the first 10–15 seconds, and thereafter the amplitude reached a plateau (see Figure 6(a)). We then recorded NMDAr eEPSCs at low frequency (0.05 Hz) over the subsequent 30 minutes. There was an initial period (5 minutes) where responses appeared to be slightly depressed and thereafter a recovery followed by a slight increase before recovery to control levels (see Figure 6(b)). However, apart from a brief period around 20 minutes there was no significant difference compared to control.

4. DISCUSSION

We originally demonstrated that the presynaptic NMDAar mediating facilitation of glutamate release in the EC was likely to be predominantly NR2B-containing, as the frequency of sEPSCs was decreased by the N2B antagonist, ifenprodil [35]. Other work supports the conclusion that preNMDAr that facilitate spontaneous glutamate release at cortical synapses are primarily NR2B-containing. We found that Ro 25-6981 but not NVP-AAM077 or Zn^{2+} reduced sEPSC frequency ([36], present study), and similar results with Ro 25-6981 and Zn^{2+} were reported for synapses in layer II/III of the visual cortex [28]. Jourdain et al. [27] reported that presynaptic NR2B receptors were responsible for the increase in mEPSC frequency in dentate granule neurones seen after stimulation of glutamate release from adjacent astrocytes, as it was blocked by ifenprodil. We now show that the same receptor is likely to mediate short-term plasticity of evoked glutamate release in layer V of the EC. Thus, the facilitation of eEPSCs at the relatively low frequency of 3 Hz was blocked by Ro 25-6981. The lack of effect of NVP-AAM077 and Zn^{2+} suggests that NR2A receptors do not contribute to facilitation of either spontaneous or evoked glutamate release at EC synapses. We cannot rule out a role of NR2A receptors at higher frequencies, although Sjöström et al. [33] have reported that frequency facilitation at 30 Hz at layer V synapses in visual cortex is greatly reduced by ifenprodil, suggesting that NR2B dominate at other presynaptic sites as well.

It is somewhat surprising that only presynaptic NR2B receptors appear to modulate release. Postembedding immunolabeling studies have shown the presence of NR1 subunits in presynaptic terminals in cortex and hippocampus [12–14, 51–53]. Whilst a host of studies have demonstrated NR2B subunits at presynaptic locations [15, 51, 54–59], similar studies have also indicated the presence of NR2A

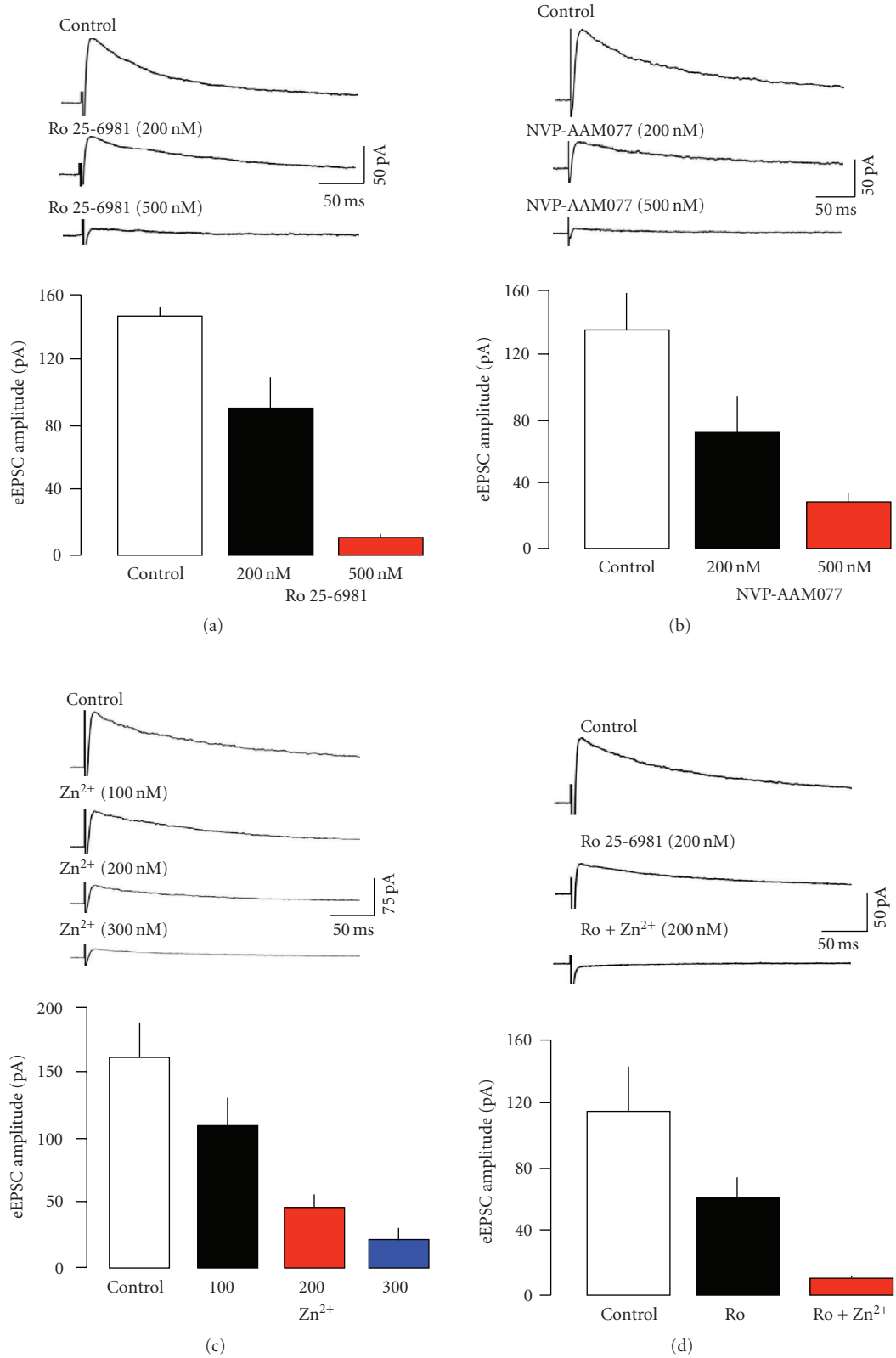

Figure 5: Effect of subunit selective antagonists on postsynaptic NMDAr-mediated eEPSCs. Slow eEPSCs were recorded at +40 mV in the presence of NBQX and bicuculline. Each response is the average of at least 8 events. (a) The NR2B antagonist, Ro 25-691, induced a concentration-dependent reduction in slow eEPSCs. They were essentially abolished at the higher concentration. (b) and (c) show that NR2A selective blockers induced a very similar blockade of slow EPSCs. (d) A combination of NR2A and NR2B antagonists also abolished slow EPSCs.

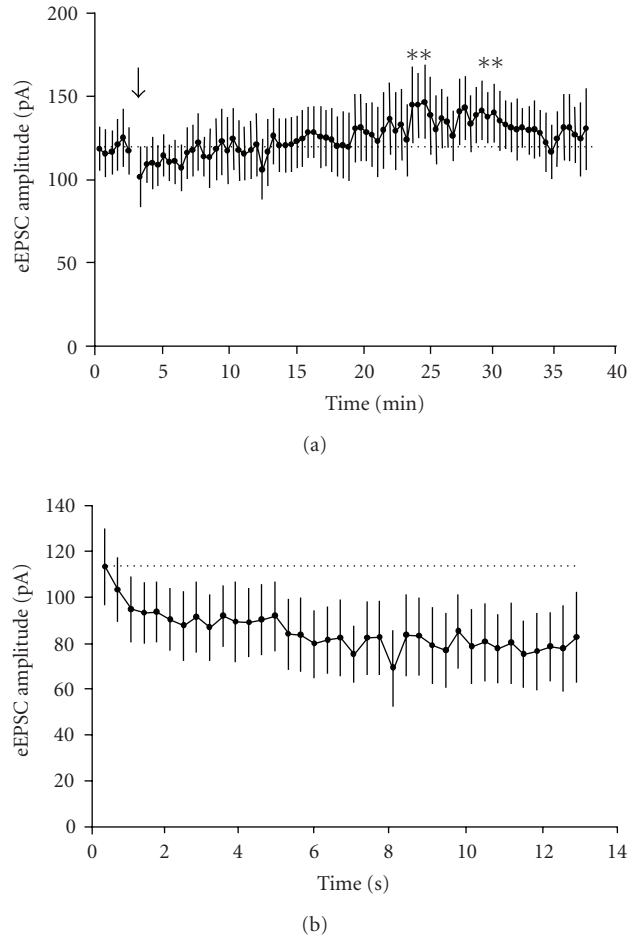

Figure 6: Changes in slow eEPSC amplitudes during and after repetitive stimulation at 3 Hz for 30 seconds. (a) shows the average response amplitudes at low frequency (0.05 Hz) recorded during 35 minutes stimulation in 7 neurones. During the period indicated by the arrow, stimulation was increased to 3 Hz for 30 seconds and the average response amplitudes (first 37 only for clarity) recorded during this period are shown in (b). The only significant differences compared to the mean control value are indicated by the asterisks in (a).

subunits [51, 52, 60–62] although, to date, there are no similar studies specifically related to the EC.

The presence of all three subunits suggests that both NR1/NR2A and NR1/NR2B diheteromeric receptors and possibly also NR1/NR2A/NR2B triheteromers could be expressed in cortical presynaptic terminals, and this may well be the case. However, it is clear from the pharmacological experiments presented here and elsewhere, that NR1/NR2B receptors are predominantly responsible for short-term NMDAr-mediated facilitation of glutamate release (but see, [63]). The properties of NR2B subunits differ from NR2A, in a way that may make them more suited to the task of presynaptic facilitation (see [6, 7, 64–66]). NR2B subunits have a higher affinity for both glutamate and glycine, and show less desensitization. The two subunits confer similar single channel conductance to diheteromeric receptors (around 50 pS), but they have very different deactivation kinetics, with NR1/NR2A receptors having decay time constants of 50–100 milliseconds, and NR1/NR2B receptors in the order of 200–400 milliseconds. Both are Ca^{2+}-permeable, but NR2B receptors exhibit a higher fractional Ca^{2+}-current than NR2A (see [66, 67]). Both subunits also display Ca^{2+}-dependent inactivation, but this is more pronounced for NR2A. The presence of NR2B subunits results in prolonged EPSPs compared to those seen when NR2A subunits dominate (see [3, 7, 66]). Thus, it seems likely that activation of presynaptic NR2B-containing receptors would mediate a slowly deactivating opening of the NMDAr channel and a greater Ca^{2+}-influx into the presynaptic terminals than any influx mediated by NR2A receptors. Ca^{2+}-influx via the NMDAr is responsible for instantaneous control of spontaneous glutamate release [35]. With a deactivation time of around 300 milliseconds, repetitive activation of NR1/NR2B receptors would readily result in temporal summation of presynaptic Ca^{2+}-entry leading to the short-term facilitation at even relatively low-frequency stimulations seen here and previously [35].

It is interesting to speculate on a physiological or pathological role for short-term plasticity mediated by preNMDAr. State-dependent rhythms and oscillatory activity at various frequencies occur in the networks of the EC including ripples and sharp waves (>100 Hz), gamma (30–80 Hz), theta (4–8 Hz), and slow waves (0.1–0.5 Hz) [68–71], and these may be involved in mnemonic processing in temporal lobe structures. There is a consensus that theta oscillations are intimately involved in declarative memory and spatial navigation (see [72–74]), and it is possible that information encoding involved in these processes is reliant on an increase in entorhinal-hippocampal delta/theta coherence [73]. The facilitation of glutamate transmission mediated by preNMDAr that we describe is readily elicited at frequencies in the low theta range. Thus, we could speculate that these receptors may be involved in the generation of theta activity in the EC, and the proposed role of this activity in short-term memory and coding of spatial information (e.g., [72, 74]).

At a pathological level, it is noteworthy that, oscillations at delta (1-2 Hz) and theta frequency may be associated with epilepsy. In patients with temporal lobe epilepsy, there is a generalized increase in EEG activity in the delta/theta range, and the most common pattern of discharges after the initiation of ictal events is a rhythmic delta/theta activity (e.g., [75, 76]). Also, in rats made chronically epileptic following kainic acid injection, epileptiform events in superficial layers of the EC were sometimes followed by spontaneous theta oscillations in layer V [77]. We recently showed that preNMDAr function declines in adulthood, but is markedly enhanced in age-matched, chronically epileptic rats [36] and there is evidence for a similar increased function in human temporal lobe epilepsy [78]. We could speculate that this increased preNMDAr function could result in enhanced generation of delta/theta activity in epileptic conditions. Of further interest in this regard is the observation that increased delta/theta EEG activity (albeit in patients with generalized absence/myoclonic seizures) is normalized by the anticonvulsant drugs, valproate, and lamotrigine [79–81].

We have also shown that at least one anticonvulsant drug (felbamate) can block the preNMDAr [42]. This raises the possibility that some anticonvulsants could alter delta/theta oscillations by targeting preNMDAr.

Whatever the function of short-term plasticity, and the involvement of preNMDAr in it, there is increasing evidence that these receptors may also contribute to longer term forms of plasticity, apparently mediating both LTD [17, 22, 33, 34] and LTP [26, 32] at a variety of synapses. In at least one case, LTD appears to be mediated by NR2B-containing receptors [33], so both short- and long-term plasticity of glutamate transmission could involve Ca^{2+}-influx via presynaptic NR2B receptors. We have also shown recently that preNMDAr are rapidly mobile and can diffuse between locations near release sites and more distal locations in the terminal membrane [82]. Trafficking of receptors in the presynaptic membrane appears to be influenced by ongoing activity levels, and exerts an intermediate (over 10 seconds of minutes) form of plasticity. Thus, presynaptic NR2B receptors may be heavily involved in both plasticity and metaplasticity at glutamate synapses in EC and other cortical synapses.

In the present study, we also present evidence for differences in pre- and postsynaptic NMDAr at layer V synapses. Whilst preNMDAr-mediated effects are exclusively dependent on NR1/NR2B-containing diheteromers, both NR2B and NR2A appear to contribute to postsynaptic responses. However, the relative contributions of the two subunits are not clear. The ability of low concentrations of both Zn^{2+} and Ro 25-6981 to reduce postsynaptic NMDAr responses could suggest that they are dependent on a mix of NR1/NR2A and NR1/NR2B diheteromeric receptors. However, concentrations of either blocker, that should largely retain selectivity at the respective subtypes, were able to almost abolish postsynaptic responses. This could suggest that the postsynaptic receptors could be largely triheteromeric NR1/NR2A/NR2B receptors. Although triheteromeric receptors do exhibit high affinity for both NR2A and NR2B selective blockers, it seems likely that they exhibit a reduced maximal inhibitory effect to either, and that maximal blockade requires occupation of both sites [83]. This does not fit well with our finding that combined application of low concentrations of Zn^{2+} and Ro 25-6981 could also abolish postsynaptic responses, which would better support a mediation by a mix of NR1/NR2A and NR1/NR2B diheteromeric receptors. It should also be noted that the ability of NMDA antagonists to block the receptors is not just dependent on the NR2 subunit present, but is also modified by which splice variant of the NR1 subunit with which it combines [47, 49]. We do not know which NR1 subunit(s) may be present in the EC. Thus, overall it is difficult to define exactly what the postsynaptic receptor population, but the most likely scenario is a mix of NR1/NR2A, NR1/NR2B, and NR1/NR2A/NR2B receptors.

A number of studies have suggested that NR1/NR2A, NR1/NR2B, and NR1/NR2A/NR2B receptors may contribute to postsynaptic responses at other cortical synapses [84–86]. There is support also for synapse-specific segregation of NR2A and NR2B-containing receptors (e.g., [87, 88]) and spatial segregation between subsynaptic and extrasynaptic sites (e.g., [86]). The controversy over whether subunit composition and spatial location are linked, and the difficulties in defining the role of triheteromeric receptors has been well reviewed recently [3]. We cannot make any firm conclusions regarding these aspects in the EC, but our data do suggest that postsynaptic NR1/NR2A, NR1/NR2B, and NR1/NR2A/NR2B receptors all contribute to postsynaptic responses at glutamate synapses in layer V of the EC, in contrast to presynaptic sites where NR1/NR2B receptors may have exclusive control. Increasing numbers of studies have documented LTP and LTD at synapses in the EC [89–95]. The EC is clearly a pivotal site in learning and memory functions resident in the temporal lobe. We have shown that preNMDAr mediate short-term forms of plasticity in the EC. In experiments employing a limited protocol of repetitive activation, we found that this short-term plasticity may lead to longer-term plasticity (either pre- or postsynaptically), and the aim now is to examine in detail the relationship between short-term effects and long-term plasticity and metaplasticity at these synapses.

ACKNOWLEDGMENTS

The authors thank the Wellcome Trust, Epilepsy Research UK and the University of Bath for financial support, the BBSRC and the University of Bristol for PhD scholarships for SELC, and JY, respectively.

REFERENCES

[1] S. G. Cull-Candy, S. Brickley, and M. Farrant, "NMDA receptor subunits: diversity, development and disease," *Current Opinion in Neurobiology*, vol. 11, no. 3, pp. 327–335, 2001.

[2] F. Gardoni and M. Di Luca, "New targets for pharmacological intervention in the glutamatergic synapse," *European Journal of Pharmacology*, vol. 545, no. 1, pp. 2–10, 2006.

[3] G. Köhr, "NMDA receptor function: subunit composition versus spatial distribution," *Cell and Tissue Research*, vol. 326, no. 2, pp. 439–446, 2006.

[4] M. Llansola, A. Sanchez-Perez, O. Cauli, and V. Felipo, "Modulation of NMDA receptors in the cerebellum. 1. Properties of the NMDA receptor that modulate its function," *The Cerebellum*, vol. 4, no. 3, pp. 154–161, 2005.

[5] P. Paoletti and J. Neyton, "NMDA receptor subunits: function and pharmacology," *Current Opinion in Pharmacology*, vol. 7, no. 1, pp. 39–47, 2007.

[6] T. Yamakura and K. Shimoji, "Subunit- and site-specific pharmacology of the NMDA receptor channel," *Progress in Neurobiology*, vol. 59, no. 3, pp. 279–298, 1999.

[7] S. G. Cull-Candy and D. N. Leszkiewicz, "Role of distinct NMDA receptor subtypes at central synapses," *Science's STKE*, vol. 2004, no. 255, p. re16, 2004.

[8] G. Bustos, J. Abarca, M. I. Forray, K. Gysling, C. W. Bradberry, and R. H. Roth, "Regulation of excitatory amino acid release by *N*-methyl-D-aspartate receptors in rat striatum: in vivo microdialysis studies," *Brain Research*, vol. 585, no. 1-2, pp. 105–115, 1992.

[9] K. Fink, H. Bönisch, and M. Göthert, "Presynaptic NMDA receptors stimulate noradrenaline release in the cerebral cortex," *European Journal of Pharmacology*, vol. 185, no. 1, pp. 115–117, 1990.

[10] M. O. Krebs, J. M. Desce, M. L. Kemel, et al., "Glutamatergic control of dopamine release in the rat striatum: evidence for presynaptic *N*-methyl-D-aspartate receptors on dopaminergic nerve terminals," *Journal of Neurochemistry*, vol. 56, no. 1, pp. 81–85, 1991.

[11] D. Martin, G. A. Bustos, M. A. Bowe, S. D. Bray, and J. V. Nadler, "Autoreceptor regulation of glutamate and aspartate release from slices of the hippocampal CA1 area," *Journal of Neurochemistry*, vol. 56, no. 5, pp. 1647–1655, 1991.

[12] C. Aoki, C. Venkatesan, C.-G. Go, J. A. Mong, and T. M. Dawson, "Cellular and subcellular localization of NMDA-R1 subunit immunoreactivity in the visual cortex of adult and neonatal rats," *The Journal of Neuroscience*, vol. 14, no. 9, pp. 5202–5222, 1994.

[13] S. DeBiasi, A. Minelli, M. Melone, and F. Conti, "Presynaptic NMDA receptors in the neocortex are both auto- and heteroreceptors," *NeuroReport*, vol. 7, no. 15–17, pp. 2773–2776, 1996.

[14] R. S. Petralia, N. Yokotani, and R. J. Wenthold, "Light and electron microscope distribution of the NMDA receptor subunit NMDAR1 in the rat nervous system using a selective anti-peptide antibody," *The Journal of Neuroscience*, vol. 14, no. 2, pp. 667–696, 1994.

[15] R. S. Petralia, Y. X. Wang, and R. J. Wenthold, "The NMDA receptor subunits NR2A and NR2B show histological and ultrastructural localization patterns similar to those of NR1," *The Journal of Neuroscience*, vol. 14, no. 10, pp. 6102–6120, 1994.

[16] N. Berretta and R. S. G. Jones, "Tonic facilitation of glutamate release by presynaptic *N*-methyl-D-aspartate autoreceptors in the entorhinal cortex," *Neuroscience*, vol. 75, no. 2, pp. 339–344, 1996.

[17] V. A. Bender, K. J. Bender, D. J. Brasier, and D. E. Feldman, "Two coincidence detectors for spike timing-dependent plasticity in somatosensory cortex," *The Journal of Neuroscience*, vol. 26, no. 16, pp. 4166–4177, 2006.

[18] A. I. M. Breukel, E. Besselsen, F. H. Lopes da Silva, and W. E. J. M. Ghijsen, "A presynaptic *N*-methyl-D-aspartate autoreceptor in rat hippocampus modulating amino acid release from a cytoplasmic pool," *European Journal of Neuroscience*, vol. 10, no. 1, pp. 106–114, 1998.

[19] M. Casado, S. Dieudonné, and P. Ascher, "Presynaptic *N*-methyl-D-aspartate receptors at the parallel fiber-Purkinje cell synapse," *Proceedings of the National Academy of Sciences of the United States of America*, vol. 97, no. 21, pp. 11593–11597, 2000.

[20] Y.-H. Chen, M.-L. Wu, and W.-M. Fu, "Regulation of presynaptic NMDA responses by external and intracellular pH changes at developing neuromuscular synapses," *The Journal of Neuroscience*, vol. 18, no. 8, pp. 2982–2990, 1998.

[21] A. J. Cochilla and S. Alford, "NMDA receptor-mediated control of presynaptic calcium and neurotransmitter release," *The Journal of Neuroscience*, vol. 19, no. 1, pp. 193–205, 1999.

[22] R. Corlew, Y. Wang, H. Ghermazien, A. Erisir, and B. D. Philpot, "Developmental switch in the contribution of presynaptic and postsynaptic NMDA receptors to long-term depression," *The Journal of Neuroscience*, vol. 27, no. 37, pp. 9835–9845, 2007.

[23] I. C. Duguid and T. G. Smart, "Retrograde activation of presynaptic NMDA receptors enhances GABA release at cerebellar interneuron-Purkinje cell synapses," *Nature Neuroscience*, vol. 7, no. 5, pp. 525–533, 2004.

[24] M. Glitsch and A. Marty, "Presynaptic effects of NMDA in cerebellar Purkinje cells and interneurons," *The Journal of Neuroscience*, vol. 19, no. 2, pp. 511–519, 1999.

[25] H. Huang and A. Bordey, "Glial glutamate transporters limit spillover activation of presynaptic NMDA receptors and influence synaptic inhibition of Purkinje neurons," *The Journal of Neuroscience*, vol. 24, no. 25, pp. 5659–5669, 2004.

[26] Y. Humeau, H. Shaban, S. Bissière, and A. Lüthi, "Presynaptic induction of heterosynaptic associative plasticity in the mammalian brain," *Nature*, vol. 426, no. 6968, pp. 841–845, 2003.

[27] P. Jourdain, L. H. Bergersen, K. Bhaukaurally, et al., "Glutamate exocytosis from astrocytes controls synaptic strength," *Nature Neuroscience*, vol. 10, no. 3, pp. 331–339, 2007.

[28] Y.-H. Li and T.-Z. Han, "Glycine binding sites of presynaptic NMDA receptors may tonically regulate glutamate release in the rat visual cortex," *Journal of Neurophysiology*, vol. 97, no. 1, pp. 817–823, 2007.

[29] C.-C. Lien, Y. Mu, M. Vargas-Caballero, and M. Poo, "Visual stimuli-induced LTD of GABAergic synapses mediated by presynaptic NMDA receptors," *Nature Neuroscience*, vol. 9, no. 3, pp. 372–380, 2006.

[30] M. Mameli, M. Carta, L. D. Partridge, and C. F. Valenzuela, "Neurosteroid-induced plasticity of immature synapses via retrograde modulation of presynaptic NMDA receptors," *The Journal of Neuroscience*, vol. 25, no. 9, pp. 2285–2294, 2005.

[31] A. Robert, J. A. Black, and S. G. Waxman, "Endogenous NMDA-receptor activation regulates glutamate release in cultured spinal neurons," *The Journal of Neurophysiology*, vol. 80, no. 1, pp. 196–208, 1998.

[32] R. D. Samson and D. Paré, "Activity-dependent synaptic plasticity in the central nucleus of the amygdala," *The Journal of Neuroscience*, vol. 25, no. 7, pp. 1847–1855, 2005.

[33] P. J. Sjöström, G. G. Turrigiano, and S. B. Nelson, "Neocortical LTD via coincident activation of presynaptic NMDA and cannabinoid receptors," *Neuron*, vol. 39, no. 4, pp. 641–654, 2003.

[34] M. Casado, P. Isope, and P. Ascher, "Involvement of presynaptic *N*-methyl-D-aspartate receptors in cerebellar long-term depression," *Neuron*, vol. 33, no. 1, pp. 123–130, 2002.

[35] G. Woodhall, D. I. Evans, M. O. Cunningham, and R. S. G. Jones, "NR2B-containing NMDA autoreceptors at synapses on entorhinal cortical neurons," *The Journal of Neurophysiology*, vol. 86, no. 4, pp. 1644–1651, 2001.

[36] J. Yang, G. L. Woodhall, and R. S. G. Jones, "Tonic facilitation of glutamate release by presynaptic NR2B-containing NMDA receptors is increased in the entorhinal cortex of chronically epileptic rats," *The Journal of Neuroscience*, vol. 26, no. 2, pp. 406–410, 2006.

[37] K. Williams, "Ifenprodil discriminates subtypes of the *N*-methyl-D-aspartate receptor: selectivity and mechanisms at recombinant heteromeric receptors," *Molecular Pharmacology*, vol. 44, no. 4, pp. 851–859, 1993.

[38] G. Fischer, V. Mutel, G. Trube, et al., "Ro 25-6981, a highly potent and selective blocker of N-methyl-D-aspartate receptors containing the NR2B subunit. Characterization in vitro," *The Journal of Pharmacology and Experimental Therapeutics*, vol. 283, no. 3, pp. 1285–1292, 1997.

[39] Y. P. Auberson, H. Allgeier, S. Bischoff, K. Lingenhoehl, R. Moretti, and M. Schmutz, "5-Phosphonomethylquinoxalinediones as competitive NMDA receptor antagonists with a preference for the human 1A/2A, rather than 1A/2B receptor composition," *Bioorganic & Medicinal Chemistry Letters*, vol. 12, no. 7, pp. 1099–1102, 2002.

[40] D. J. Brasier and D. E. Feldman, "Synapse-specific expression of functional presynaptic NMDA receptors in rat somatosensory cortex," *The Journal of Neuroscience*, vol. 28, no. 9, pp. 2199–2211, 2008.

[41] J. Neyton and P. Paoletti, "Relating NMDA receptor function to receptor subunit composition: limitations of the pharmacological approach," *The Journal of Neuroscience*, vol. 26, no. 5, pp. 1331–1333, 2006.

[42] J. Yang, C. Wetterstrand, and R. S. G. Jones, "Felbamate but not phenytoin or gabapentin reduces glutamate release by blocking presynaptic NMDA receptors in the entorhinal cortex," *Epilepsy Research*, vol. 77, no. 2-3, pp. 157–164, 2007.

[43] Y.-H. Li, T.-Z. Han, and K. Meng, "Tonic facilitation of glutamate release by glycine binding sites on presynaptic NR2B-containing NMDA autoreceptors in the rat visual cortex," *Neuroscience Letters*, vol. 432, no. 3, pp. 212–216, 2008.

[44] L. Liu, T. P. Wong, M. F. Pozza, et al., "Role of NMDA receptor subtypes in governing the direction of hippocampal synaptic plasticity," *Science*, vol. 304, no. 5673, pp. 1021–1024, 2004.

[45] S. Berberich, P. Punnakkal, V. Jensen, et al., "Lack of NMDA receptor subtype selectivity for hippocampal long-term potentiation," *The Journal of Neuroscience*, vol. 25, no. 29, pp. 6907–6910, 2005.

[46] C. Weitlauf, Y. Honse, Y. P. Auberson, M. Mishina, D. M. Lovinger, and D. G. Winder, "Activation of NR2A-containing NMDA receptors is not obligatory for NMDA receptor-dependent long-term potentiation," *The Journal of Neuroscience*, vol. 25, no. 37, pp. 8386–8390, 2005.

[47] P. Paoletti, P. Ascher, and J. Neyton, "High-affinity zinc inhibition of NMDA NR1-NR2A receptors," *The Journal of Neuroscience*, vol. 17, no. 15, pp. 5711–5725, 1997.

[48] J. Rachline, F. Perin-Dureau, A. Le Goff, J. Neyton, and P. Paoletti, "The micromolar zinc-binding domain on the NMDA receptor subunit NR2B," *The Journal of Neuroscience*, vol. 25, no. 2, pp. 308–317, 2005.

[49] S. F. Traynelis, M. F. Burgess, F. Zheng, P. Lyuboslavsky, and J. L. Powers, "Control of voltage-independent Zinc inhibition of NMDA receptors by the NR1 subunit," *The Journal of Neuroscience*, vol. 18, no. 16, pp. 6163–6175, 1998.

[50] A. Sobczyk and K. Svoboda, "Activity-dependent plasticity of the NMDA-receptor fractional Ca^{2+} current," *Neuron*, vol. 53, no. 1, pp. 17–24, 2007.

[51] M. M. Adams, S. E. Fink, W. G. M. Janssen, R. A. Shah, and J. H. Morrison, "Estrogen modulates synaptic *N*-methyl-D-aspartate receptor subunit distribution in the aged hippocampus," *The Journal of Comparative Neurology*, vol. 474, no. 3, pp. 419–426, 2004.

[52] F. Conti, P. Barbaresi, M. Melone, and A. Ducati, "Neuronal and glial localization of NR1 and NR2A/B subunits of the NMDA receptor in the human cerebral cortex," *Cerebral Cortex*, vol. 9, no. 2, pp. 110–120, 1999.

[53] V. N. Kharazia and R. J. Weinberg, "Immunogold localization of AMPA and NMDA receptors in somatic sensory cortex of albino rat," *The Journal of Comparative Neurology*, vol. 412, no. 2, pp. 292–302, 1999.

[54] J. P. Charton, M. Herkert, C.-M. Becker, and H. Schröder, "Cellular and subcellular localization of the 2B-subunit of the NMDA receptor in the adult rat telencephalon," *Brain Research*, vol. 816, no. 2, pp. 609–617, 1999.

[55] S. Fujisawa and C. Aoki, "In vivo blockade of *N*-methyl-D-aspartate receptors induces rapid trafficking of NR2B subunits away from synapses and out of spines and terminals in adult cortex," *Neuroscience*, vol. 121, no. 1, pp. 51–63, 2003.

[56] V. C. Kotak, S. Fujisawa, F. A. Lee, O. Karthikeyan, C. Aoki, and D. H. Sanes, "Hearing loss raises excitability in the auditory cortex," *The Journal of Neuroscience*, vol. 25, no. 15, pp. 3908–3918, 2005.

[57] R. O'Donnell, S. Molon-Noblot, P. Laroque, M. Rigby, and D. Smith, "The ultrastructural localisation of the *N*-methyl-D-aspartate NR2B receptor subunit in rat lumbar spinal cord," *Neuroscience Letters*, vol. 371, no. 1, pp. 24–29, 2004.

[58] J. J. Radley, C. R. Farb, Y. He, et al., "Distribution of NMDA and AMPA receptor subunits at thalamo-amygdaloid dendritic spines," *Brain Research*, vol. 1134, no. 1, pp. 87–94, 2007.

[59] J. G. Valtschanoff, A. Burette, R. J. Wenthold, and R. J. Weinberg, "Expression of NR2 receptor subunit in rat somatic sensory cortex: synaptic distribution and colocalization with NR1 and PSD-95," *The Journal of Comparative Neurology*, vol. 410, no. 4, pp. 599–611, 1999.

[60] C. Aoki, S. Fujisawa, V. Mahadomrongkul, P. J. Shah, K. Nader, and A. Erisir, "NMDA receptor blockade in intact adult cortex increases trafficking of NR2A subunits into spines, postsynaptic densities, and axon terminals," *Brain Research*, vol. 963, no. 1-2, pp. 139–149, 2003.

[61] W. G. M. Janssen, P. Vissavajjhala, G. Andrews, T. Moran, P. R. Hof, and J. H. Morrison, "Cellular and synaptic distribution of NR2A and NR2B in macaque monkey and rat hippocampus as visualized with subunit-specific monoclonal antibodies," *Experimental Neurology*, vol. 191, supplement 1, pp. S28–S44, 2005.

[62] R. S. Petralia, N. Sans, Y.-X. Wang, and R. J. Wenthold, "Ontogeny of postsynaptic density proteins at glutamatergic synapses," *Molecular and Cellular Neuroscience*, vol. 29, no. 3, pp. 436–452, 2005.

[63] E. Luccini, V. Musante, E. Neri, M. Raiteri, and A. Pittaluga, "N-methyl-D-aspartate autoreceptors respond to low and high agonist concentrations by facilitating, respectively, exocytosis and carrier-mediated release of glutamate in rat hippocampus," *Journal of Neuroscience Research*, vol. 85, no. 16, pp. 3657–3665, 2007.

[64] D. J. Laurie and P. H. Seeburg, "Ligand affinities at recombinant *N*-methyl-D-aspartate receptors depend on subunit composition," *European Journal of Pharmacology*, vol. 268, no. 3, pp. 335–345, 1994.

[65] H. Mori and M. Mishina, "Structure and function of the NMDA receptor channel," *Neuropharmacology*, vol. 34, no. 10, pp. 1219–1237, 1995.

[66] S. G. Cull-Candy and S. G. Brickley, "NMDA receptors," to appear in *Encyclopedia of Life Sciences*, http://www.els.net.

[67] A. Sobczyk, V. Scheuss, and K. Svoboda, "NMDA receptor subunit-dependent $[Ca^{2+}]$ signaling in individual hippocampal dendritic spines," *The Journal of Neuroscience*, vol. 25, no. 26, pp. 6037–6046, 2005.

[68] J. J. Chrobak, A. Lörincz, and G. Buzsáki, "Physiological patterns in the hippocampo-entorhinal cortex system," *Hippocampus*, vol. 10, no. 4, pp. 457–465, 2000.

[69] J. J. Chrobak and G. Buzsáki, "Selective activation of deep layer (V-VI) retrohippocampal cortical neurons during hippocampal sharp waves in the behaving rat," *The Journal of Neuroscience*, vol. 14, no. 10, pp. 6160–6170, 1994.

[70] M. O. Cunningham, C. H. Davies, E. H. Buhl, N. Kopell, and M. A. Whittington, "Gamma oscillations induced by kainate receptor activation in the entorhinal cortex in vitro," *The Journal of Neuroscience*, vol. 23, no. 30, pp. 9761–9769, 2003.

[71] M. O. Cunningham, D. D. Pervouchine, C. Racca, et al., "Neuronal metabolism governs cortical network response state," *Proceedings of the National Academy of Sciences of the United States of America*, vol. 103, no. 14, pp. 5597–5601, 2006.

[72] G. Buzsáki, "Theta rhythm of navigation: link between path integration and landmark navigation, episodic and semantic memory," *Hippocampus*, vol. 15, no. 7, pp. 827–840, 2005.

[73] J. Fell, P. Klaver, H. Elfadil, C. Schaller, C. E. Elger, and G. Fernández, "Rhinal-hippocampal theta coherence during declarative memory formation: interaction with gamma synchronization?" *European Journal of Neuroscience*, vol. 17, no. 5, pp. 1082–1088, 2003.

[74] R. P. Vertes, "Hippocampal theta rhythm: a tag for short-term memory," *Hippocampus*, vol. 15, no. 7, pp. 923–935, 2005.

[75] K. Alper, M. Raghavan, R. Isenhart, et al., "Localizing epileptogenic regions in partial epilepsy using three-dimensional statistical parametric maps of background EEG source spectra," *NeuroImage*, vol. 39, no. 3, pp. 1257–1265, 2008.

[76] N. Dericioglu and S. Saygi, "Ictal scalp EEG findings in patients with mesial temporal lobe epilepsy," *Clinical EEG and Neuroscience*, vol. 39, no. 1, pp. 20–27, 2008.

[77] E. A. Tolner, F. Kloosterman, E. A. van Vliet, M. P. Witter, F. H. Lopes da Silva, and J. A. Gorter, "Presubiculum stimulation in vivo evokes distinct oscillations in superficial and deep entorhinal cortex layers in chronic epileptic rats," *The Journal of Neuroscience*, vol. 25, no. 38, pp. 8755–8765, 2005.

[78] M. Steffens, H.-J. Huppertz, J. Zentner, E. Chauzit, and T. J. Feuerstein, "Unchanged glutamine synthetase activity and increased NMDA receptor density in epileptic human neocortex: implications for the pathophysiology of epilepsy," *Neurochemistry International*, vol. 47, no. 6, pp. 379–384, 2005.

[79] B. Clemens, "Valproate decreases EEG synchronization in a use-dependent manner in idiopathic generalized epilepsy," *Seizure*, vol. 17, no. 3, pp. 224–233, 2008.

[80] C. Béla, B. Mónika, T. Márton, and K. István, "Valproate selectively reduces EEG activity in anterior parts of the cortex in patients with idiopathic generalized epilepsy. A low resolution electromagnetic tomography (LORETA) study," *Epilepsy Research*, vol. 75, no. 2-3, pp. 186–191, 2007.

[81] B. Clemens, P. Piros, M. Bessenyei, and K. Hollódy, "Lamotrigine decreases EEG synchronization in a use-dependent manner in patients with idiopathic generalized epilepsy," *Clinical Neurophysiology*, vol. 118, no. 4, pp. 910–917, 2007.

[82] J. Yang, S. E. L. Chamberlain, G. L. Woodhall, and R. S. G. Jones, "Mobility of NMDA autoreceptors but not postsynaptic receptors in the rat entorhinal cortex," *The Journal of Physiology*, vol. 586, no. 20, pp. 4905–4924, 2008.

[83] C. J. Hatton and P. Paoletti, "Modulation of triheteromeric NMDA receptors by N-terminal domain ligands," *Neuron*, vol. 46, no. 2, pp. 261–274, 2005.

[84] R. A. Al-Hallaq, T. P. Conrads, T. D. Veenstra, and R. J. Wenthold, "NMDA di-heteromeric receptor populations and associated proteins in rat hippocampus," *The Journal of Neuroscience*, vol. 27, no. 31, pp. 8334–8343, 2007.

[85] J. Luo, Y. Wang, R. P. Yasuda, A. W. Dunah, and B. B. Wolfe, "The majority of *N*-methyl-D-aspartate receptor complexes in adult rat cerebral cortex contain at least three different subunits (NR1/NR2A/NR2B)," *Molecular Pharmacology*, vol. 51, no. 1, pp. 79–86, 1997.

[86] K. R. Tovar and G. L. Westbrook, "The incorporation of NMDA receptors with a distinct subunit composition at nascent hippocampal synapses in vitro," *The Journal of Neuroscience*, vol. 19, no. 10, pp. 4180–4188, 1999.

[87] I. Ito, K. Futai, H. Katagiri, et al., "Synapse-selective impairment of NMDA receptor functions in mice lacking NMDA receptor epsilon 1 or epsilon 2 subunit," *The Journal of Physiology*, vol. 500, no. 2, pp. 401–408, 1997.

[88] S. S. Kumar and J. R. Huguenard, "Pathway-specific differences in subunit composition of synaptic NMDA receptors on pyramidal neurons in neocortex," *The Journal of Neuroscience*, vol. 23, no. 31, pp. 10074–10083, 2003.

[89] A. Alonso, M. de Curtis, and R. Llinás, "Postsynaptic Hebbian and non-Hebbian long-term potentiation of synaptic efficacy in the entorhinal cortex in slices and in the isolated adult guinea pig brain," *Proceedings of the National Academy of Sciences of the United States of America*, vol. 87, no. 23, pp. 9280–9284, 1990.

[90] R. Bouras and C. A. Chapman, "Long-term synaptic depression in the adult entorhinal cortex in vivo," *Hippocampus*, vol. 13, no. 7, pp. 780–790, 2003.

[91] C. A. Chapman and R. J. Racine, "Piriform cortex efferents to the entorhinal cortex in vivo: kindling-induced potentiation and the enhancement of long-term potentiation by low-frequency piriform cortex or medial septal stimulation," *Hippocampus*, vol. 7, no. 3, pp. 257–270, 1997.

[92] M. Y. Cheong, S. H. Yun, I. Mook-Jung, Y. Kang, and M. W. Jung, "Induction of homosynaptic long-term depression in entorhinal cortex," *Brain Research*, vol. 954, no. 2, pp. 308–310, 2002.

[93] Y.-H. Chen, M.-L. Wu, and W.-M. Fu, "Regulation of presynaptic NMDA responses by external and intracellular pH changes at developing neuromuscular synapses," *The Journal of Neuroscience*, vol. 18, no. 8, pp. 2982–2990, 1998.

[94] S. Craig and S. Commins, "Plastic and metaplastic changes in the CA1 and subicular projections to the entorhinal cortex," *Brain Research*, vol. 1147, no. 1, pp. 124–139, 2007.

[95] J. Solger, C. Wozny, D. Manahan-Vaughan, and J. Behr, "Distinct mechanisms of bidirectional activity-dependent synaptic plasticity in superficial and deep layers of rat entorhinal cortex," *European Journal of Neuroscience*, vol. 19, no. 7, pp. 2003–2007, 2004.

Hindawi Publishing Corporation
Neural Plasticity
Volume 2008, Article ID 203514, 14 pages
doi:10.1155/2008/203514

Research Article

Dopaminergic Suppression of Synaptic Transmission in the Lateral Entorhinal Cortex

Douglas A. Caruana and C. Andrew Chapman

Center for Studies in Behavioral Neurobiology, Department of Psychology, Concordia University, Montréal, Québec, Canada H4B 1R6

Correspondence should be addressed to C. Andrew Chapman, andrew.chapman@concordia.ca

Received 29 March 2008; Accepted 21 June 2008

Recommended by Roland S. G. Jones

Dopaminergic projections to the superficial layers of the lateral entorhinal cortex can modulate the strength of olfactory inputs to the region. We have found that low concentrations of dopamine facilitate field EPSPs in the entorhinal cortex, and that higher concentrations of dopamine suppress synaptic responses. Here, we have used whole-cell current clamp recordings from layer II neurons to determine the mechanisms of the suppression. Dopamine (10 to 50 μM) hyperpolarized membrane potential and reversibly suppressed the amplitude of EPSPs evoked by layer I stimulation. Both AMPA- and NMDA-mediated components were suppressed, and paired-pulse facilitation was also enhanced indicating that the suppression is mediated largely by reduced glutamate release. Blockade of D_2-like receptors greatly reduced the suppression of EPSPs. Dopamine also lowered input resistance, and reduced the number of action potentials evoked by depolarizing current steps. The drop in input resistance was mediated by activation of D_1-like receptors, and was prevented by blocking K^+ channels with TEA. The dopaminergic suppression of synaptic transmission is therefore mediated by a D_2 receptor-dependent reduction in transmitter release, and a D_1 receptor-dependent increase in a K^+ conductance. This suppression of EPSPs may dampen the strength of sensory inputs during periods of elevated mesocortical dopamine activity.

Copyright © 2008 D. A. Caruana and C. A. Chapman. This is an open access article distributed under the Creative Commons Attribution License, which permits unrestricted use, distribution, and reproduction in any medium, provided the original work is properly cited.

1. INTRODUCTION

The entorhinal cortex is animportant interface that links primary sensory and association cortices to the hippocampal formation, and it is critical for the sensory and mnemonic functions of the medial temporal lobe [1–4]. In the rat, the lateral division of the entorhinal cortex receives most of its cortical inputs from the olfactory cortex and perirhinal cortex, and the medial entorhinal cortex receives visual and multimodal inputs mainly via the postrhinal cortex [5–7]. This pattern of cortical input to the medial and lateral divisions of the entorhinal cortex contributes to their different roles in sensory and cognitive processing [8–10]. In addition, neuromodulatory transmitters innervate both the medial and lateral entorhinal cortices and can have powerful effects on sensory and mnemonic function in these regions. Specifically, acetylcholine and serotonin both modulate synaptic transmission and rhythmic EEG activities in the medial entorhinal cortex [11–15]. Further, midbrain dopamine neurons send one of their largest cortical projections to the superficial layers of the lateral entorhinal cortex where they target principal cell islands [16–18]. Relatively little is known, however, regarding the neuromodulatory effects of dopamine in the lateral entorhinal cortex.

The large dopaminergic projection to the prefrontal cortex is known to regulate cellular processes related to working memory [19–21], and dopaminergic inputs to the lateral entorhinal cortex are also likely to affect mechanisms of sensory and mnemonic function. In the prefrontal cortex, activation of D_1 receptors can suppress glutamate release in layer V [22–24] but can enhance glutamatergic transmission in layer III [25, 26]. Further, the positive effect of D_1 receptor activation on working memory follows an inverted U-shaped function [27], and strong or weak stimulation of D_1 receptors can also have opposite effects on NMDA receptor-mediated synaptic currents [20, 28]. We have also found that

dopamine has dose-dependent bidirectional effects in layer II of the lateral entorhinal cortex. In awake animals, increasing levels of dopamine with a selective reuptake inhibitor facilitates synaptic responses evoked by stimulation of the piriform cortex, and field excitatory postsynaptic potentials (fEPSPs) are also facilitated by a low concentration of dopamine in vitro [29]. Higher concentrations of dopamine, however, suppress fEPSPs, and similar suppression effects have been observed by others in medial entorhinal cortex layer II [30] and layer III [31]. Dopamine can also reduce the input resistance of layer IIneurons in the medial entorhinal cortex [30] and reduce temporal summation in layer V neurons of the lateral division through an increase in the I_h current [32]. Dopamine may therefore modulate synaptic function in the lateral entorhinal cortex through multiple mechanisms.

We have used whole-cell current clamp recordings to investigate the mechanisms of the suppression of EPSPs by dopamine in electrophysiologically identified "fan" cells in layer II of the lateral entorhinal cortex. Receptor blockers were used to determine the dopamine receptors that mediate the suppression of EPSPs, and paired-pulse tests were used to assess whether the suppression is expressed pre- or postsynaptically. Changes in the intrinsic excitability of fan cells were also monitored using responses to hyperpolarizing and depolarizing current steps. In addition to a D_2-like receptor-mediated suppression of transmitter release, we show evidence that EPSPs are also reduced by an increased K^+ conductance dependent on activation of D_1 receptors.

2. MATERIALS AND METHODS

2.1. Tissue slices

Methods for obtaining whole cell current clamp recordings were similar to those described previously [13, 29, 33, 34]. Male Long-Evans rats between 4 and 6 weeks old were anesthetized with halothane, decapitated, and their brains rapidly removed and transferred into cold (4°C) artificial cerebrospinal fluid (ACSF) saturated with 95% O_2 and 5% CO_2 containing (in mM) 124 NaCl, 5 KCl, 1.25 NaH_2PO_4, 2 $MgSO_4$, 2 $CaCl_2$, 26 $NaHCO_3$, and10 dextrose (pH ≈7.3; 300–310 mOsm). All chemicals were obtained from Sigma-Aldrich, Mo, USA. Horizontal slices (300 μm thick) were cut using a vibratome (WPI, Vibroslice, Fla, USA), and slices recovered for at least one hour at 22 to 24°C. Slices were transferred individually to a recording chamber and visualized using an upright microscope (Leica, Richmond Hill, Canada, DM-LFS) equipped with differential interference contrast optics, a 40x water immersion objective, and a near-infrared camera (COHU, Inc., Calif, USA). Submerged slices were superfused with oxygenated ACSF at a rate of 1.5 to 2.0 mL/min. Slices containing the lateral entorhinal cortex were taken from ventral sections about 1.9 to 3.4 mm above the interaural line [35]. Layer IIwas identified based on the presence of cell "islands" about 150 μm from the cortical surface [36–39].

2.2. Stimulation and recording

Patch recording pipettes for whole cell recordings were prepared from borosilicate glass (1.0 mm OD, 4 to 8 MΩ) using a horizontal puller (P-97, Sutter Instr., Calif, USA) and were filled with a solution containing (in mM) 140 K-gluconate, 5 NaCl, 2 $MgCl_2$, 10 HEPES, 0.5 EGTA, 2 ATP-Tris, and 0.4 GTP-Tris (pH adjusted to 7.24–7.32 with KOH; 270–280 mOsm). Pipettes were placed in contact with somata of layer II neurons, and gentle suction was applied under voltage clamp to form a tight seal (1–3 GΩ). Whole cell configuration was achieved by increased suction, and experiments began after cells stabilized (typically within 3 to 5 minutes after break-in). Current clamp recordings were obtained using an Axopatch 200B amplifier (Axon Instr., Calif, USA) and displayed on a digital oscilloscope (Gould 1604). Recordings were filtered at 10 kHz and digitized at 20 kHz (Axon Instr., Digidata 1322A) for storage on computer hard disk. Recordings were accepted if the series resistance was ≤25 MΩ (mean = 16.9 ± 0.9 MΩ) and if input resistance and resting potential were stable. A bipolar stimulating electrode made from two tungsten electrodes (FHC, 1.0 MΩ) was positioned to span layer I near the border with layer II approximately 0.2 to 0.6 mm rostral to the recording electrode. Synaptic responses were evoked with 0.1 millisecond constant current pulses delivered using a stimulus timer and isolation unit (WPI, Mass, USA, models A300 and A360). Stimulation intensity was adjusted to evoke responses approximately 75% of maximal (75 to 300 μA).

All neurons (n = 118) included for analyses were identified as "fan" cells based on electrophysiological characteristics described previously [40, 41]. In comparison tostellate cells of the medial entorhinal cortex, fan cells show modest inward rectification during hyperpolarizing current steps, a small depolarizing afterpotential following single spikes, and do not show prominent theta-frequency membrane potential oscillations at subthreshold voltages [40–42].

2.3. Dopaminergic modulation of synaptic responses

The effects of dopamine on glutamate-mediated synaptic transmission in the lateral entorhinal cortex are largely uncharacterized. We therefore recorded both mixed and isolated components of excitatory postsynaptic potentials (EPSPs) evoked by stimulation of layer I before and after 5-minute bath-application of 1, 10, or 50 μM dopamine. Results obtained using high concentrations of dopamine must be interpreted cautiously because of the possibility of nonspecific effects. However, dopamine degrades through oxidization within the slice preparation, and similar concentrations of dopamine have been used previously, and interpreted in light of the effects of specific antagonists, in reports examining the effects of dopamine on synaptic transmission in both the entorhinal [29–32] and prefrontal [23, 43] cortices. Responses were evoked once every 20 seconds, and the mean of 10 responses was obtained for analysis. Baseline responses were obtained at resting potential and, because dopamine usually hyperpolarizes fan cells, constant current was often required to return cells

to the original membrane potential for recordings in the presence of dopamine. Sodium metabisulfite (50 μM) was coapplied to slow the oxidation of dopamine [29, 31, 43], and ambient lighting was also reduced. Possible effects of sodium metabisulfite were assessed with a vehicle control group. Drugs were routinely stored at -20°C as concentrated stock solutions until needed, but dopamine HCl was dissolved just prior to bath application.

Paired-pulse tests were used to determine whether dopamine modulates EPSPs through a pre- or postsynaptic mechanism [13]. Pairs of stimulation pulses separated by an interval of 30 milliseconds were delivered before and after 5-minute bath-application of 1, 10, or 50 μM dopamine. Stimulation intensity was reduced to evoke EPSPs approximately 50% of maximal, and ten responses were averaged for analyses. Paired-pulse facilitation was quantified by expressing the amplitude of the second response as a percentage of the first response.

Mechanisms mediating the suppression of EPSPs by high concentrations of dopamine were investigated by assessing the effects of 50 μM dopamine on isolated components of synaptic responses. After baseline recordings in normal ACSF, AMPA receptor-mediated responses were isolated with bath application of 50 μM 2-amino-5-phosphonovaleric acid (APV) and 25 μM bicuculline methiodide, or NMDA receptor-mediated responses were isolated with 20 μM 7-nitro-2,3-dioxo-1,4-dihydroquinoxaline-6-carbonitrile (CNQX) and 25 μM bicuculline. GABA-mediated IPSPs were isolated with either 1 mM kynurenic acid or 20 μM CNQX with 50 μM APV. Isolated synaptic responses were recorded before and after 5-minute application of 50 μM dopamine. Isolated AMPA receptor-mediated responses were also used to determine if dopamine suppresses EPSPs primarily throughD_1- or D_2-like receptors. Baseline responses were recorded in the presence of either the D_1 receptor antagonist SCH23390 (50 μM) or the D_2 receptor antagonist sulpiride (50 μM) [29–31], and 50 μM dopamine was then applied for 5 minutes. Sulpiride was prepared daily in a stock solution of 6% DMSO in ACSF titrated with 0.1 N HCl, and there was a final concentration of 0.1% DMSO with sulpiride.

The effects of dopamine on the intrinsic excitability of fan cells were assessed by monitoring responses to hyperpolarizing and depolarizing current steps. Changes in action potentials, afterhyperpolarizations, input resistance and inward rectification were examined before and after 5-minute bath application of 1, 10, or 50 μM dopamine. The number of action potentials elicited in response to suprathreshold current injection can be used to characterize neuronal excitability [32], and we therefore determined the number of spikes fired in response to a single 500 millisecond-duration depolarizing current pulse from a constant holding potential (typically rest) using a pulse amplitude that elicited 3 to 5 action potentials [32]. Receptors that mediate the dopamine-induced change in input resistance were investigated using SCH23390 or sulpiride, and the ionic conductances involved were assessed using 0.5 μM tetrodotoxin (TTX) or 30 mM tetraethylammonium (TEA). Blockers were preapplied for 5–10 minutes prior to coapplication of dopamine for 5 minutes.

2.4. Data analysis

Electrophysiological characteristics of fan cells and changes in synaptic responses were analyzed using the software program Clampfit 8.2 (Axon Instr., Calif, USA). The amplitudes of averaged EPSPs were measured relative to the prestimulus baseline, and paired-pulse facilitation was determined by expressing the amplitude of the second response as a proportion of the amplitude of the first response. Action potential amplitude was measured from resting potential, and action potential width and fast and medium afterhyperpolarizations were measured from threshold. Input resistance was calculated by measuring peak and steady-state voltage responses to -200 pA current steps (500 milliseconds), and inward rectification was quantified by expressing the peak input resistance as a proportion of the steady-state resistance (rectification ratio). All data were expressed as the mean $\pm$SEM for plotting, and changes in response properties were assessed using paired samples t-tests or mixed design ANOVAs.

3. RESULTS

3.1. Electroresponsiveness of layer II fan cells

A total of 118 fan cells in layer II of the lateral entorhinal cortex were identified electrophysiologically and included for analysis, and the characteristics of these cells were similar to those reported previously [40, 41]. Fan cells had a mean resting membrane potential of -58.8 ± 0.6 mV, and a peak input resistance of 99.1 ± 2.1 MΩ. Most cells (108 of 118) demonstrated a small delayed inward rectification in response to hyperpolarizing current steps (rectification ratio: 1.10 ± 0.01). Action potentials (amplitude: 128.8 ± 0.7 mV, width: 4.1 ± 0.1 milliseconds, threshold: -44.1 ± 0.8 mV) were typically followed by fast and medium afterhyperpolarizations (-3.3 ± 0.3 mV and -5.8 ± 0.3 mV) with a small depolarizing afterpotential. Averaged EPSPs evoked by stimulation of layer I had a mean amplitude of 4.4 ± 0.2 mV. Continuous recordings of membrane potential were obtained in a subset of 28 cells to assess subthreshold membrane potential oscillations and, similar to findings of Tahvildari and Alonso [40], fan cells did not display prominent oscillations (data not shown).

3.2. Dopaminergic modulation of EPSPs

We previously found concentration-dependent effects of dopamine on field EPSPs in layer II in vitro, in which 10 μM dopamine facilitated fEPSPs and 50 to 100 μM dopamine suppressed fEPSPs [29]. We obtained similar concentration-dependent effects in whole cell EPSPs recorded here before and after 5-minute bath application of dopamine. Application of 50 μM dopamine resulted in a strong suppression of synaptic response to 38.5 ± 5.8% of baseline levels (see Figure 1(a); $t_8 = 7.75$, $P < .001$; $n = 9$) that could be reversed by 15 minutes washout in normal ACSF (3 cells). We initially expected 10 μM dopamine to facilitate EPSPs [29], but foundthat10 μM dopamine instead caused a small synaptic suppression (to 87.0 ± 5.8% of baseline; see Figure 1(b); t_{15}

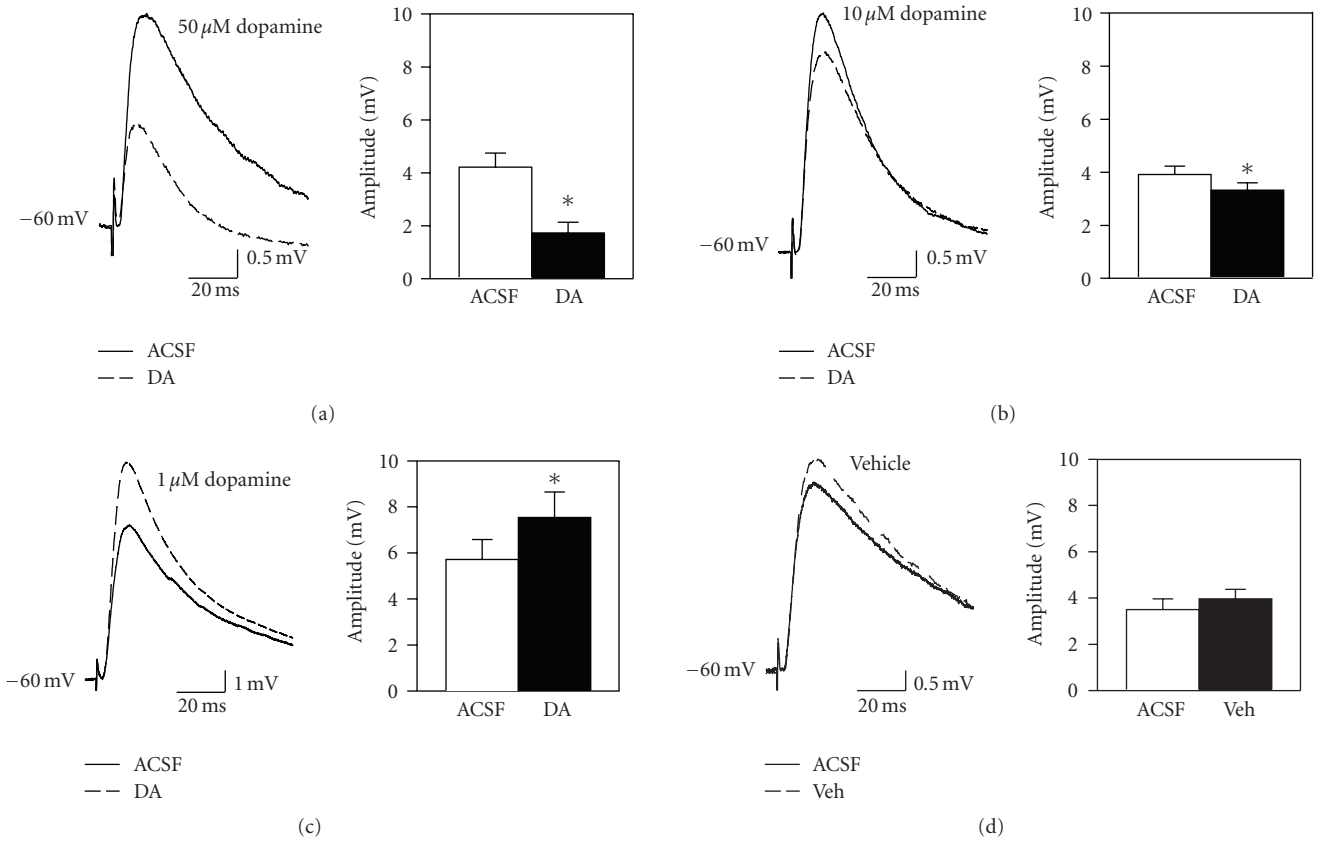

Figure 1: Dopamine has dose-dependent and bidirectional effects on the amplitude of mixed EPSPs in layer II fan cells. (a) Fifty μM dopamine significantly reduces the amplitude of synaptic responses. Traces show averaged EPSPs before (ACSF) and after 5-minute bath application of dopamine (DA) in a representative cell. Group data indicate the mean amplitude of EPSPs before and after dopamine (*, $P < .001$). Bars indicate ± 1 SEM in this and subsequent figures, and * indicates $P < .05$ unless otherwise indicated. (b) A lower concentration of 10 μM dopamine causes a smaller suppression of synaptic responses. (c) The low 1 μM concentration of dopamine enhances the amplitude of synaptic responses (*, $P < .01$). (d) Bath application of vehicle (50 μM sodium metabisulfite; Veh) does not significantly affect synaptic transmission.

= 2.31, $P < .05$; $n = 18$). However, a lower concentration of 1 μM dopamine significantly enhanced responses to 132.7 $\pm$ 4.4% of baseline levels (see Figure 1(c); $t_6 = 5.04$, $P < .01$; $n = 7$). In our previous study using a gas-fluid interface chamber, a larger bath volume and slower flow-rate may have increased dopamine oxidation and reduced the effective concentration of dopamine at the slice, and this may account for why a higher applied concentration facilitated responses in that study [29]. Bath application of the antioxidant sodium metabisulfite alone had no significant effect on the amplitude of whole cell EPSPs (see Figure 1(d); $n = 8$).

Paired-pulse tests were used to determine if synaptic suppression and facilitation effects were likely expressed pre- or postsynaptically. Pairs of pulses were delivered before and after 5-minute dopamine application, and a 30-millisecond interpulse interval was used that results in optimal paired-pulse facilitation [13, 44–46]. If EPSPs are reduced through a reduction in transmitter release, then a greater amount of transmitter should be available for release in response to the second stimulation pulse and paired-pulse facilitation should be enhanced [47–49]. Changes in EPSPs mediated by alterations in postsynaptic receptors, however, should not be associated with changes in paired-pulse ratio. High concentrations of dopamine that reduced EPSP amplitude were also found to enhance paired-pulse facilitation (see Figures 2(a), 2(b); $t_{13} = 2.78$, $P < .05$ for 10 μM; $t_8 = 2.97$, $P < .05$ for 50 μM), suggesting that dopamine reduced EPSPs by suppressing glutamate release. In contrast, the low concentration of 1 μM dopamine that facilitated EPSPs had no significant effect on paired pulse facilitation (see Figure 2(c)), suggesting that the facilitation of EPSPs was mediated primarily by an increased postsynaptic response to glutamate. The dopaminergic facilitation of the conditioning response was smaller during paired-pulse tests in which stimulus intensity was reduced to avoid spiking (see Figures 1(c) versus 2(c)) but a similar dopaminergic facilitation of fEPSPs with no effect on paired-pulse ratio has been observed in the entorhinal cortex in vivo [29].

3.3. Isolated synaptic responses

The suppression of EPSPs by high concentrations of dopamine was examined more closely using pharmacologically isolated synaptic responses. Consistent with a

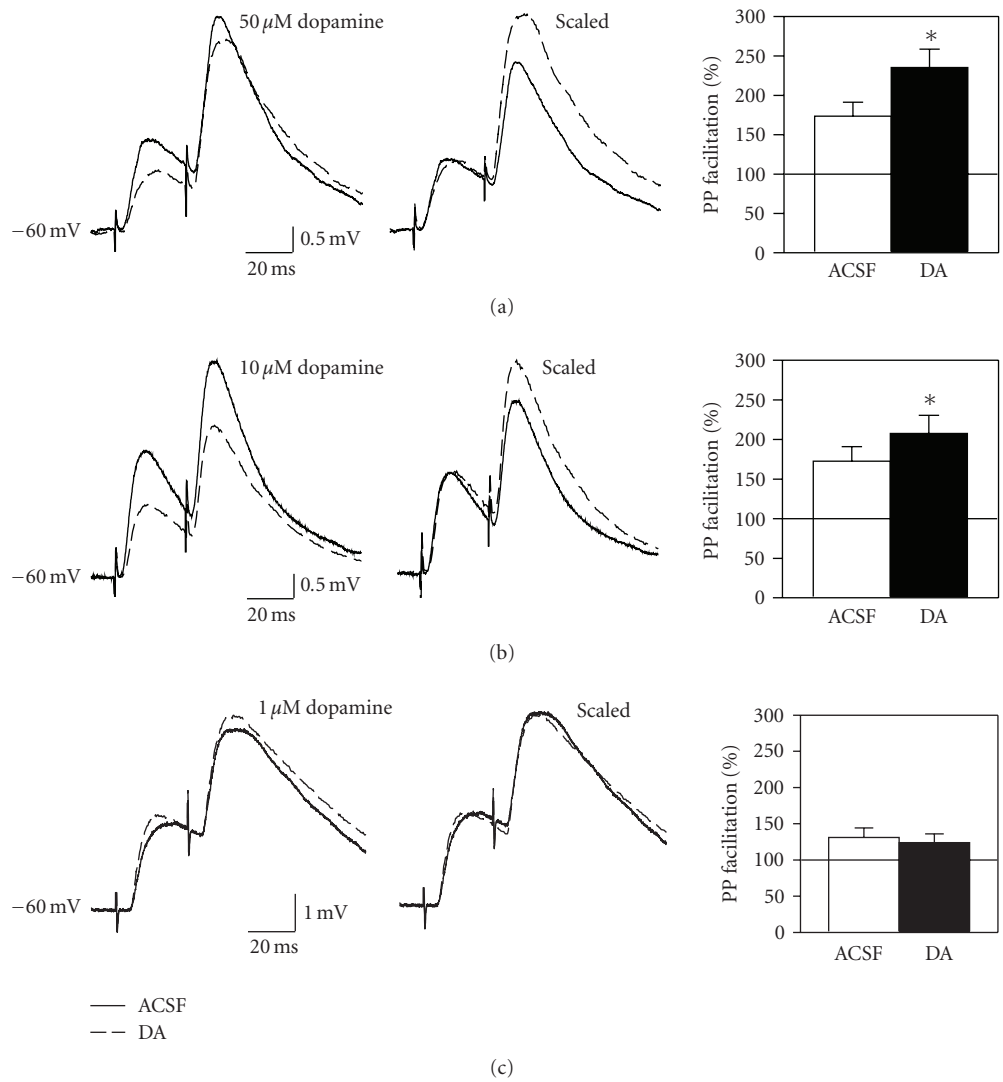

Figure 2: High concentrations of dopamine increase paired-pulse facilitation. (a) Pairs of stimulation pulses with a 30 millisecond interpulse interval were delivered before and after 5-minute bath application of 50 μM dopamine. Averaged traces at left show responses recorded before (ACSF) and after (DA) dopamine from a representative cell. Note the suppression of the response to the first pulse and the large facilitation of the second response following dopamine (dotted line). Traces at right have been scaled to the amplitude of the first response in normal ACSF to aid comparison. Group data are shown on the right. (b) Paired-pulse facilitation was also enhanced by 10 μM dopamine. (c) In contrast, the low concentration of 1 μM dopamine does not affect paired-pulse ratio.

suppression of glutamate release from presynaptic terminals, bath application of 50 μM dopamine significantly attenuated both the isolated AMPA- and NMDA-mediated responses. The NMDA component was reduced to 26.0 ± 7.5% of baseline (see Figure 3(b); $t_7 = 3.32$, $P < .05$; $n = 8$) and the AMPA component was reduced to 41.7 ± 5.6% of baseline (see Figure 3(a); $t_5 = 3.50$, $P < .05$; $n = 6$).

Dopamine receptor subtypes underlying the suppression of AMPA-mediated synaptic responses were investigated by applying 50 μM dopamine in the presence of either the D_1 receptor antagonist SCH23390 (50 μM) or the D_2 receptor antagonist sulpiride (50 μM). Similar to previous reports that have used selective agonists in the medial [30, 31] and lateral [29] entorhinal cortex, application of either the D_1 agonist SKF38393 (25 to 50 μM; $n = 9$) or the D_2 agonist quinpirole (20 to 40 μM; $n = 10$) had no effect on EPSPs (data not shown), and we therefore used receptor blockers known to affect synaptic responses in the lateral entorhinal cortex [29]. Application of antagonists alone had no effect on EPSPs, and the D_1 antagonist SCH23390 did not block the suppression of AMPA-mediated EPSPs (see Figure 4(a); $t_4 = 3.0$, $P < .05$; $n = 5$), suggesting that D_1 receptors do not mediate the suppression. However, blockade of D_2 receptors with sulpiride significantly reduced the effects of dopamine on AMPA-mediated EPSPs. Coapplication of dopamine with sulpiride ($n = 5$) resulted in a nonsignificant suppression of synaptic responses, and the size of the suppression was significantly smaller than that observed with dopamine alone (79.8 ± 7.2% versus 41.7 ± 5.6% of baseline; $F_{1,9} = 18.10$,

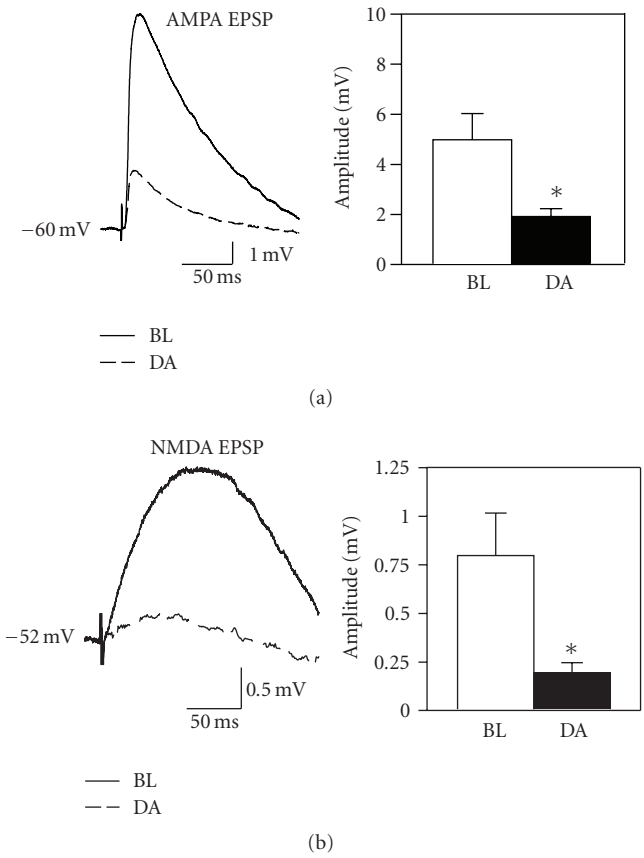

Figure 3: Dopamine suppresses the amplitude of both AMPA- and NMDA receptor-mediated components of EPSPs. (a) AMPA-mediated EPSPs recorded in the presence of APV and bicuculline were suppressed by 50 μM dopamine. Averaged traces show EPSPs recorded before (BL) and after (DA) dopamine application, and group data are shown at right. (b) Isolated NMDA receptor-mediated EPSPs recorded in the presence of CNQX and bicuculline are also suppressed by a high concentration of dopamine. Group data show a consistent suppression of the small isolated NMDA response.

$P < .001$; see Figure 4(b1)). Sulpiride also prevented the enhancement of paired-pulse facilitation induced by 50 μM dopamine (see Figure 4(b2)). Although this indicates that the dopaminergic suppression of EPSPs is largely dependent upon activation of D_2-like receptors, the suppression of responses in the presence of sulpiride was close to statistical significance ($t_4 = 2.65$, $P = .06$), suggesting that a non-D_2 receptor-mediated mechanism mediates the residual suppression.

3.4. Dopaminergic suppression of IPSPs

Biphasic IPSPs were recorded from fan cells held near action potential threshold (−51 to −48 mV) and exposed to either 1 mM kynurenic acid or a combination of 50 μM APV and 20 μM CNQX to block ionotropic glutamate transmission. A concentration of 50 μM dopamine suppressed both the early $GABA_A$- and late $GABA_B$-mediated components of the IPSP. The early IPSP was reduced to 84.5 ± 8.7% of baseline levels, and the late IPSP was reduced to 62.3 ± 11.1% of baseline levels (see Figure 5(b);early, $t_8 = 2.41$, $P < .05$, $n = 9$; late, $t_7 = 2.46$, $P < .05$, $n = 8$). The dopaminergic suppression of GABA synapses indicates that the reduction of EPSPs by dopamine is unlikely to be due to increased GABAergic inhibition of fan cells.

3.5. Modulation of intrinsic excitability

Bath application of dopamine also hyperpolarized resting membrane potential and reduced the input resistance of fan cells. Membrane potential was increased from −56.1 ± 2.0 to −59.7 ± 1.4 mV (see Figure 6(a); $t_8 = 4.73$, $P < .001$; $n = 9$), and peak input resistance was reduced from 90.3 ± 7.6 to 68.9 ± 3.1 MΩ by 50 μM dopamine (see Figure 6(b); $t_7 = 4.27$, $P < .01$; $n = 8$). Similar changes in membrane potential and input resistance were observed for 10 μM dopamine (not shown) and have also been reported following application of high concentrations of dopamine in whole-cell recordings from medial entorhinal cortex stellate cells [30]. Changes were not due to the vehicle, because control cells and cells exposed to 1 μM dopamine did not show a drop in input resistance or hyperpolarization of membrane potential.

In layer V entorhinal cortex cells dopamine causes a reduction in excitability and a drop in input resistance through an increase in the hyperpolarization-activated current I_h [32], and changes in I_h were therefore assessed in layer II fan cells. However, dopamine did not significantly affect the amount of inward rectification, and the rectification ratio remained stable (see Figure 6(d); 1.09 ± 0.02 in ACSF and in 50 μM dopamine, $t_7 = 0.00$, $P = 1.00$).

Dopamine suppressed the excitability of fan cells, and application of 10 and 50 μM dopamine reduced the number of action potentials evoked by brief 500 milliseconds depolarizing current pulses (see Figure 7). The number of spikes was reduced from 4.1 ± 0.1 to 2.8 ± 0.5 spikes by 10 μM dopamine (see Figure 7(b); $t_{17} = 2.54$, $P < .05$; $n = 18$). A higher 50 μM concentration of dopamine caused a similar reduction in the number of spikes (from 3.9 ± 0.2 to 2.8 ± 0.6) that was not statistically significant ($t_8 = 1.82$, $P = .11$; $n = 9$). The reduction in spiking could result in part from reduced input resistance, but it was not due to membrane hyperpolarization because cells were tested at the same membrane potential both before and after dopamine application.

The drop in input resistance induced by 50 μM dopamine was blocked by coapplication of the D_1 receptor antagonist SCH23390 (and there was actually a very small but reliable *increase* in R_{in} in 4 of 5 cells; $t_4 = 2.60$, $P = .06$; see Figure 8(a)). The drop in input resistance was not affected by coapplication of the D_2 receptor antagonist sulpiride ($t_4 = 9.71$, $P < .001$; $n = 5$; Figure 8(b)). The reduction in input resistance induced by dopamine is therefore dependent on activation of D_1, but not D_2, receptors.

The conductances that mediated the reduced input resistance were investigated using blockers of Na^+ and K^+ channels. The Na^+ channel blocker TTX was used to verify that reductions in input resistance were not due to an

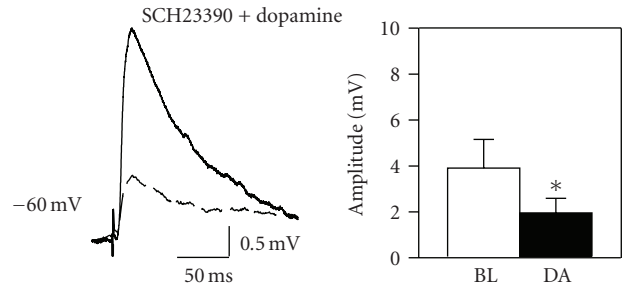

(a)

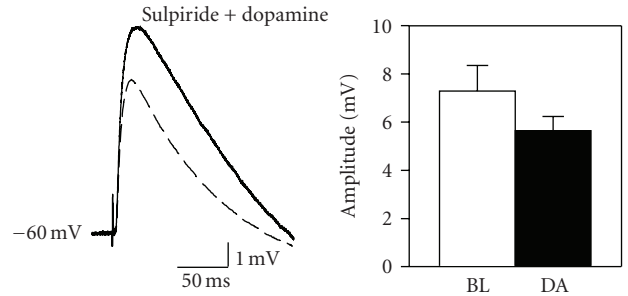

(b1)

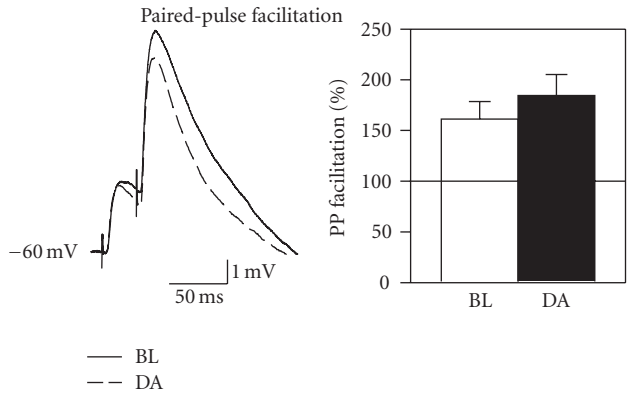

(b2)

Figure 4: Dopamine suppresses isolated AMPA-mediated EPSPs via a D_2 receptor-dependent mechanism. (a) Coapplication of the D_1 receptor antagonist SCH23390 (50 μM) did not prevent the dopamine-induced reduction in EPSP amplitude. (b) However, coapplication of the D_2 receptor antagonist sulpiride (50 μM) significantly attenuated the dopaminergic suppression of EPSPs. Sulpiride also prevented the enhancement of paired-pulse facilitation induced by dopamine (b2).

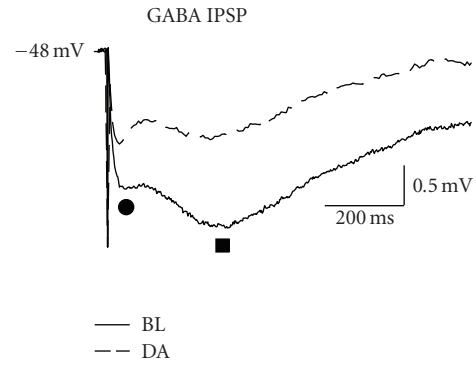

(a)

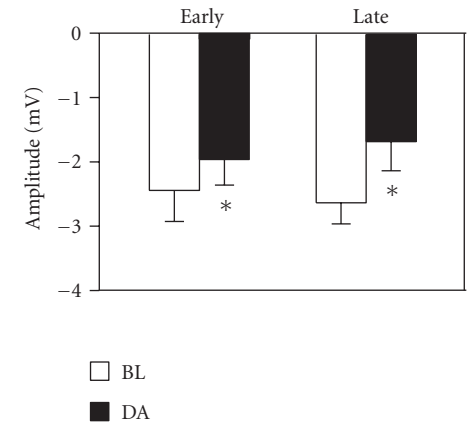

(b)

Figure 5: Dopamine suppresses both the fast and slow components of the mixed monosynaptic IPSP in fan cells. (a) GABA-mediated IPSPs were isolated pharmacologically with ionotropic glutamate receptor blockers and recorded at membrane potentials just below action potential threshold. Both the early (circle) and late (square) components of the biphasic IPSP were suppressed by 50 μM dopamine (DA). (b) Group data reflect a significant suppression of both the early and late IPSPs.

increase in action potential-dependent synaptic inputs to fan cells, or due to an altered Na^+ conductance. Blockade of Na^+ channels with TTX did not prevent the drop in input resistance induced by dopamine (see Figure 9(a); peak, $t_4 = 6.02$, $P < .01$; steady-state, $t_4 = 8.21$, $P < .01$; $n = 5$). It has been suggested that the reduced input resistance induced by dopamine in medial entorhinal cortex stellate cells might be mediated by an increased K^+ conductance [30], and we therefore assessed the effects of dopamine on input resistance in the presence of the K^+ channel blocker TEA (30 mM; $n = 5$). Coapplication of TEA blocked the reduction in input resistance induced by dopamine (see Figure 9(b)), indicating that the D_1 receptor-dependent reduction in input resistance involves an increased K^+ conductance. The increased K^+ conductance is likely to contribute to the hyperpolarization of membrane potential induced by dopamine, and may also account for the reduced excitability of fan cells (see Figure 7). The reduced input resistance may also contribute to the dopamine-induced suppression of EPSPs; the D_2 receptor blocker sulpiride did not fully prevent the suppression of AMPA-mediated EPSPs (see Figure 4(b1)), and the D_1 receptor-mediated reduction in input resistance could contribute to part of the EPSP suppression.

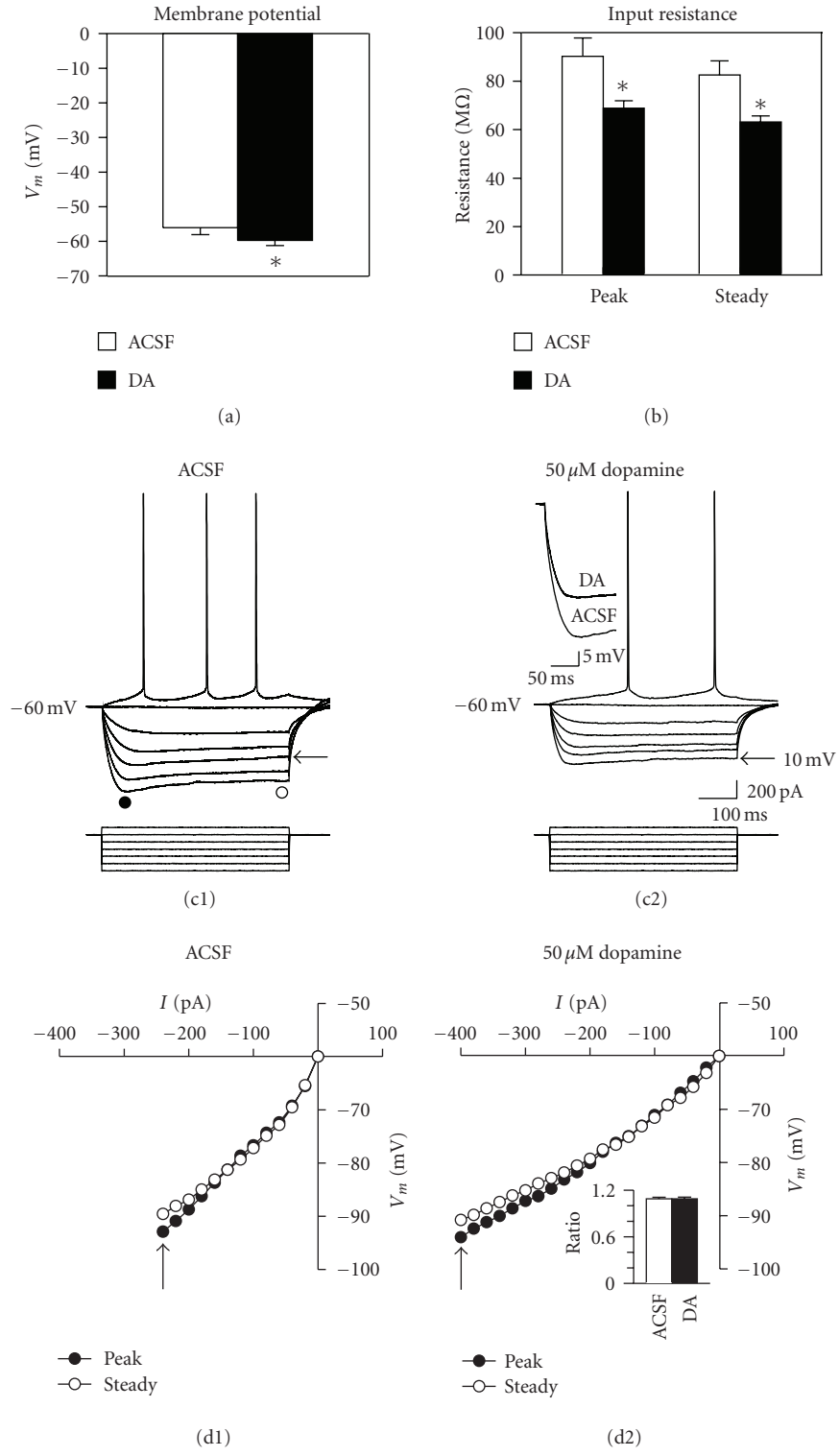

Figure 6: Dopamine hyperpolarizes membrane potential and reduces the input resistance of layer II fan cells. (a) Membrane potential was shifted to more hyperpolarized potentials by dopamine (*, $P < .001$). (b) Dopamine also reduced both peak and steady-state input resistance (*, $P < .01$). (c) Voltage responses to applied current steps before (c1) and after (c2) bath application of 50 μM dopamine in a representative cell. Action potentials are truncated. Circles in (c1) indicate the latencies at which peak and steady-state input resistance were measured. Inset traces in (c2) compare the initial voltage deflection to a −200 pA current step before and after application of dopamine. Arrows indicate voltage responses before and after dopamine that were similar in amplitude and which allow comparison of the magnitude of the inward rectification. Note also the reduced input resistance across the entire range of hyperpolarizing current pulses. (d) Current-voltage plots show peak and steady-state responses to current steps of increasing size. Arrows indicate points at which a comparable degree of inward rectification was observed during hyperpolarization to similar voltages before and after dopamine application.

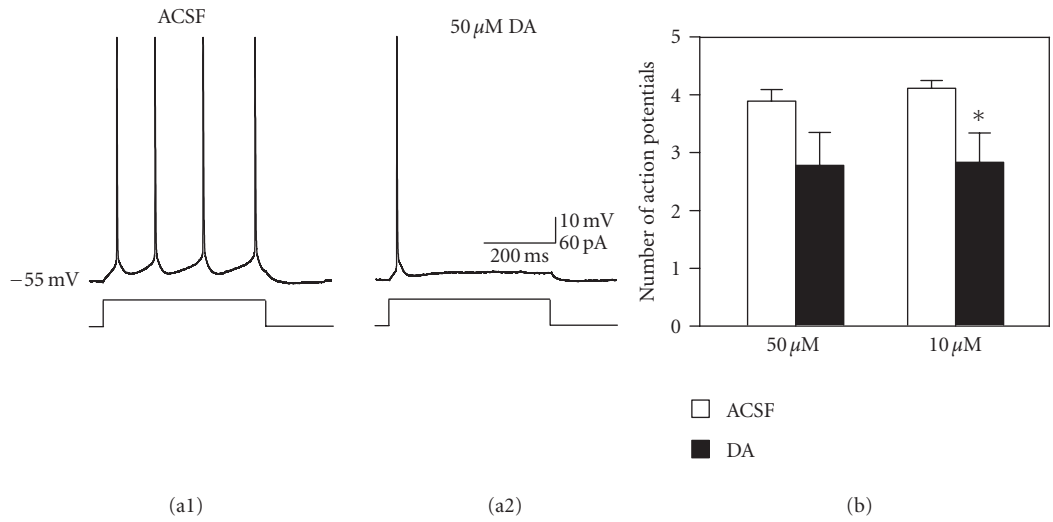

Figure 7: The number of action potentials elicited by positive current steps is reduced by dopamine. (a) Traces show action potentials generated in response to 500 milliseconds duration, 60 pA current steps before and after application of 50 μM dopamine. The example shown reflects a particularly large reduction to only one action potential following application of dopamine. Action potentials are truncated. (b) Group data show a reduction in firing for both the 10 and 50 μM conditions but only the reduction in the 10 μM condition was significant.

4. DISCUSSION

We show here that dopamine has powerful suppressive effects on glutamate-mediated synaptic transmission in layer II fan cells ofthe lateral entorhinal cortex. Our findings suggest that the suppression of EPSPs involves the combined actions of a D_2 receptor-mediated reduction in neurotransmitter release and a D_1 receptor-mediated increase in a K^+ conductance that reduces cellular input resistance. Previously, we found that field EPSPs were enhanced by low concentrations of dopamine in vitro, and by blocking dopamine reuptake in awake animals [29]. This suggested that moderate increases in dopamine release might facilitate synaptic responses in the entorhinal cortex, and enhance transmission of sensory information to the rest of the hippocampal formation. Here, we have replicated the synaptic facilitation with a low 1 μM concentration of dopamine and have also shown that high concentrations of dopamine induce a strong and reversible suppression of intracellular EPSPs. Similar suppression effects have been observed in the medial entorhinal cortex [30, 31] and prefrontal cortex [22, 23, 50, 51] using comparable doses of dopamine.

4.1. Suppression of glutamate release

The suppression of EPSPs by high concentrations of dopamine was found to be largely dependent on D_2 receptors since coapplication of the D_2 receptor antagonist sulpiride blocked most of the reduction. Dopamine also enhanced paired-pulse facilitation which suggests that the suppression of EPSPs resulted from a reduction in presynaptic glutamate release [47, 49]. The suppression of both AMPA- and NMDA-mediated components of the synaptic response is also consistent with reduced transmitter release. Although similar reductions in EPSPs have been shown in stellate cells of the medial entorhinal cortex, the suppression was dependent on D_1, and not D_2, receptor activation [30]. However, Stenkamp et al. (1998) showed a reduction in synaptic responses in layer III of the medial entorhinal cortex through activation of both D_1 *and* D_2 receptors, and results of paired-pulse tests in their study suggested that the suppression was also mediated by reduced glutamate release.

Dopamine has been shown to suppress AMPA-mediated synaptic responses in the prefrontal cortex through a D_1 receptor-mediated suppression of transmitter release [22–24]. Strong activation of D_1 receptors can also suppress synaptic responses through a retrograde signaling cascade. Weak D_1 receptor activation can enhance NMDA responses, but stronger D_1 receptor activation can lead to more intense NMDA receptor activation and the release of adenosine that suppresses transmitter release by acting on presynaptic A_1 receptors that suppress voltage-gated Ca^{2+} channels [28, 52, 53]. In the striatum, activation of presynaptic D_2 receptors suppresses *N*-type Ca^{2+} currents and inhibits acetylcholine release from striatal cholinergic interneurons [54]. D_2 receptors have also been linked to a suppression of responses in the parabrachial nucleus [55], ventral tegmental area [56], and striatum [57, 58] via a D_2-mediated reduction in glutamate release. A similar D_2-mediated mechanism underlies the suppression of GABA release from striatal inhibitory cells onto cholinergic interneurons [59]. Similar mechanisms may mediate the dopaminergic suppression of glutamate release in the entorhinal cortex.

The dopaminergic suppression of EPSPs observed here cannot be explained by increased transmission at GABA synapses because we found that dopamine reduced monosynaptic $GABA_A$ and $GABA_B$ IPSPs. The suppression is also unlikely to be due to increased activation of feedback inhibition [60] because dopamine reduced both glutamatergic

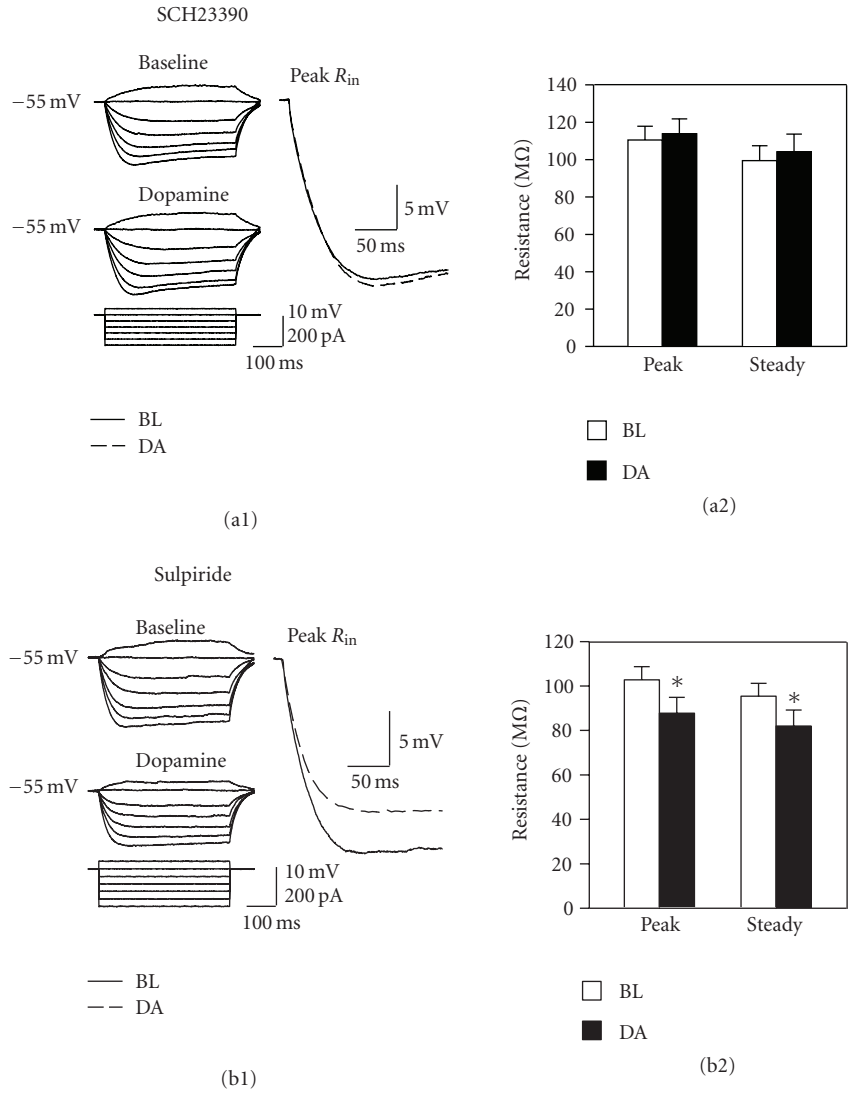

FIGURE 8: Blockade of D_1, but not D_2, receptors prevents the dopamine-induced reduction in input resistance. (a) Bath-application of the D_1 receptor antagonist SCH23390 (50 μM) prevented the reduction in input resistance induced by 50 μM dopamine. Traces at left show voltage responses to a series of current steps during baseline recordings in SCH23390 and during subsequent dopamine application. Traces at right compare the initial voltage responses to −200 pA steps before and after dopamine application. Note that input resistance is unchanged when D_1 receptors are blocked. (b) The D_2 receptor blocker sulpiride (50 μM) does not prevent changes in input resistance induced by dopamine (*, $P < .001$).

transmission and the number of spikes in fan cells (see Figure 7). The suppression of monosynaptic IPSPs that we observed may have resulted from a D_2-mediated reduction in GABA release [59, 61] and reduced input resistance in fan cells could also have contributed. These possibilities are consistent with the parallel reductions observed in $GABA_A$ and $GABA_B$ IPSPs. Recordings of spontaneous and/or miniature IPSCs would be useful to determine the mechanisms of the reduced IPSPs.

4.2. Modulation of intrinsic excitability

In addition to the D_2-mediated suppression of transmitter release, high concentrations of dopamine also appear to suppress synaptic transmission through a D_1-receptor dependent mechanism. Sulpiride did not completely block the suppression of EPSPs (see Figure 4(b1)), and a D_1 receptor-dependent activation of a TEA-sensitive K^+ conductance appears to mediate the residual suppression via a reduction in input resistance. Blockade of synaptic transmission and voltage-gated Na^+ channels with TTX did not prevent the drop in input resistance induced by dopamine indicating that it is not due to increased spontaneous synaptic drive or to an increased Na^+ conductance. However, the broadly acting K^+ channel blocker TEA prevented the drop in input resistance, indicating that dopamine activates a K^+ conductance. The drop in input resistance was also prevented by blockade of D_1, but not D_2, receptors, indicating that

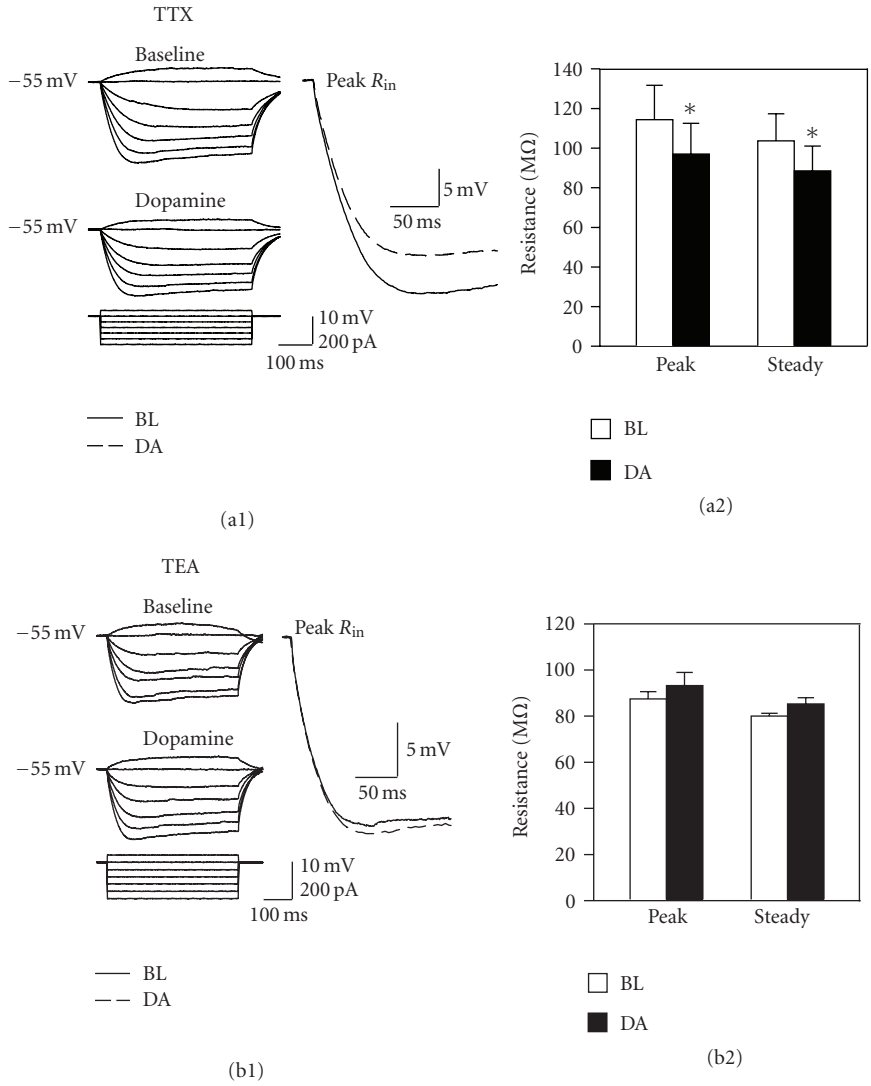

Figure 9: Blocking potassium channels prevent the dopamine-induced reduction in input resistance. (a) Blockade of Na^+ channels with 0.5 μM TTX does not prevent the reduction of peak or steady-state input resistance induced by 50 μM dopamine (*, $P < .01$). Conventions are as in Figure 8. (b) In contrast, coapplication of the K^+ channel blocker TEA (30 mM) prevented the dopamine-induced reduction in input resistance.

dopamine activates K^+ channels via D_1 receptors. High concentrations of dopamine also hyperpolarize membrane potential and reduce input resistance in stellate cells of the medial entorhinal cortex, and it was also suggested that these changes might be mediated by an increased K^+ conductance [30].

A large number of K^+ conductancesare affected by TEA, and it is therefore not clear which type(s) may be responsible for the drop in input resistance observed here. Background leak channels are insensitive to TEA [62] and are therefore not likely to contribute. Voltage-gated K^+ currents are blocked by TEA, but dopamine in the prefrontal cortex tends to enhance neuronal excitability by *suppressing* these currents (see also [43, 63]). Several reports in CA1 pyramidal cells have found that dopamine hyperpolarizes membrane potential, reduces input resistance, and increases afterhyperpolarizations through a D_1-receptor mediated increase in Ca^{2+}-activated K^+ currents ([64, 65], see also [66]), but others have found an increase in the excitability of CA1 neurons due to a *suppression* of Ca^{2+}-activated K^+ currents (see also [32, 67, 68]). Here, there was no clear increase in afterhyperpolarizations, suggesting that Ca^{2+}-dependent K^+ currents do not mediate the change in input resistance. Activation of D_1 receptors can also have dose-dependent effects on activation of inward rectifying K^+ currents (IRKCs). In the prefrontal cortex, D_1 receptor activation typically *inhibits* IRKC by direct effects of cAMP on IRK channels, but strong activation can increase IRKC via phosphorylation of the channels through elevated levels of PKA [69]. This could explain why a significant reduction in input resistance was observed here only at the higher concentrations of dopamine. Clearly, however, further experiments

will be required to determine the nature of the D_1 receptor-dependent K^+ conductance in fan cells.

We observed a decrease in fan cell firing during depolarizing current steps after dopamine, and the reduced spiking may reflect the drop in cellular input resistance. A surprising finding was that while the D_1 receptor antagonist SCH23390 prevented the dopamine-induced reduction in input resistance it did not completely eliminate the reduction in the number of spikes, suggesting that reduced input resistance cannot entirely account for the reduction in spiking, and that other mechanisms may also contribute. D_1 receptor activation can *increase* spiking in prefrontal neurons by enhancing the persistent Na^+ current (I_{NaP}) and suppressing a slowly-inactivating K^+ conductance [43, 70], but a suppression of spiking via a reduction in I_{NaP} has also been observed [71]. In layer V entorhinal cortex neurons, dopamine reduces input resistance and leads to a reduction of spiking though an increase in I_h [32]. Here, there was no apparent change in I_h in fan cells, and action potential threshold and afterhyperpolarizations were not affected, suggesting that the underlying currents were not modified. Dopaminergic effects on I_{NaP} were not directly assessed in the present study, and the drop in input resistance could mask possible reductions in depolarizing responses to current injection related to I_{NaP}. However, in tests in which SCH23390 prevented a change in input resistance, we found no reduction in the response to +20 pA pulses. This argues against a D_1-mediated reduction in I_{NaP}, but it is still possible that dopamine may reduce spiking via a D_2 receptor-mediated reduction in I_{NaP} [71].

5. CONCLUSIONS

We have shown here that dopamine has concentration-dependent, bidirectional effects on glutamate-mediated synaptic transmission in principal cells of layer II of the lateral entorhinal cortex. The lateral entorhinal cortex receives a major input from the piriform cortex [5–7], and dopaminergic innervation of the superficial layers is likely to have a strong modulatory effect on olfactory processing. In the prefrontal cortex, moderate activation of dopaminergic inputs promotes workingmemory function, but excessive dopamine activation leads to a decrement in performance [20, 27]. In the entorhinal cortex, moderate increases in dopamine concentration may enhance the salience of olfactory representations carried to the lateral entorhinal cortex (see Figure 1(c); see also 29), but large increases in dopamine associated with drug effects or acute stress [27] may dampen synaptic inputs to the superficial layers and suppress working memory function [72–74] or induction of lasting synaptic plasticity [75]. The dopaminergic suppression of synaptic transmission in layer II is also likely to inhibit the propagation of sensory information to the rest of the hippocampal formation such that only strong and synchronous inputs to the entorhinal region may be sufficient to activate entorhinal projection neurons.

ACKNOWLEDGMENTS

This research was funded by grants to Douglas A. Caruana and C. Andrew Chapman from the Natural Sciences and Engineering Research Council of Canada. C. Andrew Chapman is a member of the Center for Studies in Behavioral Neurobiology funded by the Fonds pour la Recherche en Santé du Québec.

REFERENCES

[1] L. R. Squire and S. M. Zola, "Structure and function of declarative and nondeclarative memory systems," *Proceedings of the National Academy of Sciences of the United States of America*, vol. 93, no. 24, pp. 13515–13522, 1996.

[2] P. Lavenex and D. G. Amaral, "Hippocampal-neocortical interaction: a hierarchy of associativity," *Hippocampus*, vol. 10, no. 4, pp. 420–430, 2000.

[3] R. Schwarcz and M. P. Witter, "Memory impairment in temporal lobe epilepsy: the role of entorhinal lesions," *Epilepsy Research*, vol. 50, no. 1-2, pp. 161–177, 2002.

[4] L. R. Squire, C. E. L. Stark, and R. E. Clark, "The medial temporal lobe," *Annual Review of Neuroscience*, vol. 27, pp. 279–306, 2004.

[5] R. D. Burwell, "The parahippocampal region: corticocortical connectivity," *Annals of the New York Academy of Sciences*, vol. 911, pp. 25–42, 2000.

[6] R. D. Burwell and D. G. Amaral, "Cortical afferents of the perirhinal, postrhinal, and entorhinal cortices of the rat," *Journal of Comparative Neurology*, vol. 398, no. 2, pp. 179–205, 1998.

[7] K. M. Kerr, K. L. Agster, S. C. Furtak, and R. D. Burwell, "Functional neuroanatomy of the parahippocampal region: the lateral and medial entorhinal areas," *Hippocampus*, vol. 17, no. 9, pp. 697–708, 2007.

[8] T. Hafting, M. Fyhn, S. Molden, M.-B. Moser, and E. I. Moser, "Microstructure of a spatial map in the entorhinal cortex," *Nature*, vol. 436, no. 7052, pp. 801–806, 2005.

[9] E. L. Hargreaves, G. Rao, I. Lee, and J. J. Knierim, "Major dissociation between medial and lateral entorhinal input to dorsal hippocampus," *Science*, vol. 308, no. 5729, pp. 1792–1794, 2005.

[10] T. V. Sewards and M. A. Sewards, "Input and output stations of the entorhinal cortex: superficial vs. deep layers or lateral vs. medial divisions?" *Brain Research Reviews*, vol. 42, no. 3, pp. 243–251, 2003.

[11] B. H. Bland and S. D. Oddie, "Theta band oscillation and synchrony in the hippocampal formation and associated structures: the case for its role in sensorimotor integration," *Behavioural Brain Research*, vol. 127, no. 1-2, pp. 119–136, 2001.

[12] C. R. Grünschlag, H. L. Haas, and D. R. Stevens, "5-HT inhibits lateral entorhinal cortical neurons of the rat in vitro by activation of potassium channel-coupled 5-HT(1A) receptors," *Brain Research*, vol. 770, no. 1-2, pp. 10–17, 1997.

[13] B. N. Hamam, M. Sinai, G. Poirier, and C. A. Chapman, "Cholinergic suppression of excitatory synaptic responses in layer II of the medial entorhinal cortex," *Hippocampus*, vol. 17, no. 2, pp. 103–113, 2006.

[14] L. Ma, M. H. Shalinsky, A. Alonso, and C. T. Dickson, "Effects of serotonin on the intrinsic membrane properties of layer II medial entorhinal cortex neurons," *Hippocampus*, vol. 17, no. 2, pp. 114–129, 2007.

[15] D. Schmitz, T. Gloveli, R. M. Empson, A. Draguhn, and U. Heinemann, "Serotonin reduces synaptic excitation in the superficial medial entorhinal cortex of the rat via a presynaptic mechanism," *Journal of Physiology*, vol. 508, no. 1, pp. 119–129, 1998.

[16] A. Björklund and O. Lindvall, "Dopamine-containing systems in the CNS," in *Handbook of Chemical Neuroanatomy. Vol. 2*, A. Björklund and T. Hökfelt, Eds., Classical Transmitters in the CNS, Part I, pp. 55–122, Elsevier, Amsterdam, The Netherlands, 1984.

[17] J. H. Fallon and S. E. Loughlin, "Monoamine innervation of cerebral cortex and a theory of the role of monoamines in cerebral cortex and basal ganglia," in *Cerebral Cortex*, E. G. Jones and A. Peters, Eds., pp. 41–127, Plenum, New York, NY, USA, 1987.

[18] R. D. Oades and G. M. Halliday, "Ventral tegmental (A10) system: neurobiology. 1. Anatomy and connectivity," *Brain Research*, vol. 434, no. 2, pp. 117–165, 1987.

[19] P. S. Goldman-Rakic, "The "psychic" neuron of the cerebral cortex," *Annals of the New York Academy of Sciences*, vol. 868, pp. 13–26, 1999.

[20] J. K. Seamans and C. R. Yang, "The principal features and mechanisms of dopamine modulation in the prefrontal cortex," *Progress in Neurobiology*, vol. 74, no. 1, pp. 1–58, 2004.

[21] A. G. Phillips, G. Vacca, and S. Ahn, "A top-down perspective on dopamine, motivation and memory," *Pharmacology Biochemistry and Behavior*, vol. 90, no. 2, pp. 236–249, 2008.

[22] W.-J. Gao, L. S. Krimer, and P. S. Goldman-Rakic, "Presynaptic regulation of recurrent excitation by D_1 receptors in prefrontal circuits," *Proceedings of the National Academy of Sciences of the United States of America*, vol. 98, no. 1, pp. 295–300, 2001.

[23] D. Law-Tho, J. C. Hirsch, and F. Crepel, "Dopamine modulation of synaptic transmission in rat prefrontal cortex: an in vitro electrophysiological study," *Neuroscience Research*, vol. 21, no. 2, pp. 151–160, 1994.

[24] J. K. Seamans, D. Durstewitz, B. R. Christie, C. F. Stevens, and T. J. Sejnowski, "Dopamine D1/D5 receptor modulation of excitatory synaptic inputs to layer V prefrontal cortex neurons," *Proceedings of the National Academy of Sciences of the United States of America*, vol. 98, no. 1, pp. 301–306, 2001.

[25] S. Bandyopadhyay, C. Gonzalez-Islas, and J. J. Hablitz, "Dopamine enhances spatiotemporal spread of activity in rat prefrontal cortex," *Journal of Neurophysiology*, vol. 93, no. 2, pp. 864–872, 2005.

[26] C. Gonzalez-Islas and J. J. Hablitz, "Dopamine enhances EPSCs in layer II-III pyramidal neurons in rat prefrontal cortex," *The Journal of Neuroscience*, vol. 23, no. 3, pp. 867–875, 2003.

[27] A. F. T. Arnsten, "Catecholamine modulation of prefrontal cortical cognitive function," *Trends in Cognitive Sciences*, vol. 2, no. 11, pp. 436–447, 1998.

[28] C. R. Yang and L. Chen, "Targeting prefrontal cortical dopamine D_1 and N-methyl-D-aspartate receptor interactions in schizophrenia treatment," *Neuroscientist*, vol. 11, no. 5, pp. 452–470, 2005.

[29] D. A. Caruana, R. E. Sorge, J. Stewart, and C. A. Chapman, "Dopamine has bidirectional effects on synaptic responses to cortical inputs in layer II of the lateral entorhinal cortex," *Journal of Neurophysiology*, vol. 96, no. 6, pp. 3006–3015, 2006.

[30] E. Pralong and R. S. Jones, "Interactions of dopamine with glutamate- and GABA-mediated synaptic transmission in the rat entorhinal cortex in vitro," *European Journal of Neuroscience*, vol. 5, no. 6, pp. 760–767, 1993.

[31] K. Stenkamp, U. Heinemann, and D. Schmitz, "Dopamine suppresses stimulus-induced field potentials in layer III of rat medial entorhinal cortex," *Neuroscience Letters*, vol. 255, no. 2, pp. 119–121, 1998.

[32] J. A. Rosenkranz and D. Johnston, "Dopaminergic regulation of neuronal excitability through modulation of Ih in layer V entorhinal cortex," *The Journal of Neuroscience*, vol. 26, no. 12, pp. 3229–3244, 2006.

[33] S. D. Glasgow and C. A. Chapman, "Local generation of theta-frequency EEG activity in the parasubiculum," *Journal of Neurophysiology*, vol. 97, no. 6, pp. 3868–3879, 2007.

[34] D. Mueller, C. A. Chapman, and J. Stewart, "Amphetamine induces dendritic growth in ventral tegmental area dopaminergic neurons in vivo via basic fibroblast growth factor," *Neuroscience*, vol. 137, no. 3, pp. 727–735, 2006.

[35] G. Paxinos and C. Watson, *The Rat Brain in Stereotaxic Coordinates*, Academic Press, New York, NY, USA, 1998.

[36] T. W. Blackstad, "Commissural connections of the hippocampal region in the rat, with special reference to their mode of termination," *Journal of Comparative Neurology*, vol. 105, no. 3, pp. 417–537, 1956.

[37] A. A. Carboni and W. G. Lavelle, "Ultrastructural characterizations of olfactory pathway neurons in layer II of the entorhinal cortex in monkey," *Acta Oto-Laryngologica*, vol. 120, no. 3, pp. 424–431, 2000.

[38] O. Steward, "Topographic organization of the projections from the entorhinal area to the hippocampal formation of the rat," *Journal of Comparative Neurology*, vol. 167, no. 3, pp. 285–314, 1976.

[39] J. M. Wyss, "An autoradiographic study of the efferent connections of the entorhinal cortex in the rat," *Journal of Comparative Neurology*, vol. 199, no. 4, pp. 495–512, 1981.

[40] B. Tahvildari and A. Alonso, "Morphological and electrophysiological properties of lateral entorhinal cortex layers II and III principal neurons," *Journal of Comparative Neurology*, vol. 491, no. 2, pp. 123–140, 2005.

[41] X. Wang and N. A. Lambert, "Membrane properties of identified lateral and medial perforant pathway projection neurons," *Neuroscience*, vol. 117, no. 2, pp. 485–492, 2003.

[42] A. Alonso and R. Klink, "Differential electroresponsiveness of stellate and pyramidal-like cells of medial entorhinal cortex layer II," *Journal of Neurophysiology*, vol. 70, no. 1, pp. 128–143, 1993.

[43] C. R. Yang and J. K. Seamans, "Dopamine D_1 receptor actions in layers V-VI rat prefrontal cortex neurons in vitro: modulation of dendritic-somatic signal integration," *The Journal of Neuroscience*, vol. 16, no. 5, pp. 1922–1935, 1996.

[44] R. Bouras and C. A. Chapman, "Long-term synaptic depression in the adult entorhinal cortex in vivo," *Hippocampus*, vol. 13, no. 7, pp. 780–790, 2003.

[45] D. A. Caruana and C. A. Chapman, "Stimulation of the parasubiculum modulates entorhinal cortex responses to piriform cortex inputs in vivo," *Journal of Neurophysiology*, vol. 92, no. 2, pp. 1226–1235, 2004.

[46] S. Kourrich and C. A. Chapman, "NMDA receptor-dependent long-term synaptic depression in the entorhinal cortex in vitro," *Journal of Neurophysiology*, vol. 89, no. 4, pp. 2112–2119, 2003.

[47] T. Manabe, D. J. Wyllie, D. J. Perkel, and R. A. Nicoll, "Modulation of synaptic transmission and long-term potentiation: effects on paired pulse facilitation and EPSC variance in the CA1 region of the hippocampus," *Journal of Neurophysiology*, vol. 70, no. 4, pp. 1451–1459, 1993.

[48] R. S. Zucker, "Short-term synaptic plasticity," *Annual Review of Neuroscience*, vol. 12, pp. 13–31, 1989.

[49] R. S. Zucker and W. G. Regehr, "Short-term synaptic plasticity," *Annual Review of Physiology*, vol. 64, pp. 355–405, 2002.

[50] N. N. Urban, G. González-Burgos, D. A. Henze, D. A. Lewis, and G. Barrionuevo, "Selective reduction by dopamine of excitatory synaptic inputs to pyramidal neurons in primate prefrontal cortex," *Journal of Physiology*, vol. 539, no. 3, pp. 707–712, 2002.

[51] P. Zheng, X.-X. Zhang, B. S. Bunney, and W.-X. Shi, "Opposite modulation of cortical *N*-methyl-D-aspartate receptor-mediated responses by low and high concentrations of dopamine," *Neuroscience*, vol. 91, no. 2, pp. 527–535, 1999.

[52] C. G. Craig, S. D. Temple, and T. D. White, "Is cyclic AMP involved in excitatory amino acid-evoked adenosine release from rat cortical slices?" *European Journal of Pharmacology*, vol. 269, no. 1, pp. 79–85, 1994.

[53] K. P. Scholz and R. J. Miller, "Presynaptic inhibition at excitatory hippocampal synapses: development and role of presynaptic Ca^{2+} channels," *Journal of Neurophysiology*, vol. 76, no. 1, pp. 39–46, 1996.

[54] Z. Yan, W.-J. Song, and D. J. Surmeier, "D_2 dopamine receptors reduce N-type Ca^{2+} currents in rat neostriatal cholinergic interneurons through a membrane-delimited, protein-kinase-C-insensitive pathway," *Journal of Neurophysiology*, vol. 77, no. 2, pp. 1003–1015, 1997.

[55] X. Chen, S. B. Kombian, J. A. Zidichouski, and Q. J. Pittman, "Dopamine depresses glutamatergic synaptic transmission in the rat parabrachial nucleus in vitro," *Neuroscience*, vol. 90, no. 2, pp. 457–468, 1999.

[56] E. Koga and T. Momiyama, "Presynaptic dopamine D_2-like receptors inhibit excitatory transmission onto rat ventral tegmental dopaminergic neurones," *Journal of Physiology*, vol. 523, no. 1, pp. 163–173, 2000.

[57] K.-S. Hsu, C.-C. Huang, C.-H. Yang, and P.-W. Gean, "Presynaptic D_2 dopaminergic receptors mediate inhibition of excitatory synaptic transmission in rat neostriatum," *Brain Research*, vol. 690, no. 2, pp. 264–268, 1995.

[58] M. S. Levine, L. I. Zhiwei, C. Cepeda, H. C. Cromwell, and K. L. Altemus, "Neuromodulatory actions of dopamine on synaptically-evoked neostriatal responses in slices," *Synapse*, vol. 24, no. 1, pp. 65–78, 1996.

[59] A. Pisani, P. Bonsi, D. Centonze, P. Calabresi, and G. Bernardi, "Activation of D_2-like dopamine receptors reduces synaptic inputs to striatal cholinergic interneurons," *The Journal of Neuroscience*, vol. 20 RC69, no. 7, pp. 1–6, 2000.

[60] D. M. Finch, A. M. Tan, and M. Isokawa-Akesson, "Feedforward inhibition of the rat entorhinal cortex and subicular complex," *The Journal of Neuroscience*, vol. 8, no. 7, pp. 2213–2226, 1988.

[61] J. K. Seamans, N. Gorelova, D. Durstewitz, and C. R. Yang, "Bidirectional dopamine modulation of GABAergic inhibition in prefrontal cortical pyramidal neurons," *The Journal of Neuroscience*, vol. 21, no. 10, pp. 3628–3638, 2001.

[62] F. Lesage, "Pharmacology of neuronal background potassium channels," *Neuropharmacology*, vol. 44, no. 1, pp. 1–7, 2003.

[63] Y. Dong and F. J. White, "Dopamine D_1-class receptors selectively modulate a slowly inactivating potassium current in rat medial prefrontal cortex pyramidal neurons," *The Journal of Neuroscience*, vol. 23, no. 7, pp. 2686–2695, 2003.

[64] L. S. Benardo and D. A. Prince, "Dopamine modulates a Ca^{2+}-activated potassium conductance in mammalian hippocampal pyramidal cells," *Nature*, vol. 297, no. 5861, pp. 76–79, 1982.

[65] N. Berretta, F. Berton, R. Bianchi, M. Capogna, W. Francesconi, and M. Brunelli, "Effects of dopamine, D-1 and D-2 dopaminergic agonists on the excitability of hippocampal CA1 pyramidal cells in guinea pig," *Experimental Brain Research*, vol. 83, no. 1, pp. 124–130, 1990.

[66] S. Hernández-López, J. Bargas, A. Reyes, and E. Galarraga, "Dopamine modulates the afterhyperpolarization in neostriatal neurones," *NeuroReport*, vol. 7, no. 2, pp. 454–456, 1996.

[67] R. C. Malenka and R. A. Nicoll, "Dopamine decreases the calcium-activated afterhyperpolarization in hippocampal CA1 pyramidal cells," *Brain Research*, vol. 379, no. 2, pp. 210–215, 1986.

[68] P. Pedarzani and J. F. Storm, "Dopamine modulates the slow Ca(2+)-activated K^+ current IAHP via cyclic AMP-dependent protein kinase in hippocampal neurons," *Journal of Neurophysiology*, vol. 74, no. 6, pp. 2749–2753, 1995.

[69] Y. Dong, D. Cooper, F. Nasif, X.-T. Hu, and F. J. White, "Dopamine modulates inwardly rectifying potassium currents in medial prefrontal cortex pyramidal neurons," *The Journal of Neuroscience*, vol. 24, no. 12, pp. 3077–3085, 2004.

[70] N. A. Gorelova and C. R. Yang, "Dopamine D1/D5 receptor activation modulates a persistent sodium current in rat prefrontal cortical neurons in vitro," *Journal of Neurophysiology*, vol. 84, no. 1, pp. 75–87, 2000.

[71] E. Geijo-Barrientos and C. Pastore, "The effects of dopamine on the subthreshold electrophysiological responses of rat prefrontal cortex neurons in vitro," *European Journal of Neuroscience*, vol. 7, no. 3, pp. 358–366, 1995.

[72] J. McGaughy, R. A. Koene, H. Eichenbaum, and M. E. Hasselmo, "Cholinergic deafferentation of the entorhinal cortex in rats impairs encoding of novel but not familiar stimuli in a delayed nonmatch-to-sample task," *The Journal of Neuroscience*, vol. 25, no. 44, pp. 10273–10281, 2005.

[73] B. Tahvildari, E. Fransén, A. A. Alonso, and M. E. Hasselmo, "Switching between "On" and "Off" states of persistent activity in lateral entorhinal layer III neurons," *Hippocampus*, vol. 17, no. 4, pp. 257–263, 2007.

[74] B. J. Young, T. Otto, G. D. Fox, and H. Eichenbaum, "Memory representation within the parahippocampal region," *The Journal of Neuroscience*, vol. 17, no. 13, pp. 5183–5195, 1997.

[75] D. A. Caruana, S. J. Reed, D. J. Sliz, and C. A. Chapman, "Inhibiting dopamine reuptake blocks the induction of long-term potentiation and depression in the lateral entorhinal cortex of awake rats," *Neuroscience Letters*, vol. 426, no. 1, pp. 6–11, 2007.

Hindawi Publishing Corporation
Neural Plasticity
Volume 2008, Article ID 401645, 12 pages
doi:10.1155/2008/401645

Research Article

The Role of GLU_{K5}-Containing Kainate Receptors in Entorhinal Cortex Gamma Frequency Oscillations

Heather L. Stanger,[1] Rebekah Alford,[2] David E. Jane,[3] and Mark O. Cunningham[1]

[1] *Institute of Neuroscience, Faculty of Medical Sciences, Newcastle University, The Medical School Framlington Place, Newcastle upon Tyne NE2 4HH, UK*
[2] *The Molecular Biology, Biochemistry and Bioinformatics (MB3) Program, Towson University, Room 360, Smith Hall, 8000 York Road, Towson, MD 21251-0001, USA*
[3] *Department of Physiology and Pharmacology, MRC Centre for Synaptic Plasticity, School of Medical Sciences, University of Bristol, University Walk, Bristol BS8 1TD, UK*

Correspondence should be addressed to Mark O. Cunningham, mark.cunningham@ncl.ac.uk

Received 5 June 2008; Revised 21 July 2008; Accepted 22 September 2008

Recommended by C. Andrew Chapman

Using in vitro brain slices of hippocampus and cortex, neuronal oscillations in the frequency range of 30–80 Hz (gamma frequency oscillations) can be induced by a number of pharmacological manipulations. The most routinely used is the bath application of the broad-spectrum glutamate receptor agonist, kainic acid. In the hippocampus, work using transgenic kainate receptor knockout mice have revealed information about the specific subunit composition of the kainate receptor implicated in the generation and maintenance of the gamma frequency oscillation. However, there is a paucity of such detail regarding gamma frequency oscillation in the cortex. Using specific pharmacological agonists and antagonists for the kainate receptor, we have set out to examine the contribution of kainate receptor subtypes to gamma frequency oscillation in the entorhinal cortex. The findings presented demonstrate that in contrast to the hippocampus, kainate receptors containing the GLU_{K5} subunit are critically important for the generation and maintenance of gamma frequency oscillation in the entorhinal cortex. Future work will concentrate on determining the exact nature of the cellular expression of kainate receptors in the entorhinal cortex.

Copyright © 2008 Heather L. Stanger et al. This is an open access article distributed under the Creative Commons Attribution License, which permits unrestricted use, distribution, and reproduction in any medium, provided the original work is properly cited.

1. INTRODUCTION

KARs are made up of various combinations of five subunits: GLU_{K5}, GLU_{K6}, GLU_{K7}, KA1, and KA2 [1, 2] which are abundantly expressed in the neocortex [3]. These subunits make up tetramers of either homomeric or heteromeric assemblies, with $GLU_{K5–7}$ being able to form functional homomeric receptors [1, 4]. KA1 and KA2 cannot form functional receptors when expressed alone [5, 6], yet are able to form functional KARs when expressed heteromerically with other subunits [1, 7, 8]. Differential patterns of expression of KARs in the CNS coupled with the existence of splice variants and mRNA editing suggest complex neurophysiological roles for the various subunits, and different roles in neuronal networks depending on their localization [9, 10].

Of particular interest is the role of KARs in the generation and maintenance of network neuronal oscillatory activity in cortical regions [9, 10]. Gamma frequency oscillations occur between 30–80 Hz and have been observed in many areas of the brain, including the hippocampus [11–13] and cortical regions [14–16]. Cortical gamma oscillations are important in higher brain functions, such as learning, memory, and cognition [17–19], as well as processing of sensorimotor information [15, 16, 20]. In carrying out these functions, cortical gamma oscillations are implicated in various central processes, including long-term potentiation (LTP) and synaptic plasticity [21], with important roles in temporal regulation of neuronal activity.

Gamma frequency oscillations are recordable from the MEC during wakefulness in humans [22, 23], as well as in vivo in rodents [12], in vitro from perfused guinea pig brains [24, 25], and isolated rat brain slices [26, 27]. These gamma oscillations in the MEC play a role in the formation, processing, storage, and retrieval of memories [17, 18]. Previously it has been demonstrated in an in vitro preparation of the MEC that application of nanomolar

concentrations of kainate (200–400 nM) can induce persistent gamma frequency oscillations [26–28]. Using this in vitro model of MEC gamma frequency oscillations it has been elucidated that this activity is primarily generated by inhibitory-based neuronal networks [29–31]. A similar mechanism for the generation of gamma frequency activity has been demonstrated in both the hippocampus and neocortex [32, 33].

To date our understanding of the role of the KARs in neuronal network activity has been hampered by a paucity of selective pharmacological agents. The competitive AMPA/KAR antagonist, 2,3-dihydroxy-6-nitro-7-sulfamoyl-benzo[*f*]quinoxaline (NBQX), shows little selectivity between AMPA receptors and KARs at high concentrations, yet at low concentrations (1 μM) can be used to block AMPA receptors, and isolate KAR responses [34, 35]. However, NBQX shows no selectivity between different KAR subunits. The role of GLU_{K5} and GLU_{K6} subunits in neuronal oscillatory activity in the hippocampus has been previously investigated using receptor knockout mice [9, 10]. However, interpretation of work using transgenic models should be viewed in the light of the knowledge that compensatory factors may play a role. The recent development of pharmacological agents with specificity for distinct subunits has led to the possibility of a detailed pharmacological investigation of the role of specific KARs in cortical gamma frequency oscillations. (*S*)-3-(2-Carboxybenzyl)willardiine (UBP302) is a novel selective GLU_{K5}-containing KAR antagonist, with activity at both homomeric and heteromeric GLU_{K5}-containing receptors [36, 37]. The activity of UBP302 on GLU_{K7} is controversial, Dolman et al. [37] showed that UBP296 (racemic form of UBP302) only weakly inhibited [^{3}H]kainate binding to human GLU_{K7} (K_i value of 374 ± 122 μM). However, in an electrophysiological assay UBP302 was found to block rat homomeric GLU_{K7} receptors with an IC_{50} value of 4 μM but at a concentration of 100 μM only very weakly blocked rat GLU_{K6}/GLU_{K7} receptors [38]. 5-Carboxy-2,4-di-benzamido-benzoic acid (NS3763) is another novel glutamate antagonist, which is selective and noncompetitive for homomeric GLU_{K5}-containing KARs [39, 40]. (*RS*)-2-amino-3-(3-hydroxy-5-tert-butyl-isoxazol-4-yl)propanoic acid (ATPA) is a selective GLU_{K5}-containing receptor agonist [41]. ATPA has been shown to depress excitatory and GABAergic synaptic transmission in the hippocampus [42, 43]. However, Cossart et al. [35] demonstrated that lower concentrations of ATPA could directly depolarise hippocampal GABAergic interneurons leading to increases in the levels of tonic inhibition onto pyramidal neurons. More recently, similar concentrations of ATPA to that used in the Cossart et al. [35] study have been shown to facilitate both evoked and action potential-independent glutamate release in the neocortex [44].

The data presented here demonstrates a role of GLU_{K5}-containing KARs in the MEC by examining the contribution of these receptor subtypes to gamma frequency oscillations. Using a pharmacological approach, we have demonstrated that GLU_{K5}-containing KARs are important for the maintenance of gamma frequency oscillations in the MEC. Moreover, the selective activation of GLU_{K5}-containing KARs can induce persistent gamma frequency oscillations in the MEC. We also demonstrate that it is the specific activation of homomeric GLU_{K5}-containing KARs that is important for the generation of gamma frequency oscillations in the MEC.

2. MATERIAL AND METHODS

2.1. Preparation of EC-hippocampal slices

All procedures involving animals were carried out in accordance with UK Home Office Legislation. Male Wistar rats, weighing >150 grammes, were first anaesthetised by inhalation of the volatile anaesthetic isofluorane. This was immediately followed by intramuscular injection of a terminal dose of ≥100 mg/kg ketamine and ≥10 mg/kg xylazine. After confirmation of deep anaesthesia, rats were intracardiacally perfused with ~50 mL sucrose-modified artificial cerebral spinal fluid (aCSF), composed of (in millimolar (mM)): 252 sucrose, 3 KCl, 1.25 NaH_2PO_4, 2 $MgSO_4$, 2 $CaCl_2 \cdot 2H_2O$, 10 glucose, and 24 $NaHCO_3$. All salts were obtained from BDH Laboratory Supplies (Poole, UK), except $MgSO_4$ which was obtained from Sigma Chemical Co (Mo, USA).

The whole brain was rapidly removed and maintained in a bath of cold sucrose-modified aCSF (4-5°C) during the dissection procedure. Horizontal slices (450 μm thick) were cut using a vibroslice (Leica VT1000S). Transverse EC-hippocampal slices were then transferred either to a holding chamber or directly to the recording chamber. They were maintained at 32 ± 1°C, at the interface between a continuous perfusion (~2-3 mL/min) of NaCl-based aCSF (containing (in mM): 126 NaCl, 3 KCl, 1.25 NaH_2PO_4, 1 $MgSO_4$, 1.2 $CaCl_2 \cdot 2H_2O$, 10 glucose, 24 $NaHCO_3$) and humidified carbogen gas (95% O_2/5% CO_2). Slices were allowed to equilibrate for 60 minutes before any recordings were taken.

2.2. Electrophysiological recording and drug application

Extracellular recordings were taken using glass electrodes pulled from borosilicate glass capillaries (GC129 TF-10, 1.2 mm OD/0.94 mm ID) (Harvard Apparatus, Kent, UK) using a Flaming/Brown micropipette puller, model P-97 (Sutter Instrument Co., Calif, USA). This created electrodes with resistances of 2–4 MΩ. Electrodes were filled with NaCl-based aCSF and positioned in Layer III of the MEC. Control readings were taken from slices before drug application to confirm that any network activity seen following treatment was due to the presence of drugs.

To evoke gamma frequency oscillations, 400 nM kainic acid ((2*S*,3*S*,4*S*)-3-carboxymethyl-4-(prop-1-en-2-yl) pyrrolidine-2-carboxylic acid; Tocris Cookson, Bristol, UK) was bath applied to EC-hippocampal slices and left to equilibrate for 2-3 hours or until gamma oscillations had stabilised. All other drugs were bath applied to slices

at known concentrations: UBP302 ((*S*)-3-(2-carboxybenzyl)willardiine; gift from Dr. David Jane, Department of Pharmacology, University of Bristol, UK) at 10 μM; ATPA ((*RS*)-2-amino-3-(3-hydroxy-5-*tert*-butylisoxazol-4-yl)propanoic acid; Tocris Cookson, Bristol, UK) at 1–5 μM; NS3763 (5-carboxy-2,4-di-benzamido-benzoic acid; Tocris, Bristol, UK) at 10–15 μM; NBQX (2,3-dihydroxy-6-nitro-7-sulfamoyl-benzo[*f*]quinoxaline; Tocris, Bristol, UK) at 1–10 μM; and Carbachol (Sigma, UK) at 10–20 μM.

2.3. Data acquisition

An AppleMac computer with the Axograph OSX software package (AxographX, Dr. John Clements, Australia) was used for all data acquisition. Signals were analogue filtered at 0.01–0.3 kHz and then digitized at a frequency of 10 kHz. Power spectra were constructed, where power at a given gamma frequency was defined as the area under the peak between 20 and 80 Hz. Power spectra were generated from digitized data, using 60 second epochs of recorded activity, and it was from these spectra that values for gamma oscillation peak frequency, peak amplitude, and spectral area power in the gamma frequency band were obtained.

2.4. Data analysis

Data analysis was carried out using Excel and Kaleidagraph software packages. Kaleidagraph software was used to generate pooled power spectra, and the Excel package was used to calculate the mean and standard error of mean (SEM) of results, and to draw up histograms and line graphs. All data is presented as mean ± SEM. SigmaStat (Systat software, USA) was used for all statistical tests. Normality tests were carried out, and if data was found to be normally distributed, two-tailed paired *t-tests* were run. However, if data failed the normality test, the Wilcoxon signed rank test was carried out. This provided us with *P*-values for all data sets, and the significance level was set at 95%; values less than $P = .05$ were deemed to be statistically significant.

3. RESULTS

3.1. Induction of kainate-driven gamma oscillations in the MEC

Previously, it has been demonstrated that low concentrations of kainic acid (kainate) evoke gamma frequency activity in the rat MEC in vitro [26, 27]. In this investigation, we produced persistent gamma oscillations in the MEC by bath application of kainate (400 nM) (Figure 1). Robust gamma frequency oscillations (39.4 ± 1.6 Hz; $n = 17$) were evoked in layer III of the MEC in all slices to which kainate had been applied ($n = 17$). This activity was generated within 15 minutes of kainate superfusion, a stable baseline was observed after 60–90 minutes. As previously reported [19], application of the competitive AMPA/KAR antagonist NBQX (10 μM) effectively abolished these kainate-induced gamma oscillations ($n = 3$) (Figure 1).

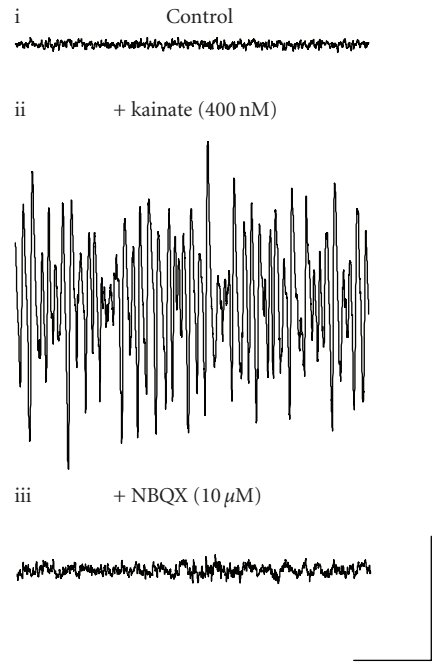

Figure 1: Gamma frequency oscillations can be induced in layer III of the MEC by application of kainate. (a) Extracellular field recordings showing 1 second epochs of activity (i) in control setting, (ii) following application of 400 nM kainate, and (iii) following application of 10 μM NBQX in the presence of 400 nM kainate. Scale bar represents 200 milliseconds and 100 μV.

3.2. A role for GLU_{K5}-containing KARs in the maintenance of kainate-driven gamma oscillations

A possible role for GLU_{K5}-containing KARs in the maintenance of kainate-driven gamma frequency oscillations in the MEC was investigated by testing the ability of the GLU_{K5} selective antagonist, UBP302, to inhibit preestablished kainate-induced gamma activity. Gamma oscillations were generated in the MEC by bath application of kainate (400 nM) and allowed to stabilise ($n = 9$) (Figure 2(a)). In the presence of UBP302 (10 μM), the amplitude of kainate-induced gamma oscillations was significantly reduced (control, 116.7 ± 44.1 μV^2/Hz; *v.* UBP302, 70.0 ± 30.3 μV^2/Hz; $P < .05$; $n = 9$), and area power of oscillations was also significantly decreased (control, 1586.0 ± 503.3 μV^2/Hz.Hz; *v.* UBP302, 1155.1 ± 441.4 μV^2/Hz.Hz; $P < .05$; $n = 9$) (Figures 2(a), 2(b)). However, following UBP302 application, the frequency of oscillations remained unchanged (control, 40.4 ± 2.1 Hz; *v.* UBP302, 38.9 ± 2.6 Hz; $P > .1$; $n = 9$). Washout of the effects of UBP302 on gamma frequency oscillations could not be achieved ($n = 9$) (Figures 2(a), 2(b)).

3.3. A role for GLU_{K5}-containing KARs in the generation of gamma oscillations in the MEC

To investigate the role that GLU_{K5}-containing KARs may play in the induction of kainate-driven gamma oscillations,

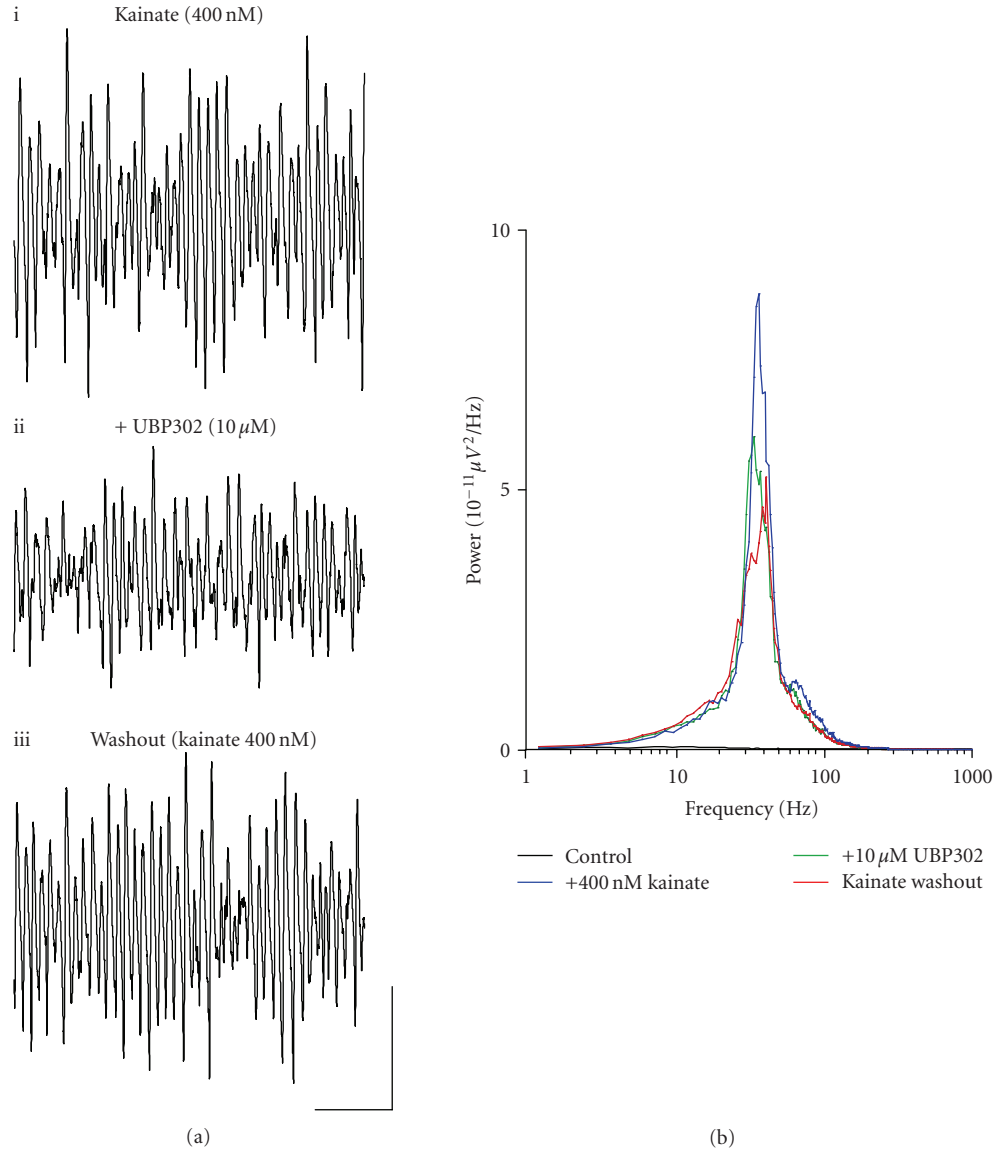

Figure 2: Antagonizing GLU_{K5}-containing KARs with UBP302 inhibits kainate-driven gamma frequency oscillations in the MEC. (a) Extracellular field recordings showing 1 second epochs of activity (i) in the presence of 400 nM kainate, (ii) following 10 μM UBP302 application, and (iii) during a washout period into 400 nM kainate. (b) Pooled power spectra ($n = 9$) produced from 60 second epochs of extracellular field recorded data, showing a control recording (black), a recording in the presence of 400 nM kainate (blue), application of 10 μM UBP302 (green), and washout back into 400 nM kainate (red). Scale bar represents 200 milliseconds and 100 μV.

we carried out two experiments, using the selective GLU_{K5}-containing KAR agonist, ATPA, and antagonist, UBP302.

First, we tested the ability of UBP302 to inhibit the generation of a kainate-driven gamma frequency oscillation in the MEC. Slices were preincubated in UBP302 (10 μM) for 30 minutes. As expected, UBP302 administration caused no neuronal network activity in slices ($n = 11$) (Figure 3(a)). However, when kainate was applied to slices following preincubation with UBP302, gamma frequency oscillations were generated in all slices ($n = 11$) (Figure 3(a)). On washout into kainate alone (400 nM), although the frequency of oscillations did not change significantly (in presence of kainate following preincubation with UBP302, 45.4 ± 2.0 Hz; *v.* 400 nM kainate alone, 40.3 ± 0.9 Hz; $P > .05$; $n = 11$), oscillations were seen to increase significantly in both peak amplitude (in presence of kainate following preincubation with UBP302, 39.2 ± 12.1 μV^2/Hz; *v.* 400 nM kainate alone, 122.9 ± 32.8 μV^2/Hz; $P < .05$; $n = 11$) and area power (in presence of kainate following preincubation with UBP302, 545.1 ± 159.6 μV^2/Hz.Hz; *v.* 400 nM kainate alone, 1302.5 ± 241.4 μV^2/Hz.Hz; $P < .05$; $n = 11$) (Figures 3(a), 3(b)).

We next investigated whether gamma frequency oscillations could be generated in the MEC by application of the GLU_{K5} selective agonist, ATPA. ATPA was bath applied to slices at concentrations of 1 μM, 2 μM, and 5 μM. ATPA induced gamma frequency oscillations in the MEC in the

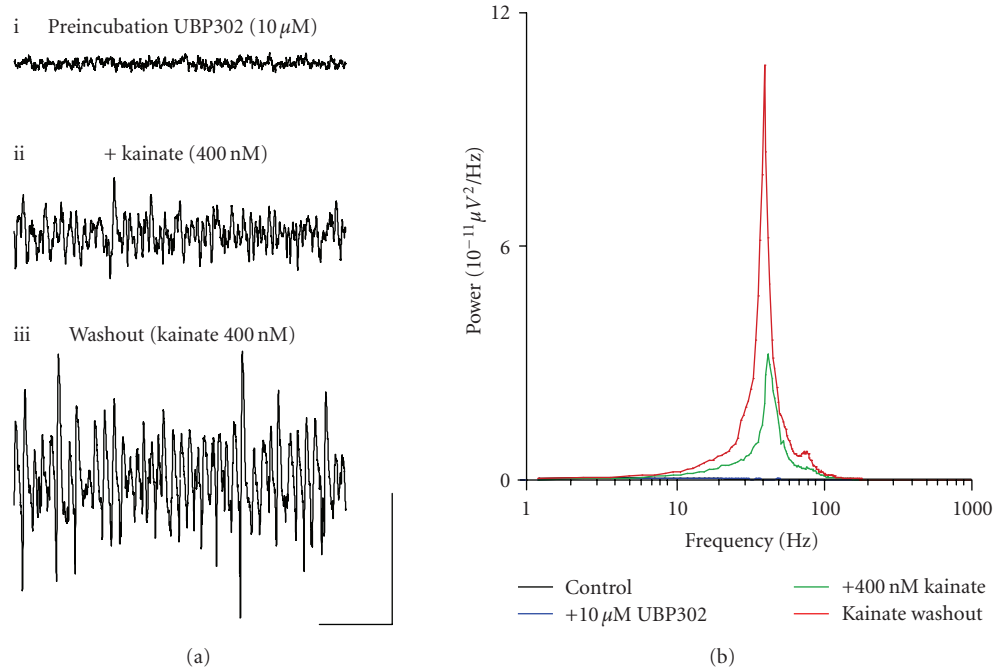

Figure 3: Preincubation of slices in UBP302 inhibits the ability of the MEC network to produce kainate-driven gamma frequency oscillations. (a) Extracellular field recordings showing 1 second epochs of activity (i) following preincubation with 10 μM UBP302, (ii) following application of 400 nM kainate onto preincubated slices, and (iii) during a washout period into 400 nM kainate. (b) Pooled power spectra ($n = 11$) produced from 60 second epochs of extracellular field recorded data, showing a control recording (black), a recording following 10 μM UBP302 preincubation (blue), 400 nM kainate application following preincubation (green), and washout into 400 nM kainate (red). Scale bar represents 200 milliseconds and 100 μV.

majority of slices to which the agonist was applied ($n = 18$ out of a total $n = 26$) (Figure 4(a)). Slices showing gamma oscillations upon ATPA application were observed to be dorsal MEC slices. Upon increasing the concentration of ATPA in slices demonstrating gamma oscillations, the mean frequency, peak amplitude, and area power of oscillations increased ($n = 10$) (Figures 4(a), 4(b)). The frequency of oscillations increased from 23.0 ± 1.9 Hz, to 34.0 ± 2.4 Hz, and to 44.2 ± 1.5 Hz ($n = 10$) (Figure 4(b)), the peak amplitude increased from 0.9 ± 0.5 μV^2/Hz, to 4.1 ± 2.3 μV^2/Hz, and to 23.3 ± 8.7 μV^2/Hz ($n = 10$) (Figure 4(b)), and the power increased from 23.1 ± 12.6 μV^2/Hz.Hz, to 88.4 ± 38.9 μV^2/Hz.Hz, and to 201.8 ± 71.0 μV^2/Hz.Hz, at the respective concentrations of ATPA (1 μM, 2 μM, and 5 μM) ($n = 10$) (Figure 4(b)). Control readings, taken before ATPA administration, showed that no network activity was spontaneously present in slices ($n = 26$) (Figure 4(a)i). ATPA-induced gamma frequency oscillations were susceptible to the AMPA/KAR antagonist NBQX (10 μM) ($n = 3$).

We next investigated the effect of UBP302 on ATPA-induced gamma frequency oscillations in the MEC. Gamma frequency oscillations were induced in slices by bath application of ATPA (2–5 μM) ($n = 4$) (Figure 5(a)i). UBP302 (10 μM) application caused no significant change in the frequency of gamma oscillations (control, 42.7 ± 3.9 Hz; *v.* UBP302, 33.9 ± 7.3 Hz; $P > .1$; $n = 4$) and yet had significant effects on both the peak amplitude (control, 20.8 ± 7.1 μV^2/Hz; *v.* UBP302, 6.6 ± 2.8 μV^2/Hz; $P < .05$; $n = 4$) and power of oscillations (control, 359.7 ± 117.9 μV^2/Hz.Hz; *v.* UBP302, 141.7 ± 61.9 μV^2/Hz.Hz; $P < .05$; $n = 4$) (Figures 5(a)ii, 5(b)). The effects of UBP302 on an ATPA-induced gamma frequency oscillations were not reversible on washout ($n = 4$).

3.4. A role for homomeric GLU_{K5}-containing KARs in gamma frequency oscillations

The GLU_{K5} selective KAR antagonist, NS3763, was used to investigate the contribution of homomeric GLU_{K5}-containing KARs to gamma activity in the MEC. NS3763 selectively antagonises homomeric GLU_{K5} KARs [39] and experiments were carried out to determine the role of these homomeric receptors in both kainate- and ATPA-induced gamma oscillations.

Application of NS3763 (10–15 μM) caused significant decreases in both peak amplitude (control, 100.2 ± 48.4 μV^2/Hz; *v.* NS3763, 46.0 ± 23.7 μV^2/Hz; $P < .05$; $n = 8$) and area power (control, 822.9 ± 273.2 μV^2/Hz.Hz; *v.* NS3763, 449.4 ± 182.3 μV^2/Hz.Hz; $P < .05$; $n = 8$) of kainate-induced gamma oscillations in the MEC (Figures 6(a), 6(b)). However, no effect was seen on the frequency of kainate-generated oscillations (control, 38.3 ± 2.7 Hz; *v.* NS3763, 36.0 ± 1.5 Hz; $P > .1$; $n = 8$) (Figure 6(b)).

Application of NS3763 (10–15 μM) to slices demonstrating ATPA-induced gamma oscillations caused no significant change in the frequency of oscillations (control,

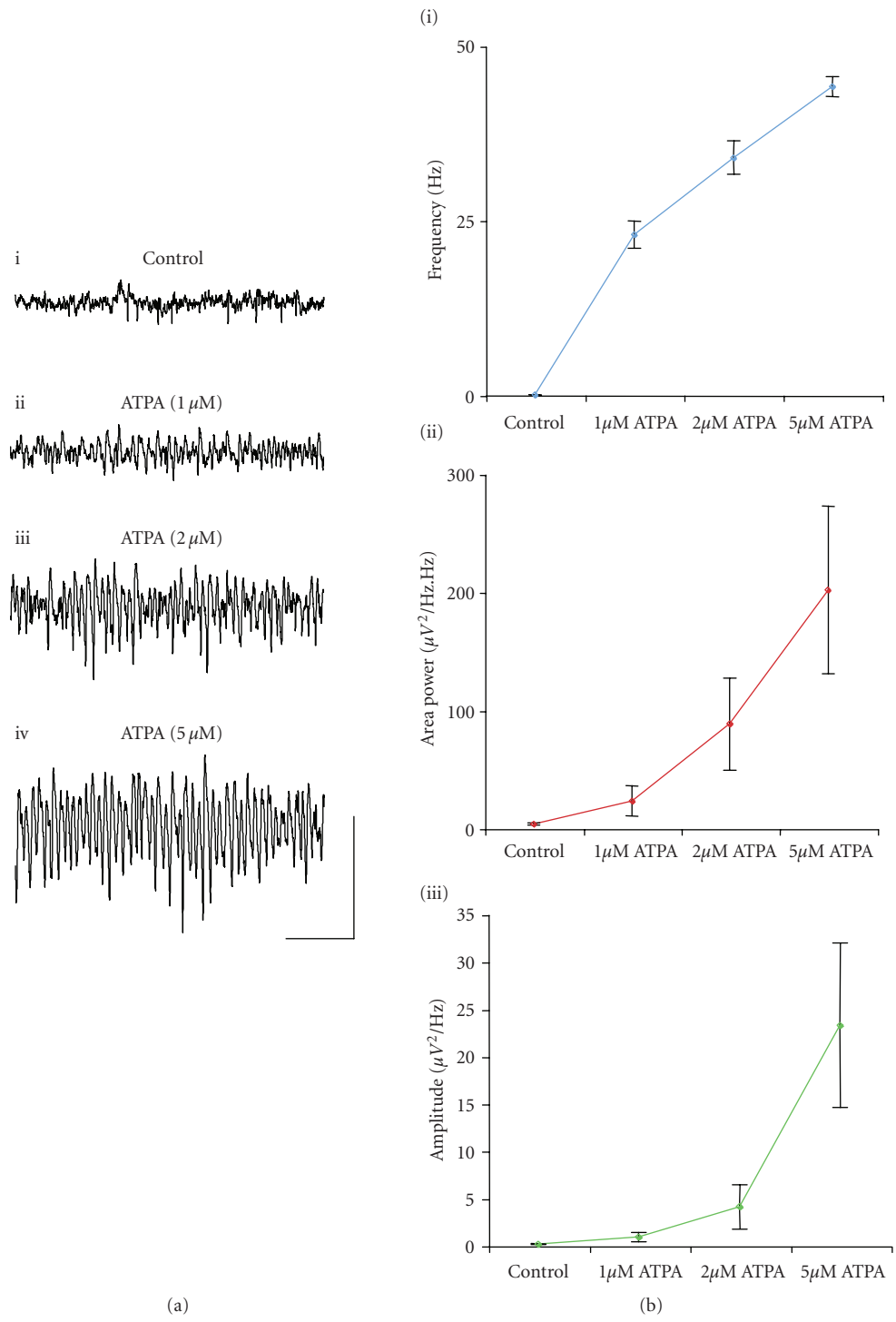

FIGURE 4: Activation of GLU_{K5}-containing KARs can induce gamma frequency oscillations in the MEC. (a) Extracellular field recordings showing 1 second epochs of activity in a control setting (i) following application of 1 μM, (ii) 2 μM (iii), and 5 μM ATPA (iv). (b) Pooled line graphs ($n = 10$) demonstrating the effects of varying ATPA concentration on (i) frequency, (ii) area power, and (iii) peak amplitude of gamma oscillations in the MEC. Scale bar represents 200 milliseconds and 100 μV.

46.7 ± 3.8 Hz; *v.* NS3763, 38.5 ± 6.2 Hz; $P > .1$; $n = 8$) (Figures 7(a), 7(b)). However, the presence of NS3763 caused a significant decrease in both the peak amplitude (control, 191.9 ± 63.1 μV^2/Hz; *v.* NS3763, 28.5 ± 13.6 μV^2/Hz; $P < .05$; $n = 8$) and area power (control, 1192.9 ± 342.8 μV^2/Hz.Hz; *v.* NS3763, 333.6 ± 120.5 μV^2/Hz.Hz; $P < .05$; $n = 8$) of gamma oscillations (Figures 7(a), 7(b)). The effects of NS3763 on either kainate- or ATPA-induced gamma

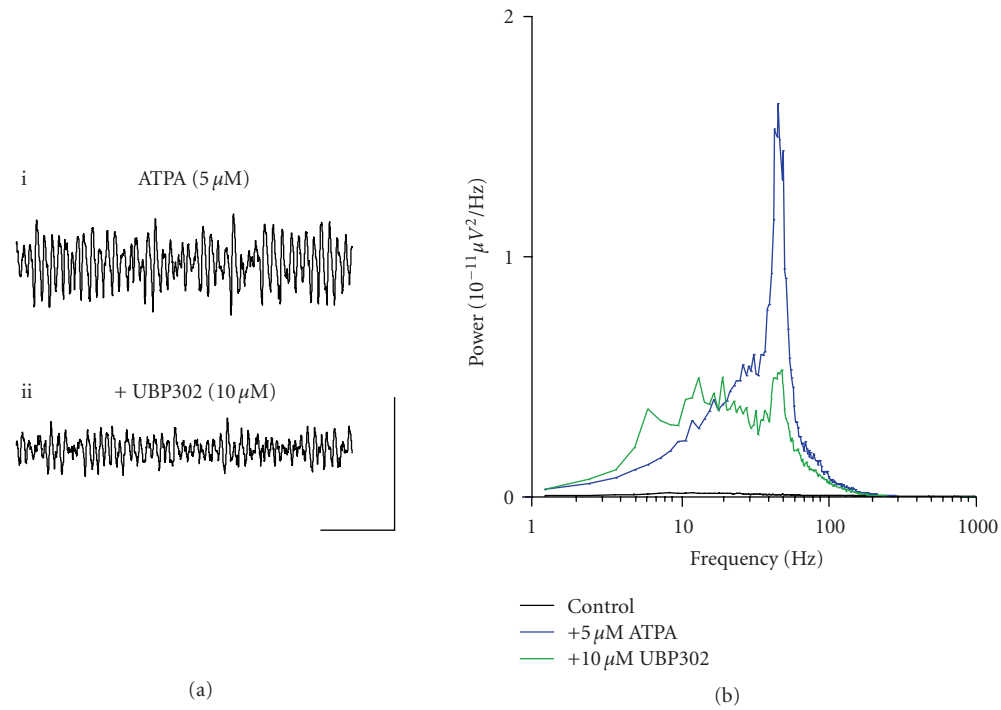

Figure 5: ATPA-generated gamma frequency oscillations in the MEC are reduced by application of the GLU_{K5} selective antagonist, UBP302. (a) Extracellular field recordings showing 1 second epochs of activity (i) in the presence of 5 μM ATPA and (ii) following application of 10 μM UBP302. (b) Pooled power spectra ($n = 4$) produced from 60 second epochs of extracellular field recorded data, showing a control recording (black), recording in the presence of 5 μM ATPA (blue), and application of 10 μM UBP302 (green). Scale bar represents 200 milliseconds and 100 μV.

frequency oscillations were not reversible on washout ($n = 12$).

3.5. A role for GLU_{K5}-containing KARs in carbachol-induced gamma oscillations

Cortical gamma frequency oscillations can also be induced by application of carbachol, an agonist at muscarinic acetylcholine receptors (mAChRs) [24, 25, 45–49]. It is unclear as to the role of GLU_{K5}-containing KARs in a cholinergic-mediated gamma frequency oscillation in the MEC. Carbachol will cause an increase in the release of glutamate in the form of rhythmic EPSPs [46]. This, in turn, may lead to activation of KARs [50]. In agreement with previous studies in the MEC [24, 25] bath application of carbachol (10–20 μM) generated persistent gamma frequency oscillations ($n = 6$) (Figure 8(a)i). Application of UBP302 (10 μM) had no significant effect on the frequency (control, 41.7 ± 1.6 Hz; *v.* UBP302, 40.3 ± 0.6 Hz; $P > .1$; $n = 6$), peak amplitude (control, 5.9 ± 3.1 μV^2/Hz; *v.* UBP302, 5.5 ± 2.5 μV^2/Hz; $P > .1$; $n = 6$) or power (control, 155.2 ± 72.7 μV^2/Hz.Hz; *v.* UBP302, 148.7 ± 62.8 μV^2/Hz.Hz; $P > .1$; $n = 6$) of preestablished carbachol-driven gamma oscillations (Figures 8(a)ii, 8(b)). This lack of effect was further demonstrated by washout back into carbachol causing no significant change in observed gamma frequency oscillations (Figures 8(a)iii, 8(b)).

4. DISCUSSION

A number of studies have examined the contribution of various KAR subunits to gamma frequency oscillations in the hippocampus in vitro. Fisahn et al. [10] focused on the roles of GLU_{K5} and GLU_{K6} subunits in kainate-induced hippocampal gamma oscillations, using brain slices from transgenic GLU_{K5} and GLU_{K6} receptor knockout mice. Knockout of GLU_{K5} caused increased sensitivity of the hippocampal network to the effects of kainate and higher susceptibility to oscillatory and epileptogenic activity. Slices from GLU_{K6}-knockout mice could not support kainate-induced gamma oscillations or epileptiform activity, suggesting distinct roles for GLU_{K5} and GLU_{K6} subunits in the hippocampus. Fisahn et al. [10] concluded that GLU_{K5}-containing receptors may be expressed on axons of hippocampal interneurons and have a function in inhibitory tone, and that GLU_{K6}-containing KARs may be found in the somatodendritic region of pyramidal cells and interneurons, and provide excitatory drive. Functional receptors of both subtypes must interact to allow generation of stable gamma oscillations in the hippocampus [9, 10].

Subsequently, Brown et al. [51] used pharmacological approaches to investigate the role of GLU_{K5}-containing receptors in hippocampal gamma oscillations. This study used the GLU_{K5}-selective agonists ATPA and iodowillardiine but found that neither could induce gamma network activity in area CA3 of rat hippocampal slices. The GLU_{K5} selective

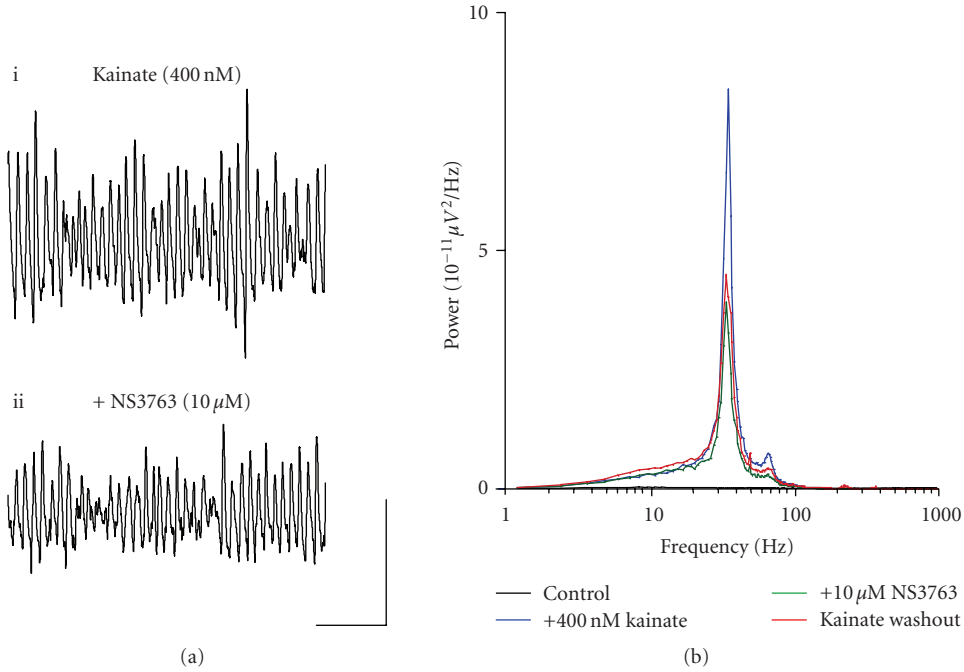

Figure 6: Blocking homomeric GLU_{K5}-containing KARs significantly reduces kainate-driven gamma frequency oscillations in the MEC. (a) Extracellular field recordings showing 1 second epochs of activity (i) in the presence of 400 nM kainate and (ii) following application of 10 μM NS3763. (b) Pooled power spectra ($n = 8$) produced from 60 second epochs of extracellular field recorded data, showing a control recording (black), recording in the presence of 400 nM kainate (blue), application of 10 μM NS3763 (green), and a washout back into 400 nM kainate (red). Scale bar represents 200 milliseconds and 100 μV.

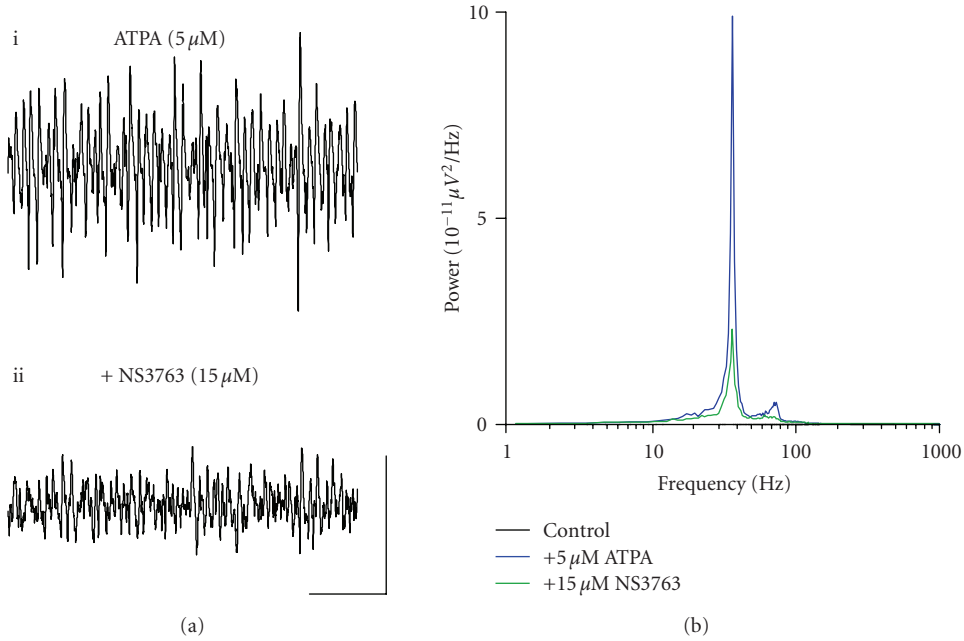

Figure 7: Blocking homomeric GLU_{K5}-containing KARs effectively reduces power and amplitude of ATPA-generated gamma frequency oscillations in the MEC (a) Extracellular field recordings showing 1 second epochs of activity (i) in the presence of 5 μM ATPA and (ii) following application of 15 μM NS3763. (b) Pooled power spectra ($n = 4$) produced from 60 second epochs of extracellular field recorded data, showing a control recording (black), recording in the presence of 5 μM ATPA (blue), and application of 15 μM NS3763 (green). Scale bar represents 200 milliseconds and 100 μV.

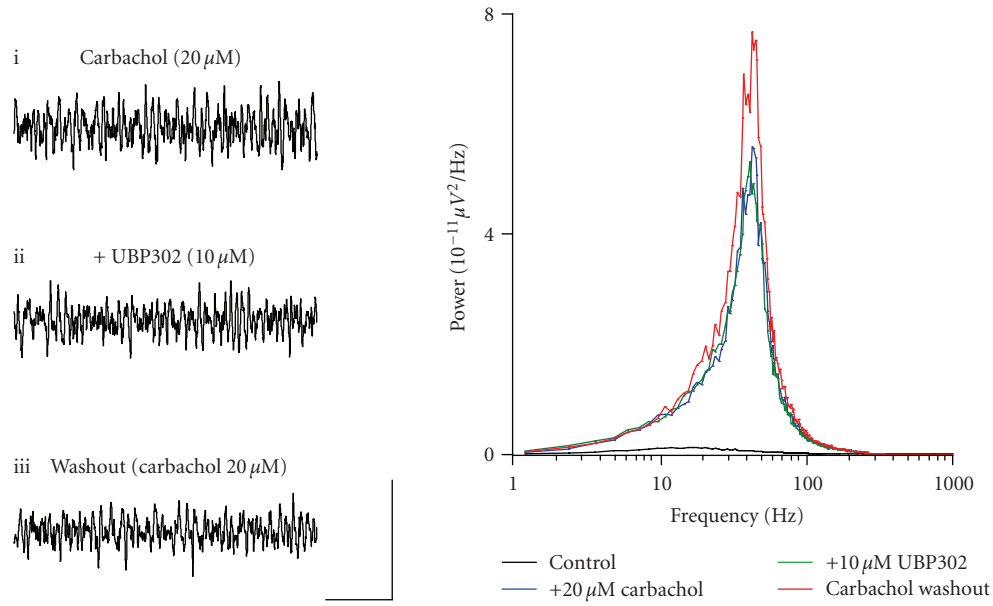

Figure 8: Carbachol-induced gamma frequency oscillations are not dependent on GLU_{K5}-containing KARs. (a) Extracellular field recordings showing 1 second epochs of activity (i) in the presence of 20 μM carbachol, (ii) following 10 μM UBP302 application, and (iii) during a washout period into 20 μM carbcahol. (b) Pooled power spectra ($n = 6$) produced from 60 second epochs of extracellular field recorded data, showing a control recording (black), recording in the presence of 20 μM carbachol (blue), application of 10 μM UBP302 (green), and washout back into 20 μM carbachol (red). Scale bar represents 200 milliseconds and 100 μV.

antagonist, UBP296, when preincubated with hippocampal slices, did not prevent induction of kainate-driven gamma oscillations. However, UBP296 produced an approximately 50% reduction in the power of preestablished kainate-induced gamma frequency oscillations. This paper concluded that GLU_{K5}-containing KARs alone cannot generate gamma oscillations in the hippocampus but may be involved in maintenance of hippocampal gamma activity generated through other KAR subtypes.

In the present study, we have demonstrated that, similarly to in the hippocampus [51], GLU_{K5}-containing KARs in the MEC have a role in the maintenance of kainate-driven oscillations. UBP302, a GLU_{K5} selective antagonist, caused reductions in peak amplitude and spectral power of preestablished kainate-induced gamma frequency oscillations in the MEC. Furthermore, pretreatment of slices with UBP302 partially inhibited generation of kainate-induced gamma frequency oscillations, suggesting that GLU_{K5}-containing KARs are at least partially responsible for the induction of gamma oscillations by kainate application. These data suggest that in the MEC, differently to in the hippocampus [5, 8, 9], activation of GLU_{K5}-containing KARs plays a role in the ability of MEC neuronal networks to generate gamma frequency oscillations. Moreover, in contrast to hippocampal gamma evoked by kainate, MEC gamma generated with GLU_{K5} agonists demonstrates a frequency increment with increased excitatory drive. This may reflect the manifestation of fundamentally different mechanisms of local circuit gamma oscillation generation in these two regions.

It was not surprising then that application of the GLU_{K5} subunit selective agonist ATPA [41] successfully evoked gamma frequency oscillations in the MEC. However, care must be taken with interpretation of this data as ATPA has recently been shown not to be entirely selective for GLU_{K5}-containing KARs [40]. In fact, ATPA can activate both homomeric and heteromeric KAR complexes containing GLU_{K5}, and also GLU_{K6}/KA2 heteromeric KARs [48]. Thus, it cannot initially be assumed that these gamma oscillations have been generated via GLU_{K5}-containing receptor complexes, since they could have been induced through GLU_{K6}/KA2 heteromeric receptors. UBP302, however, is an antagonist with selectivity for GLU_{K5}-containing KARs [36, 37]. Whilst UBP302 has been shown to block GLU_{K7} with an IC_{50} value of 4 μM—this makes it ~10-fold selective for GLU_{K5} versus GLU_{K7}—it does not have activity on GLU_{K6} or GLU_{K6}/KA2 up to 100 μM. Indeed, some controversy surrounds the activity of UBP302 on GLU_{K7} as it has been reported that UBP302 failed to demonstrate any potent activity in a binding assay on GLU_{K7} (personal communication, D.E. Jane). In any case, as UBP302 only blocks homomeric GLU_{K7} and activation of GLU_{K7} requires very high glutamate concentrations (EC_{50} value 5.9 mM) [52] it may not be relevant to this study. Application of UBP302 onto slices showing ATPA-generated network activity causes reduced peak amplitude and an approximately 60% reduction in area power of gamma frequency oscillations. This inhibition of ATPA-generated gamma oscillations by UBP302 suggests that the observed activity must, at least in part, be due to activation of GLU_{K5}-containing KARs.

Moreover, NS3763 application caused a significant reduction in peak amplitude and spectral power of preestablished kainate-driven gamma oscillations. This demonstrates that homomeric GLU_{K5}-containing KARs are at least partially responsible for the maintenance of these kainate-driven gamma frequency oscillations. Application of NS3763 to preestablished ATPA-generated oscillations caused an approximately 80% reduction in area power of gamma frequency oscillations and also a reduction in peak amplitude. This suggests that a large component of an ATPA-driven gamma oscillation is maintained through homomeric GLU_{K5} KARs. The activity of the selective homomeric GLU_{K5}-containing KAR antagonist, NS3763, on both kainate- and ATPA-generated gamma frequency oscillations, tells us that homomeric GLU_{K5}-containing KARs are involved in the observed network activity.

It has been suggested that carbachol-driven activity could cause excess glutamate release and that this overspill of glutamate could activate KARs [50]. The lack of effect of the GLU_{K5} selective antagonist, UBP302, on carbachol-induced gamma oscillations in the MEC suggests that GLU_{K5}-containing KARs are not involved in the generation or maintenance of gamma oscillations induced via activation of muscarinic cholinergic receptor. However, we cannot rule out the possibility that other KAR subtypes may be involved in these mAChR-mediated gamma oscillations.

We have shown that GLU_{K5}-containing KARs are implicated in the generation and maintenance of gamma frequency oscillations in the MEC evoked by kainate. However, we can only speculate on the cellular localisation of these GLU_{K5}-containing receptors in the MEC. Research performed by Christensen et al. [40] in the hippocampus, suggested likely localisations of KAR subtypes in hippocampal CA1 inhibitory interneurons terminating with pyramidal cells, concluding that heteromeric GLU_{K6}/KA2 receptors are expressed in somatodendritic compartments of interneurons, and that GLU_{K5} complexes, with either GLU_{K6} or KA2, are found at presynaptic terminals. It seems likely from our results that in the MEC, both homomeric and heteromeric GLU_{K5}-containing KARs are present.

Presynaptic KARs are involved in regulation and modulation of neurotransmitter release at inhibitory and excitatory synapses in the hippocampus [50, 53, 54]. In contrast, postsynaptic KARs mediate excitatory postsynaptic currents (EPSCs) in many brain regions [35, 55]. KAR activation in the hippocampus modulates GABA release at terminals of inhibitory interneurons and causes an increase in spontaneous IPSCs but a reduction in the amplitude of these IPSCs impinging on to CA1 interneurons [40]. This suggests that KARs may be present in two distinct populations in hippocampal inhibitory interneurons, and the same may be true of KARs in the MEC [2, 40]. However, other reports have demonstrated that kainate can increase the frequency and amplitude of spontaneous IPSCs, but not action potential-independent miniature IPSCs in stratum radiatum interneurons [56]. Moreover, these authors also observed that kainate can directly depolarise the axonal plexus of inhibitory interneurons producing both increased antidromic and presumably orthodromic spiking. This effect would explain the ability of KAR activation to increase spontaneous but not miniature IPSC activity. The presence of KARs at an axonal loci has been well documented in the hippocampus, most notably in mossy fibres [57, 58].

As outlined in the previous paragraph, there is a large corpus of data on the role of KAR in the hippocampus. However, with respect to the MEC there is a paucity of such information. In order to put the current results presented in this paper into context, future work will concentrate on combining intracellular recordings from individual neurones (pyramidal and interneuron), specific pharmacological KAR tools, and transgenic KAR subunit knockout animals [9, 10] to elucidate the exact nature of cellular expression of KARs in the MEC.

REFERENCES

[1] M. Hollmann and S. Heinemann, "Cloned glutamate receptors," *Annual Review of Neuroscience*, vol. 17, pp. 31–108, 1994.

[2] J. Lerma, A. V. Paternain, A. Rodríguez-Moreno, and J. C. López-García, "Molecular physiology of kainate receptors," *Physiological Reviews*, vol. 81, no. 3, pp. 971–998, 2001.

[3] W. Wisden and P. H. Seeburg, "A complex mosaic of high-affinity kainate receptors in rat brain," *The Journal of Neuroscience*, vol. 13, no. 8, pp. 3582–3598, 1993.

[4] B. Bettler and C. Mulle, "Neurotransmitter receptors II. AMPA and kainate receptors," *Neuropharmacology*, vol. 34, no. 2, pp. 123–139, 1995.

[5] P. Werner, M. Voigt, K. Keinanen, W. Wisden, and P. H. Seeburg, "Cloning of a putative high-affinity kainate receptor expressed predominantly in hippocampal CA3 cells," *Nature*, vol. 351, no. 6329, pp. 742–744, 1991.

[6] A. Herb, N. Burnashev, P. Werner, B. Sakmann, W. Wisden, and P. H. Seeburg, "The KA-2 subunit of excitatory amino acid receptors shows widespread expression in brain and forms ion channels with distantly related subunits," *Neuron*, vol. 8, no. 4, pp. 775–785, 1992.

[7] R. Chittajallu, S. P. Braithwaite, V. R. J. Clarke, and J. M. Henley, "Kainate receptors: subunits, synaptic localization and function," *Trends in Pharmacological Sciences*, vol. 20, no. 1, pp. 26–35, 1999.

[8] C. Cui and M. L. Mayer, "Heteromeric kainate receptors formed by the coassembly of GluR5, GluR6, and GluR7," *The Journal of Neuroscience*, vol. 19, no. 19, pp. 8281–8291, 1999.

[9] A. Fisahn, "Kainate receptors and rhythmic activity in neuronal networks: hippocampal gamma oscillations as a tool," *The Journal of Physiology*, vol. 562, no. 1, pp. 65–72, 2005.

[10] A. Fisahn, A. Contractor, R. D. Traub, E. H. Buhl, S. F. Heinemann, and C. J. McBain, "Distinct roles for the kainate receptor subunits GluR5 and GluR6 in kainate-induced hippocampal gamma oscillations," *The Journal of Neuroscience*, vol. 24, no. 43, pp. 9658–9668, 2004.

[11] A. Bragin, G. Jandó, Z. Nádasdy, J. Hetke, K. Wise, and G. Buzsáki, "Gamma (40–100 Hz) oscillation in the hippocampus of the behaving rat," *The Journal of Neuroscience*, vol. 15, no. 1, pp. 47–60, 1995.

[12] J. J. Chrobak and G. Buzsáki, "Gamma oscillations in the entorhinal cortex of the freely behaving rat," *The Journal of Neuroscience*, vol. 18, no. 1, pp. 388–398, 1998.

[13] J. Csicsvari, B. Jamieson, K. D. Wise, and G. Buzsáki, "Mechanisms of gamma oscillations in the hippocampus of the behaving rat," *Neuron*, vol. 37, no. 2, pp. 311–322, 2003.

[14] A. K. Engel and W. Singer, "Temporal binding and the neural correlates of sensory awareness," *Trends in Cognitive Sciences*, vol. 5, no. 1, pp. 16–25, 2001.

[15] W. Singer, "Synchronization of cortical activity and its putative role in information processing and learning," *Annual Review of Physiology*, vol. 55, pp. 349–374, 1993.

[16] C. M. Gray, P. König, A. K. Engel, and W. Singer, "Oscillatory responses in cat visual cortex exhibit inter-columnar synchronization which reflects global stimulus properties," *Nature*, vol. 388, no. 6213, pp. 334–337, 1989.

[17] J. Fell, P. Klaver, K. Lehnertz, et al., "Human memory formation is accompanied by rhinal-hippocampal coupling and decoupling," *Nature Neuroscience*, vol. 4, no. 12, pp. 1259–1264, 2001.

[18] J. Fell, P. Klaver, C. E. Elger, and G. Fernández, "The interaction of rhinal cortex and hippocampus in human declarative memory formation," *Reviews in the Neurosciences*, vol. 13, no. 4, pp. 299–312, 2002.

[19] D. Muller, I. Nikonenko, P. Jourdain, and S. Alberi, "LTP, memory and structural plasticity," *Current Molecular Medicine*, vol. 2, no. 7, pp. 605–611, 2002.

[20] W. Singer and C. M. Gray, "Visual feature integration and the temporal correlation hypothesis," *Annual Review of Neuroscience*, vol. 18, pp. 555–586, 1995.

[21] R. D. Traub, N. Spruston, I. Soltesz, A. Konnerth, M. A. Whittington, and J. G. R. Jefferys, "Gamma-frequency oscillations: a neuronal population phenomenon, regulated by synaptic and intrinsic cellular processes, and inducing synaptic plasticity," *Progress in Neurobiology*, vol. 55, no. 6, pp. 563–575, 1998.

[22] N. Hirai, S. Uchida, T. Maehara, Y. Okubo, and H. Shimizu, "Enhanced gamma (30–150 Hz) frequency in the human medial temporal lobe," *Neuroscience*, vol. 90, no. 4, pp. 1149–1155, 1999.

[23] S. Uchida, T. Maehara, N. Hirai, Y. Okubo, and H. Shimizu, "Cortical oscillations in human medial temporal lobe during wakefulness and all-night sleep," *Brain Research*, vol. 891, no. 1-2, pp. 7–19, 2001.

[24] S. Van der Linden, F. Panzica, and M. de Curtis, "Carbachol induces fast oscillations in the medial but not in the lateral entorhinal cortex of the isolated guinea pig brain," *Journal of Neurophysiology*, vol. 82, no. 5, pp. 2441–2450, 1999.

[25] C. T. Dickson, G. Biella, and M. de Curtis, "Evidence for spatial modules mediated by temporal synchronization of carbachol-induced gamma rhythm in medial entorhinal cortex," *The Journal of Neuroscience*, vol. 20, no. 20, pp. 7846–7854, 2000.

[26] M. O. Cunningham, C. H. Davies, E. H. Buhl, N. Kopell, and M. A. Whittington, "Gamma oscillations induced by kainate receptor activation in the entorhinal cortex in vitro," *The Journal of Neuroscience*, vol. 23, no. 30, pp. 9761–9769, 2003.

[27] M. O. Cunningham, D. M. Halliday, C. H. Davies, R. D. Traub, E. H. Buhl, and M. A. Whittington, "Coexistence of gamma and high-frequency oscillations in rat medial entorhinal cortex in vitro," *The Journal of Physiology*, vol. 559, no. 2, pp. 347–353, 2004.

[28] M. O. Cunningham, J. Hunt, S. Middleton, et al., "Region-specific reduction in entorhinal gamma oscillations and parvalbumin-immunoreactive neurons in animal models of psychiatric illness," *The Journal of Neuroscience*, vol. 26, no. 10, pp. 2767–2776, 2006.

[29] M. A. Whittington, R. D. Traub, and J. G. R. Jefferys, "Synchronized oscillation in interneuron networks driven by metabotropic glutamate receptor activation," *Nature*, vol. 373, no. 6515, pp. 612–615, 1995.

[30] N. Hájos, J. Pálhalini, E. O. Mann, B. Nèmeth, O. Paulsen, and T. F. Freund, "Spike timing of distinct types of GABAergic interneuron during hippocampal gamma oscillations in vitro," *The Journal of Neuroscience*, vol. 24, no. 41, pp. 9127–9137, 2004.

[31] T. Gloveli, T. Dugladze, S. Saha, et al., "Differential involvement of oriens/pyramidale interneurones in hippocampal network oscillations in vitro," *The Journal of Physiology*, vol. 562, no. 1, pp. 131–147, 2005.

[32] M. A. Whittington and R. D. Traub, "*Interneuron Diversity series*: inhibitory interneurons and network oscillations in vitro," *Trends in Neurosciences*, vol. 26, no. 12, pp. 676–682, 2003.

[33] M. O. Cunningham, M. A. Whittington, A. Bibbig, et al., "A role for fast rhythmic bursting neurons in cortical gamma oscillations in vitro," *Proceedings of the National Academy of Sciences of the United States of America*, vol. 101, no. 18, pp. 7152–7157, 2004.

[34] I. Bureau, S. Bischoff, S. F. Heinemann, and C. Mulle, "Kainate receptor-mediated responses in the CA1 field of wild-type and GluR6-deficient mice," *The Journal of Neuroscience*, vol. 19, no. 2, pp. 653–663, 1999.

[35] R. Cossart, M. Esclapez, J. C. Hirsch, C. Bernard, and Y. Ben-Ari, "GluR5 kainate receptor activation in interneurons increases tonic inhibition of pyramidal cells," *Nature Neuroscience*, vol. 1, no. 6, pp. 470–478, 1998.

[36] J. C. A. More, R. Nistico, N. P. Dolman, et al., "Characterisation of UBP296: a novel, potent and selective kainate receptor antagonist," *Neuropharmacology*, vol. 47, no. 1, pp. 46–64, 2004.

[37] N. P. Dolman, H. M. Troop, J. C. A. More, et al., "Synthesis and pharmacology of willardiine derivatives acting as antagonists of kainate receptors," *Journal of Medicinal Chemistry*, vol. 48, no. 24, pp. 7867–7881, 2005.

[38] D. Perrais, P. S. Pineiro, D. E. Jane, and C. Mulle, "Antagonism of recombinant and native GluR7-containing receptors: new tools to study presynaptic kainate receptors," submitted to *Neuropharmacology*.

[39] J. K. Christensen, T. Varming, P. K. Ahring, T. D. Jorgensen, and E. O. Nielsen, "In vitro characterisation of 5-carbozyl-2,4-di-benzamido-benzoic acid (NS3763), a non-competitive antagonist of GLU_{K5} receptors," *The Journal of Pharmacology and Experimental Theraputics*, vol. 309, pp. 1003–1010, 2004.

[40] J. K. Christensen, A. V. Paternain, S. Selak, P. K. Ahring, and J. Lerma, "A mosaic of functional kainate receptors in hippocampal interneurons," *The Journal of Neuroscience*, vol. 24, no. 41, pp. 8986–8993, 2004.

[41] V. R. J. Clarke, B. A. Ballyk, K. H. Hoo, et al., "A hippocampal GluR5 kainate receptor regulating inhibitory synaptic transmission," *Nature*, vol. 389, no. 6651, pp. 599–603, 1997.

[42] V. R. J. Clarke and G. L. Collingridge, "Characterisation of the effects of ATPA, a GLU_{K5} receptor selective agonist, on excitatory synaptic transmission in area CA1 of rat hippocampal slices," *Neuropharmacology*, vol. 42, no. 7, pp. 889–902, 2002.

[43] V. R. J. Clarke and G. L. Collingridge, "Characterisation of the effects of ATPA, a GLU_{K5} kainate receptor agonist, on GABAergic synaptic transmission in the CA1 region of rat hippocampal slices," *Neuropharmacology*, vol. 47, no. 3, pp. 363–372, 2004.

[44] S. L. Campbell, S. S. Mathew, and J. J. Hablitz, "Pre- and postsynaptic effects of kainate on layer II/III pyramidal cells in rat neocortex," *Neuropharmacology*, vol. 53, no. 1, pp. 37–47, 2007.

[45] A. Fisahn, F. G. Pike, E. H. Buhl, and O. Paulsen, "Cholinergic induction of network oscillations at 40 Hz in the hippocampus in vitro," *Nature*, vol. 394, no. 6689, pp. 186–189, 1998.

[46] R. D. Traub, A. Bibbig, A. Fisahn, F. E. N. Lebeau, M. A. Whittington, and E. H. Buhl, "A model of gamma-frequency network oscillations induced in the rat CA3 region by carbachol in vitro," *European Journal of Neuroscience*, vol. 12, no. 11, pp. 4093–4106, 2000.

[47] S. G. Hormuzdi, I. Pais, F. E. N. LeBeau, et al., "Impaired electrical signaling disrupts gamma frequency oscillations in connexin 36-deficient mice," *Neuron*, vol. 31, no. 3, pp. 487–495, 2001.

[48] J. Pálhalmi, O. Paulsen, T. F. Freund, and N. Hájos, "Distinct properties of carbachol- and DHPG-induced network oscillations in hippocampal slices," *Neuropharmacology*, vol. 47, no. 3, pp. 381–389, 2004.

[49] E. O. Mann, J. M. Suckling, N. Hajos, S. A. Greenfield, and O. Paulsen, "Perisomatic feedback inhibition underlies cholinergically induced fast network oscillations in the rat hippocampus in vitro," *Neuron*, vol. 45, no. 1, pp. 105–117, 2005.

[50] S. E. Lauri, M. Segerstråle, A. Vesikansa, et al., "Endogenous activation of kainate receptors regulates glutamate release and network activity in the developing hippocampus," *The Journal of Neuroscience*, vol. 25, no. 18, pp. 4473–4484, 2005.

[51] J. T. Brown, A. Teriakidis, and A. D. Randall, "A pharmacological investigation of the role of GLU_{K5}-containing receptors in kainate-driven hippocampal gamma band oscillations," *Neuropharmacology*, vol. 50, no. 1, pp. 47–56, 2006.

[52] H. H. Schiffer, G. T. Swanson, and S. F. Heinemann, "Rat GluR7 and a carboxy-terminal splice variant, GluR7b, are functional kainate receptor subunits with a low sensitivity to glutamate," *Neuron*, vol. 19, no. 5, pp. 1141–1146, 1997.

[53] A. Contractor, G. Swanson, and S. F. Heinemann, "Kainate receptors are involved in short- and long-term plasticity at mossy fiber synapses in the hippocampus," *Neuron*, vol. 29, no. 1, pp. 209–216, 2001.

[54] A. Contractor, A. W. Sailer, M. Darstein, et al., "Loss of kainate receptor-mediated heterosynaptic facilitation of mossy-fiber synapses in $KA2^{-/-}$ mice," *The Journal of Neuroscience*, vol. 23, no. 2, pp. 422–429, 2003.

[55] M. Vignes and G. L. Collingridge, "The synaptic activation of kainate receptors," *Nature*, vol. 388, no. 6638, pp. 179–182, 1997.

[56] A. Semyanov and D. M. Kullmann, "Kainate receptor-dependent axonal depolarization and action potential initiation in interneurons," *Nature Neuroscience*, vol. 4, no. 7, pp. 718–723, 2001.

[57] H. Kamiya and S. Ozawa, "Kainate receptor-mediated presynaptic inhibition at the mouse hippocampal mossy fibre synapse," *The Journal of Physiology*, vol. 523, no. 3, pp. 653–665, 2000.

[58] D. Schmitz, M. Frerking, and R. A. Nicoll, "Synaptic activation of presynaptic kainate receptors on hippocampal mossy fiber synapses," *Neuron*, vol. 27, no. 2, pp. 327–338, 2000.

Hindawi Publishing Corporation
Neural Plasticity
Volume 2008, Article ID 808564, 12 pages
doi:10.1155/2008/808564

Research Article

Modulation of Network Oscillatory Activity and GABAergic Synaptic Transmission by CB1 Cannabinoid Receptors in the Rat Medial Entorhinal Cortex

Nicola H. Morgan, Ian M. Stanford, and Gavin L. Woodhall

School of Life and Health Sciences, Aston University, Aston Triangle, Birmingham B4 7ET, UK

Correspondence should be addressed to Gavin L. Woodhall, g.l.woodhall@aston.ac.uk

Received 1 April 2008; Accepted 19 June 2008

Recommended by Roland S. G. Jones

Cannabinoids modulate inhibitory GABAergic neurotransmission in many brain regions. Within the temporal lobe, cannabinoid receptors are highly expressed, and are located presynaptically at inhibitory terminals. Here, we have explored the role of type-1 cannabinoid receptors (CB1Rs) at the level of inhibitory synaptic currents and field-recorded network oscillations. We report that arachidonylcyclopropylamide (ACPA; 10 μM), an agonist at CB1R, inhibits GABAergic synaptic transmission onto both superficial and deep medial entorhinal (mEC) neurones, but this has little effect on network oscillations in beta/gamma frequency bands. By contrast, the CB1R antagonist/inverse agonist LY320135 (500 nM), increased GABAergic synaptic activity and beta/gamma oscillatory activity in superficial mEC, was suppressed, whilst that in deep mEC was enhanced. These data indicate that cannabinoid-mediated effects on inhibitory synaptic activity may be constitutively active in vitro, and that modulation of CB1R activation using inverse agonists unmasks complex effects of CBR function on network activity.

Copyright © 2008 Nicola H. Morgan et al. This is an open access article distributed under the Creative Commons Attribution License, which permits unrestricted use, distribution, and reproduction in any medium, provided the original work is properly cited.

1. INTRODUCTION

Cannabinoid receptors are a family of G-protein coupled, presynaptic receptors [1, 2]. Autoradiography studies using the cannabinoid receptor ligand CP55,940 [3–5] show that CB1Rs are distributed throughout neuronal tissue. These studies report a dense binding of CP55,940 in the basal ganglia, specifically the substantia nigra *pars reticulata* the globus pallidus (GP) and also in cerebellum. In the cerebrum, the hippocampal formation and the entorhinal cortex (EC) show the highest density of staining for CB1R.

Cannabinoids are known to exert powerful control over GABAergic inhibitory signalling in the CNS [6–8], and it is reported that CB1R inhibition of $GABA_A$ receptor mediated synaptic transmission occurs through the inhibition of voltage-dependent calcium channels (VGCCs; [6]). In the hippocampus, the activation of presynaptic CB1R depresses GABA release onto postsynaptic target cells [9, 10], and in these studies, endogenous and exogenous CB1R agonists have been shown to reduce the amplitude and frequency of GABAergic spontaneous inhibitory postsynaptic currents (sIPSCs), but not to affect action-potential-independent miniature (m)IPSCs. Other studies have shown that cannabinoid receptor activation enhances network oscillatory activity [11]. However, in the parahippocampal region (PHR), the effects of cannabinoid receptors are less well described. Here, we have investigated the functional effects of CBRs on neuronal network activity modelled in vitro by kainate (KA-) induced persistent oscillations [8, 12]. Persistent oscillatory activity in the gamma frequency band (30–80 Hz) has been the most commonly reported and studied form of network activity in the in vitro slice preparation, and can be elicited by metabotropic glutamate receptors [13] or application of kainic acid [8, 12] and/or the muscarinic agonist carbachol Neuronal network oscillatory activity reflects the phasic inhibition of principal cells by GABAergic interneurones, which act to entrain and synchronize principal cell activity (Cobb et al., [14]). The mEC has been reported to express gamma oscillations (30–100 Hz) in response to application

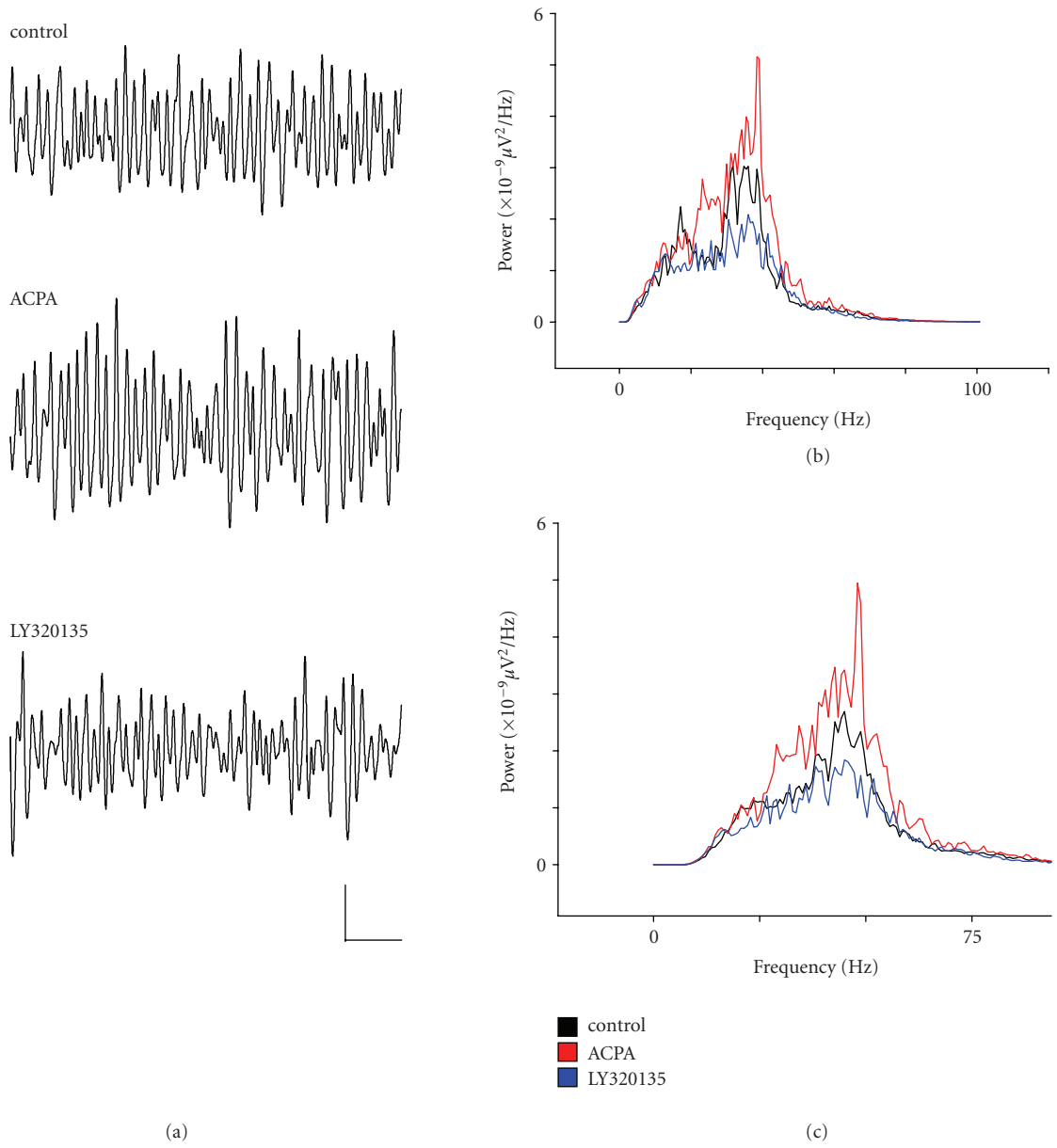

Figure 1: The effects of ACPA and LY320135 on γ-band activity in mEC layer II. (a) Example traces from layer II showing γ-oscillations under conditions in which ACPA (10 μM) or LY320135 (500 nM) were applied. (b) Plot of power spectral density during drug application (filtered between 2–100 Hz). Control (black line), ACPA (red line), LY320135 (blue line). (c) Similar plot to (b) bandpass filtered between 30–90 Hz. Scale bar = 200 milliseconds $\times$ 100 μV.

of nanomolar concentrations of kainate [15, 16], and oscillatory power was greatest in superficial layers II/III [15].

2. MATERIALS AND METHODS

Combined EC-hippocampal slices were prepared from young male Wistar rats (50–110 g) as previously described [17]. All experiments were performed in accordance with the UK Animals (Scientific Procedures) Act 1986 and European Communities Council Directive 1986 (86/609/EEC). Rats were anaesthetised with isoflurane and N_2/O_2, until cardiorespiratory arrest, and decapitated. The brain was rapidly removed and immersed in oxygenated artificial cerebrospinal fluid (ACSF) chilled to 4°C. Slices (450 μm) were cut using a vibrating microtome (MicroM, Germany), and stored in ACSF continuously bubbled with 95% O_2/5% CO_2, at room temperature. Following a recovery period of at least 1 hour, individual slices were transferred to a recording chamber mounted on the stage of an Olympus (BX50WI) upright microscope. The chamber was continuously perfused with oxygenated ACSF at 30–32°C, at a flow rate of approximately 2 mL/min. The ACSF contained the following (in mM): NaCl (126), KCl (3.25), NaH_2PO_4 (1.25), $NaHCO_3$ (24), $MgSO_4$ (2), $CaCl_2$ (2.5), and D-glucose (10). The solution

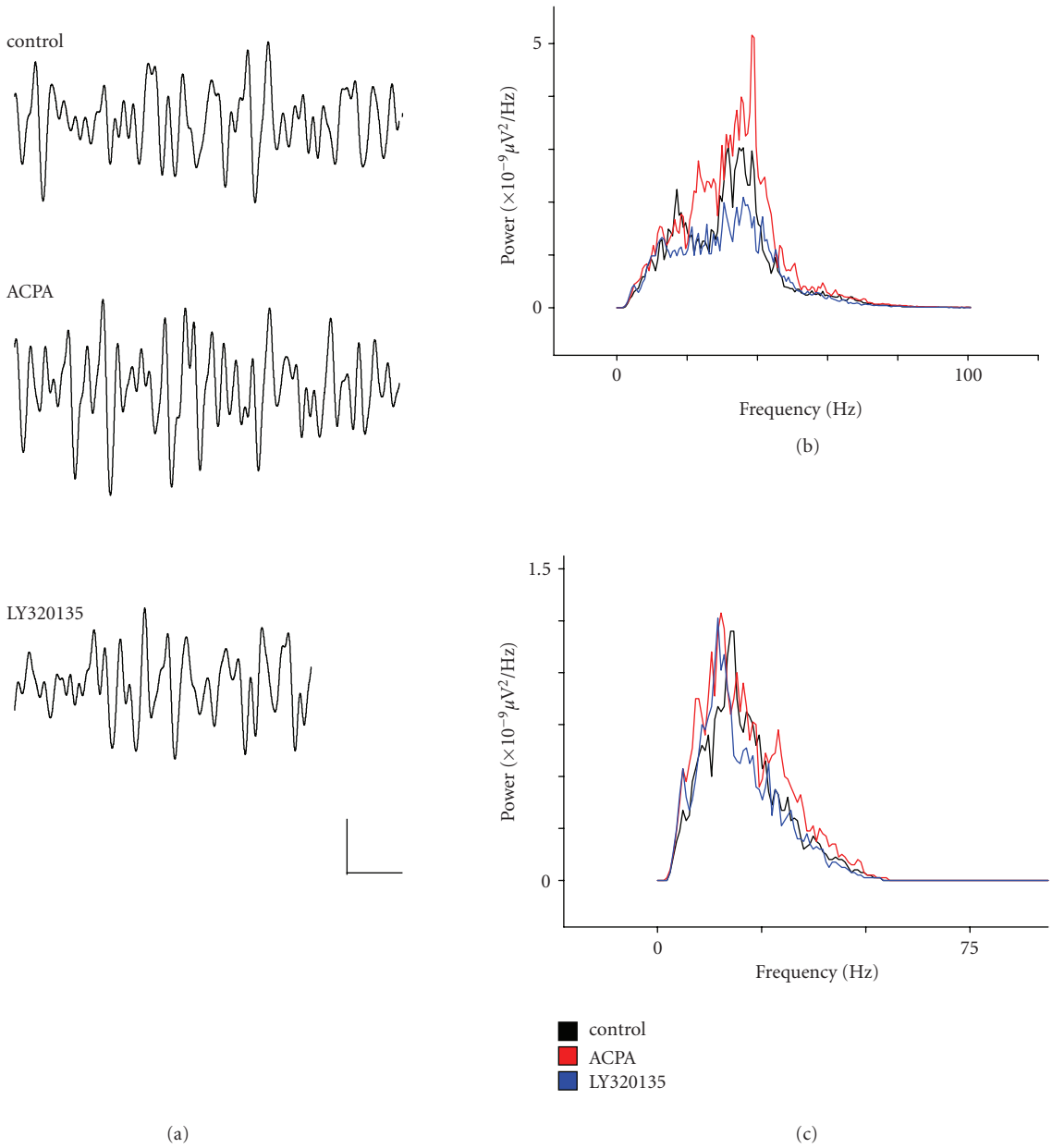

Figure 2: The effects of ACPA and LY320135 on β-band activity in mEC layer II. (a) Example traces from layer II showing β-oscillations under conditions in which ACPA (10 μM) or LY320135 (500 nM) were applied. (b) Plot of power spectral density during drug application (filtered between 2–100 Hz). Control (black line), ACPA (red line), LY320135 (blue line). (c) Similar plot to (b) bandpass filtered between 15–29 Hz. Scale bar = 200 milliseconds $\times$ 50 μV.

was continuously bubbled with 95% O_2/5% CO_2 to maintain a pH of 7.4. Neurones were visualized using differential interference contrast optics and an infrared video camera.

Patch-clamp electrodes were pulled from borosilicate glass (1.2 mm OD, 0.69 ID; Harvard Apparatus) and had open tip resistances of 4-5 MΩ. They were filled with a solution containing the following (in mM): CsCl (90), HEPES (33), QX-314 (5), EGTA (0.6), $MgCl_2$ (5.0), TEA-Cl (10), phosophocreatine (7) ATP (4), GTP (0.4). The solution was adjusted to 290 mOsmol with sucrose and to pH 7.4 with CsOH. Whole-cell voltage clamp recordings were made from neurones in layers II and V of the medial division of the EC, using an Axopatch 700 series amplifier (Molecular Devices, USA). The holding potential in all cases was –70 mV. Under these experimental conditions, layer II/V neurones exhibited sIPSCs, mediated by GABA acting primarily at $GABA_A$ receptors.

Data were recorded directly to computer hard disk using AxoScope software (Molecular Devices, USA). Mini Analysis (Synaptosoft, USA) was used for analysis of sIPSCs offline.

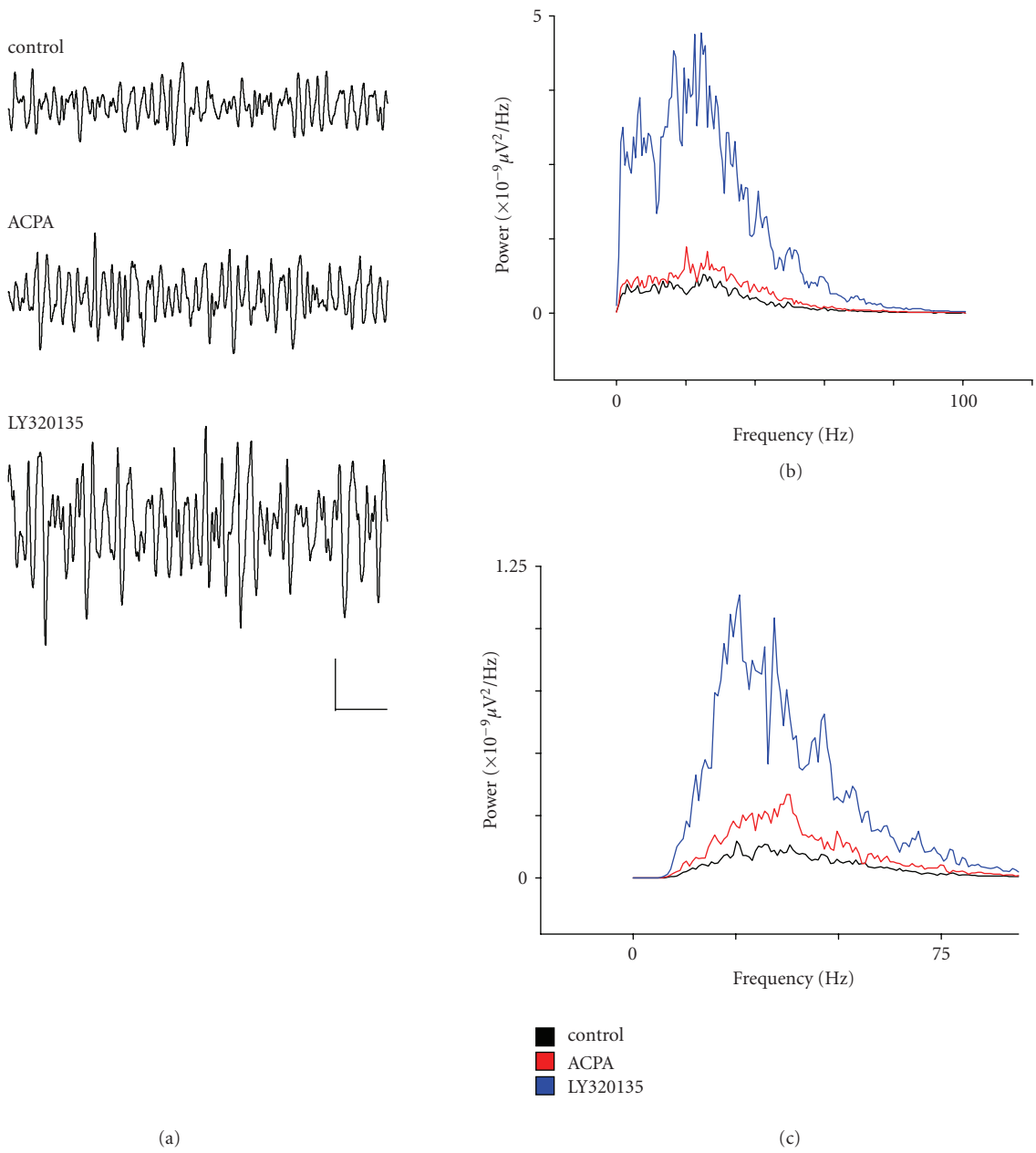

Figure 3: The effects of ACPA and LY320135 on γ-band activity in mEC layer V. (a) Example traces from layer V showing γ-oscillations under conditions in which ACPA (10 μM) or LY320135 (500 nM) was applied. (b) Plot of power spectral density during drug application (filtered between 2–100 Hz). Control (black line), ACPA (red line), or LY320135 (blue line). (c) Similar plot to (b) bandpass filtered between 30–90 Hz. Scale bar = 200 milliseconds × 50 μV.

sIPSCs were detected automatically using a threshold-crossing algorithm, and their frequency and amplitude are analysed. 200 sIPSCs were sampled during a continuous recording period for each neurone under each condition. The nonparametric Kolmogorov-Smirnoff (KS) test was used to assess the significance of shifts in cumulative probability distributions of interevent interval (IEI). Differences between drug and control situations in studies of sIPSCs were assessed by means of a one-way ANOVA. All error values stated in the text refer to the S.E.M.

All salts used in preparation of ACSF were Analar grade and purchased from Merck/BDH (UK). LY320135 and ACPA were obtained from Tocris Cookson (UK).

For field recordings of oscillatory activity, slices were placed into an interface chamber (BRSC-1, Digitimer, UK) and the chamber was continuously perfused with oxygenated ACSF at 30–32°C, at a flow rate of approximately 1-2 mL/min. Extracellular population recordings were made with glass microelectrodes filled with aCSF, of resistance 1–3 MΩ. Signals were amplified 1000-fold and recorded

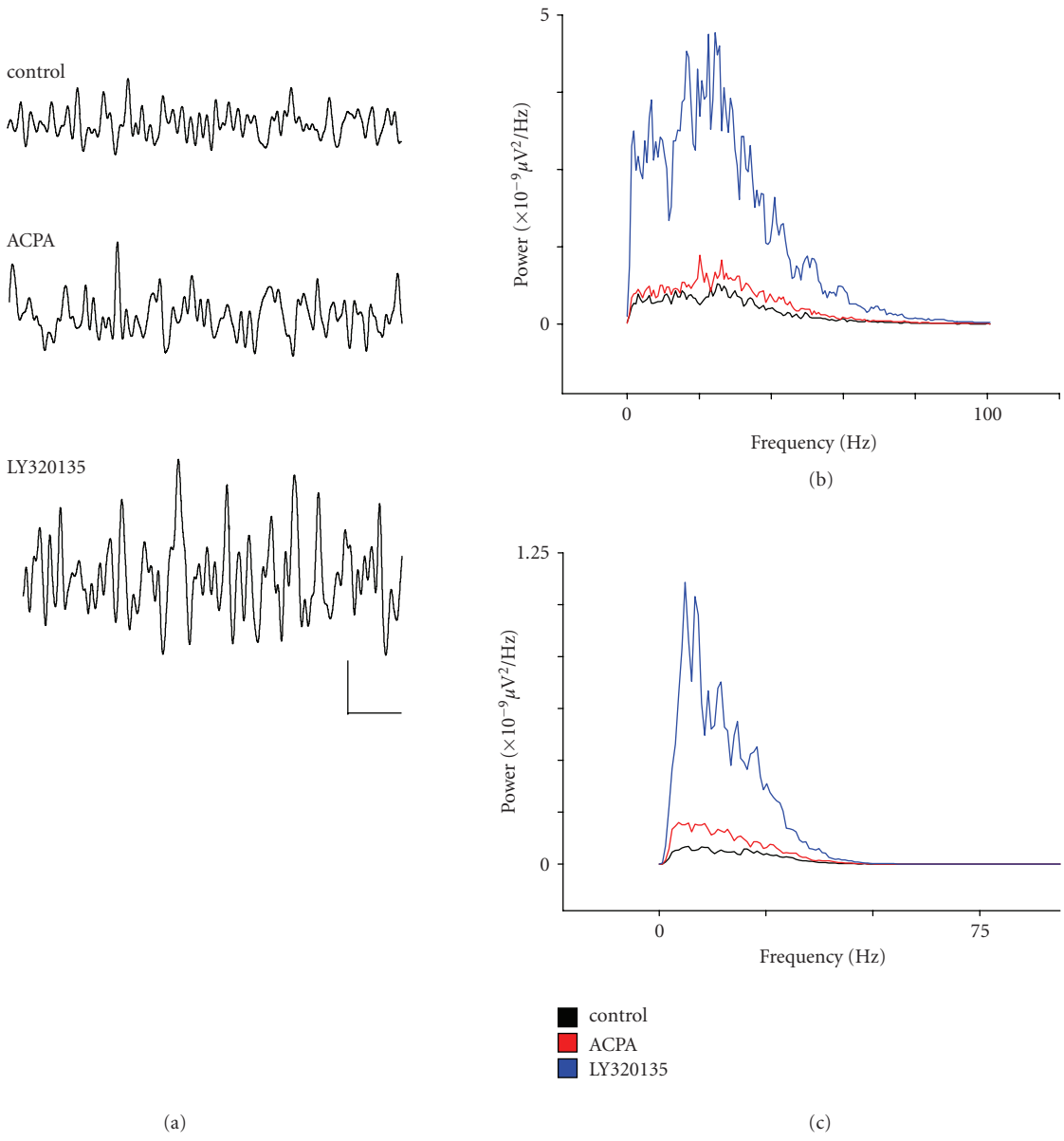

Figure 4: The effects of ACPA and LY320135 on β-band activity in mEC layer V. (a) Example traces from layer V showing β-oscillations under conditions in which ACPA (10 μM) or LY320135 (500 nM) were applied. (b) Plot of power spectral density during drug application (filtered between 2–100 Hz). Control (black line), ACPA (red line), LY320135 (blue line). (c) Similar plot to (b) bandpass filtered between 15–29 Hz. Scale bar = 200 milliseconds × 50 μV.

unfiltered. Low amplitude 50 Hz interference was removed using a HumBug (Quest Scientific, Canada). Signals were digitized and recorded at 10 kHz using an NPI EXT-02F amplifier (NPI, Germany) and pClamp 10 software (Molecular Devices, USA). Following 30–90 minutes control period of stable oscillatory activity, drugs were applied to the bath in known concentration. Pharmacological oscillatory activity was analysed using the fast Fourier transform (FFT, Clampfit 10), cross-correlation analysis and Morlet-wavelet time-frequency spectrogram analysis (MatLab 2007R, Mathworks). Student t-tests were carried out to determine statistical significance.

We analysed oscillations at beta (15–29 Hz) and gamma (30–90 Hz) bands, using bandpass filters (Clampfit 10.1) and measurement of the area under the power spectrum curve in Sigmaplot 8.0.

3. RESULTS

Whilst recording from layers II and V of the mEC, we applied the CBR agonist arachidonylcyclopropylamide (ACPA) at 10 μM, onto slices from which stable gamma activity had been induced by 300–400 nM kainate. As Figure 1(a) shows, KA-induced gamma oscillations in layer II were broadly

similar to those reported by Cunningham et al. [15]. Hence, mean area power in the γ-band was $561 \pm 179\,\mu V^2$ and mean control gamma frequency was 40.7 ± 2.4 Hz. Following 40–60 minutes bath application of ACPA, we applied the CB1R-specific inverse agonist LY320135 (500 nM; [18]). Figure 1(b) shows the power spectral density of activity bandpass filtered between 2–100 Hz, and Figure 1(c) shows similar data filtered at gamma frequency (30–90 Hz). As Figure 1(c) shows, there was a tendency towards an increase in gamma power in ACPA in some recordings, but this was not significant overall ($P \geq .19$, $n = 9$). In pooled data, ACPA did significantly reduce mean peak gamma frequency to 35.6 ± 1.8 Hz ($P \leq .04$, $n = 9$), although this effect was variable, and some recordings showed multiple peaks.

Following perfusion of the CB1R-specific inverse agonist LY320135, there was a marked reduction in normalised gamma power to $39.4 \pm 10.1\%$ of control, and this was highly significant ($P \leq .0006$, $n = 9$). In addition, mean peak frequency returned to 41.2 ± 1.8 Hz ($P \leq .04$, $n = 9$).

When beta power in layer II was measured, we noted a similar pattern of drug responses to that observed for gamma activity. Mean area power in the beta band was lower than that of gamma activity at $26 \pm 6\,\mu V^2$ and mean peak beta frequency in control conditions was 25.6 ± 1.4 Hz. Figure 2(a) shows the power spectral density of activity bandpass filtered between 2–100 Hz, and Figure 2(c) shows similar data filtered at beta frequency (15–29 Hz). As Figure 2(c) shows, there was no significant change in beta power in ACPA ($81.4 \pm 15\%$ of control, $P \geq .14$, $n = 9$), and ACPA had no significant effect on mean peak beta frequency (27.6 ± 1.43 Hz, $P \geq .25$, $n = 9$). However, when we added the CB1R-specific inverse agonist LY320135, there was a reduction in normalised beta power to $57 \pm 13\%$ of control, and this was highly significant ($P \leq .008$, $n = 9$). LY320135 had no effect on mean peak frequency (27.9 ± 0.52 Hz, $P \geq .4$, $n = 9$).

During the above experiments, we simultaneously recorded oscillatory activity in deep entorhinal cortex (layer V). Oscillatory activity in layer V was lower in power in layer V compared to layer II, with mean area gamma power just $60 \pm 10\,\mu V^2$ and mean peak frequency was similar to layer II at 39.19 ± 3.1 Hz.

When we applied ACPA whilst recording in layer V we observed a significant increase in mean gamma power (Figure 3(a)), by $38.1 \pm 13.4\%$ of control ($P \leq .03$, $n = 9$), however, baseline gamma power was very low in this layer, and the absolute change in gamma power was difficult to discern. Peak frequency was again slightly reduced to 36.0 ± 2.4 Hz, but this was not significant ($P \geq .31$, $n = 9$). On subsequent addition of the CB1R-specific inverse agonist LY320135, there was a strong increase in normalised gamma power to $108.4 \pm 58\%$ of control, and this reached significance ($P = .049$, $n = 9$). Again, LY320135 did not significantly alter mean peak gamma frequency (35.7 ± 2.41 Hz in LY320135, $P \geq .45$, $n = 9$).

When beta power in layer V was analysed, we noted a similar pattern of drug responses to that observed for gamma activity. Mean area power in the beta band was lower than that of gamma activity at $9.6 \pm 0.6\,\mu V^2$ and mean control beta frequency was 27.9 ± 0.52 Hz. Figure 4(a) shows field oscillations recorded in layer V before drug application and during ACPA and LY320135 periods. Figure 4(b) shows the power spectral density of activity bandpass filtered between 2–100 Hz, and Figure 4(c) shows similar data filtered at beta frequency (15–29 Hz). As Figure 4(c) shows, there was a slight tendency towards an increase in beta power (by $27 \pm 14\%$) in ACPA in some recordings, but this was not significant overall ($P \geq .06$, $n = 9$). ACPA had no significant effect on mean peak beta frequency (28.4 ± 0.7 Hz, $P \geq .5$, $n = 9$). When we next applied the inverse agonist LY320135, we noted an increase in normalised beta power by $142.4 \pm 88\%$ of control, and this just failed to reach significance ($P \leq .07$, $n = 9$). LY320135 (26.3 ± 1.5 Hz, $P \geq .3$, $n = 9$) had no effect on peak frequency.

We hypothesised that the lack of effects of ACPA in layer II might reflect constitutive or tonic activation of CBR, perhaps due to persistent kainate-induced activation of pyramidal neurones. To test this hypothesis, we applied LY320135 in the absence of ACPA. Application of LY320135 suppressed gamma band activity to $19.5 \pm 11\%$ of control, and this was highly significant ($P \leq .01$, $n = 5$). When beta activity was measured, it was apparent that in LY320135, there was a significant reduction in mean normalised beta power ($58.4 \pm 12\%$ of control; $P \leq .04$, $n = 5$).

The data presented up to this point indicated that, in general, gamma and beta power decreased in layer II in response to blockade or inverse agonism of CB1R, and that in layer V, the opposite was seen, with an increase in gamma and beta power. Figures 5(a)-5(b) shows summary bar charts indicating the effects of ACPA and LY320135 on normalised mean area power in the gamma and beta bands in layers II and V of the mEC.

We hypothesised that the alterations in oscillatory power seen during drug application would relate to the effects of ACPA and LY320135 on sIPSCs impinging on neurones in deep and superficial entorhinal cortex. To measure these effects, we performed whole-cell voltage clamp recordings of sIPSCs, whilst bath applying ACPA and LY320135 at concentrations similar to those used above.

4. ACPA AND LY320135 HAVE SUBTLE EFFECTS ON sIPSC AMPLITUDE AND FREQUENCY IN mEC LAYER II

Figure 6(a) shows typical recordings of inward sIPSCs made from a layer II pyramidal neurone. As Figure 6(b) shows, the application of ACPA ($10\,\mu M$) had subtle effects on sIPSCs in layer II, decreasing their frequency without affecting mean amplitude. Cumulative probability plots for sIPSC amplitude in the presence of ACPA (Figure 6(c)) indicated a shift in amplitude distribution, and mean amplitude showed a slight increase from 101.7 ± 3.2 pA in control to 108.3 ± 3.4 pA in ACPA, but this was nonsignificant ($P \geq .168$, ANOVA). When we analysed amplitude distribution using the nonparametric Kolmogorov-Smirnov test, the shift towards higher amplitude sIPSCs was just significant ($P \leq .021$ KS test). In the case of interevent interval (IEI; the reciprocal of frequency), we noted a shift to the right

in the cumulative probability plot (Figure 6(d)), indicating an increase in the likelihood of greater IEI values (reduced frequency). Mean median IEI increased from 34.6 ± 5.5 milliseconds in control to 47.6 ± 9.7 milliseconds in ACPA ($P \leq .0001$, ANOVA, $n = 5$), and the increase in IEI time distribution towards higher values was highly significant ($P \leq .006$, KS test). When we performed similar experiments using LY320135 (500 nM), we noted effects which tended towards the opposite of those seen with ACPA, that is, increased sIPSC amplitude and frequency. Figure 7(a) shows a typical recording of inward sIPSCs made from a layer-II pyramidal neurone. As Figure 7(b) shows, the application of LY320135 increased sIPSC frequency and amplitude. Mean amplitude increased from 51.7 ± 3.6 pA in control to 69.0 ± 5.9 pA in LY320135, and this was significant ($P \leq .013$, ANOVA, $n = 6$). Similarly, the shift in distribution towards larger amplitudes was highly significant ($P \leq .002$, KS test). The mean median IEI showed a slight decrease from 86.6 ± 15.8 milliseconds in control to 80.6 ± 16.1 milliseconds LY320135, but this decrease in IEI time was not significant ($P \geq .116$, ANOVA, $n = 6$).

The cumulative probability plots for sIPSC amplitude (Figure 7(c)) and IEI (Figure 7(d)) in the presence of LY320135 indicate the shifts in distribution of these parameters in the presence of LY320135.

5. ACPA AND LY320135 HAVE MARKED EFFECTS ON sIPSC AMPLITUDE AND FREQUENCY IN mEC LAYER V

In contrast to the effects observed in layer II and layer V we noted a significant reduction in sIPSC frequency in response to ACPA application. As Figure 8(a) shows, sIPSCs in layer V are considerably less frequent than those in layer II (see Woodhall et al., [17]). When ACPA was applied, sIPSC frequency was greatly attenuated (Figure 8(b)), but there was no overall shift in amplitude distribution (confirmed by a nonsignificant KS test ($P \geq .23$)). Mean amplitude rose slightly from 59.41 ± 7.33 pA in control to 70.49 ± 8.89 pA in ACPA, but this increase was not significant ($P \geq .33$, ANOVA, $n = 6$). When we analysed IEI, the change in distribution towards larger IEI values was significant ($P \leq .0001$ KS test), and mean median IEI was found to increase very significantly from 792 ± 41 milliseconds in control to 1317 ± 75 milliseconds in ACPA ($P \leq .0001$, ANOVA, $n = 6$). This effect of ACPA on IEI in layer V was consistent in all recordings. Cumulative probability plots for sIPSC amplitude (Figure 8(c)) and IEI (Figure 8(d)) illustrate the effects of ACPA on sIPSC amplitude and IEI.

When we performed similar experiments using LY320135 (500 nM), we again noted robust effects, which opposed those seen with ACPA, that is, increased sIPSC amplitude and frequency. Figure 9(a) shows a typical recording of inward sIPSCs made from a layer-II pyramidal neurone. As Figure 9(b) shows, the application of LY320135 had marked effects on sIPSCs in layer V, increasing their frequency and amplitude. Mean sIPSC amplitude in layer V increased from 47.0 pA ± 3.0 to 87.9 pA ± 7.4 pA in LY320135, and this increase was significant ($P \leq .001$, ANOVA $n = 7$). Cumulative probability plots for sIPSC amplitude in the presence of LY320135 (Figure 9(c)) show the shift in amplitude distribution, and this was confirmed statistically ($P \leq .0004$, KS test). In the case of IEI, we noted a shift to the left in the cumulative probability plot (Figure 9(d)), indicating an increase in the likelihood of lower IEI values (increased frequency). During LY320135 application the mean median IEI decreased from 477.1 ± 108.0 milliseconds in control to 300.0 ± 71.5 milliseconds in LY320135 showing that an overall increase in sIPSC frequency has occurred. The decrease in mean median IEI between control and LY320135 periods was significant ($P \leq .014$ ANOVA, $n = 7$), as was the change in distribution ($P \leq .016$, KS test).

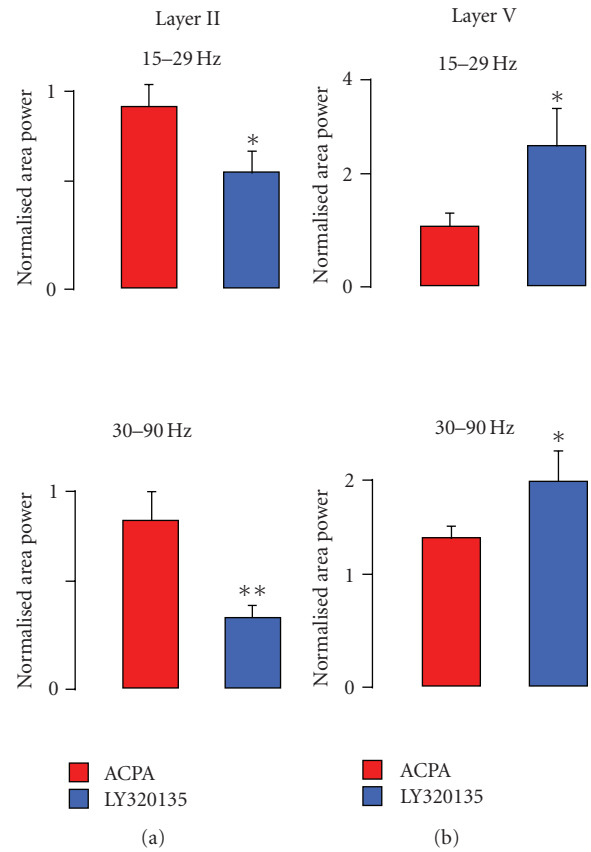

Figure 5: Summary of the effects of cannabinoid ligands on oscillatory activity in mEC. (a) Bar charts showing the effects of cannabinoid ligands in layer II on normalised area power at γ and β frequencies. (b) Bar charts showing the effects of inverse agonists alone in layer V on normalised area power at γ and β frequencies.

6. DISCUSSION

We found that the cannabinoid receptor agonist ACPA had little effect on either oscillatory activity or synaptic inhibition in superficial layers of the mEC, and that effects in deep layers were more robust, especially in the case of sIPSC frequency. However, the inverse agonist, LY320135, strongly suppressed oscillatory activity in superficial mEC even while its effects

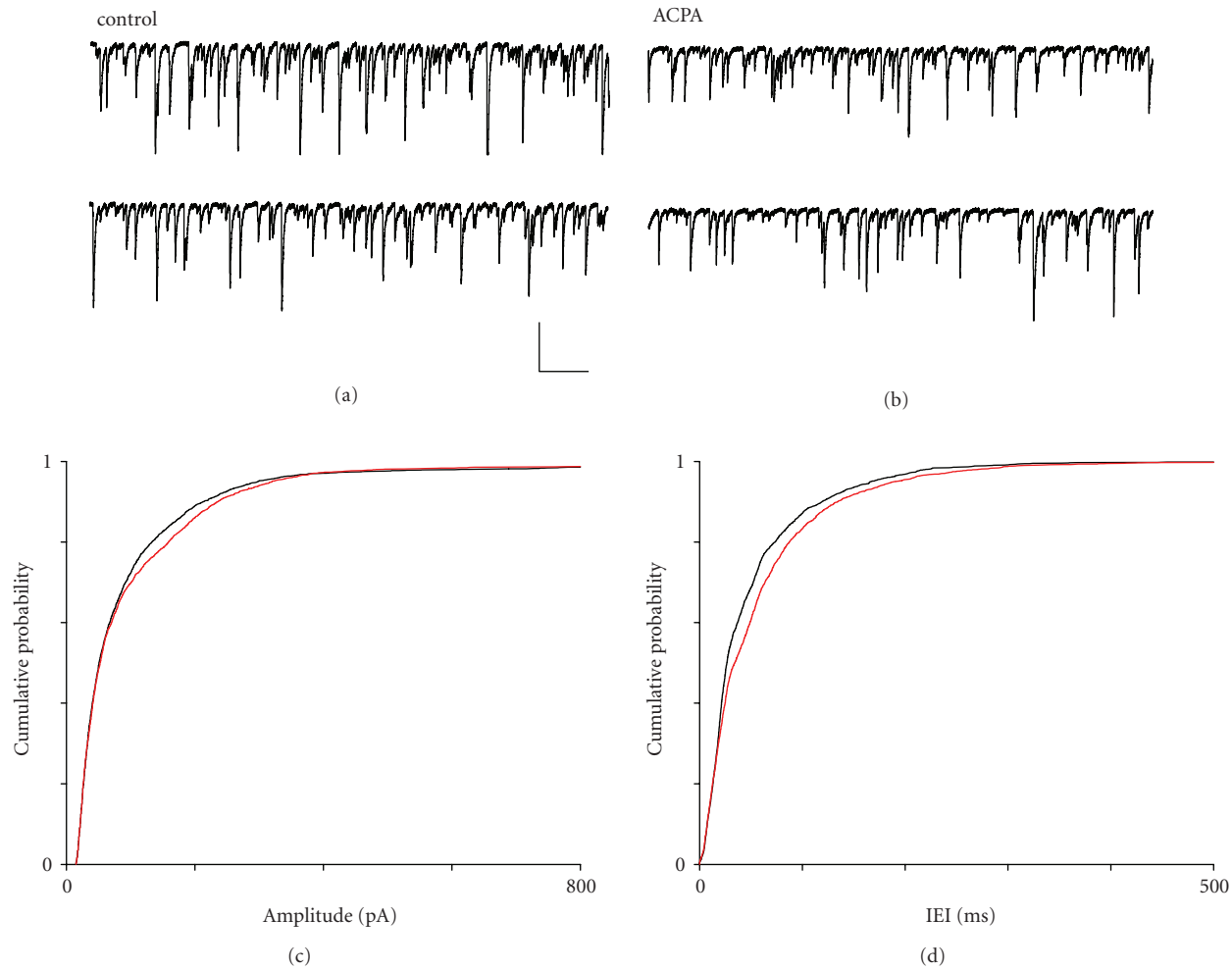

Figure 6: The effects of ACPA on sIPSCs in mEC layer II. (a) Recording from a layer II neurone under control conditions and (b) in the presence of ACPA (10 μM). (c) Cumulative probability plot for sIPSC amplitude under control (black) and ACPA (red) conditions. (d) Cumulative probability plot for sIPSC IEI under control (black) and ACPA (red) conditions. Scale bars 500 millisconds $\times$ 100 pA.

on sIPSC frequency and amplitude were not great. We also observed that suppression of oscillatory activity in layer II by LY3201235 was accompanied by augmentation of oscillatory power in layer V, and that the suppression of sIPSCs by ACPA and subsequent enhancement by LY320135 in this layer were marked.

We have reported previously [17] that spontaneous inhibition is much greater in superficial layer II of mEC than in deep layer V. In addition, more than 90% of IPSCs in layer II are action-potential (AP) independent, whereas in layer V, AP-dependent events comprise a much greater (>50%) proportion of sIPSCs. Given that CBRs act only on Ca^{2+} dependent release of GABA and have no effect on mIPSCs ([8]; it seems likely that cannabinoid ligands would show greater effects in the deep layers, where activity is low at baseline, and probably more sensitive to modulation since it is more likely to be AP-dependent.

Since, compared to layer II, both ACPA and LY320135 had more profound effects on synaptic inhibition in layer V, it seems likely that the relative dominance of mIPSCs in layer II may mask CB1R effects on the minority of AP-dependent sIPSCs to some degree. The lack of a robust effect of ACPA on oscillatory activity in layer V suggests, however, that CB1R may already be activated by ongoing network activity, and that further attempts at activation using an agonist did not increase any effect that CB1R might have on oscillatory power. This appears to be supported by the effects of the inverse agonist LY320135 in layer II. Here, we observed a robust reduction in both beta and gamma power in layer II, suggesting that CB1R do contribute to maintaining oscillatory activity in this layer. The apparently contradictory result of enhanced oscillatory activity in layer V in response to LY320125 may relate to effects that are secondary to activity in layer II, for example, Bragin [11], working in vivo, noted that ablation of superficial EC causes augmented oscillatory activity in CA3-CA1, and it may be that a similar mechanism allows suppression of oscillations in layer II to unmask activity in layer V, which receives inputs from CA1. Similarly, previous reports [15] indicate that superficial layers (especially layer III) show the strongest gamma power,

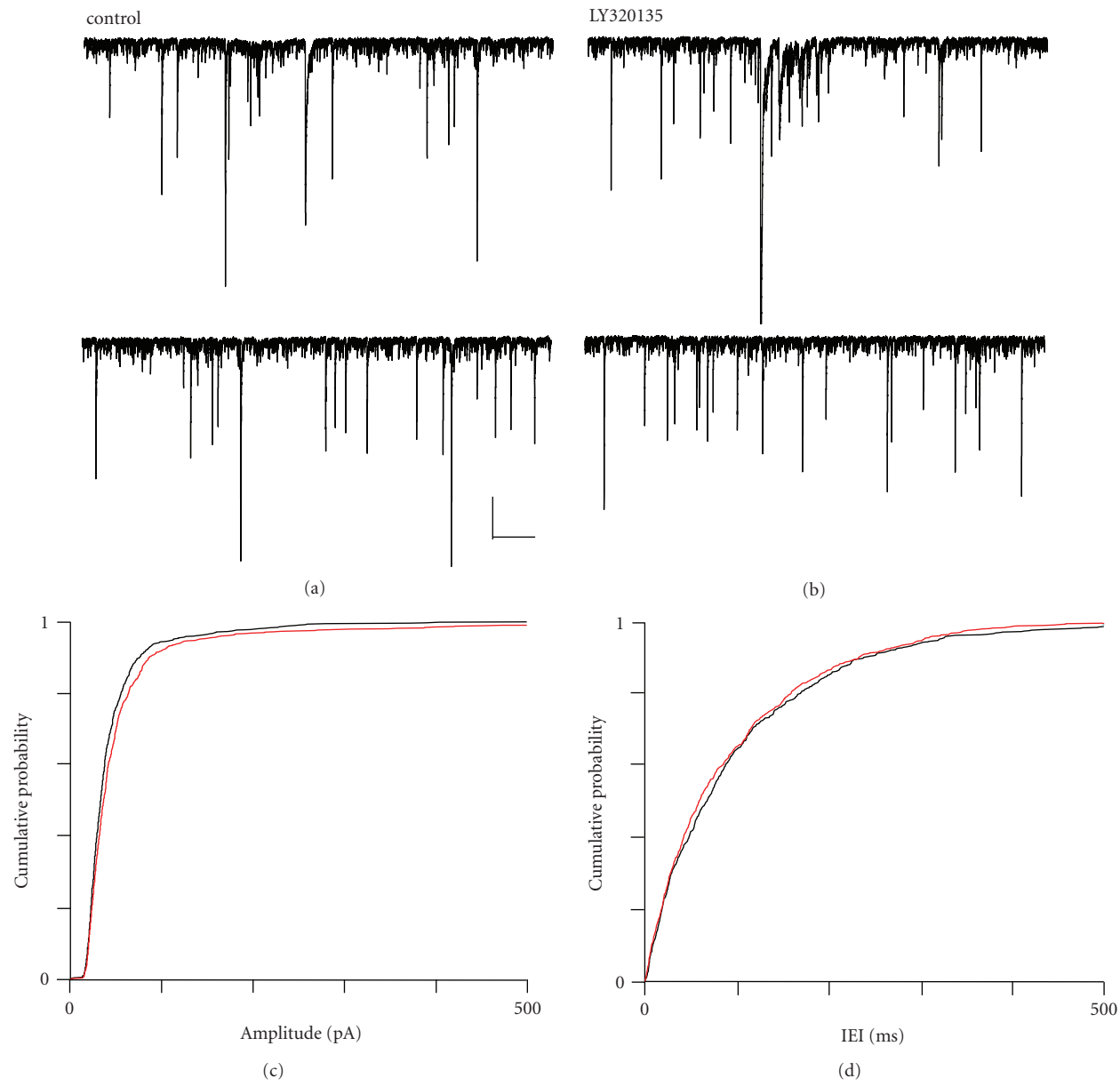

Figure 7: The effects of LY320135 on sIPSCs in mEC layer II. (a) Recording from a layer II neurone under control conditions and (b) in the presence of LY320135 (500 nM). (c) Cumulative probability plot for sIPSC amplitude under control (black) and LY320135 (red) conditions. (d) Cumulative probability plot for sIPSC IEI under control (black) and LY320135 (red) conditions. Scale bars 500 milliseconds × 250 pA.

perhaps suggesting a role in driving oscillatory activity in other layers. However, layer V is not driven directly by layers II or III [19], and hence any effect in layer V may well be indirect.

Cannabinoid receptors exert powerful control over GABA release from presynaptic terminals, with CB1 receptors having been shown to suppress both IPSPs and IPSCs in pyramidal neurones (IPSPs, [20]; IPSCs, [8]). Endocannabinoids, such as 2-arachidonyl glycerol and anandamide also suppress inhibition in CNS (see [21], for review). Cannabinoids are also believed to mediate the phenomenon of depolarisation-induced suppression of inhibition (DSI; [22–24]). Recently, studies have suggested that CB1R are present at terminals from specific subsets of inhibitory interneurones. For example, fast spiking (FS) inhibitory neurones in neocortex express parvalbumin (PV) but not CB1R, and by contrast, irregular spiking (IS) neurones express CB1R but not PV [25, 26]. Recently, Galaretta et al. [27] have demonstrated that synapses between IS neurones and pyramidal cells express CB1R and show DSI, whereas synapses between FS neurones and pyramidal cells show neither CB1R nor DSI. FS cells are thought to pace fast oscillatory network rhythms such as gamma activity ([28]; and IS cells are thought to possess properties that predispose towards nonrhythmic activity [25, 29]. A subset of neurones that express CB1R but not PV expresses cholecystokinin

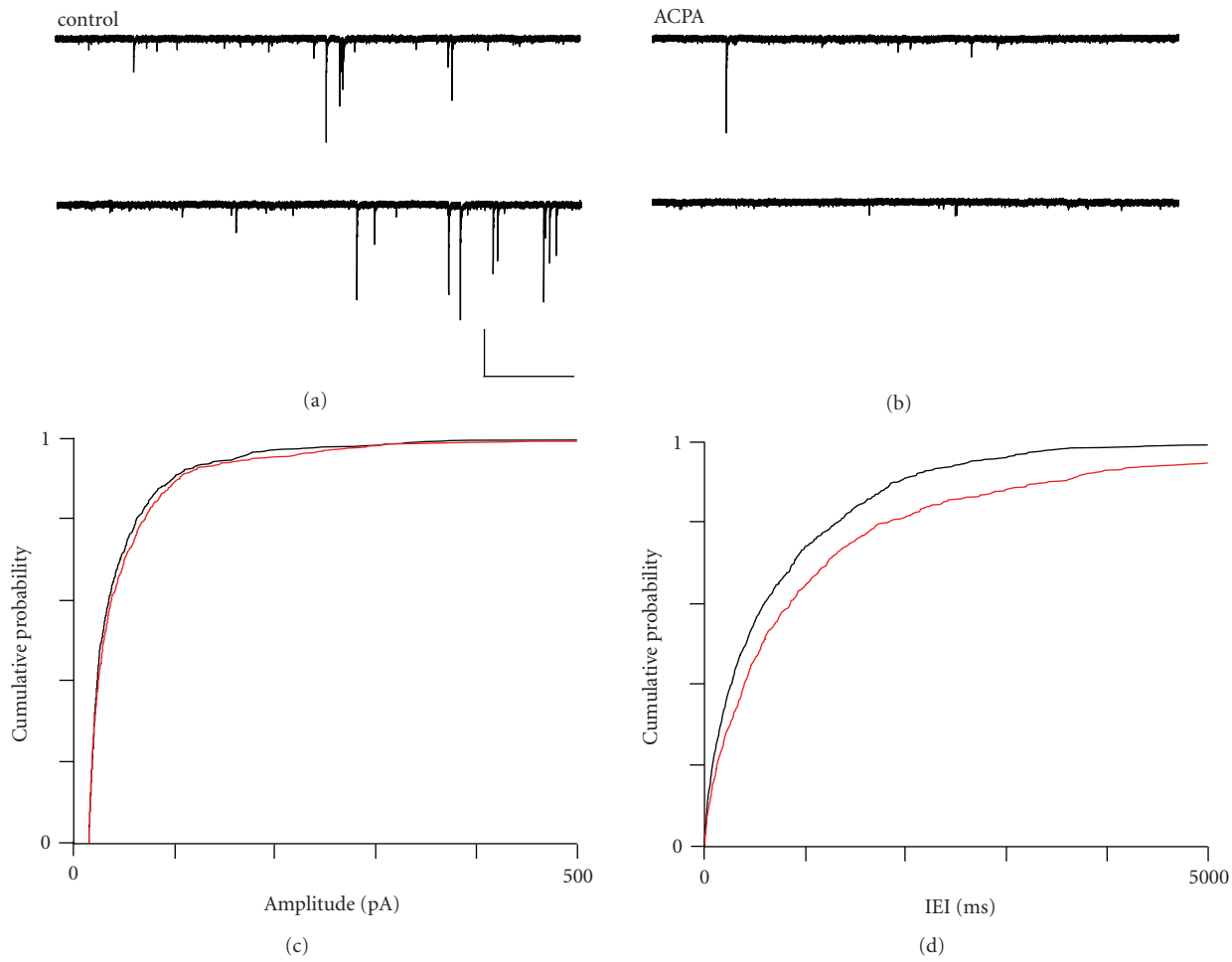

Figure 8: The effects of ACPA on sIPSCs in mEC layer V. (a) Recording from a layer V neurone under control conditions and (b) in the presence of ACPA (500 nM). (c) Cumulative probability plot for sIPSC amplitude under control (black) and ACPA (red) conditions. (d) Cumulative probability plot for sIPSC IEI under control (black) and ACPA (red) conditions. Scale bars 2000 milliseconds × 250 pA.

(CCK), and these neurones have been suggested to act, through DSI, to differentiate subgroups of pyramidal cells into neuronal assemblies which are then entrained by FS cells ("sparse coding" in place cell assemblies, [30]). In this scenario, pyramidal cell activation leads to endocannabinoid synthesis and release, which inhibits IS-cell inputs to the somata and proximal dendrites of active cells, but allows IS-cell-mediated inhibition to remain intact (and ongoing) at less active pyramids. This effect, in turn, allows FS-cells to entrain oscillatory activity only at the disinhibited population of pyramidal cells, effectively selecting that subset for rhythmic activity.

It seems possible that PV−/CCK+/CB1R+ inhibitory interneurones might similarly select populations of pyramidal cells involved in rhythmogenesis in the mEC, which contains both PV+ and PV− neurones [31, 32] and CCK+ interneurones [33], which also express CB1R [34]. We used a selective cannabinoid receptor inverse agonist to globally inhibit CB1Rs during persistent gamma and beta band oscillations in brain slices from the mEC. Under conditions in which CB1 were subject to blockade or inverse agonist effects, we observed a decrease in oscillatory power in gamma and beta bands in layer II. This is consistent with the literature described above [27, 30] and we propose that, in layer II, blockade or inverse agonism of CBRs results in increased irregular phasic inhibition from IS-cells onto pyramidal cells, decreasing the population available to participate in network oscillations and hence reducing field oscillatory power. This appears to be supported by our voltage-clamp recordings showing that LY320135 increased phasic GABAergic inhibition at principal cells in layer II.

When we measured oscillatory activity in layer V, inverse agonists at CBR *increased* gamma and beta power and this appeared to be correlated with decreased superficial beta and gamma power. At first, this appears paradoxical, however, oscillatory activity in specific laminae does not exist in isolation, and we might expect interactions between, as well as within, networks of neurones. Bragin et al. [11] have demonstrated that, in vivo, bilateral ablation of the EC suppresses gamma activity in the dentate gyrus (DG), but augments gamma oscillations in CA3-CA1. As previously discussed, superficial mEC projects to DG, and CA1

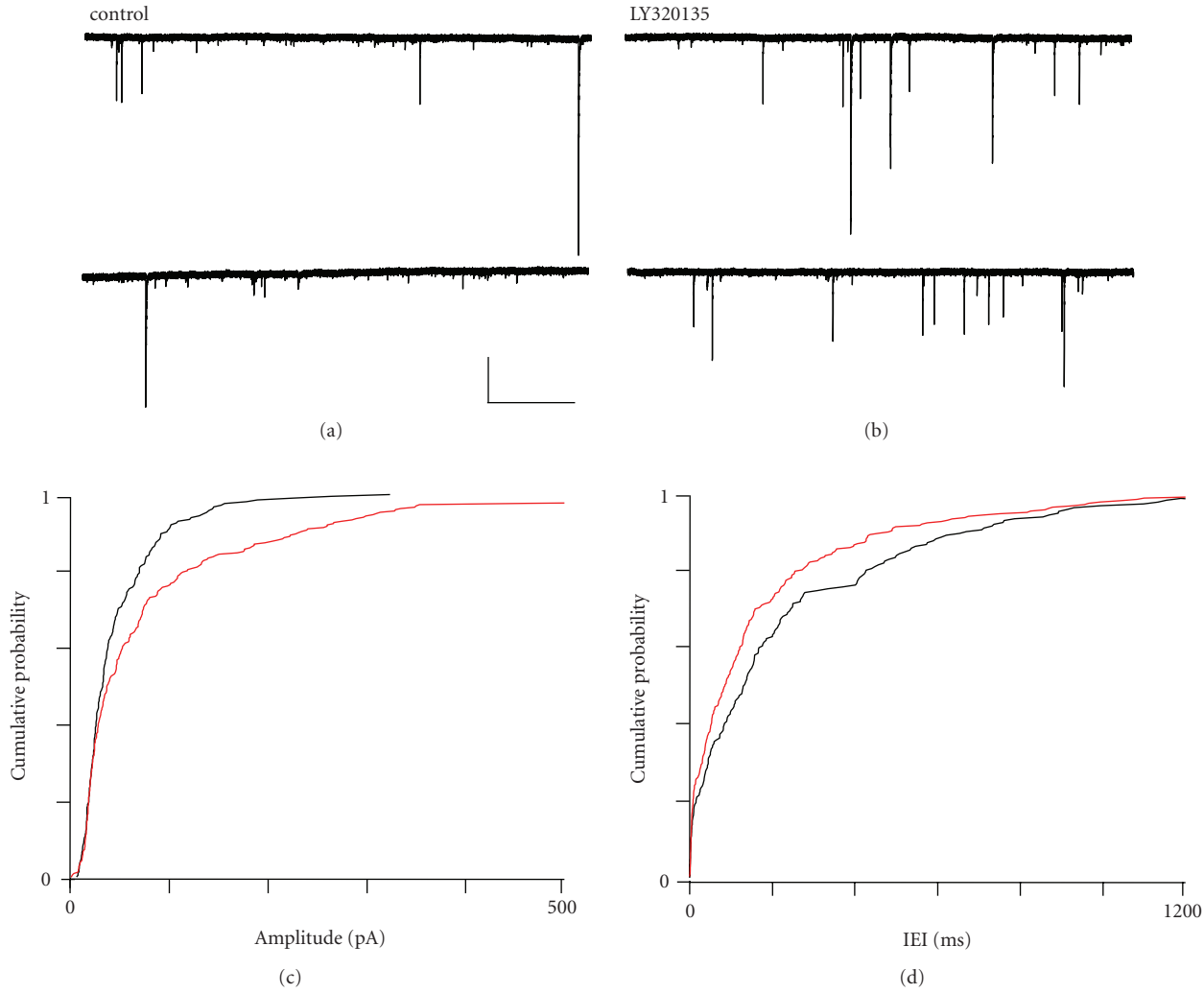

FIGURE 9: The effects of LY320135 on sIPSCs in mEC layer V. (a) Recording from a layer V neurone under control conditions and (b) in the presence of LY320135 (500 nM). (c) Cumulative probability plot for sIPSC amplitude under control (black) and LY320135 (red) conditions. (d) Cumulative probability plot for sIPSC IEI under control (black) and LY320135 (red) conditions. Scale bars 2000 milliseconds × 250 pA.

projects to deep mEC layers. Given that in our experiments, oscillatory activity in superficial mEC was suppressed, it is reasonable to suggest that this may depress gamma and/or beta activity in DG and enhance such activity in CA3-CA1. This, in turn, would feed through to layer V, where increased gamma and beta power is seen. Hence, although phasic inhibition in layer V appeared to increase in LY320135, it may be that this effect is not involved in selection of neuronal assemblies for oscillatory activity in layer V; rather, excitatory inputs to this area from hippocampus may be the dominant influence on pyramidal cell activity.

REFERENCES

[1] L. A. Matsuda, S. J. Lolait, M. J. Brownstein, A. C. Young, and T. I. Bonner, "Structure of a cannabinoid receptor and functional expression of the cloned cDNA," *Nature*, vol. 346, no. 6284, pp. 561–564, 1990.

[2] K. Mackie and B. Hille, "Cannabinoids inhibit N-type calcium channels in neuroblastoma-glioma cells," *Proceedings of the National Academy of Sciences of the United States of America*, vol. 89, no. 9, pp. 3825–3829, 1992.

[3] M. Glass, R. L. M. Faull, and M. Dragunow, "Cannabinoid receptors in the human brain: a detailed anatomical and quantitative autoradiographic study in the fetal, neonatal and adult human brain," *Neuroscience*, vol. 77, no. 2, pp. 299–318, 1997.

[4] M. Herkenham, A. B. Lynn, M. D. Little, et al., "Cannabinoid receptor localization in brain," *Proceedings of the National Academy of Sciences of the United States of America*, vol. 87, no. 5, pp. 1932–1936, 1990.

[5] M. Herkenham, A. B. Lynn, M. R. Johnson, L. S. Melvin, B. R. de Costa, and K. C. Rice, "Characterization and localization of cannabinoid receptors in rat brain: a quantitative in vitro autoradiographic study," *The Journal of Neuroscience*, vol. 11, no. 2, pp. 563–583, 1991.

[6] A. F. Hoffman and C. R. Lupica, "Mechanisms of cannabinoid inhibition of $GABA_A$ synaptic transmission in the

hippocampus," *The Journal of Neuroscience*, vol. 20, no. 7, pp. 2470–2479, 2000.

[7] I. Katona, B. Sperlágh, A. Sík, et al., "Presynaptically located CB1 cannabinoid receptors regulate GABA release from axon terminals of specific hippocampal interneurons," *The Journal of Neuroscience*, vol. 19, no. 11, pp. 4544–4558, 1999.

[8] N. Hájos, I. Katona, S. S. Naiem, et al., "Cannabinoids inhibit hippocampal GABAergic transmission and network oscillations," *European Journal of Neuroscience*, vol. 12, no. 9, pp. 3239–3249, 2000.

[9] N. Hájos, C. Ledent, and T. F. Freund, "Novel cannabinoid-sensitive receptor mediates inhibition of glutamatergic synaptic transmission in the hippocampus," *Neuroscience*, vol. 106, no. 1, pp. 1–4, 2001.

[10] R. I. Wilson, G. Kunos, and R. A. Nicoll, "Presynaptic specificity of endocannabinoid signaling in the hippocampus," *Neuron*, vol. 31, no. 3, pp. 453–462, 2001.

[11] A. Bragin, G. Jandó, Z. Nádasdy, J. Hetke, K. Wise, and G. Buzsáki, "Gamma (40–100 Hz) oscillation in the hippocampus of the behaving rat," *The Journal of Neuroscience*, vol. 15, no. 1, pp. 47–60, 1995.

[12] S. G. Hormuzdi, I. Pais, F. E. N. LeBeau, et al., "Impaired electrical signaling disrupts gamma frequency oscillations in connexin 36-deficient mice," *Neuron*, vol. 31, no. 3, pp. 487–495, 2001.

[13] M. A. Whittington, R. D. Traub, and J. G. R. Jefferys, "Synchronized oscillation in interneuron networks driven by metabotropic glutamate receptor activation," *Nature*, vol. 373, no. 6515, pp. 612–615, 1995.

[14] S. R. Cobb, E.H. Buhl, K. Halasy, O. Paulsen, and P Somogyi, "Synchronization of neuronal activity in hippocampus by individual GABAergic interneurons," *Nature*, vol. 378, no. 6552, pp. 75–78, 1995.

[15] M. O. Cunningham, C. H. Davies, E. H. Buhl, N. Kopell, and M. A. Whittington, "Gamma oscillations induced by kainate receptor activation in the entorhinal cortex in vitro," *The Journal of Neuroscience*, vol. 23, no. 30, pp. 9761–9769, 2003.

[16] M. O. Cunningham, D. M. Halliday, C. H. Davies, R. D. Traub, E. H. Buhl, and M. A. Whittington, "Coexistence of gamma and high-frequency oscillations in rat medial entorhinal cortex in vitro," *The Journal of Physiology*, vol. 559, no. 2, pp. 347–353, 2004.

[17] G. L. Woodhall, S. J. Bailey, S. E. Thompson, D. I. P. Evans, and R. S. G. Jones, "Fundamental differences in spontaneous synaptic inhibition between deep and superficial layers of the rat entorhinal cortex," *Hippocampus*, vol. 15, no. 2, pp. 232–245, 2005.

[18] C. C. Felder, K. E. Joyce, E. M. Briley, et al., "LY320135, a novel cannabinoid CB1 receptor antagonist, unmasks coupling of the CB1 receptor to stimulation of cAMP accumulation," *The Journal of Pharmacology and Experimental Therapeutics*, vol. 284, no. 1, pp. 291–297, 1998.

[19] M. P. Witter, H. J. Groenewegen, F. H. Lopes da Silva, and A. H. M. Lohman, "Functional organization of the extrinsic and intrinsic circuitry of the parahippocampal region," *Progress in Neurobiology*, vol. 33, no. 3, pp. 161–253, 1989.

[20] A. B. Ali, "Presynaptic inhibition of $GABA_A$ receptor-mediated unitary IPSPs by cannabinoid receptors at synapses between CCK-positive interneurons in rat hippocampus," *Journal of Neurophysiology*, vol. 98, no. 2, pp. 861–869, 2007.

[21] T. F. Freund, I. Katona, and D. Piomelli, "Role of endogenous cannabinoids in synaptic signaling," *Physiological Reviews*, vol. 83, no. 3, pp. 1017–1066, 2003.

[22] I. Llano, N. Leresche, and A. Marty, "Calcium entry increases the sensitivity of cerebellar Purkinje cells to applied GABA and decreases inhibitory synaptic currents," *Neuron*, vol. 6, no. 4, pp. 565–574, 1991.

[23] R. I. Wilson and R. A. Nicoll, "Endogenous cannabinoids mediate retrograde signalling at hippocampal synapses," *Nature*, vol. 410, no. 6828, pp. 588–592, 2001.

[24] R. I. Wilson and R. A. Nicoll, "Neuroscience: endocannabinoid signaling in the brain," *Science*, vol. 296, no. 5568, pp. 678–682, 2002.

[25] M. Galarreta, F. Erdélyi, G. Szabó, and S. Hestrin, "Electrical coupling among irregular-spiking GABAergic interneurons expressing cannabinoid receptors," *The Journal of Neuroscience*, vol. 24, no. 44, pp. 9770–9778, 2004.

[26] Á. L. Bodor, I. Katona, G. Nyíri, et al., "Endocannabinoid signaling in rat somatosensory cortex: laminar differences and involvement of specific interneuron types," *The Journal of Neuroscience*, vol. 25, no. 29, pp. 6845–6856, 2005.

[27] M. Galarreta, F. Erdélyi, G. Szabó, and S. Hestrin, "Cannabinoid sensitivity and synaptic properties of 2 GABAergic networks in the neocortex," *Cerebral Cortex*. In press.

[28] M. Bartos, I. Vida, M. Frotscher, et al., "Fast synaptic inhibition promotes synchronized gamma oscillations in hippocampal interneuron networks," *Proceedings of the National Academy of Sciences of the United States of America*, vol. 99, no. 20, pp. 13222–13227, 2002.

[29] J. R. Gibson, M. Belerlein, and B. W. Connors, "Two networks of electrically coupled inhibitory neurons in neocortex," *Nature*, vol. 402, no. 6757, pp. 75–79, 1999.

[30] T. Klausberger, L. F. Marton, J. O'Neill, et al., "Complementary roles of cholecystokinin- and parvalbumin-expressing GABAergic neurons in hippocampal network oscillations," *The Journal of Neuroscience*, vol. 25, no. 42, pp. 9782–9793, 2005.

[31] F. G. Wouterlood, E. Mugnaini, and J. Nederlof, "Projection of olfactory bulb efferents to layer I GABAergic neurons in the entorhinal area. Combination of anterograde degeneration and immunoelectron microscopy in rat," *Brain Research*, vol. 343, no. 2, pp. 283–296, 1985.

[32] F. G. Wouterlood, W. Härtig, G. Brückner, and M. P. Witter, "Parvalbumin immunoreactiv neurones in the entorhinal cortex of the rat: localization, morphology, connectivity and ultrastrucure," *Journal of Neurocytology*, vol. 24, no. 2, pp. 135–153, 1995.

[33] C. Köhler and V. Chan-Palay, "The distribution of cholecystokinin-like immunoreactive neurons and nerve terminals in the retrohippocampal region in the rat and guinea pig," *The Journal of Comparative Neurology*, vol. 210, no. 2, pp. 136–146, 1982.

[34] G. Marsicano and B. Lutz, "Expression of the cannabinoid receptor CB1 in distinct neuronal subpopulations in the adult mouse forebrain," *European Journal of Neuroscience*, vol. 11, no. 12, pp. 4213–4225, 1999.

Hindawi Publishing Corporation
Neural Plasticity
Volume 2008, Article ID 658323, 12 pages
doi:10.1155/2008/658323

Review Article

Linking Cellular Mechanisms to Behavior: Entorhinal Persistent Spiking and Membrane Potential Oscillations May Underlie Path Integration, Grid Cell Firing, and Episodic Memory

Michael E. Hasselmo and Mark P. Brandon

Center for Memory and Brain, Department of Psychology and Program in Neuroscience, Boston University, 2 Cummington Sreet, Boston, MA 02215, USA

Correspondence should be addressed to Michael E. Hasselmo, hasselmo@bu.edu

Received 11 January 2008; Accepted 14 May 2008

Recommended by Roland S.G. Jones

The entorhinal cortex plays an important role in spatial memory and episodic memory functions. These functions may result from cellular mechanisms for integration of the afferent input to entorhinal cortex. This article reviews physiological data on persistent spiking and membrane potential oscillations in entorhinal cortex then presents models showing how both these cellular mechanisms could contribute to properties observed during unit recording, including grid cell firing, and how they could underlie behavioural functions including path integration. The interaction of oscillations and persistent firing could contribute to encoding and retrieval of trajectories through space and time as a mechanism relevant to episodic memory.

Copyright © 2008 M. E. Hasselmo and M. P. Brandon. This is an open access article distributed under the Creative Commons Attribution License, which permits unrestricted use, distribution, and reproduction in any medium, provided the original work is properly cited.

1. INTRODUCTION

The entorhinal cortex plays an important role in memory function. In the rat, entorhinal cortex lesions impair performance in both spatial memory tasks [1] as well as in odor memory tasks [2]. In monkeys, memory function in delayed match to sample tasks is impaired by lesions of entorhinal cortex [3] and adjacent parahippocampal structures [4]. This article describes cellular and circuit mechanisms in the entorhinal cortex that could underlie its role in spatial and episodic memory functions. Computational modeling links data across multiple levels of function, including: (a) properties of single cell physiology, including persistent spiking and membrane potential oscillations, (b) properties of unit recording, including grid cells, place cells, and head direction cells, and (c) the role of entorhinal cortex in spatial path integration and episodic memory function. This article will review physiological data and modeling across these different levels.

2. PHYSIOLOGICAL DATA

Recordings from neurons in slice preparations of entorhinal cortex demonstrate important cellular properties including (i) persistent spiking and (ii) membrane potential oscillations. These cellular properties could contribute to properties described in unit recordings from entorhinal cortex in awake, behaving rats.

2.1. Persistent spiking

In slices, pyramidal neurons in different layers of entorhinal cortex demonstrate the capacity to display persistent spiking activity after a depolarizing current injection or a period of repetitive synaptic input [5–8]. Pyramidal neurons in layer II of medial entorhinal cortex show persistent spiking that tends to turn on and off over periods of many seconds [5]. This cyclical persistent spiking is shown in Figure 1(a). As described below, this could underlie the spatial periodicity of grid cells. Pyramidal neurons in deep layers of entorhinal cortex can maintain spiking at different graded frequencies for many minutes [8] as shown in Figure 2(a). The persistent spiking appears to due to muscarinic or metabotropic glutamate activation of a calcium-sensitive nonspecific cation current [7, 9, 10]. This graded persistent firing could allow these neurons to integrate synaptic input over extended periods. Persistent firing has also been shown in layer III of lateral entorhinal cortex [6].

2.2. Membrane potential oscillations

Entorhinal layer II stellate cells show prominent subthreshold membrane potential oscillations when depolarized near firing threshold [11, 12]. These are small oscillations of a few millivolts in amplitude that can influence the timing of action potentials [13] and can contribute to network oscillations [14, 15]. The frequency of membrane potential oscillations differs systematically along the dorsal to ventral axis of the medial entorhinal cortex [16]. A model presented below discusses how the membrane potential oscillation properties could underlie differences in grid cell firing properties along the dorsal to ventral axis [16–19]. The oscillations appear to be due to a hyperpolarization activated cation current or h-current [20], that differs in time constant along the dorsal to ventral axis [21]. Depolarizing input increases the frequency of these oscillations such that the phase of the oscillation integrates the depolarizing input over time. Membrane potential oscillations do not usually appear in layer II or layer III pyramidal cells [12], but are observed in layer V pyramidal cells, where they may be caused by M-current [22]. Membrane potential oscillations do not appear in neurons of the lateral entorhinal cortex [23].

2.3. Unit recording data

Recordings of neural activity in awake behaving rats provide important clues to the functional role of entorhinal cortex. In particular, many cells in medial entorhinal cortex fire as "grid cells." A single grid cell responds as a rat forages in a hexagonal array of different locations in an open-field environment [24, 25]. Examples of the pattern of firing in modeled grid cells are shown in Figures 1 and 2. Grid cells differ in spatial periodicity along the dorsal to ventral axis of medial entorhinal cortex, with larger spacing between larger fields in more ventral regions [24, 25].

Grid cells appear in all layers of entorhinal cortex, but in layers V and VI of entorhinal cortex the grid cells often only respond when the rat is facing in a particular direction [25]. This resembles head direction cells in areas such as the postsubiculum (dorsal presubiculum), which respond at all locations in the environment but only when the rat faces a particular direction [26–30]. The conjunctive grid-by-direction cells resemble the theta-modulated place-by-direction cells observed in the post- and parasubiculum, which respond only when the rat faces a preferred direction while occupying a single location [31].

3. PATH INTEGRATION

The cellular mechanisms described above may contribute to the function of path integration. Path integration involves an animal using its self-motion cues to maintain an accurate representation of the angle and distance from its start position, even during performance of a complex trajectory through the environment [32–35]. Many species demonstrate the behavioral capacity to remember the distance as well as the angle of return to the starting location (here represented in Cartesian coordinates by a two component

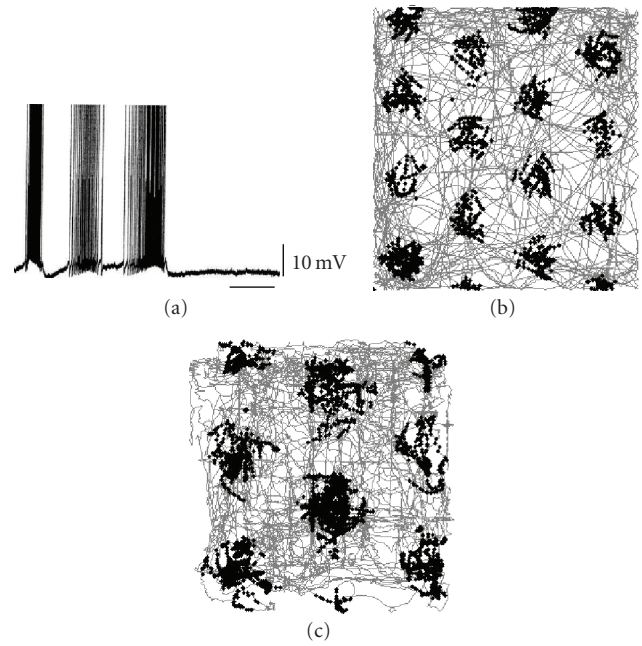

Figure 1: (a) Example of persistent firing in layer II pyramidal cell showing alternating cycles of spiking and nonspiking in data from Klink and Alonso [5]. (b) Simulation of grid cell firing dependent upon cyclical persistent spiking gated by random movement in a two-meter square environment. Spiking shown as black dots on trajectory in gray. (c) Simulation from same model using rat trajectory from experimental data in an 85 cm square environment.

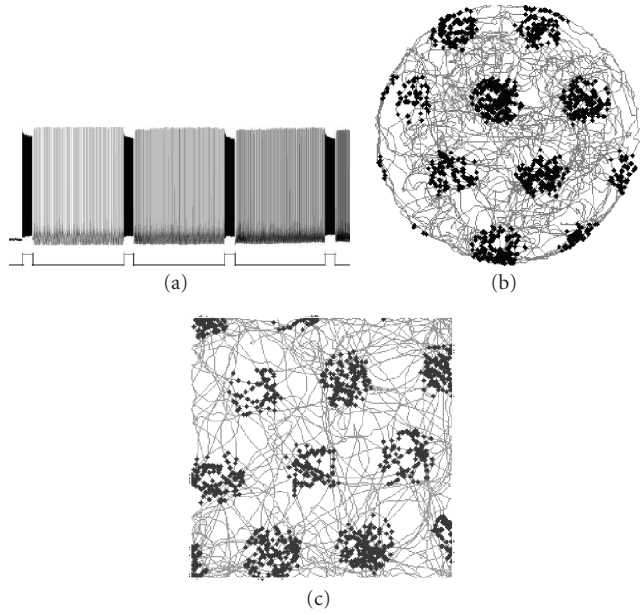

Figure 2: (a) Example of graded persistent firing in a layer V pyramidal cell from Egorov et al. [8]. (b) Simulation of grid cell firing based on persistent firing in cells from deep layers of medial entorhinal cortex. The spiking activity shown as black dots arises from convergent input from three neurons with the same baseline persistent firing frequency, with phase of input neurons influenced by input from different speed modulated head direction cells during movement (trajectory shown in gray). (c) Simulation of grid cell firing based on membrane potential oscillations in dorsal layer II stellate cells in medial entorhinal cortex.

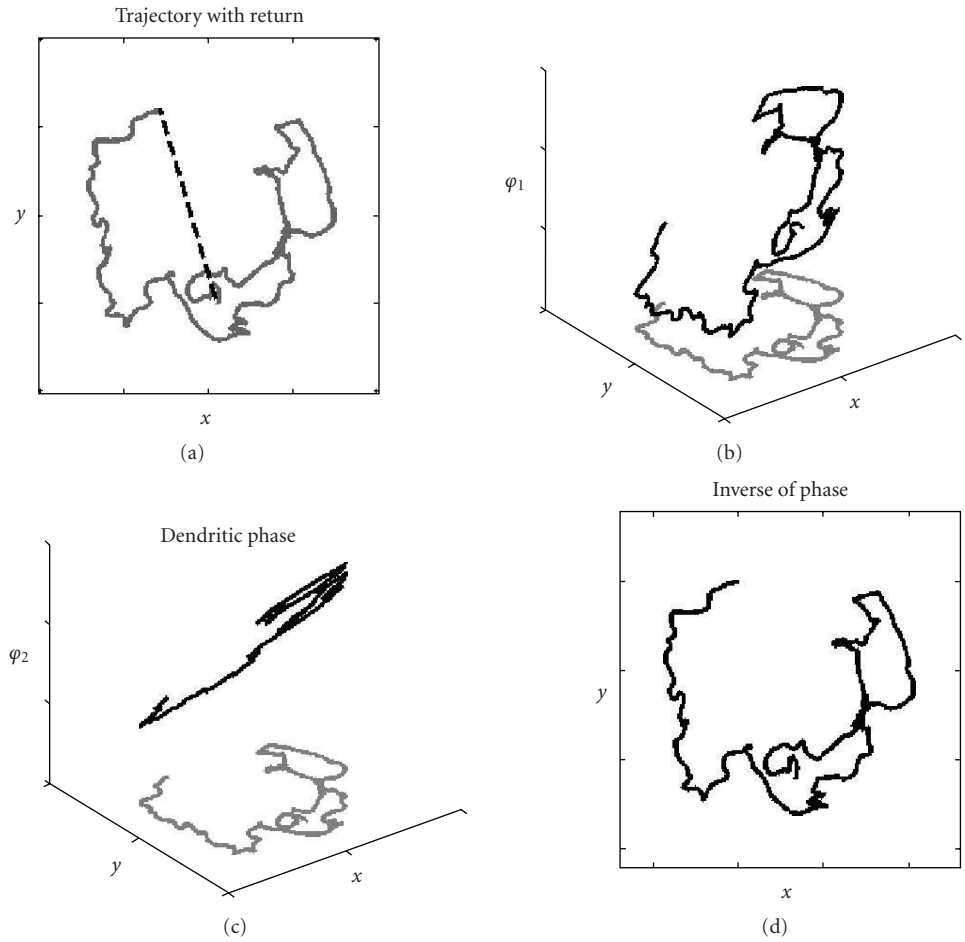

Figure 3: Coding of location by phase. (a) Actual trajectory run by the rat is shown in gray. If phase is reset at start location, the inverse transform of phase at any position yields a return vector with angle and distance leading back to start (shown with black dashed line). (b) Plot of membrane potential oscillation phase φ in a single dendrite of a simulated grid cell, showing linear change in phase with one dimension of location (dendrite receives input from head direction cell with angle preference zero). (c) Phase of another dendrite receiving input from head direction with angle preference 120. (d) Performing the inverse transform of oscillation phases at each point in time effectively reconstructs the full trajectory.

return vector). As shown here, persistent firing provides a single neuron mechanism to integrate the distance and angle of trajectory segments to compute the overall distance and angle from start location to an end or goal location. Here, the vector from start to goal is called the goal vector (and the negative of the goal vector is called the return vector). An example of a return vector is shown as a dashed line in Figure 3(a).

In general, the location of an agent can be determined by computing the integral of the velocity vector. In Cartesian coordinates, the velocity vector is $\vec{v} = [dx/dt, dy/dt]$. Integration of the velocity vector over a period of time T after starting at location $\vec{x}_0$ yields the location vector $\vec{x} = [x, y]$ at time T:

$$\vec{x}\,(T) = \vec{x}_0 + \int_0^T \vec{v}\,(t)dt. \tag{1}$$

For example, if the velocity of an animal is 10 cm/sec in the x direction and 5 cm/sec in the y direction, integration over 5 seconds yields a final location of $[x,y]$ = [50 cm, 25 cm] relative to the start location. Note that this integral corresponds to the goal vector $\vec{g}\,(T) = \vec{x}\,(T) - \vec{x}_0$, which is the negative of the return vector.

4. INTEGRATION BY PERSISTENT FIRING CAN CODE LOCATION

Integration of the goal vector or return vector could be provided by the mechanism of graded persistent firing in deep layer entorhinal neurons [7, 8]. These neurons could integrate a velocity vector coded by neurons responsive to the head direction of the rat and to the speed of the rat. Head direction cells have been shown in deep entorhinal cortex [25] and in the postsubiculum, which provides direct input to the entorhinal cortex [26, 27]. Head direction cells respond selectively when the rat is heading in a specific allocentric direction. Some neurons show sensitivity to speed (translational motion) in the postsubiculum [27] as well as

in the hippocampus [36] and in the medial mammillary nucleus which receives output from the postsubiculum and medial entorhinal cortex [37]. Here, the activity of a population of head direction cells modulated by speed is represented by multiplying the velocity vector of the rat with a head direction matrix H. The head direction matrix consists of rows with unit vectors representing the preference angles of individual speed modulated head direction cells, that transforms the velocity vector into a head direction vector $\vec{h} = H\,\vec{v}$. For example, a matrix representing two head direction cells with preference angles θ_1 and θ_2 has two rows: $H = \left[\begin{smallmatrix} \cos\theta_1 & \sin\theta_1 \\ \cos\theta_2 & \sin\theta_2 \end{smallmatrix}\right]$. For a cell with a preference angle of 0, the activity of the head direction cell would be $\cos(0) * dx/dt + \sin(0) dy/dt = dx/dt$. This framework has the advantage that it allows for a simple inverse transform turning head direction space back into Cartesian coordinates. The inverse [38] of the matrix H is

$$H^{-1} = \begin{bmatrix} \sin\theta_2 & -\sin\theta_1 \\ -\cos\theta_2 & \cos\theta_1 \end{bmatrix} / (\cos\theta_1 \sin\theta_2 - \sin\theta_1 \cos\theta_2). \tag{2}$$

Note that this framework assumes that the response of head direction cells is like a cosine function, whereas head direction cells usually only show positive activity and have narrower, triangular response functions with no activity outside this range. Head direction input corresponding to a cosine function of actual input could be provided by summed input converging from a population of head direction cells with different magnitudes of tuning for values at different angles from the preferred direction. Note also that this representation combines the properties of different neurons responding to translational velocity or to head direction in the postsubiculum [27] and other regions [36, 37]. If head direction is not computed based on velocity, then it could be integrated from angular velocity as a distinct element of the state vector or could be computed based on angle to a different reference point.

Using this mathematical representation of head direction input, the firing rate of a set of graded persistent firing cells could integrate the input from a set of head direction cells to yield a firing rate as follows:

$$\vec{a}\,(T) = \beta \int_{t=0}^{T} H(\vec{v}\,(t)dt) = \beta H(\vec{x}\,(T) - \vec{x}\,(0)), \tag{3}$$

where vector $\vec{a}\,(T)$ represents the firing rate of a population of graded persistent firing cells at time T. For example, imagine two cells a_1 and a_2 with capacity for graded persistent spiking that receive input from two head direction cells with preference angles of 0 degrees and 60 degrees. Imagine that the rat moves at 10 cm/sec in the x direction for 4 seconds, and the scaling factor β is 0.25 Hz/cm. Moving in the x direction is equivalent to moving at 0 degrees, which would result in the head direction cells having the activity $h_1 = 1$ and $h_2 = 0.5$. The computation in (3) would then result in the frequency of the graded persistent firing cells as follows: $a = \beta \left[\begin{smallmatrix} \cos\theta_1 & \sin\theta_1 \\ \cos\theta_2 & \sin\theta_2 \end{smallmatrix}\right] \left[\begin{smallmatrix} x \\ y \end{smallmatrix}\right] = 0.25 \left[\begin{smallmatrix} 1 & 0 \\ 0.5 & 0.87 \end{smallmatrix}\right] \left[\begin{smallmatrix} 40 \\ 0 \end{smallmatrix}\right] = \left[\begin{smallmatrix} 10 \\ 5 \end{smallmatrix}\right]$. Thus, the graded persistent firing cells would increase their activity to $a_1 = 10$ Hz and $a_2 = 5$ Hz. Mathematically, the inverse transform of this firing rate vector computes the location vector $\vec{x}\,(T) = H^{-1}\,\vec{a}\,(T)/\beta$ in Cartesian coordinates (see Figure 3(a)). However, the difference in neural activity could guide behavior without use of the inverse transform. This could involve forming associations between the start location and this pattern of graded firing, and then forming associations between this pattern of graded firing and the associated head direction signal. At the start location, the pattern of graded firing could be activated, and this could retrieve the associated head direction signal. The animal could change directions until its actual head direction matched this retrieved head direction. This could give the animal the correct angle to the goal.

The same mechanism computes both the goal vector and its negative, the return vector. The return vector allows a rat to return to the starting location from any arbitrary location in the environment. In contrast, the goal vector can be used to store the distance and angle to important locations in the environment. For example, if a rat is started in one location in an open field, and wanders until it finds food in another location, the integrated activity vector at that point is the goal vector—it provides a simple description of the angle and distance from the start to the goal. This goal vector could be associated with all elements of the preceding path by backward replay of place cells coding the full pathway [39, 40]. This could allow storage of an association between place cells active at the start location and the subsequent goal vector. Retrieval of the goal vector at the start location could then allow the rat to go directly to the location of food reward. If the spatial locations leading to a goal are associated with the goal vector at each goal location, and then integration is reset, a sequential series of trajectories to goals could be stored separately. The rat could then use this activity to sequentially retrieve pathways to different rewarded locations in the environment, as in some behavioral tasks [41]. The resetting of integration activity could underlie the different pattern of place cell firing shown with this type of directed task compared to open field activity. Thus, the resetting of integration could explain the shift in firing location for place cells between scavenging in an open field and following sequential trajectories between reward locations [41] as well as the shift in firing location for grid cells between open field scavenging and running on a long hairpin track [42] in which the view of each new segment could cause phase reset.

Graded persistent spiking could also hold initial head direction $\theta_{\mathrm{HD}}(0)$ and update this by integrating input from neurons coding angular head velocity $\dot{\theta}_{\mathrm{AHV}}(t)$ in areas such as the postsubiculum [27].

5. PERSISTENT SPIKING COULD UNDERLIE GRID CELL FIRING

Because the neurons that show persistent firing can integrate the synaptic input from speed modulated head direction cells, and thereby can code spatial location, these persistent firing neurons could potentially be the grid cells recorded in

awake behaving animals [24, 43, 44]. This section describes two potential mechanisms for persistent firing neurons to contribute to the activity of grid cells. The first mechanism involves the cyclical persistent firing shown in layer II (see Figure 1(a)). The second mechanism involves the graded persistent firing shown in layer V (see Figure 2(a)).

In a general manner, the experimental data on firing of single grid cells can be described by

$$g(t) = \prod_{\theta} \cos(\omega H \vec{x}(t) + \varphi), \tag{4}$$

where $g(t)$ is the probability of firing of the grid cell over time. The product sign Π represents multiplication of the output from each row (each head direction θ) of the head direction transform matrix H described above. The description of the experimental data here directly uses the vector representation of location over time $x(t)$. Orientation of the grid is determined by the head directions θ in H, the spatial phase is determined by φ, and the spacing between fields is determined by the angular frequency ω. This equation resembles other representations of grid cells [18, 45] but simplifies the representation by using the head direction transform matrix.

5.1. Cyclical persistent firing

The pattern of periodic spatial firing of grid cells could arise from the pattern of cyclical persistent firing as shown in Figure 1(a). The tendency for persistent firing to turn on and off could contribute to grid cell firing if the oscillation could be gated by integration of input from different populations of head direction cells with different preferred angles. Simulations shown in Figures 1(b) and 1(c) show that the following equations can generate grid cell firing properties:

$$\begin{aligned} \frac{dh^+}{dt} &= -\omega^2 V(t)(H\vec{v}^{+}(t))^{3/2}, \\ \frac{dh^-}{dt} &= \omega^2 V(t)(H\vec{v}^{-}(t))^{3/2}, \\ \frac{dV}{dt} &= h^+(H\vec{v}^{+}(t))^{1/2} - h^-(H\vec{v}^{-}(t))^{1/2}, \\ g(t) &= \left[\prod V(t)\right], \end{aligned} \tag{5}$$

where h^+ represents changes in current due to positive components of the head direction input (note that this uses cosine modulated head direction input), and h^- represents current due to negative components of the cosine modulated head direction input. Note that the equations separately use positive and negative elements of the speed modulated head direction matrix H transforming the rat movement velocity $v(t)$. The parameter ω determines the time scaling of input effects on activity levels. In the equations, $V(t)$ represents the voltage change in individual compartments each of which receive input from the positive and negative components of one head direction input. As noted above, the cosine modulated head direction input could be provided by summing over head direction cells with different angles of preference. The negative influence of head direction in the equation could be due to feedforward inhibition or inhibitory GABAergic projections from the postsubiculum to the medial entorhinal cortex. The function $g(t)$ represents the firing of grid cells over time. The square brackets [] indicate that spiking occurs whenever $V(t)$ crosses a threshold.

This pattern of activity could be obtained if neurons respond to different head direction inputs with cyclical persistent firing (Klink and Alonso, 1997), as shown in Figure 1(a). In this case, when going one direction, head direction input will cause phasic changes in firing in that direction, possibly due to build up first of calcium and then of calcium inactivation. When going the exact opposite direction, head direction input would have to activate the reverse processes, possibly reducing calcium inactivation and then reducing calcium.

Examples of grid field plots obtained with this model are shown in Figures 1(b) and 1(c). The grid fields are more stable in the trajectory data from the Moser laboratory than in randomly created trajectories (see Figure 1(b)) or in a trajectory obtained in our own laboratory (see Figure 1(c)). This indicates that the statistics of rat movement can determine appearance of the grid in this new model, and this could underlie variability in detection of grid cell firing properties depending on the trajectory of rat movement in the behavioral foraging task.

5.2. Graded persistent firing

As an alternative to cyclical persistent firing, graded persistent firing as shown in Figure 2(a) could provide the basis for grid cell firing. In this framework, different graded persistent firing cells start out with the same baseline frequency of spiking and provide convergent input to a grid cell that fires whenever the inputs are in synchrony. Speed modulated head direction input to different graded persistent firing cells will transiently alter the frequency and thereby the phase of firing. Therefore, if the rat moves, it shifts the frequency of a graded cell out of phase with the other cells and thereby reduces or stops the grid cell firing until the phase is shifted enough to come into phase with the other neurons. A grid cell simulated with this model is shown in Figure 2(b). This mechanism uses graded persistent firing in a manner similar to the mechanism of membrane potential oscillations described in the following section.

Both of these models will yield a pattern of firing similar to grid cells as long as the head direction cells providing input have preference angles at multiples of 60 degrees. For path integration, the head direction angles used for integration might be determined at the start location. For example, a single pyramidal cell showing persistent firing might receive input from three head direction cells that code the heading angle at the start, as well as the angle of eye direction. Rats have binocular overlap of about 60 degrees [46]. If the total visual field of one eye is 180 degrees and the center of view is at 90 degrees, then the center of view for each eye should be offset about 60 degrees from head direction. Therefore, a rat may choose angles of 0, −60, and

60 degrees for path integration. These angles have the 60-degree difference necessary for the head direction input to cause hexagonal arrays in the grid cell model. The rat can use these initial angles of view as reference angles, but if it turns far enough from the initial heading (e.g., 180 degrees from the initial head direction), then it may need to select additional reference angles at 60-degree intervals from the previous reference angles.

Some grid cells respond selectively only for certain head direction [25]. These head direction sensitive grid cells might result from the input only being suprathreshold for a population of head direction cells responding near one preferred angle, with input being subthreshold from other populations of head direction cells coding other preferred angles (e.g., at 60 or 120 degrees differences).

6. INTEGRATION BY MEMBRANE POTENTIAL OSCILLATION PHASE CAN CODE LOCATION

As an alternative mechanism for path integration, the phase of membrane potential oscillations in medial entorhinal stellate cells can also be used to integrate speed modulated head direction input. This mechanism was proposed in a model of grid cells developed by Burgess et al. [18] and O'Keefe and Burgess [47]. This mechanism uses the physiological fact that depolarizing inputs to stellate cells cause a change in frequency of membrane potential oscillations [16]. This could change oscillation phase based on an integral of the depolarizing input.

6.1. Model of grid cells using membrane potential oscillations

This computational model shows how activity of a single grid cell could arise from membrane potential oscillations within that cell modulated by depolarizing input from head direction cells:

$$g(t) = \left[\prod\left(\cos\omega t + \cos\left(\omega t + \omega\beta_H \int_0^t H(\vec{v}\ (\tau)d\tau + x_0)\right)\right)\right], \tag{6}$$

where $g(t)$ is the firing in time and space of a single modeled grid cell. ω represents the baseline angular frequency of membrane potential oscillations ($2*\pi*f$) in different portions of the neuron. β_H is the experimentally determined scaling factor relating membrane potential oscillations to grid cell spacing. The input from head direction cells is determined by the matrix H and the velocity vector $\vec{v}$. The inner product of each row of H with the velocity vector $\vec{v}$ represents input to one dendrite from one head direction cell modulated by the speed of the rat. This input alters the frequency of dendritic membrane potential oscillations and thereby shifts the phase of the dendritic oscillations in proportion to the integral of the velocity vector over time. Both the starting location of the rat and the spatial phase of the grid cell are combined in the initial location vector x_0. This initial location vector is also transformed by the matrix H. The square brackets [] represent a Heaviside step function generating a spiking output for each time point when the product crosses a threshold (set at 1.8).

This model generates grid cell firing fields with spacing between fields dependent upon the frequency of membrane potential oscillations [16–18]. A grid cell created with this model is shown in Figure 2(c). The model generated the prediction that the systematic change in spacing of grid cell firing fields along the dorsal to ventral axis of entorhinal cortex would depend upon a systematic difference in frequency of membrane potential oscillations in entorhinal neurons. This prediction was tested and supported by whole cell patch recordings from entorhinal layer II stellate cells [16]. Based on experimental data alone, it appears that membrane potential oscillation frequency f is scaled to grid cell spacing G by a constant factor $f*G = H$ [16, 17].

As noted above, membrane potential oscillations appear in specific medial entorhinal populations such as layer II stellate cells and layer V pyramidal cells, but not in other cells such as layer II pyramidal cells, or neurons in medial entorhinal layer III, or in the lateral entorhinal cortex. Based on these data, the generation of grid cells responses based on membrane potential oscillations would only occur in layer II stellate cells and layer V pyramidal cells, and would appear in other neurons due to network interactions or due to the persistent spiking mechanisms described above.

6.2. Grid cell activity codes location

In the model, the depolarizing input from head direction cells increases the frequency of membrane potential oscillations in proportion to the velocity vector. This shift in frequency alters the phase of oscillations in proportion to the integral of the velocity vector transformed by head direction: $\int_{t=0}^{T} H(\vec{v}\ (t)dt + x_0) = H\ \vec{x}\ (T)$. In addition, the interference pattern increases and decreases in proportion to the difference in oscillation frequency of the soma and dendrite, so that the vector of angular phases of interference is $\varphi(t) = \omega\beta H\ \vec{x}\ (t)$ (see Figures 3(b) and 3(c)) and the equation for grid cell activity can be written for location as $g(t) = [\prod \cos(\omega\beta_H H\ \vec{x}\ (t))]$.

The location can be extracted from grid cell phase by using the inverse of the head direction transform matrix as follows: $\vec{x}\ (t) = H^{-1}\ \vec{\varphi}\ (t)/\omega\beta$. Figure 3(d) shows the trajectory obtained from this inverse transform of phase.

6.3. Theta phase precession

In addition to replicating the spatial periodicity of grid cell firing fields, the model based on interference of membrane potential oscillations also replicates experimental data showing systematic changes in phase of grid cell firing relative to network theta rhythm oscillations [48], a phenomenon known as theta phase precession. The phenomenon of theta phase precession was initially shown for place cell firing in the hippocampal formation [49, 50] and was proposed to arise from the interaction of network theta rhythm oscillations with cellular theta rhythm oscillations [49, 51, 52]. As

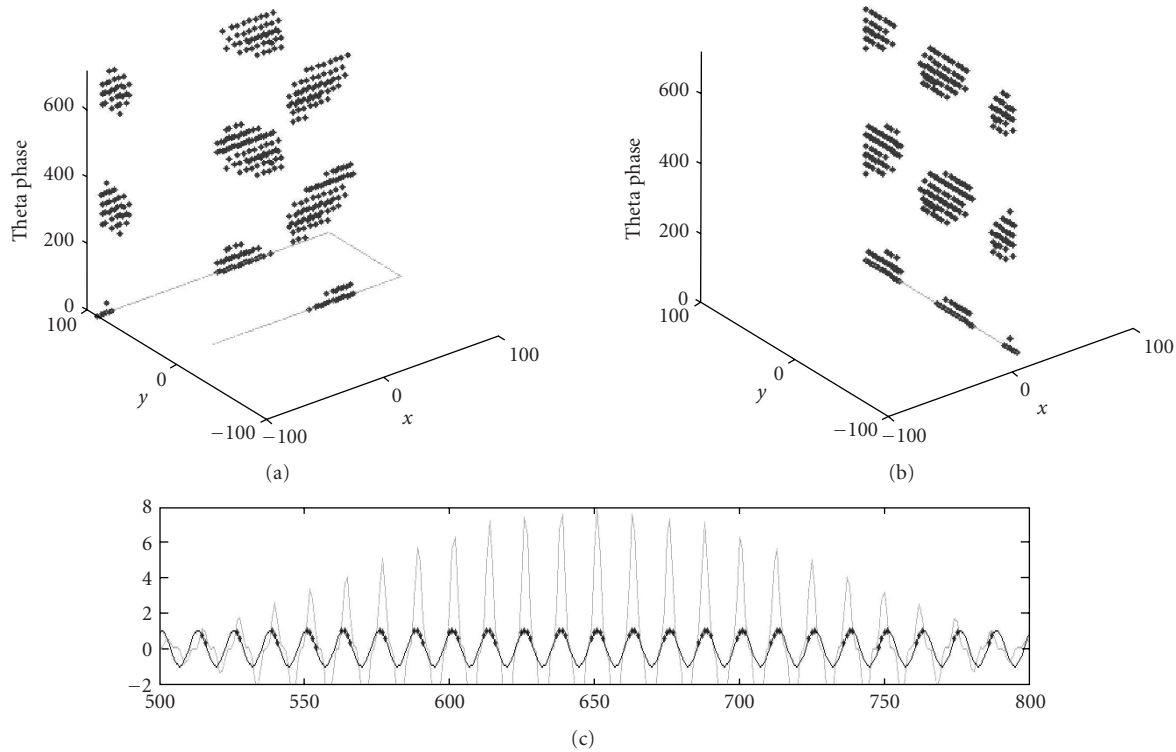

Figure 4: Simulation of theta phase precession in grid cell model based on membrane potential oscillations. (a) Theta phase plotted on vertical axis as a simulated rat runs through a grid cell firing field in west to east and east to west directions. (b) Theta phase during run from south to north. (c) Spike times (filled circles) of summed oscillations in a neuron relative to oscillation in the soma of that neuron (negative of network theta oscillation).

an alternative model, precession was proposed to arise from the readout of sequences of place cell activity [53–55].

The oscillatory interference model of grid cells [18, 47] extended the models of hippocampal phase precession and can account for grid cell phase precession [48]. In the oscillatory interference model, the interference has two components that appear physiologically: (1) as described above, the size of grid fields is determined by the envelope that has a frequency depending on the difference of the two angular frequencies $\omega_d - \omega_s$, and (2) the pattern of phase precession depends on a higher frequency component that corresponds to the mean of the two frequencies $(\omega_s + \omega_d)/2$. The phase of this second-high frequency component of the summed oscillation is $\varphi_{\text{sum}} = \omega t + \omega\beta\int_0^t H\ \vec{v}\ (\tau)d\tau/2$. The spiking will occur near the peak phase of this summed oscillation which is equal to some multiple n of the full cycle: $\varphi_{\text{sum}} = n2\pi$.

The spiking caused by the phase of the summed oscillations can then be plotted relative to the network theta rhythm by plotting the phase of the soma at the time of each spike. This can be obtained analytically from the above equation if we consider the case of the movement at a constant speed continuously in the preferred direction of one head direction cell. In this case, the integral of head direction for that cell is simply the integral of speed, which is equal to the location $x = \int_0^t H\ \vec{v}\ (\tau)d\tau$. Note also that the phase of the soma oscillations is the product of soma frequency and time: $\varphi_{\text{soma}} = 2\pi f t$. Therefore, the equation for the phase of the summed oscillation can be reduced to $\varphi_{\text{sum}} = \varphi_{\text{soma}} + \omega Bx/2$.

Plotting of theta phase precession essentially involves plotting the timing of spikes (which occur when $\varphi_{\text{sum}} = n2\pi$) relative to the phase of the network oscillations (which here correspond to the phase of the soma because the soma is being driven by network oscillations with fixed frequency ω). Thus, the vertical axis of a plot of theta phase precession shows the phase of the soma oscillation at the time of each spike: $\varphi_{\text{soma}} = n2\pi - \pi f Bx$ plotted relative to location x on the horizontal axis. Figure 4 shows the plotting of spikes in the simulation during runs on a linear track through the firing field of the neuron. Note that the phase precession in this model resembles the phase precession found in experimental data [50] but only covers about 180 degrees of the network theta oscillation cycle.

Note that the phase precession for a single direction gives a partial readout of the phase code of location, but when considering the phase in two-dimensional space, it confounds the phase of the two or more dendrites, so it is radially symmetric and dependent upon the direction of trajectory through the field (see Figure 5(a)). Thus, the phase precession code is less accurate for use in path integration, in contrast to the overall mean firing rate that would be observed in a grid cell due to persistent firing with a very large firing field, which could code location for distances smaller than one half the spacing between two grid fields (e.g., for 80 cm spacing, distances less than 40 cm could be coded).

6.4. Mechanism for path integration

As noted above, path integration involves an animal using its self-motion cues to maintain an accurate representation of angle and distance from start position. In the grid cell model, the update of oscillation phase by speed-modulated head direction integrates the velocity vector, thereby integrating the distance from the starting position in specific directions determined by H. If oscillation phases are reset to zero at the starting location, the return vector $\mathbf{r}$ giving distance and direction back to the starting location can be obtained by applying the inverse of the head direction matrix to the dendritic phase vector at any position $\vec{r} = -H^{-1}\ \vec{\varphi}\ /\omega\beta$. Figure 3(a) shows that after resetting phase at the starting location, applying the inverse head direction transform to the dendritic phase vector, and taking the negative of this vector gives the direction and angle directly back to the starting location (dotted line).

6.5. Interaction of path integration and visual stimuli

Path integration based on idiothetic cues alone builds up substantial error [34] that is usually corrected by comparison with sensory cues such as visual stimuli [35]. Grid cells show dependence upon visual stimuli in the environment. They maintain the same properties when returned to a familiar room [24], and they change their scale during a period of time after manipulations of environment size [44]. This influence of visual stimuli could result from the fact that the angle to visual stimuli has the same properties as phase of grid cell oscillations. Figure 5 shows how the angle of a single distal visual stimulus changes as a rat moves in a manner that is consistent with the change in phase of individual dendrites of a single modeled grid cell.

Alternately, the grid cell could be influenced by the angle and distance to visual stimuli, and neural mechanisms could update the expected angle and distance to visual stimuli in a manner similar to the mechanism for updating the angle and distance from start location (return vector). This requires updating the angles of the initially selected stimuli (that might be determined by eye direction) according to the direction and velocity of movement. This will update the expected absolute angle of visual stimuli. The further computation of expected relative angle (the actual visual input) requires combining absolute angle with current head direction. The process of updating head direction could depend upon input from cells coding angular velocity of movement. These have been shown in the postsubiculum [27, 56] as well as in structures including the anterior dorsal thalamic nucleus [29]. Grid cells appear to be more consistent when there are clear barriers on the edge of the open field, suggesting that rats might use the vertical angle of a boundary to judge distance.

The basic grid cell model assumes speed modulation of head direction cells, but most head direction cells show stable persistent firing even when the rat is motionless. In contrast, place cells show more speed modulation. In keeping with the physiological data that shows stable persistent firing for head direction cells and speed dependent firing for place cells, it might be appropriate to represent state as the static head direction cell activity combined with visual stimulus angle, and to use the speed-dependent activity of place cells as the action of the rat.

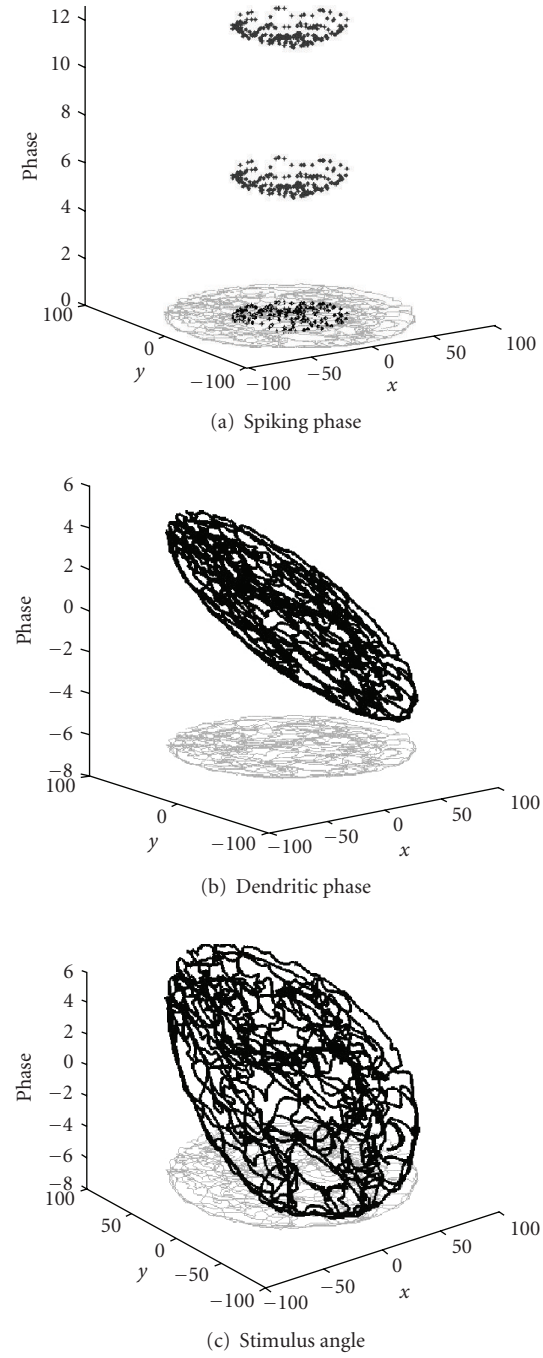

Figure 5: Phase relative to location in the environment. (a) Spiking phase due to precession (with refractory period). Note that phase depends upon location, but is circularly symmetric. (b) Dendritic phase of oscillations contains more complete continuous representation of location. (c) Plot of the angle of a single distal visual stimulus as a rat moves around in an environment, indicating similarity of allocentric stimulus angle to integrated dendritic phase in a grid cell.

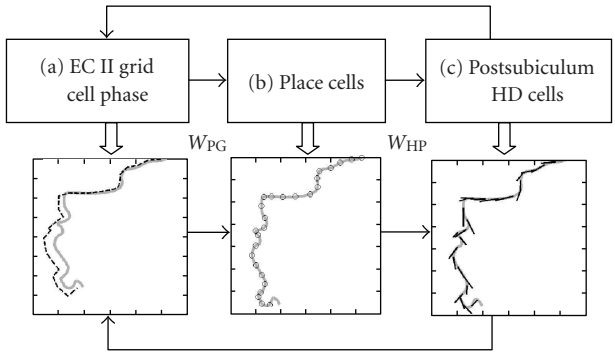

Figure 6: Model of episodic encoding and retrieval of trajectories. Top: Schematic representation of connectivity between grid cells, place cells, and head direction (HD) cells. Bottom: example of trajectory retrieval activity in each region. Trajectory experienced during encoding is shown in gray. (a) The location coded by the oscillation phase of entorhinal grid cell membrane potential is plotted as a dashed line that follows the actual trajectory in gray. Grid cell phase is put through the inverse head direction transformation to obtain coded location. Phase shifts are driven by retrieved head direction until next place cell is activated, then phase moves in new direction dependent on next active head direction cell. (b) Sequentially activated place cell representations are shown as open circles. (c) Each place cell activates a corresponding head direction representation, with direction shown as a short, straight, black line. This drives the next period of update of the grid cell phase.

6.6. *Grid cell phase represents continuum of locations for reinforcement learning*

The grid cells can be used as a representation of state for goal directed behavior. Many reinforcement learning theory models have used discrete representations of state for goal directed behavior. However, this causes difficulties for representing movement in continuous space. The phase of oscillations in the grid cell models is a continuous representation of space that can be updated in a continuous manner by actions held by persistent spiking. As noted previously [16, 57], this could allow grid cells to provide an effective mechanism for representations of state and action in continuous space and time.

7. MODEL OF EPISODIC MEMORY

The interaction of head direction cells and grid cells described here provides a potential mechanism for episodic memory involving the storage of trajectories through space and time [57]. As shown in Figure 6, this model uses a functional loop that encodes and retrieves trajectories via three stages: (1) head direction cells $h(t)$ update grid cells, (2) grid cells $g(t)$ update place cells, and (3) place cells $p(t)$ activate associated head direction activity [57]. This model is consistent with the anatomical connectivity (see Figure 6). The head direction cells could update grid cells via projections from the postsubiculum (dorsal presubiculum) to the medial entorhinal cortex [58–60], causing updating of persistent firing as described above, or influencing the phase of membrane potential oscillations [16–18]. Grid cells can update place cells via the extensive projections from entorhinal cortex layer II to dentate gyrus and CA3 and from layer III to region CA1 [45, 61]. The connectivity from grid cells to place cells could be formed by different computational mechanisms [45, 62, 63]. Place cells can become associated with head direction activity via direct projections from region CA1 to the postsubiculum [58], or via indirect projections from region CA1 to the subiculum [61, 64], and projections from the dorsal and distal regions of the subiculum to the postsubiculum and medial entorhinal cortex [65], both of which contain head direction cells.

During initial encoding of a trajectory in the model, the head direction cell activity vector would be set by the actual head direction of the rat during exploration, and associations would be encoded between place cell activity and head direction activity. These associations would be stored in the form of a synaptic connectivity matrix W_{HP} with strengthened connections between active place cells $p(t)$ and the head direction cell activity vector $h(t)$ as follows:

$$W_{HP} = \sum_{p} \vec{h}_p(t)\ \vec{p}\ (t)^T. \tag{7}$$

In this equation, head direction vectors associated with individual place cell locations are identified with the place cell index p. During retrieval, the head direction activity depends upon synaptic input from place cell representations as follows: $h(t) = W_{HP}p(t)$.

This model has the capacity for performing episodic encoding and retrieval of trajectories in simulations [57], including trajectories based on experimental data or trajectories created by an algorithm replicating foraging movements of a rat in an open field [17]. During encoding, a series of place cells $p(t)$ is created associated with particular locations $x_p = x(t)$. Each place cell is also associated with input from the grid cell population activity $g(t)$ and with the head direction vector $h_p = h(t)$ that occurred during the initial movement from that location. For retrieval, the simulation is cued with the grid cell phase vector $\varphi(t_0)$ and head direction vector $h(t_0)$ present at the start location. The head direction vector updates the grid cell phase vector $\varphi_d(t)$, which alters the activity of grid cells. The grid cell firing drives place cells p associated with subsequent locations on the trajectory. These mechanisms are summarized in Figure 6.

The activation of each new place cell activates a new head direction vector h_p associated with that place cell. This new head direction vector then drives the further update of dendritic phases of grid cells. This maintenance of the head direction vector might require graded persistent spiking [8] of head direction cells in deep layers of entorhinal cortex. Essentially, the retrieval of the place cell activity representing the state drives the retrieval of the new head direction vector representing the action from that state. This action is then used for a period of time to update the grid cell state representation until a new place cell representation is activated.

Because retrieval of the trajectory depends on updating of phase by head direction cells, this allows retrieval of a

trajectory at a time course similar to the initial encoding. This can allow effective simulation of the slow time course of place cell replay observed in previous experimental data collected during REM sleep [66]. The spread of activity from place cells to cells coding head direction could contribute to patterns of firing in the postsubiculum that appear as cells responding dependent on both place and head direction [31]. These cells might code the action value for retrieval of a trajectory from a particular location, firing only when actual head direction matches the head direction previously associated with specific place cell activity. The strong theta phase specificity of these cells could be due to separate dynamics for encoding and retrieval within each cycle of theta rhythm [67]. These cells might selectively fire during the retrieval phase.

7.1. Enhancement by arc length cells

The retrieval mechanism mediated by place cells can be enhanced by inclusion of cells that fire dependent upon the arc length of the trajectory [57], or by the time interval alone [17]. These types of responses help prevent a breakdown in trajectory retrieval caused by overlaps in the trajectory. The associations between place cells and head direction cells cannot disambiguate between two segments of a trajectory passing through the same location with different head directions. However, coding of arc length or time since the start of the trajectory can disambiguate these overlapping locations. Oscillatory interference between neurons directly modulated by speed but not head direction can activate arc length cells coding arc length from the start of a trajectory, or from the last time that oscillations are reset along the trajectory. Simulations based on this coding of arc length can account for many features of unit recording data in behavioral tasks. Persistent spiking in layer III of entorhinal cortex could provide a means for driving the coding of arc length (or time) along a trajectory. Persistent spiking in layer III with specific frequencies [6] could activate neurons in region CA1 with different phases relative to arc length (or time) on a trajectory. During retrieval, arc length cells from one portion of a trajectory can activate associated speed modulated cells to trigger the next arc length cell along a trajectory. This retrieval process can be accelerated or decelerated via modulation of the frequency of entorhinal oscillations during persistent firing.

7.2. Predictions of arc length model

Since the output of arc length cells is essentially dependent upon distance, a simple manipulation of running distance should directly influence spatial specificity of arc length cells. For example, in a rat running continuously clockwise around a circular track with a circumference of two meters, an arc length cell may match the periodicity of the track and display a stable place field somewhere on the track. Here, the cell is firing at an arc length of two meters. If we expand the track by a small amount to say, a circumference of 2.1 meters, the arc length cell would be expected to continue to fire at two-meter intervals, thus the field will translocate in the counterclockwise direction (or backwards in relation to the rat) by 10 centimeters for each lap.

The reset version of the arc length coding model assumes that oscillations reset at a specified location or during a key event such as food reward. This is supported experimentally given that the theta oscillation does reduce when an animal stops or consumes food. By using the same manipulation on the circular track as before, a similar but quite different prediction surfaces. Here, the field will shift counterclockwise abruptly, but will remain at that location for subsequent laps. This location stability is a direct consequence of stability of the food reward location since now the oscillatory interference is anchored to the food reward, and not from the previous location that the cell had discharged. Interestingly, the distance a field moves will be linearly proportional to the distance the original field was from the food reward location. Thus, a field will move 10 centimeters only if the field was originally located at the end of a lap (at the feeder), and a field will shift 5 centimeters if the original field was located at the midpoint of the lap.

The reset model prediction of the expanded circular track leads us to a further prediction. Since the discharge of an arc length cell in the reset model is dependent on and anchored to the reward location, a manipulation of the location of food reward will cause a relative movement of the location of the arc length's discharge. For example, the movement of the food reward by 10 centimeters in the clockwise directly will cause an arc length cell to correspondingly shift its field 10 centimeters in the clockwise direction.

8. CONCLUSIONS

The cellular physiological phenomena described in this paper provide mechanisms important for behavioral functions including path integration and the episodic encoding and retrieval of trajectories. Detailed computational models demonstrate the potential behavioral role of cellular mechanisms of persistent spiking and membrane potential oscillation, demonstrate how these could underlie unit recording data such as grid cell firing, and generate predictions for future experimental studies.

ACKNOWLEDGMENTS

Research supported by Silvio O. Conte Center grants NIMH MH71702 and MH60450, by NIMH R01 grants MH60013 and MH61492, by NSF SLC SBE 0354378, and by NIDA grant DA16454 (part of the CRCNS program).

REFERENCES

[1] H.-A. Steffenach, M. Witter, M.-B. Moser, and E. I. Moser, "Spatial memory in the rat requires the dorsolateral band of the entorhinal cortex," *Neuron*, vol. 45, no. 2, pp. 301–313, 2005.

[2] T. Otto and H. Eichenbaum, "Complementary roles of the orbital prefrontal cortex and the perirhinal-entorhinal cortices in an odor-guided delayed-nonmatching-to-sample task," *Behavioral Neuroscience*, vol. 106, no. 5, pp. 762–775, 1992.

[3] B. W. Leonard, D. G. Amaral, L. R. Squire, and S. Zola-Morgan, "Transient memory impairment in monkeys with bilateral lesions of the entorhinal cortex," *The Journal of Neuroscience*, vol. 15, no. 8, pp. 5637–5659, 1995.

[4] S. Zola-Morgan, L. R. Squire, and S. J. Ramus, "Severity of memory impairment in monkeys as a function of locus and extent of damage within the medial temporal lobe memory system," *Hippocampus*, vol. 4, no. 4, pp. 483–495, 1994.

[5] R. Klink and A. Alonso, "Muscarinic modulation of the oscillatory and repetitive firing properties of entorhinal cortex layer II neurons," *Journal of Neurophysiology*, vol. 77, no. 4, pp. 1813–1828, 1997.

[6] B. Tahvildari, E. Fransén, A. A. Alonso, and M. E. Hasselmo, "Switching between "On" and "Off" states of persistent activity in lateral entorhinal layer III neurons," *Hippocampus*, vol. 17, no. 4, pp. 257–263, 2007.

[7] E. Fransén, B. Tahvildari, A. V. Egorov, M. E. Hasselmo, and A. A. Alonso, "Mechanism of graded persistent cellular activity of entorhinal cortex layer V neurons," *Neuron*, vol. 49, no. 5, pp. 735–746, 2006.

[8] A. V. Egorov, B. N. Hamam, E. Fransén, M. E. Hasselmo, and A. A. Alonso, "Graded persistent activity in entorhinal cortex neurons," *Nature*, vol. 420, no. 6912, pp. 173–178, 2002.

[9] M. H. Shalinsky, J. Magistretti, L. Ma, and A. A. Alonso, "Muscarinic activation of a cation current and associated current noise in entorhinal-cortex layer-II neurons," *Journal of Neurophysiology*, vol. 88, no. 3, pp. 1197–1211, 2002.

[10] M. Yoshida, E. Fransén, and M. E. Hasselmo, "Cholinergic-independent persistent firing in entorhinal layers III and V neurons," *Society for Neuroscience Abstract*, vol. 33, p. 935.9, 2007.

[11] A. Alonso and R. R. Llinás, "Subthreshold Na^+-dependent theta-like rhythmicity in stellate cells of entorhinal cortex layer II," *Nature*, vol. 342, no. 6246, pp. 175–177, 1989.

[12] A. Alonso and R. Klink, "Differential electroresponsiveness of stellate and pyramidal-like cells of medial entorhinal cortex layer II," *Journal of Neurophysiology*, vol. 70, no. 1, pp. 128–143, 1993.

[13] E. Fransén, A. A. Alonso, C. T. Dickson, J. Magistretti, and M. E. Hasselmo, "Ionic mechanisms in the generation of subthreshold oscillations and action potential clustering in entorhinal layer II stellate neurons," *Hippocampus*, vol. 14, no. 3, pp. 368–384, 2004.

[14] C. D. Acker, N. Kopell, and J. A. White, "Synchronization of strongly coupled excitatory neurons: relating network behavior to biophysics," *Journal of Computational Neuroscience*, vol. 15, no. 1, pp. 71–90, 2003.

[15] A. Alonso and E. García-Austt, "Neuronal sources of theta rhythm in the entorhinal cortex of the rat. I. Laminar distribution of theta field potentials," *Experimental Brain Research*, vol. 67, no. 3, pp. 493–501, 1987.

[16] L. M. Giocomo, E. A. Zilli, E. Fransén, and M. E. Hasselmo, "Temporal frequency of subthreshold oscillations scales with entorhinal grid cell field spacing," *Science*, vol. 315, no. 5819, pp. 1719–1722, 2007.

[17] M. E. Hasselmo, L. M. Giocomo, and E. A. Zilli, "Grid cell firing may arise from interference of theta frequency membrane potential oscillations in single neurons," *Hippocampus*, vol. 17, no. 12, pp. 1252–1271, 2007.

[18] N. Burgess, C. Barry, and J. O'Keefe, "An oscillatory interference model of grid cell firing," *Hippocampus*, vol. 17, no. 9, pp. 801–812, 2007.

[19] N. Burgess, C. Barry, K. J. Jeffery, and J. O'Keefe, "A grid and place cell model of path integration utilizing phase precession versus theta," in *Proceedings of the 1st Annual Computational Cognitive Neuroscience Conference*, Washington, DC, USA, April 2005.

[20] C. T. Dickson, J. Magistretti, M. H. Shalinsky, E. Fransén, M. E. Hasselmo, and A. Alonso, "Properties and role of I(h) in the pacing of subthreshold oscillations in entorhinal cortex layer II neurons," *Journal of Neurophysiology*, vol. 83, no. 5, pp. 2562–2579, 2000.

[21] L. M. Giocomo and M. E. Hasselmo, "Time constant of I(h) differs along dorsal to ventral axis of medial entorhinal cortex," submitted.

[22] M. Yoshida and A. Alonso, "Cell-type-specific modulation of intrinsic firing properties and subthreshold membrane oscillations by the M(Kv7)-current in neurons of the entorhinal cortex," *Journal of Neurophysiology*, vol. 98, no. 5, pp. 2779–2794, 2007.

[23] B. Tahvildari and A. Alonso, "Morphological and electrophysiological properties of lateral entorhinal cortex layers II and III principal neurons," *The Journal of Comparative Neurology*, vol. 491, no. 2, pp. 123–140, 2005.

[24] T. Hafting, M. Fyhn, S. Molden, M.-B. Moser, and E. I. Moser, "Microstructure of a spatial map in the entorhinal cortex," *Nature*, vol. 436, no. 7052, pp. 801–806, 2005.

[25] F. Sargolini, M. Fyhn, T. Hafting, et al., "Conjunctive representation of position, direction, and velocity in entorhinal cortex," *Science*, vol. 312, no. 5774, pp. 758–762, 2006.

[26] J. S. Taube, R. U. Muller, and J. B. Ranck Jr., "Head-direction cells recorded from the postsubiculum in freely moving rats. I. Description and quantitative analysis," *The Journal of Neuroscience*, vol. 10, no. 2, pp. 420–435, 1990.

[27] P. E. Sharp, "Multiple spatial/behavioral correlates for cells in the rat postsubiculumml: multiple regression analysis and comparison to other hippocampal areas," *Cerebral Cortex*, vol. 6, no. 2, pp. 238–259, 1996.

[28] H. T. Blair and P. E. Sharp, "Anticipatory head direction signals in anterior thalamus: evidence for a thalamocortical circuit that integrates angular head motion to compute head direction," *The Journal of Neuroscience*, vol. 15, no. 9, pp. 6260–6270, 1995.

[29] J. S. Taube, "Head direction cells and the neurophysiological basis for a sense of direction," *Progress in Neurobiology*, vol. 55, no. 3, pp. 225–256, 1998.

[30] R. U. Muller, J. B. Ranck Jr., and J. S. Taube, "Head direction cells: properties and functional significance," *Current Opinion in Neurobiology*, vol. 6, no. 2, pp. 196–206, 1996.

[31] F. Cacucci, C. Lever, T. J. Wills, N. Burgess, and J. O'Keefe, "Theta-modulated place-by-direction cells in the hippocampal formation in the rat," *The Journal of Neuroscience*, vol. 24, no. 38, pp. 8265–8277, 2004.

[32] M. Muller and R. Wehner, "Path integration in desert ants, cataglyphis fortis," *Proceedings of the National Academy of Sciences of the United States of America*, vol. 85, no. 14, pp. 5287–5290, 1988.

[33] R. Wehner and M. Muller, "The significance of direct sunlight and polarized skylight in the ant's celestial system of navigation," *Proceedings of the National Academy of Sciences of the United States of America*, vol. 103, no. 33, pp. 12575–12579, 2006.

[34] A. Cheung, S. Zhang, C. Stricker, and M. V. Srinivasan, "Animal navigation: the difficulty of moving in a straight line," *Biological Cybernetics*, vol. 97, no. 1, pp. 47–61, 2007.

[35] R. Wehner, B. Michel, and P. Antonsen, "Visual navigation in insects: coupling of egocentric and geocentric information,"

Journal of Experimental Biology, vol. 199, part 1, pp. 129–140, 1996.

[36] J. O'Keefe, N. Burgess, J. G. Donnett, K. J. Jeffery, and E. A. Maguire, "Place cells, navigational accuracy, and the human hippocampus," *Philosophical Transactions of the Royal Society B*, vol. 353, no. 1373, pp. 1333–1340, 1998.

[37] P. E. Sharp and S. Turner-Williams, "Movement-related correlates of single-cell activity in the medial mammillary nucleus of the rat during a pellet-chasing task," *Journal of Neurophysiology*, vol. 94, no. 3, pp. 1920–1927, 2005.

[38] G. Strang, *Linear Algebra and Its Applications*, Harcourt Brace Jovanovich, San Diego, Calif, USA, 1988.

[39] D. J. Foster and M. A. Wilson, "Reverse replay of behavioural sequences in hippocampal place cells during the awake state," *Nature*, vol. 440, no. 7084, pp. 680–683, 2006.

[40] R. A. Koene and M. E. Hasselmo, "Reversed and forward buffering of behavioral spike sequences enables retrospective and prospective retrieval in hippocampal regions CA3 and CA1," *Neural Networks*, vol. 21, no. 2-3, pp. 276–288, 2008.

[41] E. J. Markus, Y.-L. Qin, B. Leonard, W. E. Skaggs, B. L. McNaughton, and C. A. Barnes, "Interactions between location and task affect the spatial and directional firing of hippocampal neurons," *The Journal of Neuroscience*, vol. 15, no. 11, pp. 7079–7094, 1995.

[42] D. Derdikman, M. Fyhn, T. Hafting, M. B. Moser, and E. I. Moser, "Breaking up the entorhinal grid in a hairpin maze," *Society for Neuroscience Abstract*, vol. 33, p. 68.10, 2006.

[43] M. Fyhn, T. Hafting, A. Treves, M.-B. Moser, and E. I. Moser, "Hippocampal remapping and grid realignment in entorhinal cortex," *Nature*, vol. 446, no. 7132, pp. 190–194, 2007.

[44] C. Barry, R. Hayman, N. Burgess, and K. J. Jeffery, "Experience-dependent rescaling of entorhinal grids," *Nature Neuroscience*, vol. 10, no. 6, pp. 682–684, 2007.

[45] T. Solstad, E. I. Moser, and G. T. Einevoll, "From grid cells to place cells: a mathematical model," *Hippocampus*, vol. 16, no. 12, pp. 1026–1031, 2006.

[46] C. P. Heesy, "On the relationship between orbit orientation and binocular visual field overlap in mammals," *The Anatomical Record. Part A*, vol. 281, no. 1, pp. 1104–1110, 2004.

[47] J. O'Keefe and N. Burgess, "Dual phase and rate coding in hippocampal place cells: theoretical significance and relationship to entorhinal grid cells," *Hippocampus*, vol. 15, no. 7, pp. 853–866, 2005.

[48] T. Hafting, M. Fyhn, M.-B. Moser, and E. I. Moser, "Phase precession and phase locking in entorhinal grid cells," *Society for Neuroscience Abstract*, vol. 32, p. 68.8, 2006.

[49] J. O'Keefe and M. L. Recce, "Phase relationship between hippocampal place units and the EEG theta rhythm," *Hippocampus*, vol. 3, no. 3, pp. 317–330, 1993.

[50] W. E. Skaggs, B. L. McNaughton, M. A. Wilson, and C. A. Barnes, "Theta phase precession in hippocampal neuronal populations and the compression of temporal sequences," *Hippocampus*, vol. 6, no. 2, pp. 149–172, 1996.

[51] A. P. Maurer, S. R. VanRhoads, G. R. Sutherland, P. Lipa, and B. L. McNaughton, "Self-motion and the origin of differential spatial scaling along the septo-temporal axis of the hippocampus," *Hippocampus*, vol. 15, no. 7, pp. 841–852, 2005.

[52] M. Lengyel, Z. Szatmáry, and P. Érdi, "Dynamically detuned oscillations account for the coupled rate and temporal code of place cell firing," *Hippocampus*, vol. 13, no. 6, pp. 700–714, 2003.

[53] M. V. Tsodyks, W. E. Skaggs, T. J. Sejnowski, and B. L. McNaughton, "Population dynamics and theta rhythm phase precession of hippocampal place cell firing: a spiking neuron model," *Hippocampus*, vol. 6, no. 3, pp. 271–280, 1996.

[54] G. V. Wallenstein and M. E. Hasselmo, "GABAergic modulation of hippocampal population activity: sequence learning, place field development, and the phase precession effect," *Journal of Neurophysiology*, vol. 78, no. 1, pp. 393–408, 1997.

[55] O. Jensen and J. E. Lisman, "Hippocampal CA3 region predicts memory sequences: accounting for the phase precession of place cells," *Learning & Memory*, vol. 3, no. 2-3, pp. 279–287, 1996.

[56] P. E. Sharp and K. Koester, "Lesions of the mammillary body region severely disrupt the cortical head direction, but not place cell signal," *Hippocampus*. In press.

[57] M. E. Hasselmo, "Arc length coding by interference of theta frequency oscillations may underlie context-dependent hippocampal unit data and episodic memory function," *Learning & Memory*, vol. 14, no. 11, pp. 782–794, 2007.

[58] T. van Groen and J. M. Wyss, "The postsubicular cortex in the rat: characterization of the fourth region of the subicular cortex and its connections," *Brain Research*, vol. 529, no. 1-2, pp. 165–177, 1990.

[59] M. Caballero-Bleda and M. P. Witter, "Regional and laminar organization of projections from the presubiculum and parasubiculum to the entorhinal cortex: an anterograde tracing study in the rat," *The Journal of Comparative Neurology*, vol. 328, no. 1, pp. 115–129, 1993.

[60] C. Köhler, "Intrinsic projections of the retrohippocampal region in the rat brain. I. The subicular complex," *The Journal of Comparative Neurology*, vol. 236, no. 4, pp. 504–522, 1985.

[61] D. G. Amaral and M. P. Witter, "The 3-dimensional organization of the hippocampal formation: a review of anatomical data," *Neuroscience*, vol. 31, no. 3, pp. 571–591, 1989.

[62] M. C. Fuhs and D. S. Touretzky, "A spin glass model of path integration in rat medial entorhinal cortex," *The Journal of Neuroscience*, vol. 26, no. 16, pp. 4266–4276, 2006.

[63] E. T. Rolls, S. M. Stringer, and T. Elliot, "Entorhinal cortex grid cells can map to hippocampal place cells by competitive learning," *Network*, vol. 17, no. 4, pp. 447–465, 2006.

[64] L. W. Swanson, J. M. Wyss, and W. M. Cowan, "An autoradiographic study of the organization of intrahippocampal association pathways in the rat," *The Journal of Comparative Neurology*, vol. 181, no. 4, pp. 681–715, 1978.

[65] P. A. Naber and M. P. Witter, "Subicular efferents are organized mostly as parallel projections: a double-labeling, retrograde-tracing study in the rat," *The Journal of Comparative Neurology*, vol. 393, no. 3, pp. 284–297, 1998.

[66] K. Louie and M. A. Wilson, "Temporally structured replay of awake hippocampal ensemble activity during rapid eye movement sleep," *Neuron*, vol. 29, no. 1, pp. 145–156, 2001.

[67] M. E. Hasselmo, C. Bodelón, and B. P. Wyble, "A proposed function for hippocampal theta rhythmml: separate phases of encoding and retrieval enhance reversal of prior learning," *Neural Computation*, vol. 14, no. 4, pp. 793–817, 2002.

Hindawi Publishing Corporation
Neural Plasticity
Volume 2008, Article ID 563028, 7 pages
doi:10.1155/2008/563028

Research Article

Enhancement of Neocortical-Medial Temporal EEG Correlations during Non-REM Sleep

Nikolai Axmacher,[1,2] Christoph Helmstaedter,[1] Christian E. Elger,[1,2] and Juergen Fell[1]

[1] *Department of Epileptology, University of Bonn, 53105 Bonn, Germany*
[2] *Life and Brain Academic Research, University of Bonn, 53105 Bonn, Germany*

Correspondence should be addressed to Nikolai Axmacher, nikolai.axmacher@ukb.uni-bonn.de

Received 21 December 2007; Revised 17 March 2008; Accepted 13 May 2008

Recommended by C. Andrew Chapman

Interregional interactions of oscillatory activity are crucial for the integrated processing of multiple brain regions. However, while the EEG in virtually all brain structures passes through substantial modifications during sleep, it is still an open question whether interactions between neocortical and medial temporal EEG oscillations also depend on the state of alertness. Several previous studies in animals and humans suggest that hippocampal-neocortical interactions crucially depend on the state of alertness (i.e., waking state or sleep). Here, we analyzed scalp and intracranial EEG recordings during sleep and waking state in epilepsy patients undergoing presurgical evaluation. We found that the amplitudes of oscillations within the medial temporal lobe and the neocortex were more closely correlated during sleep, in particular during non-REM sleep, than during waking state. Possibly, the encoding of novel sensory inputs, which mainly occurs during waking state, requires that medial temporal dynamics are rather independent from neocortical dynamics, while the consolidation of memories during sleep may demand closer interactions between MTL and neocortex.

Copyright © 2008 Nikolai Axmacher et al. This is an open access article distributed under the Creative Commons Attribution License, which permits unrestricted use, distribution, and reproduction in any medium, provided the original work is properly cited.

1. INTRODUCTION

Memory consolidation has been suggested to occur in two subsequent steps: while initial encoding depends on the integrity of the medial temporal lobe (MTL) (e.g., [1, 2]) and is linked to the formation of transient assemblies via fast synaptic plasticity in the entorhinal cortex and hippocampus, subsequent consolidation requires the transfer of information to the neocortex, where more permanent networks are built [3–6]. During both waking state and sleep, communication of the hippocampus with the neocortex mainly proceeds via polymodal regions within the rhinal cortex [7]. The rhinal cortex receives rich input from modality-specific regions in higher-order sensory areas which are located in the inferior temporal neocortex. The inferior temporal cortex is the final processing stage of the ventral visual stream and comprises object-specific regions such as the fusiform face area [8, 9]. Recently, Klopp and colleagues [10] used intracranial EEG to show that activity within this area was coherent with activity in widespread brain regions selectively during face processing. Furthermore, fusiform and rhinal cortices are synchronized during memory retrieval [11]. These data indicate that during waking state, interactions between sensory and medial temporal regions are required.

In an influential model, Buzsáki [3] hypothesized that during waking state, and particularly during exploratory phases, information is transferred into the hippocampus and induces rapid though transient forms of synaptic plasticity (see also [12]). Physiologically, strong cholinergic inputs during waking state inhibit feedback excitation in the CA3 region of the hippocampus and induce θ (4–8 Hz) and γ (20–44 Hz) oscillations; during sleep, a reduced level of acetylcholine leads to disinhibition of hippocampal pyramidal cells, which consequently engage in highly synchronized population bursts [4]. These bursts have been linked to replay of previously acquired information and transfer into the neocortex, where more stable representations are being built [5]. Taken together, these studies suggest a bidirectional information flow between MTL and neocortex, with transmission from the neocortex into the hippocampus during exploration and from the hippocampus into the neocortex during rest and sleep.

The close connection between memory consolidation and sleep [13] suggests that interactions of neocortical and medial temporal EEG activity also undergo circadian fluctuations. However, there are very few data on the interaction between neocortical and medial temporal EEG oscillations during waking state and sleep in humans, partly due to the difficulty of obtaining EEG recordings from the human MTL. Neocortical as well as MTL θ and γ oscillations were suggested to underlie declarative memory encoding and retrieval (e.g., [12, 14–16]. On the other hand, neocortical slow wave activity (i.e., <4 Hz activity, which includes both δ activity between 1 and 4 Hz and slow oscillations <1 Hz) as well as sleep spindles in the β (12–20 Hz) range, was shown to be important for the consolidation of previously acquired declarative memories during sleep (e.g., [17, 18]). It is unknown, however, whether there are state specific correlations between the amplitudes of neocortical and medial temporal EEG oscillations. To investigate this question, we analyzed scalp and intracranial EEG recordings in patients with pharmacoresistant focal epilepsy undergoing presurgical evaluation for exact localization of the seizure onset zone.

2. MATERIALS AND METHODS

During presurgical evaluation, polysomnography and intracranial EEG were recorded from ten patients (six women; mean age 40.1 ± 22.6 years) with pharmacoresistant unilateral temporal lobe epilepsy. Mean duration of epilepsy was 21.4 ± 11.3 years. Scalp EEG was recorded from positions Cz, C3, C4, and O1 (10–20 system). Electro-ocular activity was registered at the outer canthi of both eyes, and submental electromyographic activity was acquired with electrodes attached to the skin. Scalp as well as depth electroencephalograms were referenced to linked mastoids, bandpass filtered (0.01 Hz (6 dB/octave) to 70 Hz (12 dB/octave)), and recorded with a sampling rate of 200 Hz.

Multicontact depth electrodes were implanted stereotactically along the longitudinal axis of each MTL [19]. The placement of electrode contacts within the hippocampus and the anterior parahippocampal gyrus, which is covered by the rhinal cortex, was ascertained by magnetic resonance imaging in each patient. For each patient, one contact within the rhinal cortex, one within the anterior part (anterior third), and one within the posterior part of the hippocampus (posterior third) were selected. Only invasive EEG recordings of the MTL contralateral to the zone of seizure origin were analyzed. These data were compared with the central electrode of scalp EEG (C3/C4) ipsilateral to the nonepileptic MTL.

Visual sleep stage scoring was carried out for each 20-second epoch according to Rechtschaffen/Kales criteria [20] by two experts. Subsequently, epochs were divided into the following categories: waking state, REM sleep, and non-REM sleep. All EEG epochs were visually inspected for movement artifacts and epileptiform activity. Epochs containing artifacts were discarded irrespective of the duration of artifacts. Furthermore, all epochs with power values above 50 μV^2 in the upper γ band (36–44 Hz) were discarded, to avoid high-frequency contamination, which may survive visual artifact rejection. In total, 53.0% of all EEG epochs were excluded from further analysis (45.1% based on step one, 7.9% based on step two).

Power spectra of all artifact-free epochs were calculated for each 20 seconds epoch. To increase statistical reliability of power estimates, we partitioned each 20 seconds EEG epoch into 16 nonoverlapping subsegments of 1.25 seconds duration. We used a fast Fourier transform (cosine windowing), and the frequency range was divided up into the following bands: δ (1–4 Hz), θ (4–8 Hz), α (8–12 Hz), β_1 (12–16 Hz), β_2 (16–20 Hz), γ_1 (20–28 Hz), γ_2 (28–36 Hz), and γ_3 (36–44 Hz). Pearson's correlations between power values for scalp EEG (C3/C4) and all three locations of the medial temporal depth electrodes were calculated. Correlation values were Fisher z-transformed, and group differences against zero were evaluated with two-tailed t-tests.

3. RESULTS

Figure 1 presents raw data from one exemplary subject. Visually, there appeared to be an increased correlation of δ band activity during non-REM sleep. To quantify the effect of different sleep stages on interactions of EEG dynamics within neocortex and MTL, we performed a three-way ANOVA with "locus" (C3/4 compared to rhinal cortex, anterior hippocampus, or posterior hippocampus) and "sleep stage" (waking state, REM-sleep, and non-REM sleep) as repeated measures and "frequency band" as independent variable. Figure 2 depicts average values of Fisher z-transformed correlation values for the different frequency bands during waking state, REM-sleep, and non-REM sleep. We observed a highly significant effect of "sleep stage" ($F_{2,144} = 6.49$; $P = 0.002$) and a near significant effect of "frequency band" ($F_{7,72} = 2.13$; $P = 0.051$), but no effect of "locus" and no interaction. This result indicates that interactions of EEG dynamics within neocortex and MTL depended significantly on sleep stage. Neocortical and medial temporal EEG oscillations were more closely correlated during sleep than during waking state.

Although we did not find a significant "sleep stage" × "frequency band" interaction, we were interested in frequency-specific effects and thus conducted two-way ANOVAs with "locus" and "sleep stage" (waking state, REM sleep, and NREM sleep) as repeated measures separately for the different frequency bands. We found a significant effect of "sleep stage" ($F_{2,18} = 6.00$; $P = 0.010$) and a trend for a "sleep stage" × "locus" interaction ($F_{4,36} = 2.14$; $P = 0.096$) in the δ range, but not in any other frequency bands. To identify differences between pairs of sleep stages in the different frequency bands, we conducted two-way ANOVAs with "locus" and "sleep stage" (either waking state and REM sleep; or waking state and NREM sleep; or REM sleep and NREM sleep) as repeated measures separately for the different frequency bands. In the δ band, we found a significant effect of "sleep stage" for the comparison of waking state and NREM sleep ($F_{1,9} = 7.11$; $P = 0.026$). While there was no significant difference between waking

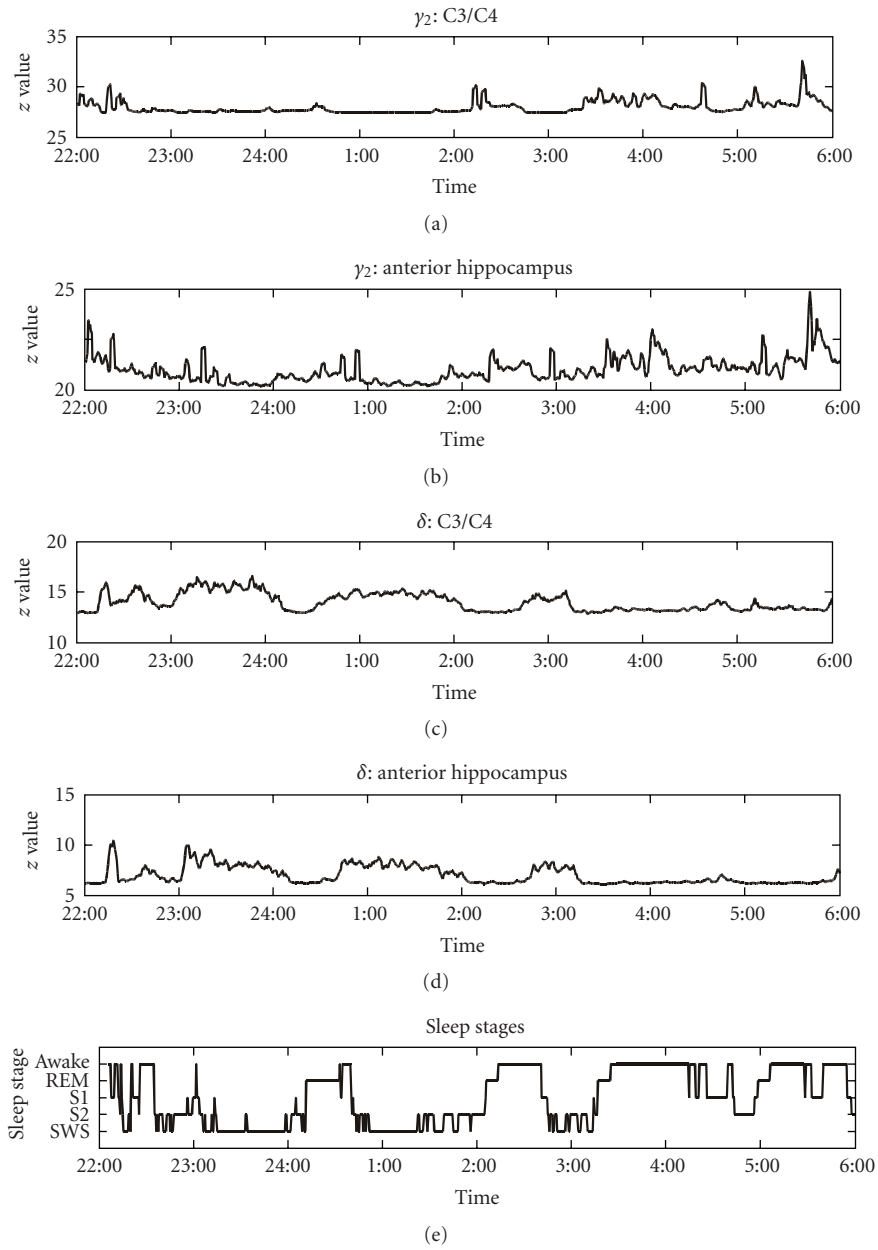

FIGURE 1: Time course of γ_2 and δ band activity in scalp EEG and in the anterior hippocampus and sleep stages during one night in one exemplary subject. S1: sleep stage 1, S2: sleep stage 2, SWS: slow wave sleep.

state and REM sleep, the comparison of REM sleep and NREM sleep also revealed a significant effect of "sleep stage" ($F_{1,9} = 7.95$; $P = 0.020$) and a significant "sleep stage" $\times$ "locus" interaction ($F_{2,18} = 3.99$; $P = 0.037$). We thus calculated separate one-way ANOVAs for the different pairs of electrodes. We found a significant difference between NREM and REM sleep at the posterior hippocampus-Cz pair ($F_{1,9} = 16.76$; $P = 0.0027$), and trends for the anterior hippocampus-Cz pair ($F_{1,9} = 4.27$; $P = 0.0687$) and the rhinal-Cz pair ($F_{1,9} = 3.56$; $P = 0.091$).

Besides these effects in the δ frequency range, we also conducted separate two-way ANOVAs with "locus" and pairs of "sleep stage" as repeated measure in the other frequency bands. We found a trend for a difference between NREM and REM sleep both in the α ($F_{1,9} = 3.83$; $P = 0.0819$) and in the γ_2 range ($F_{1,9} = 3.39$; $P = 0.0987$).

It might be argued that the effect of sleep stage on power correlations is contaminated by differences of power in the different sleep stages. Power values depend on sleep stage, and thus in stages with low EEG power in a given frequency band, the noise may be too large to detect the correlation. In other words, the increased correlation in the δ band during NREM sleep as compared to waking state might be related to the fact that δ power is maximal during NREM sleep. However, it is unlikely that the effect of sleep stage on correlation observed in our data depends

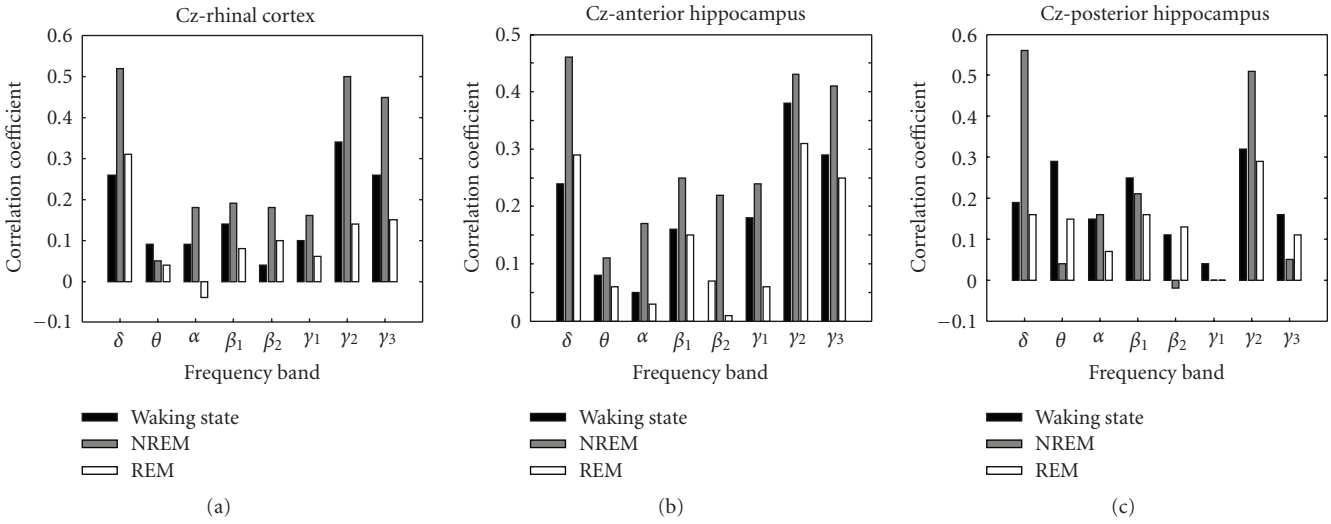

Figure 2: Pearson's correlation coefficient (Fisher z-transformed) between power densities in scalp EEG (C3/C4) versus medial temporal locations; averages across subjects are depicted. Both in the δ and in higher (α and γ_2) frequency range, correlation values were maximal during NREM sleep.

on power values for the following reasons. In the three-way ANOVA with "sleep stage" and "locus" as repeated measures and "frequency band" as independent variable reported above, we observed a main effect of "sleep stage" but no "frequency band" × "sleep stage" interaction, indicating that the effect of sleep stage did not depend on frequency band. Indeed, we did not only observe increased correlations during NREM sleep as compared to waking state in the δ range, but also trends for increased correlations in the α and γ_2 range, which have a lower power during NREM sleep than waking state. The effects of sleep stage on power values are usually substantially different. δ and θ power increase during NREM sleep as compared to waking state, whereas power in higher frequency ranges decreases. This typical relationship occurred in our data as well (see Figure 3). A three-way ANOVA of power values with "sleep stage" and "locus" as repeated measures and "frequency band" as independent variable revealed a significant "sleep stage" × "frequency band" interaction ($F_{14,144} = 9.771$; $P < 10^{-10}$; $\varepsilon = 0.707$), indicating that sleep had different effects on power in the different frequency bands.

To directly assess whether the effect of "sleep stage" on the correlation of power values depends on differences in power, we calculated the correlation of (Fisher z-transformed) correlation values with power across regions and frequency bands. None of these correlations reached significance (Pearson's correlation values were <0.2 in each test, corresponding to P values >0.6).

4. DISCUSSION

Our findings indicate that oscillations within the MTL and the neocortex are more closely correlated during sleep, in particular during non-REM sleep, than during waking state. This is consistent with the hypothesis that encoding of novel inputs into long-term memory, which occurs mainly during waking state, requires that medial temporal EEG dynamics are rather independent from neocortical dynamics [3], with the exception of interactions in the θ and γ range (e.g., [12, 14–16]. On the other hand, the consolidation of declarative memories during sleep may demand closer correlation of neocortical and medial temporal EEG dynamics [3], not only in the γ range, but also with respect to δ and β (spindle) oscillations (e.g., [17, 18]). Interestingly, correlations in the spindle frequency range only reached significance during slow-wave sleep, but not during the entire period of non-REM sleep. This might suggest that neocortical-medial temporal interactions in this frequency range are less prominent in sleep stage 2, which is most commonly associated with sleep spindles, than in deeper sleep stages.

Even though we only analyzed data from the hemisphere contralateral to the seizure onset zone, a relatively large number of epochs (53%) contained at least one epileptiform event or a movement artifact. All EEG epochs were inspected twice for movement artifacts and epileptiform activity. Artifact segments were discarded irrespective of artifact duration; for example, if a single spike or movement artifact occurred during a 20-second epoch, the entire epoch was discarded because artifacts might otherwise spuriously contribute to power estimates. As a result, the number of discarded epochs was relatively large; however, because we analyzed EEG during entire nights, the remaining data set was still extensive (mean ± std.: 178.3 ± 117.3 minutes per night).

Activity in the frequency range between 0.5 Hz and 1 Hz, that is, below the δ frequency range, has been termed "slow activity" (SA) and is probably due to different mechanisms than δ activity [21]. In principle, it would have been interesting to analyze correlation of SA between the neocortex and the MTL as well. However, the subsegments of 1.25 seconds durations which were used to analyze power values (see Methods) contain only a single cycle, or even less, of 0.5–1 Hz activity, which would have resulted in imprecise

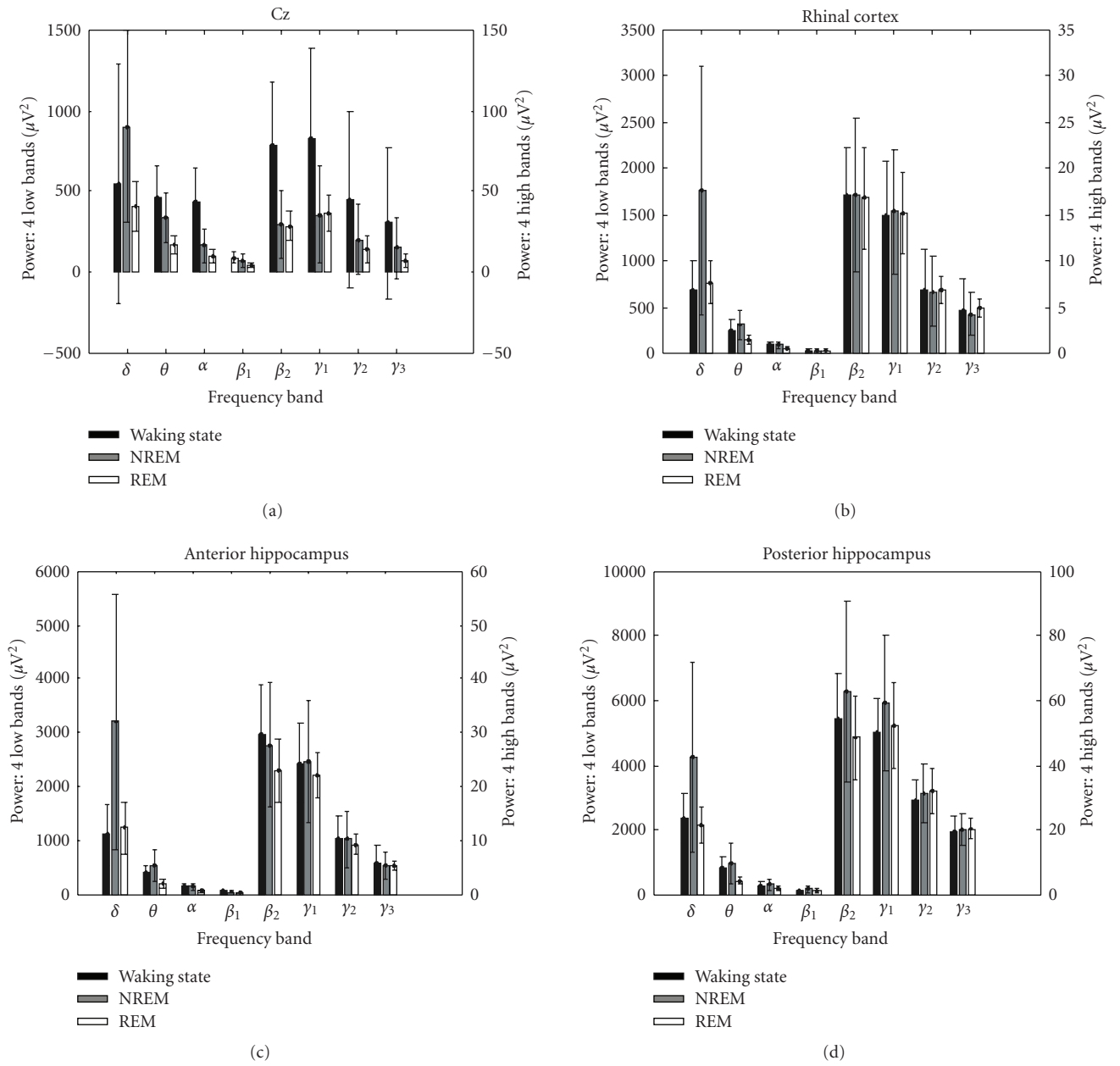

Figure 3: Power values (mean and standard deviation across epochs) in scalp EEG and medial temporal locations. Please note that to improve visibility of effect of sleep stage, ordinate scaling differs for low- (δ to β_1) and high- (β_2 to γ_3) frequency bands. In contrast to the effect of sleep on power correlations (see Figure 2), power values in the high-frequency band were maximal during waking state.

estimations of power values. We thus decided to omit this frequency range.

Previous studies on correlation of activity between hippocampus and neocortex found that hippocampal θ oscillations occurred in brief bursts and were most abundant during REM sleep, where they were independent of neocortical θ band activity [22]. While they were virtually absent during SWS, there were also longer θ bursts during transition from REM sleep to waking state, which occurred simultaneously with neocortical θ activity. These results are somewhat different from our findings that coupling was most pronounced during NREM sleep. However, it should be noted that different measures were used. While we calculated correlations of power values across 20 seconds epochs, Cantero and colleagues [22] analyzed partial directed coherence. In another study, Cantero et al. [23] reported a decrease of cortico-hippocampal coherence during sleep in a γ band (35–58 Hz) corresponding roughly to (but exceeding) our γ_3 band (36–44 Hz). In our study, the average correlation in the γ_3 range between Cz and the posterior hippocampus was also higher during waking state than during NREM sleep (see Figure 2), although this difference did not reach

significance and was opposite between Cz and the other MTL locations. Further research is necessary to explain these divergent findings.

In particular, it would be interesting to investigate cortico-hippocampal coupling during replay of previously acquired information similar to results from animal studies. In rats, place cells in the hippocampus represent spatial positions by their firing rate [24]. Various studies found that during sleep periods following exploration of new environments (and thus following development of new place representations; [25]), these activity sequences are being replayed [26, 27]. Most importantly, such replay has been observed not only in the hippocampus, but also simultaneously in the neocortex as well [28]. In humans, stimulus-specific activity has only been observed in the hippocampus [29], but not in the neocortex. It is unknown, however, if this activity is replayed during consecutive sleep periods. Such relative preservation of the mechanisms underlying memory consolidation across species might be suggested by studies showing that medial temporal high-frequency bursts ("ripples"), which appear to correspond to condensed information replay [12], are coupled to neocortical sleep spindles both in rats [30–32] and humans [33].

In our analyses, we assessed functional connectivity by measuring the correlation of power values averaged across episodes of 20 seconds. While this approach lacks temporal resolution, it allows to clearly assign correlation values to specific sleep stages. Of course, correlations may depend on the investigated timescale. In principle, an evaluation of correlations at shorter time scales might allow for more mechanistic interpretations. Here, we intended to analyze state-related correlations across 20 seconds epochs defined by Rechtschaffen and Kales criteria [20], because classification of sleep stages on a smaller time scale has not been validated. Previous bivariate measures of intracranial EEG data utilized either power correlation [34, 35] or phase synchronization [14, 36]. The latter approach is particularly well suited to study interactions of intracranial EEG with a high temporal resolution. However, phase synchronization between scalp and intracranial EEG is problematic because of the different properties of scalp and intracranial EEG, and because scalp activity is transferred through structures with strong low-pass filtering properties such as bone and skin [37], which may lead to phase distortions. In contrast, the reported analysis of power correlation is probably less hampered by these difficulties. Further recordings in patients with both medial temporal depth electrodes and subdural electrodes are required to calculate phase synchronization during different sleep stages.

Taken together, our findings support the idea that medial temporal and neocortical dynamics are more integrated during sleep, in particular NREM sleep, than during waking state [38].

ACKNOWLEDGMENT

This research was supported by the Deutsche Forschungsgemeinschaft (DFG El-122-8).

REFERENCES

[1] H. Eichenbaum, "A cortical-hippocampal system for declarative memory," *Nature Reviews Neuroscience*, vol. 1, no. 1, pp. 41–50, 2000.

[2] S. Zola-Morgan and L. R. Squire, "Neuroanatomy of memory," *Annual Review of Neuroscience*, vol. 16, pp. 547–563, 1993.

[3] G. Buzsáki, "Two-stage model of memory trace formation: a role for "noisy" brain states," *Neuroscience*, vol. 31, no. 3, pp. 551–570, 1989.

[4] M. E. Hasselmo, "Neuromodulation: acetylcholine and memory consolidation," *Trends in Cognitive Sciences*, vol. 3, no. 9, pp. 351–359, 1999.

[5] R. Stickgold, J. A. Hobson, R. Fosse, and M. Fosse, "Sleep, learning, and dreams: off-line memory reprocessing," *Science*, vol. 294, no. 5544, pp. 1052–1057, 2001.

[6] B. J. Wiltgen, R. A. M. Brown, L. E. Talton, and A. J. Silva, "New circuits for old memories: the role of the neocortex in consolidation," *Neuron*, vol. 44, no. 1, pp. 101–108, 2004.

[7] M. P. Witter and D. G. Amaral, "Entorhinal cortex of the monkey: V. Projections to the dentate gyrus, hippocampus, and subicular complex," *The Journal of Comparative Neurology*, vol. 307, no. 3, pp. 437–459, 1991.

[8] C. Ranganath, J. DeGutis, and M. D'Esposito, "Category-specific modulation of inferior temporal activity during working memory encoding and maintenance," *Cognitive Brain Research*, vol. 20, no. 1, pp. 37–45, 2004.

[9] P. E. Downing, A. W.-Y. Chan, M. V. Peelen, C. M. Dodds, and N. Kanwisher, "Domain specificity in visual cortex," *Cerebral Cortex*, vol. 16, no. 10, pp. 1453–1461, 2006.

[10] J. Klopp, K. Marinkovic, P. Chauvel, V. Nenov, and E. Halgren, "Early widespread cortical distribution of coherent fusiform face selective activity," *Human Brain Mapping*, vol. 11, no. 4, pp. 286–293, 2000.

[11] S. Knake, C. M. Wang, I. Ulbert, D. L. Schomer, and E. Halgren, "Specific increase of human entorhinal population synaptic and neuronal activity during retrieval," *NeuroImage*, vol. 37, no. 2, pp. 618–622, 2007.

[12] N. Axmacher, F. Mormann, G. Fernández, C. E. Elger, and J. Fell, "Memory formation by neuronal synchronization," *Brain Research Reviews*, vol. 52, no. 1, pp. 170–182, 2006.

[13] R. Stickgold, "Sleep-dependent memory consolidation," *Nature*, vol. 437, no. 7063, pp. 1272–1278, 2005.

[14] J. Fell, P. Klaver, K. Lehnertz, et al., "Human memory formation is accompanied by rhinal-hippocampal coupling and decoupling," *Nature Neuroscience*, vol. 4, no. 12, pp. 1259–1264, 2001.

[15] J. Fell, P. Klaver, H. Elfadil, C. Schaller, C. E. Elger, and G. Fernández, "Rhinal-hippocampal theta coherence during declarative memory formation: interaction with gamma synchronization?" *European Journal of Neuroscience*, vol. 17, no. 5, pp. 1082–1088, 2003.

[16] P. B. Sederberg, M. J. Kahana, M. W. Howard, E. J. Donner, and J. R. Madsen, "Theta and gamma oscillations during encoding predict subsequent recall," *The Journal of Neuroscience*, vol. 23, no. 34, pp. 10809–10814, 2003.

[17] S. Gais and J. Born, "Declarative memory consolidation: mechanisms acting during human sleep," *Learning & Memory*, vol. 11, no. 6, pp. 679–685, 2004.

[18] L. Marshall, H. Helgadóttir, M. Mölle, and J. Born, "Boosting slow oscillations during sleep potentiates memory," *Nature*, vol. 444, no. 7119, pp. 610–613, 2006.

[19] D. Van Roost, L. Solymosi, J. Schramm, B. van Oosterwyck, and C. E. Elger, "Depth electrode implantation in the length

axis of the hippocampus for the presurgical evaluation of medial temporal lobe epilepsy: a computed tomography-based stereotactic insertion technique and its accuracy," *Neurosurgery*, vol. 43, no. 4, pp. 819–826, 1998.

[20] A. Rechtschaffen and A. Kales, *A manual of standardized terminology, techniques, and scoring system for sleep stages of human subjects*, Public Health Service, US Government Printing Office, Washington, DC, USA, 1968.

[21] M. Steriade, *Neuronal Substrates of Sleep and Epilepsy*, Cambridge University Press, Cambridge, UK, 2003.

[22] J. L. Cantero, M. Atienza, R. Stickgold, M. J. Kahana, J. R. Madsen, and B. Kocsis, "Sleep-dependent θ oscillations in the human hippocampus and neocortex," *The Journal of Neuroscience*, vol. 23, no. 34, pp. 10897–10903, 2003.

[23] J. L. Cantero, M. Atienza, J. R. Madsen, and R. Stickgold, "Gamma EEG dynamics in neocortex and hippocampus during human wakefulness and sleep," *NeuroImage*, vol. 22, no. 3, pp. 1271–1280, 2004.

[24] J. O'Keefe, "Place units in the hippocampus of the freely moving rat," *Experimental Neurology*, vol. 51, no. 1, pp. 78–109, 1976.

[25] G. Dragoi, K. D. Harris, and G. Buzsáki, "Place representation within hippocampal networks is modified by long-term potentiation," *Neuron*, vol. 39, no. 5, pp. 843–853, 2003.

[26] M. A. Wilson and B. L. McNaughton, "Reactivation of hippocampal ensemble memories during sleep," *Science*, vol. 265, no. 5172, pp. 676–679, 1994.

[27] K. Louie and M. A. Wilson, "Temporally structured replay of awake hippocampal ensemble activity during rapid eye movement sleep," *Neuron*, vol. 29, no. 1, pp. 145–156, 2001.

[28] D. Ji and M. A. Wilson, "Coordinated memory replay in the visual cortex and hippocampus during sleep," *Nature Neuroscience*, vol. 10, no. 1, pp. 100–107, 2007.

[29] R. Q. Quiroga, L. Reddy, G. Kreiman, C. Koch, and I. Fried, "Invariant visual representation by single neurons in the human brain," *Nature*, vol. 435, no. 7045, pp. 1102–1107, 2005.

[30] A. G. Siapas and M. A. Wilson, "Coordinated interactions between hippocampal ripples and cortical spindles during slow-wave sleep," *Neuron*, vol. 21, no. 5, pp. 1123–1128, 1998.

[31] A. Sirota, J. Csicsvari, D. Buhl, and G. Buzsáki, "Communication between neocortex and hippocampus during sleep in rodents," *Proceedings of the National Academy of Sciences of the United States of America*, vol. 100, no. 4, pp. 2065–2069, 2003.

[32] M. Mölle, O. Yeshenko, L. Marshall, S. J. Sara, and J. Born, "Hippocampal sharp wave-ripples linked to slow oscillations in rat slow-wave sleep," *Journal of Neurophysiology*, vol. 96, no. 1, pp. 62–70, 2006.

[33] Z. Clemens, M. Mölle, L. Erőss, P. Barsi, P. Halász, and J. Born, "Temporal coupling of parahippocampal ripples, sleep spindles and slow oscillations in humans," *Brain*, vol. 130, no. 11, pp. 2868–2878, 2007.

[34] V. V. Nikouline, K. Linkenkaer-Hansen, J. Huttunen, and R. J. Ilmoniemi, "Interhemispheric phase synchrony and amplitude correlation of spontaneous beta oscillations in human subjects: a magnetoencephalographic study," *NeuroReport*, vol. 12, no. 11, pp. 2487–2491, 2001.

[35] T. Womelsdorf, J.-M. Schoffelen, R. Oostenveld, et al., "Modulation of neuronal interactions through neuronal synchronization," *Science*, vol. 316, no. 5831, pp. 1609–1612, 2007.

[36] J.-P. Lachaux, E. Rodriguez, J. Martinerie, and F. J. Varela, "Measuring phase synchrony in brain signals," *Human Brain Mapping*, vol. 8, no. 4, pp. 194–208, 1999.

[37] R. Srinivasan, P. L. Nunez, and R. B. Silberstein, "Spatial filtering and neocortical dynamics: estimates of EEG coherence," *IEEE Transactions on Biomedical Engineering*, vol. 45, no. 7, pp. 814–826, 1998.

[38] Y. Isomura, A. Sirota, S. Özen, et al., "Integration and segregation of activity in entorhinal-hippocampal subregions by neocortical slow oscillations," *Neuron*, vol. 52, no. 5, pp. 871–882, 2006.